UNIVERSITY OF SOUTHAMPTON

FACULTY OF NATURAL AND ENVIRONMENTAL SCIENCES

Ocean and Earth Sciences

Mechanisms of Calcification in Coccolithophores

Charlotte Elizabeth Walker

Thesis for the degree of

DOCTOR OF PHILOSOPHY

MARCH 2018

UNIVERSITY OF SOUTHAMPTON

ABSTRACT

FACULTY OF NATURAL AND ENVIRONMENTAL SCIENCES

Ocean and Earth Sciences

Doctor of Philosophy

MECHANISMS OF CALCIFICATION IN COCCOLITHOPHORES

By Charlotte Elizabeth Walker

Coccolithophores are unicellular marine algae characterised by the production of calcite coccoliths. As a result of their calcification they contribute significantly to global biogeochemical cycles. Comprehensive understanding of the mechanisms behind calcification remains elusive, due in part to the research focus on one species, *Emiliania huxleyi*; the most globally abundant of all coccolithophores. It is imperative to investigate calcification in other species to better understand this biogeochemically important process, especially as the ecological success of *E. huxleyi* may be due to certain physiological differences with other species. This study set out to explore differences between species in the mechanisms of calcification in three primary areas. Firstly, the physiological requirement for calcification remains poorly understood, particularly as non-calcifying strains of *E. huxleyi* grow normally in laboratory culture. This study identified a contrast in the requirement for calcification between *E. huxleyi* and the ecologically important *Coccolithus braarudii*. Calcification disruption had no negative impacts on *E. huxleyi* but resulted in major growth defects in *C. braarudii* demonstrating an obligate requirement for calcification in this species. Secondly, the previous identification of Si transporters in some coccolithophores was further investigated using a combination of physiological and expression studies to identify that Si plays a role in heterococcolith calcification during their diploid life stage. *C. braarudii* Si transporters were also found to be regulated in response to available Si and shown to be expressed in natural populations. Finally, coccolith associated polysaccharides (CAPs) are an integral component of the calcification mechanism known to modulate the precipitation of calcite. The data presented here show that extracellular CAPs differ in structure and composition between species and that they also play an important role in the organisation of the coccosphere, expanding upon their role and importance in calcification. These findings mark crucial physiological differences between coccolithophore species. The identification of a requirement for calcification in coccolithophores highlights the importance of maintaining a coccosphere. The requirement for Si in some species suggests major physiological differences between species which may influence their ecology. Consequently, these contrasting physiological characteristics may contribute to significant differences in the response of coccolithophores to future ocean conditions.

List of Contents

List of Tables and Figures

1. Introduction

2. The Effect of Ge on Coccolithophores

3. The requirement for Calcification Differs Between Ecologically Important Coccolithophore Species

4. The Molecular Characterisation of Si Transporters in *Coccolithus braarudii*

5. Investigating Coccolith Associated Polysaccharides

1. General Discussion

List of Appendices

Appendix I: Chapter 2 Supplementary Information

Appendix II: Chapter 3 Supplementary Information

Appendix III: Chapter 4 Supplementary Information

Appendix IV: Chapter 5 Supplementary Information

Academic Thesis: Declaration Of Authorship

I, CHARLOTTE ELIZABETH WALKER declare that this thesis and the work presented in it are my own and has been generated by me as the result of my own original research.

Mechanisms of calcification in coccolithophores

I confirm that:

1. This work was done wholly or mainly while in candidature for a research degree at this University;
2. Where any part of this thesis has previously been submitted for a degree or any other qualification at this University or any other institution, this has been clearly stated;
3. Where I have consulted the published work of others, this is always clearly attributed;
4. Where I have quoted from the work of others, the source is always given. With the exception of such quotations, this thesis is entirely my own work;
5. I have acknowledged all main sources of help;
6. Where the thesis is based on work done by myself jointly with others, I have made clear exactly what was done by others and what I have contributed myself (overleaf);
7. Either none of this work has been published before submission, or parts of this work have been published as: [please list references below]:

Durak GM, Taylor AR, Walker CE, Probert I, De Vargas C, Audic S, Schroeder D, Brownlee C, Wheeler GL. 2016. A role for diatom-like silicon transporters in calcifying coccolithophores. *Nat Commun* 7 (Appendix 1)

Signed: 

Date: 26.3.18

Declaration of authorship continued: outline of work conducted jointly with or by others presented in this thesis (information pertaining to point 6 on previous page).

Chapter 2: The effect of Ge on coccolithophore

The majority of the experimental work was conducted by C. E. Walker with the following exception:
1. The concentration of Si in the seawater utilised in these experiments was measured by Dr M. Woodward from Plymouth Marine Laboratory in collaboration with this project.

The data presented was published in part in Durak *et al*. 2016 (Appendix I).

Chapter 3: The requirement for calcification differs between ecologically important coccolithophore species

The majority of the experimental work was conducted by C. E. Walker with the following exceptions:
1. Dr G. Wheeler conducted the growth experiment presented in Figure 3.3b and took images presented in Supplementary Figure II.1c (Appendix II).
2. Dr G. Durak conducted the immunofluorescence study presented in Figure 3.6 during her Ph.D studies at the Marine Biological Association.
3. Dr I. Probert from Roscoff Culture Collection provided the information pertaining to Supplementary Table II.2 (Appendix II) in collaboration with this project.
4. The concentration of Si in the seawater utilised in these experiments was measured by Dr M. Woodward from Plymouth Marine Laboratory in collaboration with this project.

This work is currently in review at New Phytologist

Chapter 4: Molecular characterisation of Si-transporters in *C. braarudii*

The majority of the experimental work was conducted by C. E. Walker with the following exception:
1. The L4 environmental samples were collected by the MBA RV Sepia crew.
2. The concentration of Si in the seawater utilised in these experiments was measured by Dr M. Woodward from Plymouth Marine Laboratory in collaboration with this project.

Chapter 5: Exploring coccolith associated polysaccharides

The majority of the experimental work was conducted by C. E. Walker with the following exceptions:
1. Dr D. Salmon aided in the GC-MS analysis described in Figure 5.6. C. E. Walker conducted the preparation of samples for analysis up to the derivatisation stage whereby Dr D. Salmon completed the method reported here (section 5.2.7).
2. Dr S. Heath completed some of the initial polysaccharide imaging as part of her MRes project at the Marine Biological Association. The Images she captured are presented in Figure 5.7 and Supplementary Figure IV.4 (Appendix IV).

The work conducted is in submission at Frontiers in Marine Biology for a special issue on Biomineralisation.

Acknowledgments

Formerly, I would like to thank the Natural Environment Research Council for funding my project and the University of Southampton and the Marine Biological Association of the UK for hosting me. Additionally, I would like to acknowledge the Gillings Fund (University of Southampton) and the British Phycological Association for additional travel awards that made this project more enriching.

I would like to say thank you to all of those who have been part of my PhD experience. This has been both a joy and a challenge. None of this would have been possible alone so please excuse me these extensive acknowledgements and I hope it imparts upon any who read it just how many people have influenced this experience.

First and foremost, a huge thank you to Dr Glen Wheeler who has been my primary advisor throughout my studentship. You have patiently and skilfully taught me how to channel my enthusiasm into robust and exciting research. Thank you for many hours discussing, reviewing and improving my work, for which I am so grateful. I have truly enjoyed our time working together and I hope this continues in the future.

To Prof. Colin Brownlee, thank you so much for advising me on everything from the interpretation of data and continuation of experiments, to helping me report our research with the impact it deserves. It has been great being part of your lab, thank you for making it so.

I would also like to thank my supervisor Prof. Toby Tyrrell for you have been incredibly helpful in framing my work in a wider oceanographic context, an invaluable component to my personal study in this process. Also to Prof. Mark Moore, you both have been central in linking my experience at the MBA in Plymouth to progressing through the University of Southampton programme of study. Thank you both for being so supportive.

Although I have three official supervisors, I have been fortunate enough to adopt others along this journey who have improved and enriched my research development. Firstly, thank you Dr Gerald Langer who has taught me more about the intricate workings of crystallisation and coccolithophores than I thought I could ever comprehend. You have selflessly given me your time and always listened with interest and respect to what I have to contribute. I will aspire to impart the same feeling on others as it has had such a positive effect upon me. Secondly, Dr Alison Taylor, your meticulous and excellent work ethic impacted upon me during my time in your lab at UNCW. I am truly grateful for the detail in which you taught me, how welcome you made me feel and how you have continued to influence my work as our labs work collaboratively together. Finally, Dr Katherine Helliwell, thank you for imparting confidence, perspective and always finding the time to discuss research and academic life with me. It is intimidating to be venturing into this career path and your realistic and friendly discussion has helped me greatly throughout this process.

There are many who have made this research possible and this list is by no mean exhaustive. Firstly I would like to thank all members of the Cell and Molecular group at the MBA for their friendship and support, particularly Angela Ward, Shae Bailey and Claire Jasper for their impeccable technical support and Susie Wharem and Andrea Highfield for your excellent knowledge and help in the lab. Thank you to the crew of the RV MBA Sepia, who kindly collected the seawater and plankton tow samples I have used throughout my

experiments. I would like to thank Drs Julie Koester and Mark Gay for their support while I was at UNCW. Thank you to Dr Ian Probert from Roscoff Culture Collection for his unmatched understanding of coccolithophore culturing. Thank you to Malcolm Woodward from PML for nutrient analysis assistance. Thank you to Dr Renee Lee from the University of Reading, Dr Debbie Salmon and Prof Nick Smirnoff from the University of Exeter for their assistance in polysaccharide extraction and analysis. Thank you also to the Plymouth University Electron Microscopy facility, particularly Glenn Harper for his technical help and productivity encouraging chocolate biscuits.

The MBA is an incredible place to work and I have been so happy there these last few years. I consider it a privilege to have been part of such a great organisation. This would not be possible without my fellow PhD students Sam, Harriet and Harry who have been with me every step of the way. You all grounded my experience and made it infinitely better; I am truly in awe of your skills as scientists and your generosity as friends. My time MBA started with a person who has become the greatest friend, dog walking companion and the only person who is actually louder than me. Thank you to Costanza for supporting me through this whole experience and reminding me there is a world beyond this PhD.

Thank you especially to Taylor, who has steadily taken on all the chaos I create in life. Your never ending support and willingness to move our life around this planet is the most awe-inspiring show of faith anyone could ask for. Here's to an exciting next chapter, may it bring us all we hope.

I would like to thank my Mum, Dad and James for being the foundation that I can always turn to. You make me smile, keep me going and bring me back down to Earth. My Mum has tirelessly read my whole thesis with a red pen in hand, yes, she is a bit old school but she will proudly go down in history as one of the few that has read the whole thing. I am so lucky to come from a foundation of belief and encouragement and I struggle to express how grateful I am to all three of you. I am fortunate enough to have more parents than most, I have an extra circle of love and support in the form of my WSM Janey and CP Mark. I hope you both know how grateful I am that you have been such a positive influence in my life. I would also like to specially thank my grandparents, all of whom bestow upon me great encouragement and more pride than I could ever deserve.

I would like to finish by remembering my Grandfather Peter, who saw me start this journey but did not see me finish. You are and will always be the standard to which I aspire and the friend I will always miss.

List of Abbreviations

ASW	Artificial Seawater
CAP	Coccolith Associated Polysaccharide
cDNA	Complementary Deoxyribose Nucleic Acid
C_i	Inorganic Carbon
C_o	Organic Carbon
CT	Controlled Temperature
CV	Coccolith Vesicle
d	Day
DDSW	Diatom Depleted Seawater
DIC	Dissolved Inorganic Carbon
dSi	Dissolved Silicon
[dSi]	Concentration of Dissolved Silicon
EFL	Elongation Factor
ER	Endoplasmic Reticulum
FSW	Filtered Seawater
GC	Gas Chromatography
h	Hour
HRM	High Resolution Melt
LM	Light Microscopy
min	Minute
MS	Mass Spectrometry
MYA	Million Years Ago
pCO_2	Partial Pressure of CO_2
PCR	Polymerase Chain Reaction
PM	Plasma Membrane
ppm	Parts Per Million
ppt	Parts Per Thousand
qPCR	Quantitative Polymerase Chain Reaction
RB	Reticular Body
rDNA	Ribosomal Deoxyribose Nucleic Acid
RNA	Ribose Nucleic Acid
RPS1	Ribosomal Protein S1
SEM	Scanning Electron Microscopy
SGR	Specific Growth Rate
SIT	Silicon Transporter
SITL	Diatom-like Silicon Transporter
TATB	TATA Box Binding Protein
TEM	Transmission Electron Microscopy
TMD	Transmembrane Domain
µ	Growth Rate

1. Introduction

1.1. Coccolithophore Introduction

Coccolithophores (Haptophyta) are unicellular marine algae characterised by elaborate calcite platelets (coccoliths) found on the cell surface (Marsh, 2003; Brownlee & Taylor, 2004) (Figure 1.1). Coccolithophores are key components of global phytoplankton communities with approximately 200 extant species in modern oceans (Young *et al.*, 2003) and an extensive fossil record covering the last 220 million years (Bown, 1998; Brown et al., 2004). Following their origin in the Triassic period (Brown et al., 2004) coccolithophores have increased in abundance and have played a key role in biogeochemical cycling ever since (Rost & Riebesell, 2004).

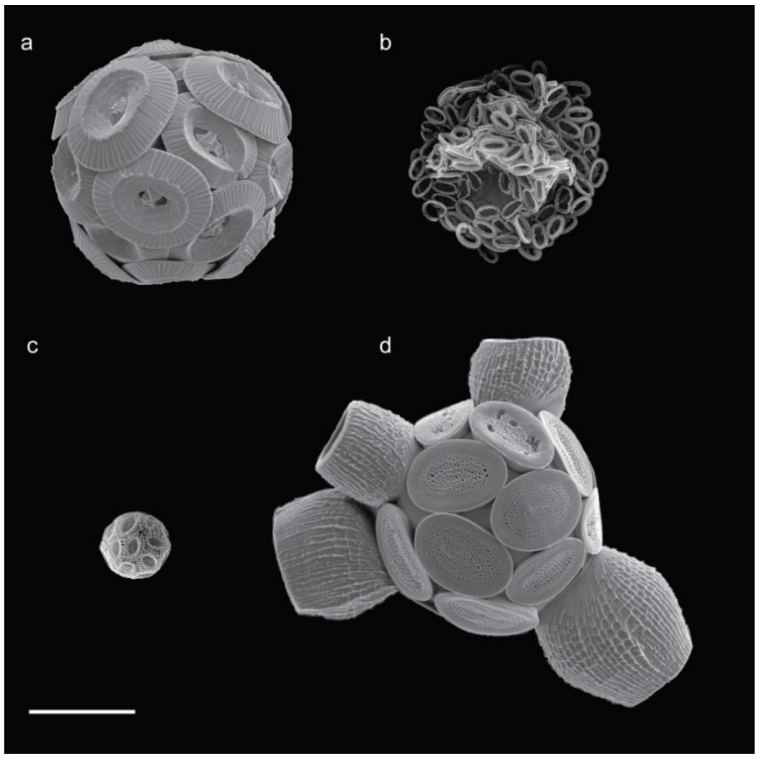

Figure 1.1 Coccolithophores
Scanning electron microscopy images of diploid heterococcolith bearing (a) *Coccolithus braarudii*, (b) *Chrysotila carterae*, (c) *Emiliania huxleyi* and (d) *Scyphosphaera apsteinii.* Scale bar denotes 10 µM.

Coccolithophores inhabit coastal and open ocean environments and can thrive in oligotrophic waters. Their small size (3 – 40 µM including coccosphere) and high surface to volume ratio decreases nutrient diffusion limitation (Brand, 2006). Coccolithophores are often associated with large blooms, with the majority of large-scale blooms formed by only two species, *Emiliania huxleyi* and *Gephyrocapsa oceanica* (Westbroek *et al.*, 1993; Brand, 2006). Coccolithophores are often thought to dominate in warm, stratified, nutrient-poor waters (Brand, 2006) and to optimise on low Si conditions following diatom blooms (Leblanc *et al.*, 2009; Balch *et al.*, 2014; Hopkins *et al.*, 2015). The current

research focusses heavily on *E. huxleyi* but there are many other influential species, such as *Calcidiscus leptoporus and Coccolithus pelagicus*. These species contribute significantly to calcification in the oceans (Baumann *et al.*, 2004; Daniels *et al.*, 2014), do not form dense blooms and thrive in different ecological conditions. It is becoming increasingly obvious that different species have clear light intensity, temperature and nutrient optima making them subject to seasonal, vertical stratification and biogeographic distributions (Thierstein & Young, 2004; De Vargas *et al.*, 2007).

Coccolithophores significantly impact the fate of inorganic carbon (C_i) and organic carbon (C_o) on Earth through two important components of the carbon cycle; the organic carbon pump and the carbonate counter pump. The organic carbon pump involves the utilisation of CO_2 for photosynthesis and as a result, coccolithophores increase long term atmospheric O_2 and photosynthetically fix C_i into C_o (Westbroek *et al.*, 1993; Falkowski *et al.*, 2005). Consequentially they are estimated to be responsible for between 1-10% of global carbon fixation (Poulton *et al.*, 2007), increasing locally to as much as 40% under bloom conditions (Poulton *et al.*, 2013). As coccolithophores sink a high proportion of the C_o remineralises through degradation and respiration, releasing CO_2 at depth.

Coccolithophores contribute to the carbonate counter pump through the formation of calcite, of which they are responsible for approximately 50% of the global production (Milliman, 1993). The use of HCO_3^- as the C_o substrate for calcification leads to reduced alkalinity in surface waters and reduced capacity for carbonate and pH buffering. Moreover, the calcification process generates CO_2, potentially leading to increased pCO_2 in surface waters (Westbroek et al., 1993). The production of coccoliths causes a continuous rain of calcium carbonate from surface waters to depth, maintaining the vertical alkalinity gradient of the water column through calcite dissolution (Archer, 1996; Milliman *et al.*, 1999) and forming vast sedimentary deposits (Milliman, 1980; Steinmetz, 1994), for example the White Cliffs of Dover. Additionally, coccoliths act as a ballast which induces sinking of associated organic matter, aiding the transfer of organic matter to the deep ocean (Thierstein *et al.*, 1977; Klaas & Archer, 2002).

1.2. Coccoliths and Calcification

Coccolith morphology varies significantly between species (Figure 1.1). and a comprehensive morphology-driven species-level taxonomy is clearly established (Jordan & Green, 1994; Winter & Siesser, 2006). Two categories of coccolith are associated with different life-cycle stages, heterococcoliths and holococcoliths. Diploid cells bear multicrystalline heterococcoliths which are produced internally in a specially derived

cellular compartment and are extruded to the cell surface once fully formed (Dixon, 1900; Taylor *et al.*, 2007). Species such as *Scyphosphaera apsteinii* even exhibit two distinct heterococcolith types (dimorphic) (Figure 1.1d), found in variable arrangements. In contrast, holococcoliths are formed from single calcite crystals, are present in the haploid stage of the life cycle and are thought to be synthesised outside the cell (Rowson *et al.*, 1986; Young *et al.*, 1999; Cros *et al.*, 2000). For the purpose of this review, only heterococcoliths will be referred to from now on unless specified otherwise.

Although coccolith production is pivotal to the biogeochemical importance of coccolithophores, many of the cellular mechanisms behind the process remain elusive. Coccolith production occurs internally, involving specially adapted cell organelles. The cell structures known to be closely associated with calcification include the coccolith vesicle (CV) and the reticular body (RB) (Figure 1.2). The CV is a Golgi-derived cellular compartment in which the coccolith is produced. The CV allows for the control of the intracellular environment within which calcification can be controlled by multiple cellular mechanisms (Brownlee & Taylor, 2004). The RB is a membranous structure closely associated with the CV and is thought to be key in providing calcification raw material (De Jong *et al.*, 1976).

For calcification to take place HCO_3^- and Ca^{2+} have to be transported from the surrounding seawater into the CV (Figure 1.2). The transport of HCO_3^- (Buitenhuis *et al.*, 1999; Herfort *et al.*, 2002) is thought to involve Na^+ co-transporters and Cl^- antiporters (Mackinder *et al.*, 2010). Ca^{2+} ions are also acquired from the environment: a study into *E. huxleyi* showed the strong upregulation of Ca^{2+}/H^+ antiporters in calcifying cells. It is suggested that Ca^{2+} is transported into the cell through protein channels down a strong Ca^{2+} gradient, it is then actively transported into the CV with Ca^{2+}/H^+ antiporters most likely operating to bring about loading of Ca^{2+} into the endomembrane system (Mackinder *et al.*, 2010; Mackinder *et al.*, 2011; Holtz *et al.*, 2013).

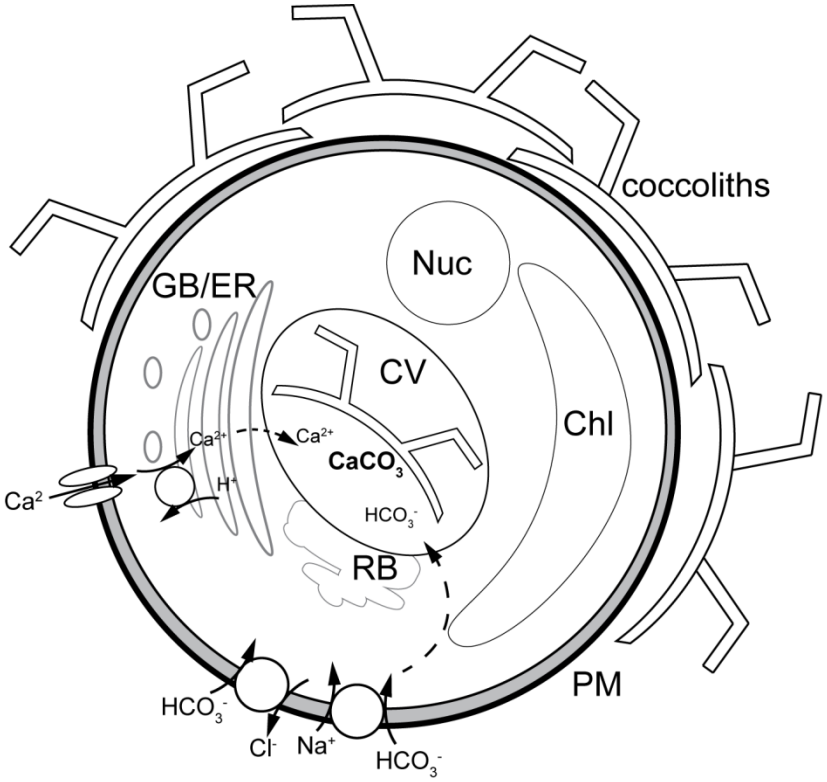

Figure 1.2 Schematic of coccolithophore calcification
General intracellular structures including the nucleus (Nuc), chlorplast (Chl), plasma membrane (PM), cytoplasm (Cyt) are shown alongside calcification associated organelles, Golgi body (GB), endoplasmic reticulum (ER), coccolith vesicle (CV) and reticular body (RB). The transport of calcification precursors Ca^{2+} and HCO_3^- is depicted, based on previous studies (Mackinder *et al.*, 2010; Mackinder *et al.*, 2011; Holtz *et al.*, 2013). See text for further details.

A number of studies have explored the molecular mechanisms behind the transport processes shown in Figure 1.2. However, it should be noted there is a significant absence of genetic manipulation tools for any coccolithophore species which presents obstacles for progression in this field of study. Progress has been made in the identification of potential calcification relevant genes: firstly, GPA a coccolith associated protein thought to bind to Ca^{2+} was identified in extracellular polysaccharides of diploid calcifying *E. huxleyi* (Corstjens *et al.*, 1998) and also analysed in gene expression studies (Mackinder *et al.*, 2011). Other Ca^{2+} related proteins involved in a range of processes within the cell have also been identified (Wahlund *et al.*, 2004; Quinn *et al.*, 2006), including carbonic anhydrases which catalyse the interconversion of CO_2 and H_2O to HCO_3^- and H^+ (Quinn *et al.*, 2006). Additionally, genes which have been found to be involved in biomineralisation in other organisms have also been identified (Nguyen *et al.*, 2005). At this stage the findings from the studies are correlative, although it is very likely these genes are involved in calcification, we cannot be sure they do not have alternative functions.

Other potential calcification related genes identified include components involved in H^+ transport. The calcification process produces H^+ which may exert pressure on the internal pH homeostasis of the cell (Brownlee & Taylor, 2004; Suffrian *et al.*, 2011). There are two H^+ ion transporters thought to maintain the internal pH of a coccolithophore, one is a channel and one is an ATPase. Channels are transporters (co- or anti-) which utilise the gradient of an ion to drive the transport of another. In contrast, ATPases transport ions against their electrochemical gradients and use chemical energy derived from ATP to do so. The first of the two H^+ ion transporters is a plasma membrane voltage-gated H^+ channel (HVCN1), which was identified as active by electrophysiology (Taylor *et al.*, 2011). Although HVCN1 is clearly involved in pH maintenance, gene expression studies indicate it is expressed in both calcifying diploid and non-calcifying haploid *E. huxleyi* and therefore may serve a more general pH homeostasis role (Mackinder *et al.*, 2011). The second is a vacuolar H^+-ATPase which was shown to be upregulated in calcifying *E. huxleyi* (Mackinder *et al.*, 2011), it is likely that this transporter is upregulated to cope with the increase in production of H^+ during calcification and removal of H^+ from the calcifying compartment. Correlating gene expression studies with electrophysiology strengthens the conclusions drawn about the functions of the HVCN1 channel, multidisciplinary approaches are essential in elucidating the function of transporters in the absence of genetic manipulation tools.

With the publication of the *E. huxleyi* genome (Read *et al.*, 2013) more work can now be undertaken to investigate functional characterisation through expression studies, heterologous characterisation and localisation studies. These approaches would enable a greater understanding of the genes which control calcification in *E. huxleyi.* In addition, essential comparisons can be made to other species in the future through the use of the transcriptomes of five additional coccolithophore species available from the Marine Microbial Eukaryote Transcriptome Sequencing Project (MMETSP): *C. braarudii, C. leptoporus, S. apsteinii, G. oceanica* and *C. carterae* (Keeling *et al.*, 2014).

Following the delivery of HCO_3^- and Ca^{2+} ions into the CV the nucleation of calcite crystals occurs in a proto-coccolith ring around an organic base-plate scale. Subsequent crystal growth occurs in various directions to produce a complete coccolith (Young *et al.*, 1999). The formation of crystals is thought to be strongly regulated by coccolith associated polysaccharides (CAPs) and specific proteins (Van der Wal, P. *et al.*, 1983b; Marsh, 2003; Kayano & Shiraiwa, 2009; Hirokawa, 2013). The CAPs, CV and surrounding cytoskeleton are thought to shape the coccoliths into their species-specific form (Young *et al.*, 1999). Once the coccolith is fully formed, the CV fuses with the plasma membrane to extrude the coccolith onto the cell surface where it forms part of the coccosphere. The

CAPs remain associated with the coccoliths and are hypothesised to play a role in coccosphere organisation (van Emburg *et al.*, 1986) and protecting the calcite from dissolution (Van der Wal, P. *et al.*, 1983b).

1.3. The Evolution of Calcification in Coccolithophores

It is widely acknowledged that the evolution of photosynthetic haptophytes and the evolution of calcification are distinct (De Vargas *et al.*, 2007). However, the phylogeny surrounding the origin of the haptophytes is uncertain. Haptophytes have previously been placed in the chromalveolates, a Eukaryotic super group (Cavalier-Smith, 2003). The chromalveolates contain chlorophyll-c and are thought to have originated through a single secondary endosymbiotic event when an Amoebozoic host engulfed a red alga (Cavalier-Smith, 1982). However this grouping has now been challenged. Subsequent phylogenies placed the haptophytes in the Hacrobia (Burki *et al.*, 2012) and most recently it has been suggested they acquired their plastid from the Stramenopiles (Stiller *et al.*, 2014; Dorrell *et al.*, 2017). Although there is a lot of uncertainty surrounding the origin of the haptophytes, the phylogeny within the haptophytes has been well resolved due to multiple gene phylogeny studies (Medlin *et al.*, 2008; Liu *et al.*, 2010).

Coccolithophores are distinguished from other haptophytes because of calcification. Other haptophytes include the Pavlovales, Phaeocystales and Prymnesiales. All of which are non-calcified but have the characteristic haptonema, an organelle thought to be involved in feeding and/or attachment (Lewin, 1992). As a result of their calcite coccoliths, coccolithophores have been reliably identified in the fossil record as early as ~220 million years ago (MYA) (Bown *et al.*, 2004). However, it is suggested that early coccolithophores predominantly occurred in coastal waters where conditions for preservation in the sediments are unfavourable (Young *et al.*, 2005). As a result, the fossil record may not be completely accurate in its depiction of calcification evolution.

It is clearly important to include multiple lines of evidence when trying to deduce the point at which calcification evolved in haptophytes. Combining the fossil data and comparing this to molecular analysis is one such method to attempt to accurately infer the point of calcification evolution. In this case, the evidence for the origin of potentially calcifying haptophytes is supported by both the molecular clock data and the fossil records. The molecular data places the origin at ~270-240 and ~200MYA for the small subunit (SSU) and large subunit (LSU) ribosomal DNA clocks respectively (De Vargas *et al.*, 2007). These findings correlate with the previously mentioned ~220MYA fossil data (Brown *et*

al., 2004). It is possible to conclude that there is reasonably robust evidence for the timescale of coccolithophore evolution.

In order to fully understand the evolution of calcification it is important to reflect on the ocean environment coccolithophores would have inhabited in the late Triassic. Coccolithophores originated in a period where the atmospheric CO_2 concentration was four to six times higher than today (Katz *et al.*, 2007), which is interesting as current and predicted high CO_2 levels have widely been considered a threat to calcifying organisms (Doney *et al.*, 2009). The CO_2 in the atmosphere forms a net flux of CO_2 into the surface ocean, therefore the more CO_2 released by anthropogenic activity causes an increase in ocean pCO_2. The ocean pH is causatively reduced and the carbonate (CO_3^{2-}) ion concentration lowered, resulting in a reduction in the calcite saturation state (Ω) of the ocean. The result of these factors is that the conditions for the formation of calcareous structures are less favourable (Doney *et al.*, 2012). The factors that may have buffered the Triassic carbonate chemistry to enable calcite deposition within these conditions remain debated, however it is considered that a relaxation of the calcification inhibitory chemistry in the Paleozoic is a large contributor (De Vargas *et al.*, 2007). In addition to these changes, seawater was considered to be highly oversaturated with respect to calcite and aragonite (Ridgwell & Zeebe, 2005) due to little or no calcification occurring at the time combined with the weathering of exposed carbonates (Walker *et al.*, 2002). These factors lead to the available HCO_3^- necessary for calcification.

Ca^{2+} was also readily available 220 MYA and at higher concentration (approximately 15 mM) than in modern oceans (10 mM) (Hönisch *et al.*, 2012). Interestingly calcification has been suggested as a method to cope with Ca^{2+} poisoning (Müller *et al.*, 2015). Ca^{2+} homeostasis is of upmost importance as it is a vital cell signalling molecule and excessive influx can be lethal (Clapham, 1995) therefore, the utilisation of large amount of Ca^{2+} for calcification may buffer the influx of Ca^{2+} from the environment.

It is likely the environmental conditions played a role in the evolution of calcification in coccolithophores; it has been suggested that the mechanisms for calcification were already in place in the cells but the environmental conditions at the time drove them into novel roles resulting in calcification (Westbroek & Marin, 1998). De Vargas et al. (2007) reviews the evidence that the mechanisms behind calcification were already present prior to the evolution of coccolithophore calcification, and that calcification is the result of new associations in existing biochemical pathways (De Vargas et al., 2007). One such example is the polysaccharides that are associated with coccolith construction, notably the regulation of calcite precipitation (Marsh, 2003). Polysaccharides that inhibit

calcification and control skeleton growth have been reported to have first evolved in oceans in the Proterozoic Era (Marin et al., 1996), suggesting the polysaccharides involved in coccolith production existed long before their recruitment to a calcification role in coccolithophores. Supporting this theory is the estimate that carbonate (calcite or aragonite) skeletons evolved independently at least 28 times in eukaryotes (Knoll, 2003). In light of this observation, it also prompts the question as to whether coccolithophores evolved calcification once or multiple times independently.

Biomineralisation within the haptophytes is not limited to the coccolithophores, which may support the theory that the cellular mechanisms for calcification were present in coccolithophores prior to calcification evolution. For example, *Prymnesium neolepis* (formerly *Hyalolithus neolepis*) is a Prymnesiales that has evolved the ability to biomineralise using silicon (Si) as opposed to calcite. *P. neolepis* is covered with coccolith-like silica scales (Yoshida *et al.*, 2006; Edvardsen *et al.*, 2011) which are produced intracellularly and then deposited outside the plasma membrane in a comparable mechanism to coccolith secretion (Yoshida *et al.*, 2006; Taylor *et al.*, 2007). The Prymnesiales are estimated to have diverged from the coccolithophores around 280 MYA (Liu *et al.*, 2010) and *P. neolepis* is the only known extensively silicified haptophyte. Understanding whether common cellular mechanisms contribute to silica scale production in *P. neolepis* and coccolith formation in the coccolithophores may help us to understand how these different forms of biomineralisation have evolved within the haptophyte tree. As an example of independently evolved biomineralisation within the photosynthetic haptophytes, *P. neolepis* also supports the theory that independent evolution of calcification within the coccolithophores is possible.

The lineage of Isochrysidales (Figure 1.3) is of particular interest as it contains species with various degrees of calcification, it has been hypothesised that these species may be evidence of multiple independent emergences of calcification. There are examples of non-calcifying coccolithophores within the Isochrysidales: *Isochrysis spp.* and *Ruttnera lamellosa*. (formerly *Chrysotila lamellose). R. lamellosa* produces organic base-plate scales, a suggested pre-cursor for coccoliths (De Vargas *et al.*, 2007) and mucus-containing polysaccharides, potentially similar in function to those that are involved in the regulation of coccolith production (Green & Course, 1983). *E. huxleyi* is found within the Isochrysidales and is generally considered an atypical coccolithophore (Paasche, 2001). One of the reasons is that *E. huxleyi* only produces a singular coccolith at any one time (Van der Wal, P. *et al.*, 1983b), whereas *C. pelagicus* and *Chrysotila carterae* (formerly *Pleurochrysis*) can have multiple coccoliths in production at one time (Van der Wal, P. *et al.*, 1983b).

Additionally *E. huxleyi* and closely related genus *Gephyrocapsa* have a non-calcifying haploid life cycle stage (Cros *et al.*, 2000) (unlike other genera). *E. huxleyi* is also able to grow in culture in a non-calcified state, these cultures are fully-calcified on initial isolation but lose the ability over time with no apparent negative impact on cellular fitness (Paasche, 1998). However, whether or not this is the case for other species of coccolithophore remains largely unknown.

It is also important to consider that the loss of the calcification mechanism in *Isochrysis* is also possible. The loss of the calcification mechanism in *Isochrysis* in terms of evolutionary events would require one loss event, whereas the independent evolution of calcification would require at least two events within the coccolithophores. Although the field has not yet fully elucidated the evolutionary state of calcification within the Isochrysidales, more research into differences in calcification mechanisms would shed light on this debate.

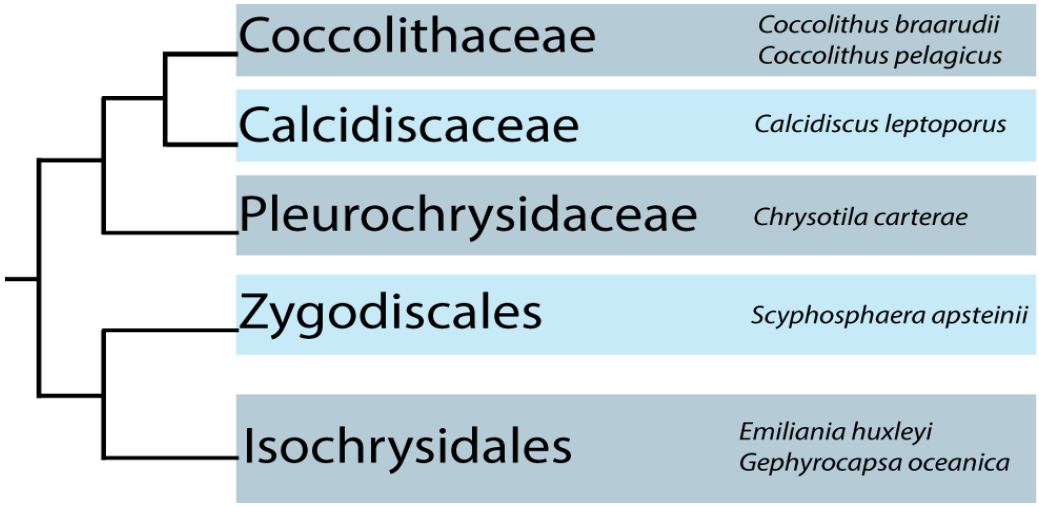

Figure 1.3 Coccolithophore phylogeny
Schematic tree based on multi-gene phylogeny (Liu et al., 2010) depicting families and species of extant coccolithophores focussed on within this thesis.

The *Braarudosphaera* genus is another interesting example of potential independent calcification evolution to consider. *Braarudosphaera* is a pentalith calcifying haptophyte genus, although the coccoliths are relatively simple in structure in comparison to heterococcoliths. *Braarudosphaera* was previously considered to be a coccolithophore due to the coccolith structure and single gene phylogenetic studies (Takano *et al.*, 2006). Some recent single gene phylogenetic studies have been published (Thompson *et al.*, 2012; Hagino *et al.*, 2013) suggesting its close relation to the Prymnesiales. These findings suggest that *Braarudosphaera* has evolved calcification independently to the other coccolithophores, supporting the theory that calcification may have evolved

independently on multiple occasions. However, currently these studies are only based on single gene phylogenies and leave uncertainty about the true location of *Braarudosphaera* in the haptophyte tree, this is largely due to the difficulty to culture this genus.

To conclude, calcification is likely to have evolved approximately 220 MYA, supported by both molecular clock and fossil data. There is evidence that the cellular components were present prior to the evolution of the calcification mechanism and that favourable environmental conditions may have driven the development of the process. There is evidence for multiple emergences of calcification in both the coccolithophores, however this is yet to be fully resolved.

1.4. The Role of Calcification

Another discussion surrounding coccolithophore calcification that is closely linked to its evolution is why coccolithophores calcify (Monteiro *et al.*, 2016). The most prominent theory is that the coccoliths evolved protect the coccolithophore mechanically (Dixon, 1900; Young, 1987; Jaya *et al.*, 2016) and from a variety of external factors: grazing, bacterial infection, viral attachment and excessive light exposure (Tyrrell & Merico, 2004; Monteiro *et al.*, 2016). However, there are studies that have reported that the coccoliths do not significantly protect the cells against other organisms, detailed below. For these studies *E. huxleyi* is very useful as it has both calcified and non-calcified states, i.e. some laboratory cultures have lost the ability to calcify over time with no known negative impacts on cellular fitness. These studies revealed that there is some ambiguity when comparing the rate of grazing on calcified and non-calcified *E. huxleyi.* Studies have shown that calcified cells are ingested at a slower rate (Kolb & Strom, 2013; Harvey *et al.*, 2015), an equal rate or at a faster rate than non-calcified cells (Sikes & Wilbur, 1982; Harris, 1994; Hansen *et al.*, 1996; Harvey *et al.*, 2015). Additionally, despite the production of an intact coccosphere, diploid cells of *E. huxleyi* are still subject to viral infection. Indeed viruses have been shown to play important roles in the termination of blooms of *E. huxleyi* (Wilson *et al.*, 2002).

There is evidence that some species utilise the coccosphere to regulate light entering the cell. Calcium carbonate reflects light and therefore blocks a proportion of light hitting the cell. This may potentially protect cells from photoinhibition or other forms of stress arising from high light. However, mixed results have been observed in experiments designed to test the role of coccoliths in prevention of photoinhibition, *E. huxleyi* cells can increase coccolith production at higher intensities of UV radiation (Guan & Gao,

2010) and are also a dominant component of the phytoplankton communities at high light intensities (Nanninga & Tyrrell, 1996). In contrast, *E. huxleyi* has been shown to be resistant to photoinhibition even without a coccosphere (Balch *et al.*, 1992; Houdan *et al.*, 2005). *S. apsteinii*, the previously described dimorphic coccolithophore, exhibits a change in the ratio of coccolith type in response to different light intensities. Under high light intensities there are fewer large, barrel shaped lopadoliths produced as opposed to the small, ovoid shaped, muroliths. The different coccoliths (Figure 1.1) may play a different role in the light protection of the cell, however very little work has been done on this species and a lot remains unclear as to the role of the two distinct coccolith types (Drescher *et al.*, 2012). In contrast, light channelling for photosynthesis has been suggested for deep water species *Florisphaera profunda* and *Gladiolithus flabellatus* where the coccoliths are arranged in a flower-like cup-shaped structure, reviewed Monteiro *et al.* (2016). Unfortunately these species are not able to be kept in culture which limits the application of experimental approaches to understand the roles of calcification.

Until recently it was considered the ballast effect of the calcite may play a role in regulation of sinking: coccoliths affect the velocity at which coccolithophores sink (Buitenhuis *et al.*, 2001; Bach *et al.*, 2012; Hoffmann *et al.*, 2015), sinking was thought to enable the coccolithophores to regulate their environmental factors such as nutrient availability (Gerecht *et al.*, 2015), predator avoidance or light regulation. However, modelling data has demonstrated it there is little statistical support for the ballast effect hypothesis (Monteiro *et al.*, 2016).

A highly debated proposed function for calcification is its potential role in providing CO_2 for photosynthesis. The carbon concentrating mechanism (CCM) is a crucial process in coccolithophores and the organic carbon pump. CCMs are required in phytoplankton as CO_2 diffusion rates are not high enough to account for the photosynthetic rates (Falkowski & Raven, 2013). Coccolithophores have biophysical CCMs, which act to specifically increase the concentration of CO_2 at the point of C-fixation by influencing the transport of DIC. They involve carbonic anhydrases (CA), DIC transport mechanisms and pH regulation (Falkowski & Raven, 2013), which all combine to enhance the delivery of CO_2 to Rubisco (Reinfelder, 2011). Calcification produces H^+, if HCO_3^- is used as the external substrate and these H^+ could be used to drive the dehydration of HCO_3^- to CO_2, presumably catalysed by carbonic anhydrase (Paasche, 2001). Calcification could therefore potentially act as a CCM. However, a number of studies have shown that it is possible to inhibit calcification through reducing external calcium whilst photosynthesis and growth remains unaffected (Paasche, 1964; Herfort *et al.*, 2002; Trimborn *et al.*,

2007; Leonardos *et al.*, 2009). Moreover, Bach *et al.* showed, by manipulating the external carbonate chemistry, rather than providing a source of DIC for photosynthesis, calcification appeared to be in direct competition with photosynthesis for available DIC. These results indicate calcification does not function as a CCM (Bach *et al.*, 2013) and are supported by other investigations (Buitenhuis *et al.*, 1999; Riebesell *et al.*, 2000; Zondervan *et al.*, 2001).

There is very little information available on the cellular and molecular mechanisms of the CCM in coccolithophores, Bach *et al*. show multiple upregulated genes in *E. huxleyi* at low DIC which have the characteristics of a CCM that is responsive to CO_2 and HCO_3^- (Bach *et al.*, 2013). Although it is known that *E. huxleyi* has an inducible CCM under low DIC, the molecular mechanisms of the CCM have not been explored in other coccolithophores.

Many studies have explored the question, why do coccolithophores calcify? Taking each theory presented here into account it is likely that different species rely more heavily on different adaptations of coccoliths, hence their differences in morphology. This does not mean they did not evolve the mechanism for the same initial purpose, but have adapted to the different benefits calcification can provide. This hypothesis is strongly supported by the recent review by Monteiro *et al.* (2016) which concludes that a protective role is the most likely origin of calcification. Additionally the review also proposed that other roles may be more important in certain ecological niches, for example light focusing coccoliths in deep-waters species. The evidence presented here indicates a need to treat species with a degree of separation and not rely on the *E. huxleyi* model across the coccolithophore phylogenetic tree. To fully appreciate the variety among coccolithophores we need to understand more about the physiology and role of calcification in diverse extant species.

1.5. Differences between Species

Coccolithophores exhibit a high level of morphological diversity (Figure 1.1), which underpins a morphology-driven taxonomy (Jordan & Green, 1994; Winter & Siesser, 2006). How these morphological differences are achieved are unknown and have prompted investigation into differences within the cellular mechanisms of coccolith production in different species. It is important to consider the reported differences between species of coccolithophores, detailed below. It is prudent at this point to reiterate that studies have largely focussed on *E. huxleyi* so most comparisons will be made in reference to this species.

There are some variations in cell ultrastructure between species, particularly in calcification associated organelles. These variations produce small logistical differences in coccolith production. Microscopy studies have shown the number of coccoliths in production inside a cell differs between species. The CV is singular in *E. huxleyi* with only one coccolith being produced at a time, within *C. carterae* and *C. pelagicus* multiple CVs have been observed with coccoliths at varying stages of production (Van der Wal, P. *et al.*, 1983b). However it important to note that in *C. pelagicus* this observation is uncommon. The RB has been widely reported in *E. huxleyi* (Brownlee & Taylor, 2004). Similar structures have been observed in *Gephyrocapsa oceanica, Coccolithus braarudii* (Taylor *et al.*, 2007) and *S. apsteinii* (Drescher *et al.*, 2012) but appear to be absent in *C. carterae* (Marsh, 1994).

It has been suggested that polysaccharides play a key role in the delivery of Ca^{2+} to the CV in the absence of a RB (Marsh, 1994; Marsh, 1996) in addition to their role in regulating the precipitation of calcite (De Jong *et al.*, 1976; Marsh, 1994; Marsh, 1996; Ozaki *et al.*, 2007). *Chrysotila sp.* have three CAPs associated with the CV, an additional two more than other studied species (Marsh, 1994; Ozaki *et al.*, 2004; Ozaki *et al.*, 2007; Kayano & Shiraiwa, 2009). Based on these observations attempts have been made to quantify the cost of producing such a large quantity of polysaccharide. In *C. carterae* CAP production has been estimated to cost up to 50% of the total fixed organic carbon, a high cost of production (Brownlee & Taylor, 2004). However, these estimates are based on the hypothesis that Ca^{2+} transport to the site of calcification is achieved by polysaccharide binding. The direct quantification of polysaccharide per coccolith has resulted in estimates showing CAPs produced by *E. huxleyi* and *C. braarudii* require 7% and 0.2% of fixed organic carbon respectively (Monteiro *et al.*, 2016). Further work is clearly needed to more accurately determine the metabolic cost of CAP production in different species.

Lee *et al.* (2016) extracted CAPs integrated within the crystal structure of the coccoliths and found differences in polysaccharide size and uronic acid content between species and strain. Uronic acid is of interest as the negatively charged acidic groups may bind to Ca^{2+} and modulate calcite precipitation (De Jong *et al.*, 1976; Ozaki *et al.*, 2007; Kayano & Shiraiwa, 2009). The study found that uronic acid content is linked to the extent to which a strain is calcified, i.e lightly calcified *E. huxleyi* cells had a very low uronic acid content and highly calcified cells had a higher uronic acid content. These observations directly correlate with the proposed role of uronic acid residues in the CAPS. Other studies have extracted CAPs, however different studies have used different extraction procedures. Some investigations include the whole cell (Kayano & Shiraiwa, 2009), some

have isolated the coccoliths (Ozaki *et al.*, 2007) and in others the coccoliths have been stripped of all exterior organic material (Lee *et al.*, 2016). There is a lack of clarity in the definition of the CAPs in current literature; differences observed between species highlight the need for further study into their role or, more likely, multiple roles. Following clear definition of function we can accurately extrapolate the energetic expenditure the cells exert into the production of CAPs.

Coccolith composition also varies between species, notably the presence of Si, which has been identified in *S. apsteinii* coccoliths but has not currently been reported in the coccoliths of other species (Drescher *et al.*, 2012). Furthermore, Durak *et al.* (2016) have identified diatom-like Si transporters known as SITs and SITLs in a selection of haptophytes, not only in the silicified species *P. neolepis* but also in some important coccolithophore species (Durak *et al.*, 2016). This is very surprising as it has been largely assumed that coccolithophores do not have a Si requirement, allowing them to colonise diatom Si-depleted waters (Yool & Tyrrell, 2003). Not all of the species analysed were found to have the SITs or SITLs: *E. huxleyi* and *G. oceanica,* bloom forming species, are not among those with identified Si transporters. Those that were found to have SITLs include the important marine calcifiers, *C. braarudii* and *C. leptoporus,* which contribute significantly to calcite flux to the deep ocean in large parts of the Atlantic (Baumann *et al.*, 2004; Daniels *et al.*, 2014). The cellular mechanisms through which Si contributes to the calcification process are yet unknown. Durak *et al.* (2016) hypothesise Si may stabilise an amorphous calcium carbonate phase during the formation of the coccoliths (Gal *et al.*, 2012; Durak *et al.*, 2016), however no evidence of an amorphous calcium carbonate phase has yet been identified in coccolithophores. A Si requirement in some, but not all species, may explain why *E. huxleyi* and *G. oceanica* are able to form large blooms in diatom Si-depleted water whereas *C. braarudii* and *C. leptoporus* blooms do not achieve the same cell density. More research is needed to fully understand this requirement.

Some calcification mechanisms appear to differ between species, but the fundamental requirement to calcify at all may furthermore separate species. Some coccolithophores have the ability to grow in a non-calcified state. For example, it is has been widely shown that in low Ca^{2+} experiments, *E. huxleyi* will switch to a non-calcified state and continue to grow (Herfort *et al.*, 2004; Trimborn *et al.*, 2007; Leonardos *et al.*, 2009). *Chrysotila sp.* have shown a similar adaptation (Marsh, 2003). In addition to this response to low Ca^{2+}, *E. huxley*i has been observed both losing and gaining the ability to calcify in low phosphorus conditions (Paasche, 1998). This range of studies suggests there is no obligate requirement for calcification in coccolithophores. However, we do not know if

this is the case for all species, for example *C. braarudii* has not been shown to exhibit these adaptations (Marsh, 2003). Further exploration of this is needed to fully understand the reliance and role of calcification.

There is clear evidence for different mechanisms and requirements for calcification between different species of extant coccolithophore. When looking into their evolutionary history we see evidence of either multiple independent evolutionary events of calcification, or the progressive loss of these characteristics. Further exploration into whether or not coccolithophores calcify by the same mechanisms will shed light on the role and origin of the calcification mechanism.

1.6. Current Study

The variation in coccolith morphology, requirement for calcification and known mechanisms of coccolith production points towards the need to examine mechanisms of calcification in a broad range of coccolithophores. The field has seen an overreliance on *E. huxleyi* as a model organism, the evidence presented here clearly outlines the atypical nature of this species and the need to include others when investigating the coccolithophores as a whole.

This review has outlined some distinct physiological differences between species, including the presence of Si transporters in some ecologically important species; ambiguities in the requirement for calcification; and physiological and biochemical differences in species CAPs. These observations create the foundations for the investigations conducted in this thesis, each of which is outlined below.

1. **The effect of germanium on coccolithophores**

   Germanium (Ge) was used to explore the role Si plays following the identification of Si transporters (SITs and SITLs) in some species of calcifying coccolithophore. Ge is a Si analogue, known to disrupt Si transport and silicification in other organisms. Ge was used on a range of coccolithophore species, including those with and without Si transporters, to elucidate the process in which Si is required.

2. **The differing requirement for calcification in ecologically important coccolithophores**

   E. huxleyi is known to be able to exist in a non-calcified state in laboratory culture, however it is not clear if this ability is widespread throughout the coccolithophores. This chapter investigates the requirement for calcification in *C. braarudii*, an

ecologically important species not known to grow in laboratory culture in a non-calcified state. Multiple independent calcification disruption tools were utilised to disentangle the impact of calcification disruption upon these species, whilst using *E. huxleyi* as an important comparison with which to ground the results.

3. **Molecular characterisation of Si transporters in *Coccolithus braarudii***

   In order to clearly define the requirement for Si in coccolithophores, Chapter 4 explores the regulation of SITLs in *C. braarudii* in response to changing Si availability; compares haploid and diploid SITL expression; and explores whether SITLs are actively expressed in natural populations.

4. **Investigating coccolith associated polysaccharides**

   CAPs have been identified as an important calcification component but additionally have been cited as the source of some clear species differences. This chapter focusses on examining diversity in role and structure of extracellular polysaccharides in a variety of coccolithophore species.

2. The Effect of Germanium on Coccolithophores

2.1. Abstract

Calcification by coccolithophores and silicification by diatoms play an important role in ocean biogeochemical cycles. It was previously thought that coccolithophores do not require silicon (Si) which allowed them to often succeed diatoms following Si depletion by diatom silicification. The recent identification of diatom-like Si transporters (SITLs) in some species of calcifying coccolithophore has thrown this into question. In this study we utilise the Si analogue Ge to investigate the role Si transport plays in species of coccolithophore with SITLs. Ge has been well documented to disrupt Si transport in other organisms, here we demonstrate that the application of Ge has a dramatic effect on the calcification mechanism in coccolithophores with SITLs, implying a role for Si in calcification. At low Ge/Si ratios the Ge causes the production of aberrant coccoliths which cannot integrate into the coccosphere and are subsequently discarded. Using a range of physiological measurements it was shown that Ge has no general toxic effects on cellular health. Additionally we saw a close correlation between the effect of Ge on calcification disruption and the distribution of SITLs as Ge did not negatively impact coccolithophore species without Si transporters. As a result, we hypothesise that Si is directly involved in calcification, indicating that Si contributes to very different forms of biomineralisation in diatoms and coccolithophores.

2.2. Introduction

Coccolithophores are unicellular marine algae characterised by elaborate calcite platelets (coccoliths) which they produce internally and extrude to the cell surface (Marsh, 2003; Brownlee & Taylor, 2004; Taylor *et al.*, 2017). Diatoms, another important group of unicellular marine eukaryotes, produce a two-part silica frustule that encases the cell body. Coccolithophores and diatoms dominate global eukaryotic phytoplankton communities, often forming vast blooms and contributing as much as 10% (Poulton *et al.*, 2007) and 20% (Falkowski *et al.*, 1998) to global carbon fixation, respectively. Biomineralisation in coccolithophores and diatoms is of particular importance for ocean nutrient cycling. Seasonal succession models infer that coccolithophores often succeed diatoms following Si depletion by diatom silicification, leading to limitation to diatom growth and allowing the non-Si requiring coccolithophores to out-compete the diatoms for other available nutrients (Balch *et al.*, 1992; Leblanc *et al.*, 2009; Hopkins *et al.*, 2015). However, the identification of diatom and diatom-like Si transporters (SITs and SITLs) in some species of coccolithophore has raised the question of the role these transporters play in calcifying organisms (Durak *et al.*, 2016).

SITs, first described in diatoms (Hildebrand *et al.*, 1997), are Na-coupled silicic acid uptake transporters. Each SIT is comprised of two identical sets of five transmembrane domains (TMDs) (Figure 2.1a). The transport site of each set of five TMDs is proposed around repeated EGxQ and GRQ motifs, featuring at TMD2-3 and TMD7-8. SITs have been well characterised in diatoms and their expression linked to Si availability, frustule formation and life-cycle stage (Thamatrakoln & Hildebrand, 2007). SITs have also been identified in other organisms including choanoflagellates (Marron *et al.*, 2013) and haptophytes (Durak *et al.*, 2016).

The initial identification of SITs in haptophytes was in *Prymnesium neolepis*. *P. neolepis* diverged from the coccolithophores approximately 280 MYA (Liu *et al.*, 2010) and differs in biomineralisation mechanism by producing a cell covering of silica scales in place of calcite coccoliths (Yoshida *et al.*, 2006; Edvardsen *et al.*, 2011). Analogous to coccoliths, the silica scales are produced internally and extruded to the cell surface (Yoshida *et al.*, 2006; Taylor *et al.*, 2007). Investigation into the *P. neolepis* transcriptome (Keeling *et al.*, 2014) revealed a protein encoding sequence exhibiting similarity to diatom-SITs. *P. neolepis* SITs also have 10 TMDs and the pair of transport motifs (EGxQ and GRQ) between TMD2-3 and TMD7-8 (Durak *et al.*, 2016). Surprisingly SITs were also identified in the calcifying coccolithophore *Scyphosphaera apsteinii* in the same study (Durak *et al.*, 2016). The discovery of SITs in *P. neolepis* is both interesting and logical; as a

silicified organism, it clearly requires Si transport. However, to find apparent components (i.e. Si transporter genes) of conserved biomineralisation mechanisms between diatoms and haptophytes is unprecedented.

Further analysis of the *S. apsteinii* transcriptome revealed the presence of another similar transporter made up of five TMDs, exhibiting similarity to the repeated five TMDs in diatom SITs. It was termed a diatom-like Si transporter (SITL) and was identified in other coccolithophore species, *Coccolithus braarudii and Calcidiscus leptoporus* (Durak *et al.*, 2016) (Figure 2.1a). In contrast, the bloom forming species *Emiliania huxleyi* and *Gephyrocapsa oceanica*, and the well-studied *Chrysotila carterae* (formerly *Pleurochrysis carterae*), did not have SITLs present in their transcriptome (Keeling *et al.*, 2014), or genome in the case of *E. huxleyi* (v1) (Nordberg *et al.*, 2013). The currently limited information on SIT/L distribution in coccolithophores is shown in Figure 2.1b.

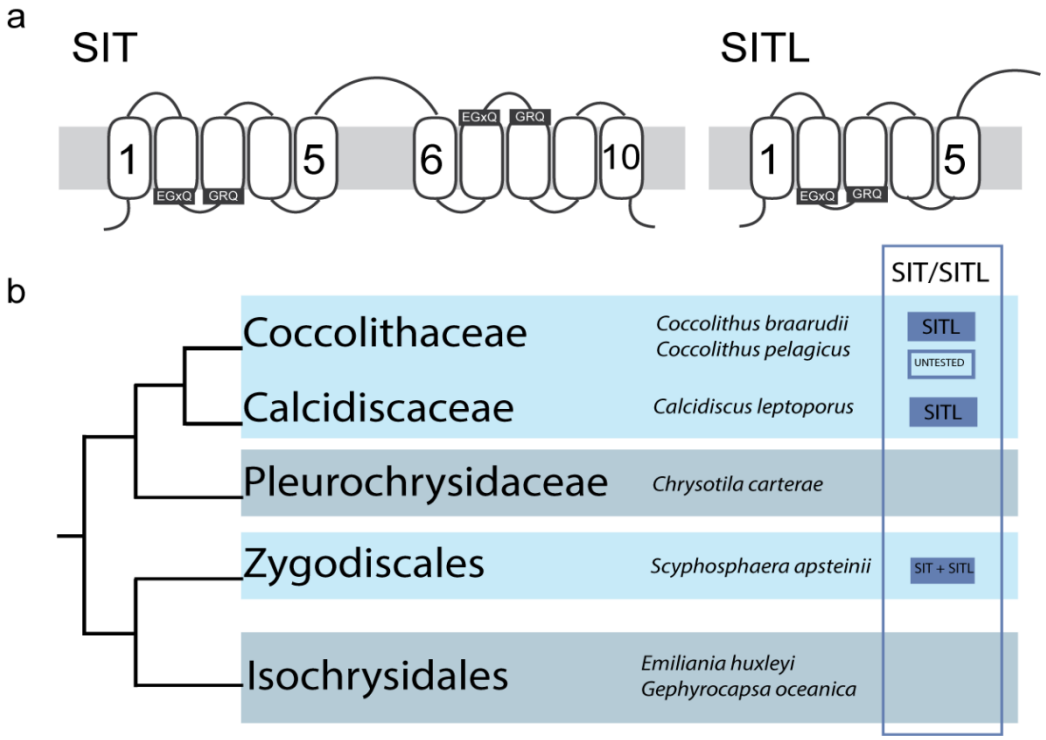

Figure 2.1 The structure and distribution of SITs and SITLs in coccolithophores
a) A schematic image of the domain architecture of the SITs and the SITLs indicating the approximate position of the transmembrane domains and of the conserved motifs. b) A schematic tree adapted from Durak *et al.* (2016), based on multiple gene phylogenies (Liu *et al.*, 2010), transcriptome (Keeling *et al.*, 2014) and genome (Nordberg *et al.*, 2013) analysis to show the distribution of SITs and SITLs in coccolithophores. Interestingly there is a lack of identified Si transporters in two distinct groups, the Pleurochrysidaceae and Isochrysidales.

The presence of SITLs in some species of calcifying haptophytes is a particularly interesting revelation. In fact, recent research has found SITLs in various eukaryotic and

prokaryote lineages (Marron, Alan O. *et al.*, 2016). Marron, Alan O. *et al.* (2016) proposes that SITLs are actually the ancestral form of Si-transporters that potentially acted as efflux transporters that maintained low cellular Si levels in the high seawater Si concentration in the Precambrian period. It has been proposed that the duplication and fusion of the five TMD SITL in a common ancestor of haptophytes and diatoms has led to the wide distribution of SITs with multiple cases of gene loss occurring throughout evolution leading to the absence of SITs in many lineages. It is clear that a thorough understanding of the SITL functionality and role they play in non-silicified organisms is essential to elaborating on this interesting hypothesis.

In addition to understanding the evolution of Si transporters, the production of biosilica is of particular interest for commercial utilisation, including as drug delivery vehicles, biosensors, catalytic systems and tissue engineering scaffolds (Gordon *et al.*, 2009; Patwardhan, 2011). Biosilica structures are incredibly strong, diatom frustules are amongst the strongest known biological material per unit of density (Aitken *et al.*, 2016). Moreover, biosilicification occurs at ambient temperatures and pressures, producing an amazing diversity of nanostructured frameworks which artificial production methods have yet to achieve (Mann & Ozin, 1996; Kröger *et al.*, 1999). A full understanding of the role Si plays in coccolithophores will add to the greater understanding of biogenic Si utilisation and the roles it plays in additional mineralised structures.

Biomineralisation is an incredibly important process as it greatly influences global biogeochemical cycling. The Si cycle is of specific interest due its close coupling to the carbon cycle (Treguer *et al.*, 1995). Si is particularly influential in the surface ocean environment and therefore identification of the role Si plays in coccolithophores is imperative. Until this revelation coccolithophores were not thought to utilise Si, and the distinction between calcification and silicification is thought to allow coccolithophores to be unaffected by very low levels of Si that occur as a result of Si removal by diatom silicification (Sullivan & Volcani, 1981; Treguer *et al.*, 1995; Leblanc *et al.*, 2009; Balch *et al.*, 2014; Hopkins *et al.*, 2015; Marron, Alan O. *et al.*, 2016). This may still be the case for those species without SIT/Ls but until we fully understand the role Si plays in other coccolithophores we cannot appreciate the extent to which Si availability affects their physiology and ecology.

One way to explore the role of Si is to utilise germanium (Ge), a Si analogue which is known to disrupt Si transport in biological systems (Azam & Volcani, 1981). Ge and Si are both found in group 14 in the periodic table and have similar atomic radii (2.11 and 2.10 Å respectively) which results in similar chemical properties (Jolly, 1966; Azam &

Volcani, 1981; Chemistry, 2018). Diatom SITs have been shown to uptake Si from seawater in the form of $Si(OH)_4$ (Hildebrand *et al.*, 1997; Hildebrand *et al.*, 1998) which is also likely to be the case for haptophyte SIT and SITLs, although this is yet to be demonstrated. It is thought that Ge is competitively transported through SITs in the form of $Ge(OH)_4$, demonstrated by its successful utilisation as a radiotracer for $Si(OH)_4$ uptake in diatoms (Thamatrakoln & Hildebrand, 2008) and modelling studies in choanoflagellates (Marron, A. O. *et al.*, 2016). The reason Si transport is not disrupted by naturally occurring Ge is thought to be because Si is far more abundant which negates any effect of naturally occurring Ge. Si forms 27.7% of the lithosphere whereas Ge only forms 1.4×10^{-4}% (Tréguer & Rocha, 2013). A similar scenario also exists in the oceans; the average concentration of Si is 70 µM however, as a result of diatom uptake the concentration is often <10 µM in surface waters (Martin-Jézéquel *et al.*, 2000). The Ge concentration has been shown to be tightly correlated at Ge/Si ratio of 0.76×10^{-6} (Sutton *et al.*, 2010) whereby the average surface water Ge concentration is <7.6 pM.

Although Ge is not shown to be disruptive to Si transport in marine environments (pM), when utilised at higher concentrations (µM) *in vitro* it has a significant effect on the formation of biosilica. Uptake of Ge into siliceous structures has been well documented in sponges (Simpson, 1981; Simpson *et al.*, 1985), chrysophytes (Klaveness & Guillard, 1975; Lee, 1978) diatoms (Safonova *et al.*, 2007; Basharina *et al.*, 2012) and choanoflagellates (Marron, A. O. *et al.*, 2016). In sponge studies Ge has been found to cause spicule deformations (Simpson, 1981; Simpson *et al.*, 1985) and in diatoms causes the production of aberrant frustules (Safonova *et al.*, 2007). Ge is cited as a direct and specific competitive inhibitor of Si transport and is known to prevent Si uptake at a Ge/Si ratios >0.05 in diatoms (Thamatrakoln & Hildebrand, 2008). Other studies into silicified algae Ge-Si interactions include *Synura petersenii* (Chrysophyceae) (Klaveness & Guillard, 1975) and *Pararphysomonas vestita* (Chrysophyceae) (Lee, 1978) whereby Ge was shown to reduce growth but was competitively relieved by increased Si. Studies that included non-siliceous species found that Ge is not broadly toxic to algae, even at relatively high concentrations (3.8 mM) and specifically interacts with Si metabolism (Lewin, 1966; Durak *et al.*, 2016).

In this study we utilise Ge to disrupt Si transport in coccolithophores in order to identify the cellular process in which Si is involved. Through this approach we identify that Ge disrupts calcification in species of coccolithophore with SITLs but has no general toxic effects on coccolithophores, confirmed by Ge addition to species without SITLs. We propose that Si in species with SITLs is utilised in coccolithophore calcification, an

exciting revelation that links the mechanisms of calcification and silicification for the first time.

2.3. Materials and Methods

2.3.1. Algal strains and culture conditions

Coccolithophores were grown in batch cultures and incubated in a controlled temperature (CT) room at 15^{O}C, except the Northern Atlantic *C. pelagicus* (RCC4092) which was incubated at 7^{O}C. Cells were illuminated with 55-65µmol photons m^{-2} s^{-1} on a 16:8 light:dark cycle. Natural seawater (collection and filtration described below) was used for all culture media. *C. braarudii* (PLY182g) and *E. huxleyi* (CCMP1516) were grown in f/2 media (Guillard & Ryther, 1962), *C. leptoporus* (RCC1130) and *C. carterae* (PLY406) were grown in 90% f/2 media (Guillard & Ryther, 1962) with 10% K medium (Keller *et al.*, 1987), and *C. pelagicus* (RCC4092) was grown in K/2 medium (Keller *et al.*, 1987).

Seawater for culture media was collected in 25 L carboys from the L4 survey station, 10 nautical miles SW of Plymouth in the English Channel. In order to manipulate the Ge/Si ratio a low concentration of dissolved Si (dSi) in the seawater used was required. The seawater was collected in May, after the diatom spring bloom, to ensure naturally low [dSi] (Observatory, 2017).The seawater was kept in the dark at 15^{O}C prior to filtration using a 30kDa hollow fibre filter (Sartorius, UK). To minimise contamination by Si, all procedures were undertaken in plastic equipment. After filtration the seawater was autoclaved before nutrients were added. The [dSi] was determined using a silicate molybdate-ascorbate assay (Kirkwood, 1989) and was found to be 2 µM. Where required, the [dSi] was amended by the addition of $Na_2SiO_3.5H_2O$.

Ge was added as GeO_2 for a range of concentrations (0.5-20 µM) to seawater containing 2, 20 and 100µM of Si. Cultures were subjected to short term (48 h) and long term (5 d) experimental periods under conditions described in 2.3.1, with physiological measurements taken as described below.

2.3.2. Physiological measurements

2.3.2.1. Cell counts

Cells were counted using light microscopy (LM) and a Sedgewick-Rafter counting chamber at regular intervals (specified). Cultures were treated and analysed during mid-exponential phase with starting cell densities of >8, 000 cell ml^{-1} for *C. braarudii, C. leptoporus* and *C. pelagicus,* >340, 000 cell ml^{-1} for *E. huxleyi* and >26, 000 cell ml^{-1} for *C. carterae.* Growth rates (d^{-1}) were calculated for the duration of the incubation experiments (48 h and 5 d, specified) and determined from the initial and final cell densities ($N_{t0,}$ N_{t1} respectively) using the formula below.

Formula 1: Growth Rate

$$\mu = (\ln(N_{t1}) - \ln(N_{t0})) / t)$$

2.3.2.2. Chlorophyll Fluorimetry

Measurements of chlorophyll fluorescence were also taken to assess the performance of the photosynthetic apparatus. In the case of *C. braarudii,* an initial cell density of 12,000 cells mL^{-1} was used to ensure sufficient biomass was available. The maximum quantum yield (F_v/F_m) of photosystem II was determined using a Z985 AquaPen chlorophyll fluorimeter (Qubit Systems, Kingston, Canada).

2.3.2.3. Microscopy

Cells were imaged by LM using differential interference contrast (DIC) optics on a Nikon Eclipse Ti Light Microscope and processed using ImageJ (Abràmoff *et al.*, 2004).

Ge causes the production of aberrant coccoliths in coccolithophores with SITLs. In selected experiments, discarded coccoliths were recorded to demonstrate the extent of the Ge affect between treated cells and controls. Regular and aberrant coccoliths were not distinguishable using LM as the resolution is not high enough.

Scanning electron microscopy (SEM) was used to obtain high-resolution data on the morphological effects of Ge on *C. braarudii*. Samples for SEM were filtered onto a 13 mm 0.4 µm Isopore filter (Millipore EMD) and rinsed with 5 ml of 1 mM HEPES buffered (pH 8.2) MilliQ water to remove any salt. Filters were air dried, mounted onto an aluminium stub and sputter coated with 10 nm Pt/Pd (Cressington, USA). Samples were examined using a Phillips XL30S FEG SEM (FEI-Phillips, USA) and imaged in high-resolution secondary electron mode with beam acceleration of 5 kV.

2.3.2.4. Data Analysis

Statistical analysis was carried out with SigmaPlot v12.0 software (Systat Software Inc, London, UK). All datasets were subjected to normal distribution (Shapiro Wilk) and equal variance tests (Levene's mean) prior to analysis of variance. When distribution and variance tests were passed a one-way ANOVA with *post hoc* (specified) was conducted and when failed the non-parametric equivalent, Kruskal-Wallis One Way Analysis of Variance on Ranks followed by an All Pairwise Multiple Comparison Procedures (Tukey Test) was conducted. All statistical tests conducted are specified in figure legends.

2.4. Results

2.4.1. Effect of Ge exposure on *Coccolithus braarudii*

C. braarudii cells were treated with 0, 0.25, 0.5 or 1.0 Ge/Si (2 µM Si) for 48 h. The addition of Ge caused an increase in discarded coccoliths across all treatments (Figure 2.2a). This effect was statistically significant between the control and 1.0 Ge/Si treatment over 48 h (p=<0.05). LM data (Figure 2.2b) show some coccolith malformations were present, however regular and aberrant coccoliths were not discriminated between at this stage as the resolution in LM is not high enough to definitively distinguish between the two. It is also clear that from the LM images that Ge treated cells have partial coccospheres after 48 h, consistent with the high numbers of discarded coccoliths.

Photosynthetic efficiency of photosystem II (F_v/F_m) and growth were measured to assess the overall cellular health following 48 h of Ge treatment. F_v/F_m measures the auto fluorescence of photosystem II, part of the photosynthetic machinery in the chlorophyll, and therefore is a proxy for photosynthetic potential and general cell health. There was no difference in F_v/F_m between Ge treatments and control (Figure 2.2c). Increasing Ge/Si ratios resulted in eventual inhibition of growth with statistically significant inhibition occurring at 1.0 Ge/Si compared with the control (p=<0.05). The data in Figure 2.2 show clearly that inhibition of growth at higher Ge/Si ratios was not related to decreased photosynthetic efficiency.

SEM was used to obtain high resolution images of the morphological effects of Ge on *C. braarudii* on cells grown in a 0.2 Ge/Si for 48 h (100 µM Si). SEM micrographs (Figure 2.3) enable a clear visualisation of the aberrant coccoliths produced in the Ge treated cultures, not present in the control. It is also possible to see discarded coccoliths; it is most likely the aberrant coccoliths cannot integrate within the coccosphere and are shed into the media. It was not possible to visualise the partial coccospheres seen in LM (Figure 2.2b) using SEM, as the preparation process involves subjecting the cells to vacuum conditions, this causes the partial structures to collapse, also seen in previous study on *C. leptoporus* (Langer & Bode, 2011).

The data presented in Figure 2.2 and Figure 2.3 suggest that Ge causes the production of aberrant coccoliths after 48 h that cannot integrate into the coccosphere and are subsequently discarded into the media. Ge, at low Ge/Si ratios, appears to act specifically on the calcification mechanism and does not disrupt the general health of the cells.

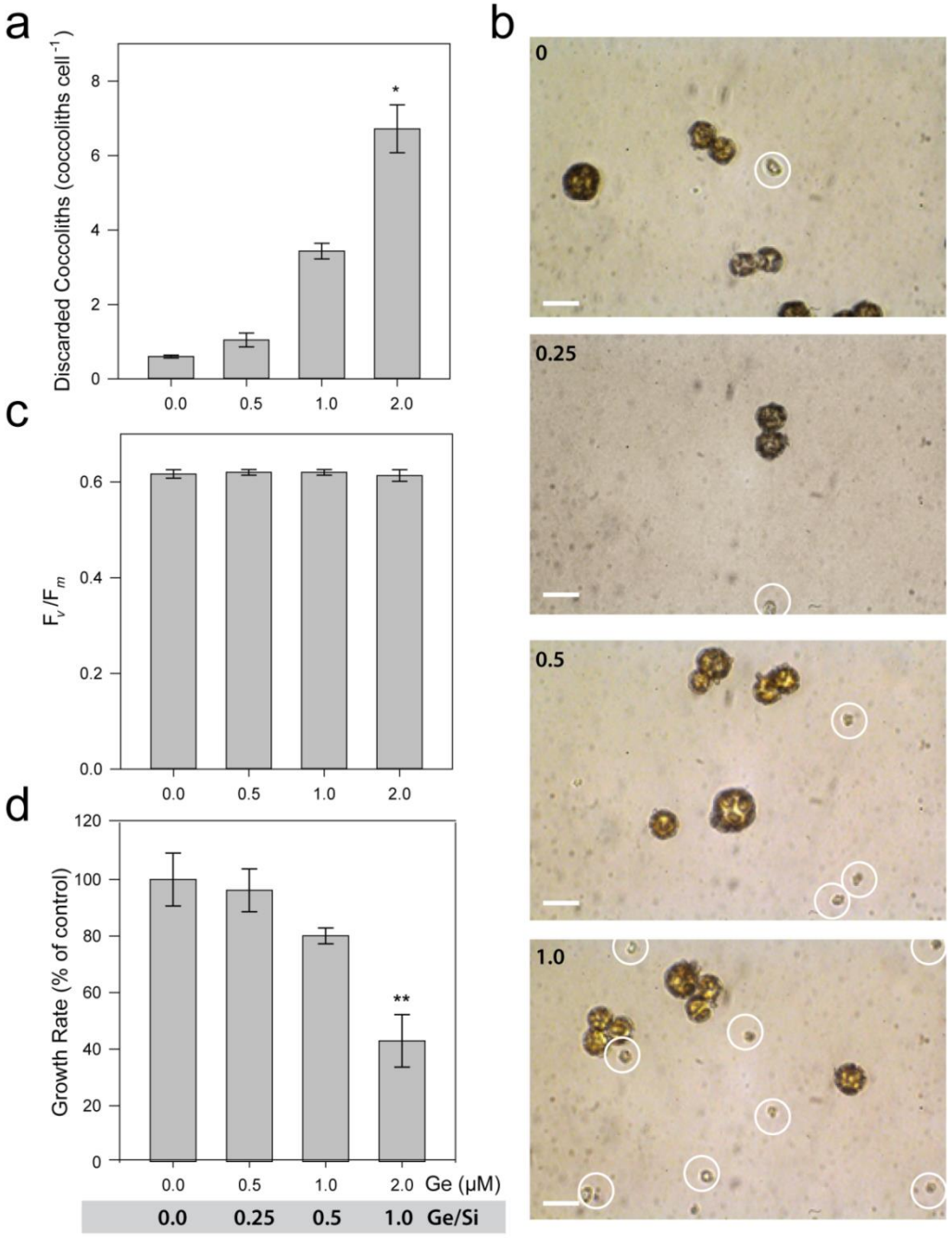

Figure 2.2 Effect of Ge on *C. braarudii*

Cells were treated with 0, 0.25, 0.5 or 1.0 Ge/Si for 48 h (2 µM Si). Discarded coccoliths are presented (a) alongside LM images of each Ge/Si treatment (b). The number of discarded coccoliths (coccoliths cell^{-1}) in the 1.0 Ge/Si were significantly higher than the control, analysed using a Kruskal-Wallis One Way Analysis of Variance on Ranks followed by all pairwise multiple comparison procedures (Tukey Test), n=3, p=<0.05 (*). This data is supported by a visible increase in discarded coccoliths seen in 0.5 and 1.0 Ge/Si images (circled) (b). The photosynthetic efficiency F_v/F_m (c) and growth rate (d) are also presented to assess general cell health. No change in F_v/F_m was observed at any Ge/Si ratio. The growth rate is presented as a % of control (SGR = 0.35 ± 0.03 d^{-1}). The 1.0 Ge/Si treatment grew significantly less than the control (one-way ANOVA with Holm-Sidak post hoc test, n=3, p=<0.01 (**)). Error bars denote standard errors. Image labels denote Ge/Si ratio and scale bars represent 20 µm.

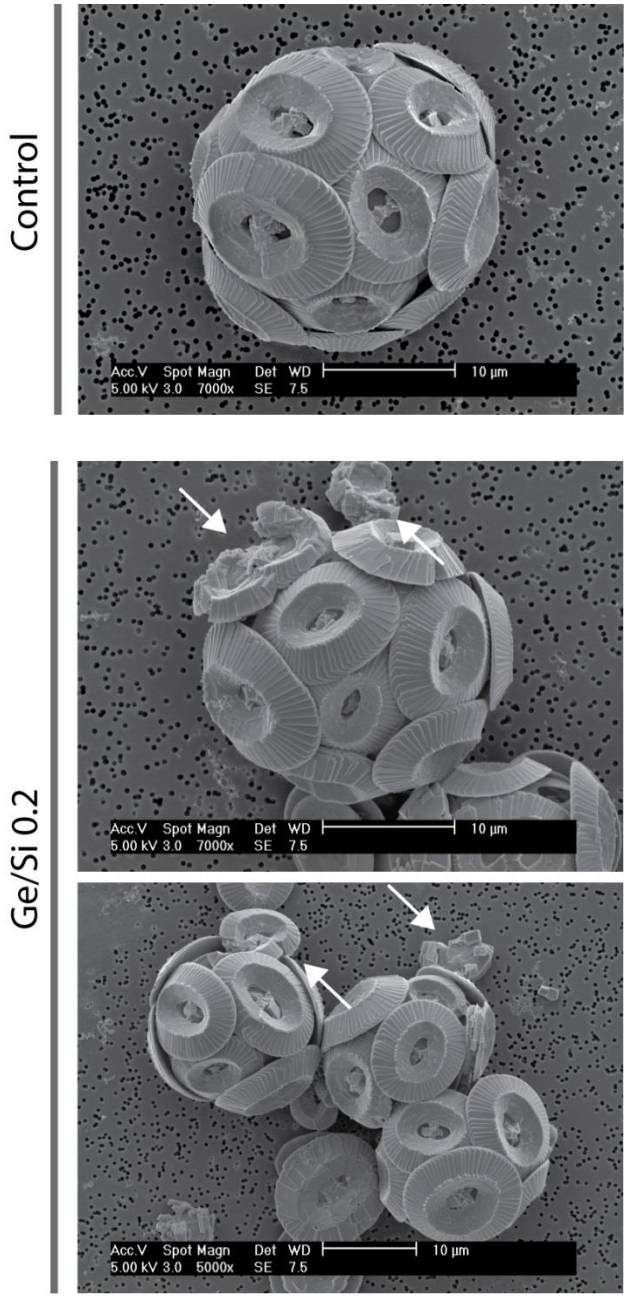

Figure 2.3 Morphological effect of Ge on *C. braarudii*
Cells were grown in 0.2 Ge/Si for 48 h (100 µM Si). SEM images taken of control and Ge treated cells clearly show the presence of aberrant and discarded coccoliths (arrows) in the Ge treatment but not in the control.

In addition to short-term exposure to Ge, the longer-term effect on *C. braarudii* was also investigated. After 5 d there was a significant reduction in growth rate in all Ge-treated cultures when compared to the control (p=<0.01) and a significant increase in discarded coccoliths between the control and 0.5 Ge/Si (2 µM Si) (p=<0.01) (Figure 2.4). Over 5 d, disruption of calcification occurred in conjunction with the reduction in the growth of *C. braarudii*, we can hypothesise that the disruption of calcification is apparent within 48 h (Figure 2.2 and Figure 2.3) and the reduction in growth is more apparent during longer Ge treatment (up to 5 d).

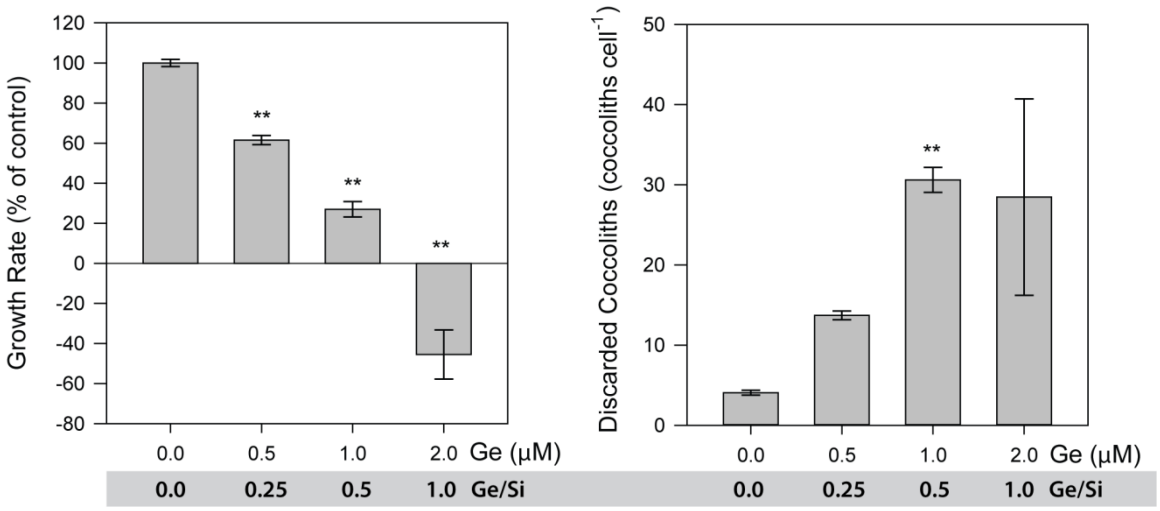

Figure 2.4 Longer-term effects of Ge on *C. braarudii*
Cells were treated with 0, 0.25, 0.5, 1.0 Ge/Si for 5 d in seawater containing 2 µM Si. The growth rates for all cultures treated with Ge is significantly lower than the control (SGR 0.49 ± 0.009 d^{-1}), analysed using a one-way ANOVA with Holm-Sidak *post hoc* test, n=3, p=<0.01 (**). The number of discarded coccoliths in the 0.5 Ge/Si treatment is significantly higher than the 0 Ge/Si control, analysed using a Kruskal-Wallis One Way Analysis of Variance on Ranks followed by an all pairwise multiple comparison procedures (Tukey Test), n=3, p=<0.01 (**). Error bars denote standard errors.

2.4.2. The ratio of Ge/Si

In order to determine further whether Ge was interacting competitively with Si, we examined whether the effect of Ge was influenced by the availability of Si at different Ge/Si ratios. *C. braarudii* cells were treated with various Ge/Si ratios ranging between 0 and 10 (full details in Figure 2.5) (0, 2, 5 or 20 µM Ge in seawater containing 2, 20 and 100 µM Si) for 48 h. The data presented demonstrates that the ratio of Ge/Si, and not simply the concentration of Ge, is crucial to the effect of Ge on *C. braarudii*, i.e. at 2 µM Si 2 µM Ge (1.0 Ge/Si) causes many discarded coccoliths to be produced (Figure 2.5a), however when the Si is increased to 20 and 100 µM the effect is dramatically reduced (Figure 2.5b, c). As Ge/Si ratios of >1.0 exhibit a reduction in discarded coccoliths compared to those of ≤1.0 in longer term experiments, it is possible that Ge at high ratios completely inhibits calcification whereas lower ratios disrupts the process and causes the production of aberrant coccoliths. It is also possible that the inoculum of untreated cells, the starting cells, bias the data in this treatment as no growth occurs. This would bias the discarded coccolith data if the cells are not growing or calcifying. Both scenarios are possible, further experimentation into the effect of higher ratios is required.

Consistent with previous observations, very little variation in F_v/F_m was observed in Ge treatments, except the highest concentration of 20 µM Ge in the 2 and 20 µM Si treatments (10.0 and 1.0 Ge/Si respectively) (Figure 2.5) which were significantly lower than control (p=<0.01). The effect was reduced in 100 µM Si treatment, where no reduction in F_v/F_m was observed, implying the higher concentration of Si reduced the effect of Ge on the cells.

We saw in previous experiments that high Ge/Si ratios caused a reduction in growth after 48 h and in all Ge treated cultures after 5 d. In *C. braarudii* high Ge/Si ratios (≥1) inhibit growth after 48 h (p=<0.01) (Figure 2.5). The effect on growth at higher ratios may be linked to the disruption of calcification.

The results suggest that Ge effects calcification in *C. braarudii*, however the ratio of Ge/Si is crucial for the disruption of growth and F_v/F_m and the disruption or inhibition of the calcification mechanism, indicating that the inhibitory and/or toxic effects of Ge are mitigated in the presence of Si.

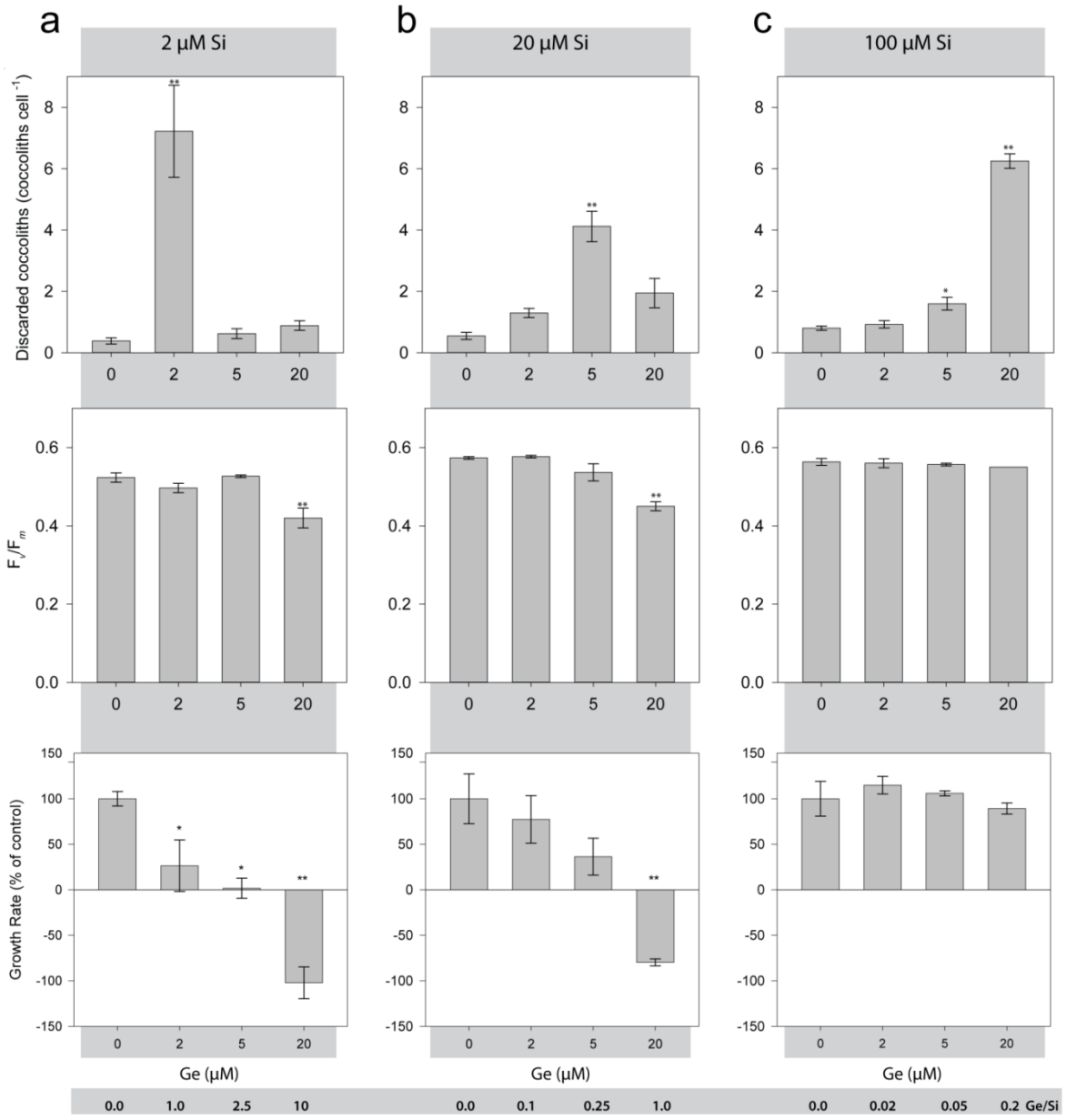

Figure 2.5 The effect of changing Ge/Si ratio on *C. braarudii*

Cells were treated with a range of Ge/Si ratios (specified) by utilising 0, 2, 5 or 20 µM Ge in seawater containing 2 (a), 20 (b) and 100 µM (c) Si for 48 h. The treatments that differ significantly from the 0 Ge/Si control were analysed by a one-way ANOVA with Holm-Sidak *post hoc* test, n=3, p=<0.05 (*) and p=<0.01 (**). Growth rate is presented as percentage of control, alongside F_v/F_m and discarded coccoliths (coccoliths cell^{-1}). The effect of Ge is dependent on the Ge/Si ratio, i.e. Ge had a much lower impact on coccolithophore physiology at higher Si concentrations. Error bars denote standard errors.

2.4.3. Effect of Ge on *Coccolithus pelagicus* and *Calcidiscus leptoporus*

To gain a broader insight into the effect of Ge on coccolithophores the responses of two coccolithophore species closely related to *C. braarudii*, *Calcidiscus leptoporus* and *C. pelagicus,* to a range of Ge/Si ratios (0, 1, 2.5 and 10) were compared. *C. leptoporus* has been identified as possessing SITLs (Durak *et al.*, 2016) but *C. pelagicus* transcriptome data is not yet available and it is not yet known if they have SITLs, however it is closely related to *C. braarudii* and similarities may be expected between the two species (Sáez *et al.*, 2003).

High Ge/Si ratios were utilised to test Ge sensitivity in *C. pelagicus.* C. pelagicus showed a similar response to Ge to that of *C. braarudii* (Figure 2.6 cf. Figure 2.5a for *C. braarudii* data) exhibiting a significant increase in discarded coccoliths in the 2.5 and 10 Ge/Si treatments (2 µM Si) (p=<0.01) and a significant reduction in growth in the 10 Ge/Si ratio (p=<0.05). *C. pelagicus* may have a lower sensitivity to Ge than *C. braarudii*, as no increase in discarded coccoliths at Ge/Si ratio of 1.0 and a lesser reduction in growth was observed after 48 h. However, these observations may be because it is likely *C. pelagicus* has slower calcification and growth rates due to the colder culture conditions required for this strain (see section 2.3.1).

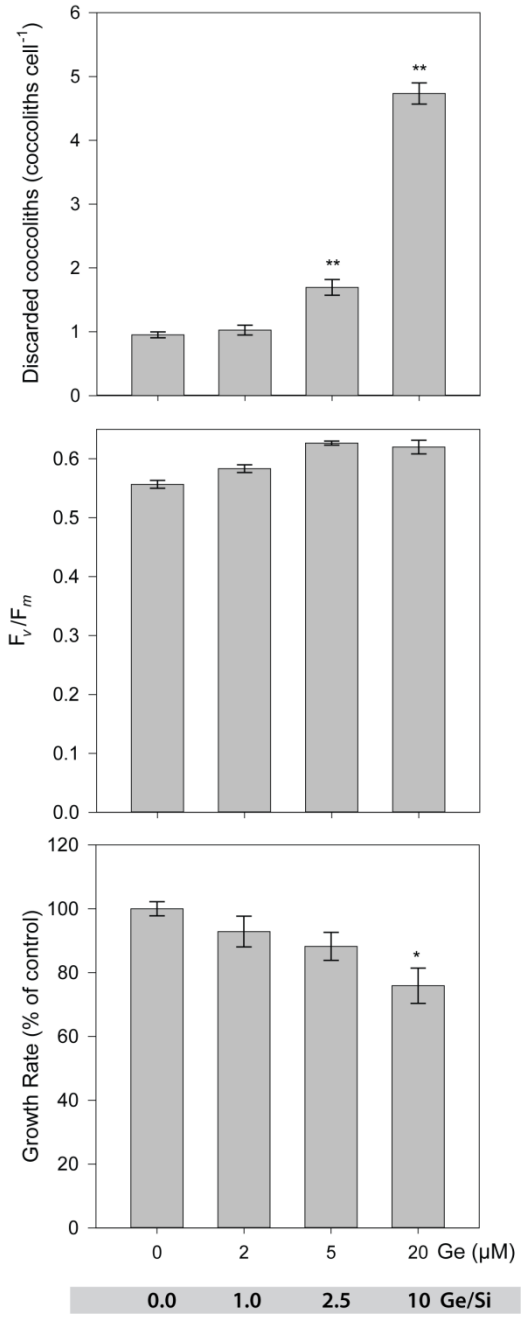

Figure 2.6 The effect of Ge on *C. pelagicus*

Cells were treated with 0, 1.0, 2.5 and 10 Ge/Si for 48 h (2 µM Si). Discarded coccoliths were found to be significantly increased in the 2.5 and 10 Ge/Si treatments when compared to the control, analysed using a one-way ANOVA with Holm-Sidak *post hoc* test, n= 3 p=<0.01 (**). Growth data is presented as percentage of control (SGR 0.31 ± 0.007, n= 3). A significant decrease in growth in the 10 Ge/Si treatment, analysed using a one-way ANOVA with Holm-Sidak *post hoc* test, n= 3 p=<0.05 (*). No change in F_v/F_m was observed, consistent with other species treated with Ge. Error bars denote standard errors.

C. leptoporus was also subjected to high Ge/Si ratio conditions and exhibited an increase in discarded coccoliths in all Ge treatments (Figure 2.7), that was significant in the 10.0 Ge/Si ratio (2 µM Si) (p=<0.01). Under laboratory conditions *C. leptoporus* is a slow growing species and the control cultures grew very slowly during the 48 h experimental period (SGR 0.04 ± 0.07). However, those cultures treated showed a reduction in growth rate compared to the control, similar to that of *C. braarudii* (Figure 2.5a), (p<0.05). It is clear that the impact of Ge on calcification on *C. leptoporus* is consistent to that of other tested species. Subsequent analysis also indicated that Ge does affect calcification in *C. leptoporus* (Durak *et al.*, 2016).

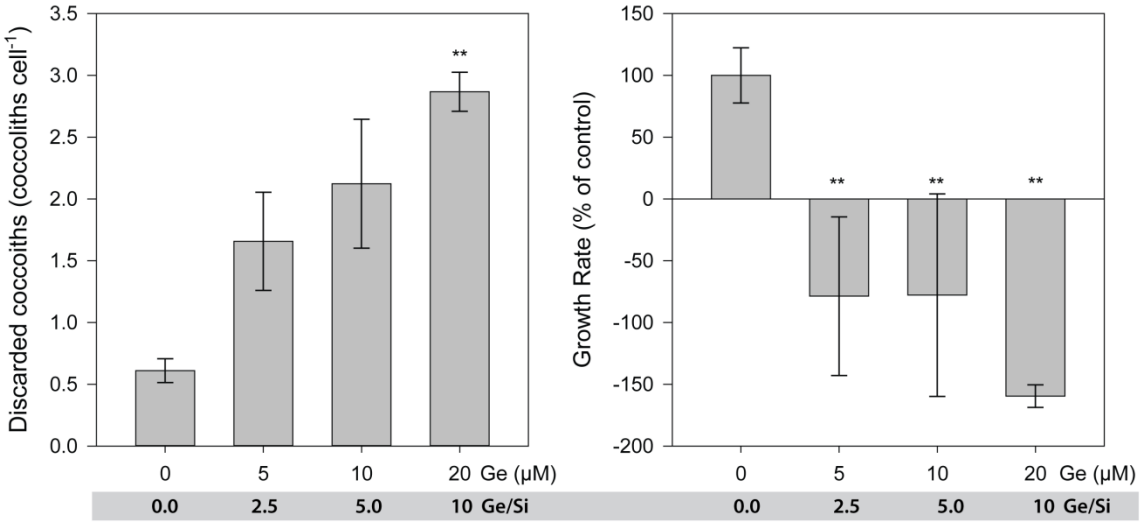

Figure 2.7 The effect of Ge on *C. leptoporus*
Cells were treated with 0, 1.0, 2.5 and 10 Ge/Si for 48 h (2 µM Si). Numbers of discarded coccoliths were significantly increased in 10 Ge/Si treatment when compared to the control analysed using one-way ANOVA with Holm-Sidak *post hoc* test, n = 3, p=<0.01 (**). Growth data is presented as percentage of control (SGR 0.04 ± 0.07, n= 3). A decrease in growth was observed in all Ge treatments, analysed using a one-way ANOVA with Holm-Sidak *post hoc* test, n= 3 p<0.01 (**). Error bars denote standard errors.

2.4.4. Effect of Ge on *Emiliania huxleyi* and *Chrysotila carterae*

The impact of Ge on species confirmed to lack SITLs (Durak *et al.*, 2016) was examined to ensure the effects we were observing were specific to the Si transport mechanism. We used Ge/Si on *E. huxleyi* (Figure 2.8) and *C. carterae* (Figure 2.9), at 0, 1.0 2.2 and 10 Ge/Si ratios (2 µM Si), and found no effects on growth or F_v/F_m in either species. This is in clear contrast to the effects of similar Ge/Si ratios on *C. braarudii*. Discarded coccoliths were not scored in these preliminary experiments as the coccoliths present in both these species are very small (approximately 2-3 µm in length) (Young *et al.*, 2003) and cannot

clearly be identified by LM. However, Inspection of the cells by LM confirmed that the cells were calcified, corroborated by published data (Durak *et al.*, 2016). These results suggest that Si plays an important role in calcification in coccolithophores that possess SITLs, but this requirement for Si is not universal amongst coccolithophores. Further experimentation found no malformations were observed in Ge treated *E. huxleyi* (Durak *et al.*, 2016).

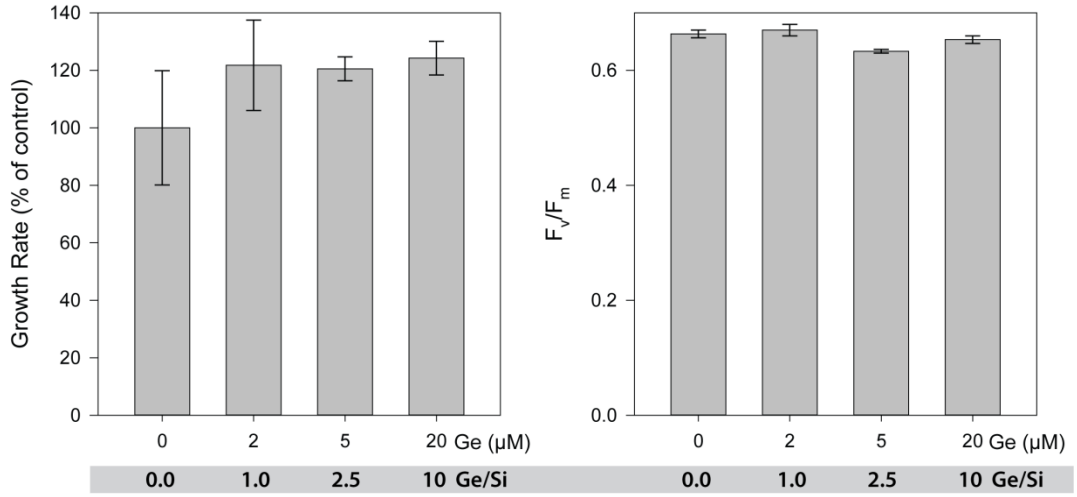

Figure 2.8 The effect of Ge on *E. huxleyi*
Cells were grown in four Ge/Si ratios (0, 1.0, 2.5 and 10) in 2 μM Si seawater for 48 h. The data shows Ge has no effect on growth rate or photosynthetic efficiency in *E. huxleyi.* Error bars denote standard error.

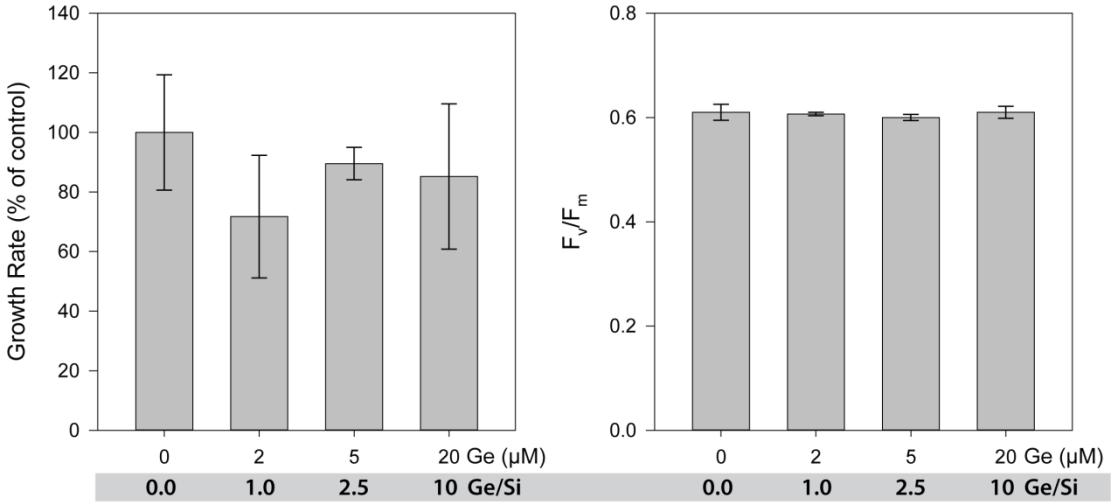

Figure 2.9 The effect of Ge on *C. carterae*
Cells were grown in four Ge/Si ratios (0, 1.0, 2.5 and 10) in 2 μM Si seawater for 48 h. The data shows Ge has no significant effect on growth rate or photosynthetic efficiency in *C. carterae.* Error bars denote standard error.

The currently known distribution of SITS and SITLs show a close correlation with the effectiveness of Ge disruption on coccolithophore calcification, summarised in Figure 2.10. SIT/Ls were identified using transcriptome (Keeling *et al.*, 2014) and genome (Nordberg *et al.*, 2013) sequence data. Species *C. braarudii, C. pelagicus, Calcidiscus leptoporus, Chrysotila carterae* and *E. huxleyi* were investigated here. Additionally the disruption of calcification in the coccolithophore *S. apsteinii* by Ge and lack of effect on *G. oceanica* was demonstrated by further experimentation (Durak *et al.*, 2016). From this study we can conclude that SITLs are involved directly in the calcification mechanism in species where they are present and that addition of Ge specifically affects the calcification mechanism.

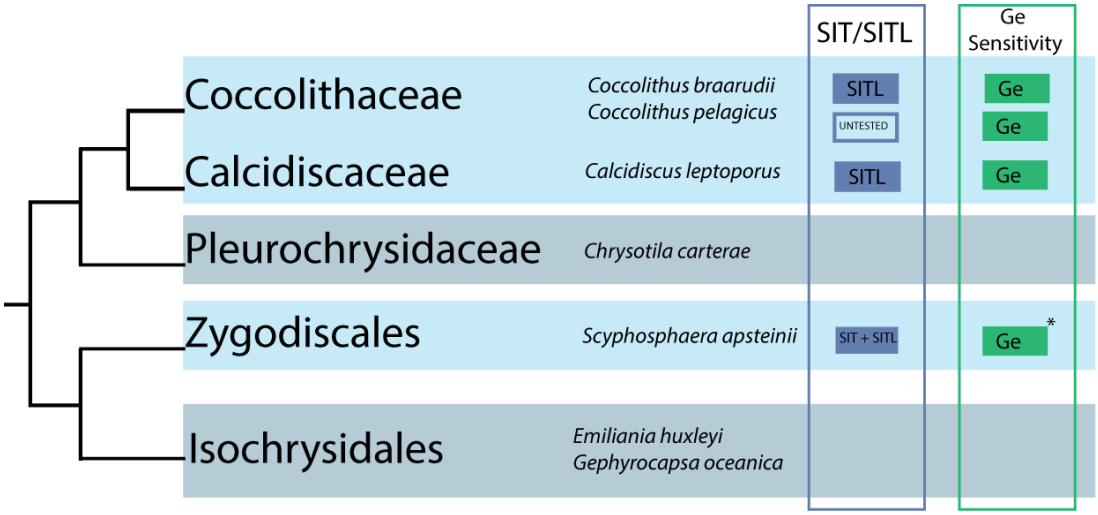

Figure 2.10 The distribution of SIT/Ls in coccolithophores correlated with their sensitivity Ge. A schematic tree adapted from Durak *et al.* (2016), based on multiple gene phylogenies(Liu *et al.*, 2010), transcriptome(Keeling *et al.*, 2014) and genome analysis(Nordberg *et al.*, 2013). Ge sensitivity in *S. apsteinii* is referenced from published work (Durak *et al.*, 2016).

2.5. Discussion

In this study it was shown that the addition of Ge disrupts calcification in species of coccolithophore that possess SITLs (Durak *et al.*, 2016). Ge was not found to have any negative impacts on the cell health and the calcification process in species without SIT/Ls, even at high Ge/Si ratios (>1.0). It was also shown that the Ge effect on calcification is dependent on the availability of Si, indicating a competitive interaction between Ge and the Si transport system in these species. As a result of these observations, we have identified a likely requirement for Si in the calcification process in coccolithophores with SITLs. If coccolithophores do require Si for calcification, this would imply a common requirement for Si in two previously distinct mechanisms of biomineralisation, calcification and silicification. Additionally, we propose *C. braarudii* as an excellent species to study calcification due to its ease of culture, distinct uniform coccosphere and sensitivity to Ge as a potential calcification disruption tool.

In this investigation it is important to consider the potential toxicity of Ge to coccolithophores. There are multiple lines of evidence from the data presented to suggest that Ge is not broadly toxic at the Ge/Si ratios utilised in this study: Firstly, we identified that at low Ge/Si (<1.0) ratios there were no adverse effects on general cell health after 48 h in *C. braarudii*. Secondly, the evidence suggests Ge specifically interacts with the Si transport system and not additional cellular processes. The ratio of Ge/Si is pivotal in the effect Ge has on the cells implying that the two interact competitively for the Si transport system, with Si able to mitigate the response of Ge when increased in the medium. Finally, the use of a broad range Ge/Si ratios (0 - 10) on species without SITLs (*C. carterae* and *E. huxleyi*) demonstrated no adverse effects on the growth or photosynthetic efficiency of these species.

However, it is important to note that there have been recorded cases where Ge has been shown to have toxic effects, for example a study on Chinese Hamster Ovary (CHO) cells observed cytotoxic effects at a Ge concentration of 5 mM but did not report on the availability of Si (Chiu *et al.*, 2002). The concentration of Ge utilised in the CHO cell study is significantly higher than that utilised here. In the data presented here there is evidence of potential toxicity in the higher Ge/Si ratios (≥1.0) which caused a reduction in F_v/F_m and growth after 48 h in *C. braarudii*. In other species with SITLs, reduction in growth was observed at 10.0 Ge/Si in *C. pelagicus* and >1.0 Ge/Si in *Calcidiscus leptoporus* after 48 h. There were no observed negative effects of high Ge/Si ratios (> 1.0) on species without SITLs (*E. huxleyi* and *C. carterae*) it is possible that the Ge may not have a toxic effect as it may not be able to enter the cell due to the lack of Si-transporters to

facilitate uptake in these species. Although the effects on growth may be due to toxic effects of Ge, they may also be due to the effect on calcification, as evidenced from the short-term effect on calcification (represented in discarded coccoliths) in *C. braarudii* after 48 h but the effect on growth not appearing at lower Ge/Si ratios until 96 h. More work is needed to explore whether or not the effect on growth is from Ge or the calcification disruption. An additional insight into the effect of Ge would be to explore the response of coccolithophores to low Si conditions. These experiments have been conducted in a subsequent study within this thesis (Chapter 3).

The evidence suggests that Ge specifically disrupts calcification in species of coccolithophore with SITLs. The investigation predominantly focussed on *C. braarudii* to disentangle the effect of Ge, whereby we identified that low Ge/Si ratios caused the production of aberrant coccoliths and an increase in discarded coccoliths after 48h. It is likely that the malformations disrupt the overlapping structure of the interlocking placoliths and result in the inability to integrate within the coccosphere, the coccoliths subsequently detach from the cell surface. The cells continue to calcify, producing aberrant coccoliths, at the low Ge/Si (<1.0 Ge/Si) ratios but as Ge is increased (≥1.0 Ge/Si) discarded coccoliths cease to be produced. It appears the calcification mechanisms continues at the lower ratios and is completely stopped at higher ratios. This may be due to saturation of SITL membrane proteins by Ge causing a reduction in coccolith production. The effect may also be as a result of the effect on growth, however it is unclear whether the reduced growth causes the disruption of calcification or the inverse effect, this is explored further in subsequent work (Chapter 3). We suggest that low Ge disrupts calcification and higher ratios cause complete inhibition of the process.

The influence of the Ge/Si ratio in coccolithophores bears certain similarities to effect in certain silicifying organisms. In diatoms (Davis & Hildebrand, 2008); ratios of <0.01 Ge/Si do not have an inhibitory effect on silicification, but ratios >0.05 Ge/Si inhibit Si uptake and also disrupt Si metabolism within the cell (Darley & Volcani, 1969; Azam *et al.*, 1973; Simpson & Volcani, 2012). The phenomenon is also seen in loricate (silicified structures) choanoflagellates (Marron, A. O. *et al.*, 2016), whereby low Ge/Si ratios (0.01-0.03) caused the production of incomplete or absent loriceae. At 0.01 Ge/Si the choanoflagellates continued to grow normally until 6 d had passed, after which growth rates reduced significantly. Higher Ge/Si ratios (≥0.05) were lethal to the choanoflagellate cultures. In this investigation we see a similar effect: Ge does not reduce growth of *C. braarudii* at ratios of <1.0 Ge/Si over 48 h but does in all Ge treated cultures measured over 5 d. This may be due to an intracellular pool of Si mitigating the effects. Higher Ge/Si ratios (≥1.0) significantly reduce growth over 48 h. The disruption of calcification is clear

after 48 h at low Ge/Si ratios (<1.0) and the impact on growth at this ratio occurs after 5 d. We can hypothesise that the impact on calcification may cause the decrease in growth in this species. However, more work is needed to disentangle this effect to see if the two effects co-occur or Ge disruption of calcification is causative of the growth reduction.

The mechanism by which Ge disrupts Si transport is largely thought to involve molecular mimicry in the form of $Ge(OH)_4$ which is transported through the SIT in the place of $Si(OH)_4$. This is analogous to the transport of another metalloid arsenate, which is transported through trans-membrane phosphate transporters (major intrinsic proteins) and disrupts phosphate homeostasis in animals (Bienert *et al.*, 2008). To date the proposed transport of $Si(OH)_4$ and $Ge(OH)_4$ is through SITs and therefore cannot be confidently be applied to SITLs until their functionality is fully elucidated.

In addition to the transport of Ge into the cell, there is the disruption of the biosilicification process itself. This has recently been modelled in silicified choanoflagellates using density function theory by Marron, A. O. *et al.* (2016). The study concluded that Ge acts as a competitive inhibitor of Si uptake and (in the form of $Ge(OH)_4$) is disruptive to internal Si polymerisation by incorporating into the ends of the polymerising Si structure. As the Ge/Si ratio increases more Ge "caps" are incorporated into the SiO_2 structure causing deformities in the silicification process. Although we do not know the role Si is currently playing in coccolithophore calcification, as more is divulged about the role of Si, this model may prove relevant in the explanation of Ge disruption in coccolith production.

The cellular mechanisms through which Si contributes to the calcification process in coccolithophores remain unknown. One comparison which may shed light on the role is found in terrestrial plants: It has been demonstrated that Si plays an important role in formation of cystoliths, small calcium carbonate deposits that are found in the leaves of certain plants (Gal *et al.*, 2010; Gal *et al.*, 2012). Although Si is only a minor component, it is essential for the formation of amorphous calcium carbonate, which comprises the majority of the cystoliths (Gal *et al.*, 2012). Si could potentially modulate the formation of coccoliths by stabilising an amorphous calcium carbonate phase of production, however there is no current evidence of amorphous calcium carbonate in coccolithophore calcification but it has not yet been ruled out. Further elucidation of its precise role will enable important insight into the cellular mechanisms of calcification in coccolithophores, which remain poorly understood.

The data presented here divulge that it would be possible to manipulate the Ge/Si ratio to conduct controlled calcification disruption experiments. Previous studies have relied largely on the removal of Ca^{2+} to disrupt calcification (Riebesell *et al.*, 2000; Marsh,

2003). However, the essential role of Ca^{2+} in a wide range of cellular functions (Clapham, 1995; Riebesell *et al.*, 2000; Sanders *et al.*, 2002) means that such manipulations are not specific to the calcification process. Utilising Ge may prove incredibly useful in dissecting the impact of calcification disruption in this species, as it appears to act specifically on the calcification mechanism and not additional cellular functions.

There is a strong correlation between SIT/Ls and Ge sensitivity. As disruption of calcification was also observed in C. *pelagicus* we are able to propose that this species is likely to be positive for Si transporters. Interestingly, the presence of SITLs has also been identified in a range of other organisms including the calcified foraminifera *Ammonia sp*. and the copepod *Calanus finmarchicus*, which has silicified teeth (Marron, Alan O. *et al.*, 2016). The distribution of SITLs in various eukaryotic lineages provides a list of organisms for the effects of Ge to be explored further.

The lack of SIT/Ls and Ge effects on *E. huxleyi* and *C. carterae* raises interesting implications about the ecology of coccolithophores. *E. huxleyi* is the most globally abundant species of coccolithophore and forms extensive blooms in Si-depleted waters, which has likely contributed to its considerable ecological success (Leblanc *et al.*, 2009; Balch *et al.*, 2014; Hopkins *et al.*, 2015). Another bloom-forming species, *Gephyrocapsa oceanica* was also found not to have SITLs (Durak *et al.*, 2016). These bloom-forming coccolithophores (Noelaerhabdaceae) may have developed an alternative cellular mechanism to replace the role of Si in coccolith formation. The marked decline of surface ocean [SiO_4] in the Cenozoic period to the present suggests that loss of the requirement for Si would be beneficial for a species which diverged later. This divergence would have been 250,000 years ago in the case of *E. huxleyi* (Liu *et al.*, 2010). This raises the interesting possibility that a Si requirement may even be a disadvantage to coccolithophores with SITLs in a Si deplete, diatom dominant Ocean.

The exact role and requirement for Si during calcification remains unclear but we can hypothesise that the amount of Si required is likely to be significantly lower than extensively silicified organisms. However, it is noteworthy that the coccolithophores affected by Ge in this study are crucial marine calcifiers, with *C. braarudii* and *Calcidiscus leptoporus* contributing significantly to calcite flux to the deep ocean in large parts of the Atlantic Ocean (Yool & Tyrrell, 2003; Baumann *et al.*, 2004; Daniels *et al.*, 2014). Therefore, it is possible that if these species encounter significant Si limitation in natural seawaters and whether they can compete effectively for this resource with diatoms and other silicified plankton will impact the fate of these important calcifiers. We can conclude that differing requirements for Si may therefore have had a

profound impact on the physiology of modern coccolithophores and contributed significantly to the evolution and global distribution of this important calcifying lineage. It is clear there is need of more focus in the future on Si and its role in calcification in coccolithophores to fully elucidate the biomineralisation activities in the oceans.

3. The Requirement for Calcification Differs Between Ecologically Important Coccolithophore Species

3.1. Abstract

Coccolithophores are globally distributed unicellular marine algae that are characterised by their covering of calcite coccoliths. Calcification by coccolithophores contributes significantly to global biogeochemical cycles. However, the physiological requirement for calcification remains poorly understood as non-calcifying strains of some commonly used model species, such as *Emiliania huxleyi*, grow normally in laboratory culture. To determine whether the requirement for calcification differs between coccolithophore species, we utilised multiple independent methodologies to disrupt calcification in two important species of coccolithophore, *E. huxleyi* and *Coccolithus braarudii.* We investigated their physiological response and used time-lapse imaging to visualise the processes of calcification and cell division in individual cells. Disruption of calcification resulted in major growth defects in *C. braarudii*, but not in *E. huxleyi*. We find no evidence that calcification supports photosynthesis in *C. braarudii* but show that an inability to maintain an intact coccosphere results in cell cycle arrest. We find that *C. braarudii* is very different from *E. huxleyi* as it exhibits an obligate requirement for calcification. The identification of a growth defect in *C. braarudii* resulting from disruption of the coccosphere may be important in considering their response to future changes in ocean carbonate chemistry.

3.2. Introduction

Coccolithophores (Calcihaptophycidae) are globally abundant, single celled marine phytoplankton characterised by the production of elaborate calcite platelets (coccoliths). These are produced in an intracellular compartment (coccolith vesicle) and secreted to the cell surface where they are arranged extracellularly to form a coccosphere (Marsh, 2003; Brownlee & Taylor, 2004; Taylor *et al.*, 2017). Due to their global prevalence and ability to form vast blooms (Westbroek et al., 1993), coccolithophores are estimated to be responsible for up to 10% of the global carbon fixation (Poulton et al., 2007) and are major producers of oceanic biogenic calcium carbonate. Calcification by coccolithophores contributes to a rain of calcite from surface waters to depth, which can remineralise and contribute to a vertical alkalinity gradient in the water column (Milliman, 1993) or form vast sedimentary deposits on the ocean floor (Thierstein et al., 1977). Additionally, sinking coccoliths ballast particulate organic matter enabling the transfer of organic carbon to depth (Ziveri et al., 2007). Consequently, coccolithophores are crucial contributors to ocean biogeochemical cycles and much research has focussed on how calcification may be impacted by future changes in ocean carbonate chemistry (Riebesell et al., 2000; Rost & Riebesell, 2004; Ridgwell et al., 2009; Meyer & Riebesell, 2015).

Given the biogeochemical importance of calcification, it is surprising that the ecological and physiological reasons underlying coccolith production remain uncertain (Tyrrell & Merico, 2004; Monteiro et al., 2016). Several species exhibit the ability to grow without coccoliths in laboratory culture, most notably *Emiliania huxleyi* and *Chrysotila carterae* (formerly *Pleurochrysis carterae*) (Paasche, 2001; Marsh, 2003). The diploid heterococcolith-bearing life stages of these species are invariably fully calcified on initial isolation, although many strains that have been maintained in laboratory culture for several years are only partially calcified or have lost the ability to calcify entirely (Paasche, 2001; Marsh, 2003). Non-calcifying strains of *E. huxleyi* are genetically diverse, suggesting that this characteristic is not restricted to a single lineage or morphotype (Kegel *et al.*, 2013; Read *et al.*, 2013). These observations suggest that calcification is not essential for the growth of coccolithophores, at least when they are maintained in laboratory culture. In turn, this finding has important implications for our understanding of coccolithophore ecology, especially when we consider the potential impact of future changes in ocean carbonate chemistry on the calcification process (Riebesell et al., 2000).

However, there is currently little experimental evidence examining the requirement for calcification in other coccolithophore species and there is evidence suggesting that commonly used laboratory models *E. huxleyi* and *C. carterae* may not be typical of all coccolithophores. For example, the large, heavily calcified species such as *Calcidiscus leptoporus* and *Coccolithus braarudii*, which contribute significantly to calcification in our global oceans (Daniels et al., 2014), always appear to be fully calcified in exponentially growing diploid cultures. Additionally, there are some indications of mechanistic differences in the process of calcification between coccolithophores. For example, several species including *C. braarudii* exhibit a requirement for silicon (Si) in the calcification process, whereas this requirement is entirely absent from other species, such as *E. huxleyi* (Durak et al., 2016). It is also likely that coccolith production fulfils multiple roles within coccolithophores, which may differ between species (Monteiro et al., 2016). In light of these contrasts, it is essential to question whether these species exhibit an obligate dependence on calcification for cellular fitness that relates to important differences in either the process or the function of calcification between coccolithophore lineages.

The availability of non-calcifying strains of *E. huxleyi* has been used to assess the potential role of calcification in this species. Surprisingly, the absence of calcification, either in non-calcifying strains or by depletion of Ca^{2+} in calcifying strains, has little obvious impact on *E. huxleyi* physiology in laboratory cultures, with no reduction in growth rate or photosynthesis (Herfort et al., 2004; Trimborn et al., 2007; Leonardos et al., 2009). Although calcification in E*. huxleyi* commonly occurs at a similar rate to photosynthesis, current evidence does not support a role for calcification as a carbon concentrating mechanism in this species (Herfort et al., 2002; Trimborn et al., 2007; Leonardos et al., 2009; Bach et al., 2013). There is also no evidence to suggest that calcified *E. huxleyi* cells are better protected from zooplankton grazing (Harris, 1994) or viral infection (Wilson et al., 2002). Several studies have also indicated that the coccosphere does not contribute to the protection from photoinhibition (Nanninga & Tyrrell, 1996; Trimborn et al., 2007), although recent evidence indicates that the non-calcifying strains may be more sensitive to UV radiation and grow less well under natural light (Xu et al., 2016). Given that there are few clear physiological differences between calcifying and non-calcifying *E. huxleyi* strains, evidence in support of the many proposed roles of calcification remains limited.

The absence of non-calcifying strains has precluded similar investigations into the requirement for calcification in most other coccolithophore species. However, it is possible to disrupt calcification in coccolithophores experimentally by using a range of

different techniques. For example, *E. huxleyi* cells grown at 0.1 mM Ca^{2+} in artificial seawater media are non-calcified, whilst cells grown at 1 mM Ca^{2+} produce very poorly calcified coccoliths with extensive malformations (Herfort et al., 2002; Herfort et al., 2004; Trimborn et al., 2007; Leonardos et al., 2009). At 1 mM Ca^{2+} *E. huxleyi* cells grow normally, although cells grown at extremely low Ca^{2+} (<0.1 mM) exhibit minor growth defects (Trimborn et al., 2007; Mackinder et al., 2011). *Chrysotila haptonemofera* (formerly *Pleurochrysis haptonemofera*) exhibited reduced calcification at concentrations <10 mM Ca^{2+} but growth was negatively impacted at concentrations <5 mM Ca^{2+} (Katagiri et al., 2010). As Ca^{2+} is essential for many cellular processes, most notably cell signalling, extreme Ca^{2+} depletion could potentially affect many wider aspects of cell physiology. An alternative mechanism to inhibit calcification is the application of bisphosphonates such as HEDP, which inhibit calcification through their ability to chelate metal ions and prevent the growth of calcium carbonate crystals. HEDP has been used extensively in other calcified organisms (e.g. fresh water algae (Heath et al., 1995) and corals (Yamashiro, 1995)) and also inhibits calcification in the coccolithophores *E. huxleyi* (1 mM) (Sekino & Shiraiwa, 1994) and *C. carterae* (0.5 and 1 mM) (Asahina, 2004). In addition, we have recently identified that the silicon analogue germanium (Ge) may be used to disrupt calcification in the coccolithophore species that exhibit a requirement for silicon in coccolith production (Durak et al., 2016).

In this study, we have examined whether the ecologically important species *C. braarudii* exhibits an obligate dependence on calcification for growth. *C. braarudii* and the closely related species *C. pelagicus* are abundant in subarctic regions of the Atlantic and Pacific oceans and their large coccoliths contribute significantly to the sedimentary deposition of calcite from the photic zone (Ziveri et al., 2004; Daniels et al., 2016; Tsutsui et al., 2016). Although *C. braarudii* strains have been maintained in laboratory culture for many years, non-calcifying diploid strains have not been identified. Previous experiments to manipulate calcification in coccolithophores have primarily utilised a single technique, which limits the ability to identify non-specific impacts of the treatment on other cellular functions. We have therefore employed multiple methodologies to disrupt calcification to ensure that our observations are primarily due to a defect in coccolith production. We show that disruption of calcification using four different methods leads to inhibition of growth in *C. braarudii*. We do not find evidence for a link between calcification and photosynthetic function, but find that cell division is inhibited in cells that are unable to form a complete coccosphere.

3.3. Materials and Methods

3.3.1. Algal strains and culture conditions

C. braarudii (PLY182g) (formerly *Coccolithus pelagicus ssp braarudii*) and *E. huxleyi* (CCMP1516) were grown in filtered seawater (FSW) with added f/2 nutrients (Guillard & Ryther, 1962) and added [dSi] 10 µM (unless specified). Cells were grown in triplicate batch cultures, incubated at 15^{O}C and illuminated with 65-75 µmol photons m^{-2} s^{-1} on a 16:8 light:dark cycle.

3.3.2. Cell growth and discarded coccoliths

Cells were counted using light microscopy and a Sedgewick-Rafter counting chamber. Growth rates (d^{-1}) were determined from the initial and final cell densities (Nt_0, Nt_1) using the formula: $SGR = (\ln(Nt_1) - \ln(Nt_0)) / t$). Discarded coccoliths were also counted by light microscopy. We did not discriminate between regular and aberrant coccoliths for this count. Statistics were completed using SigmaPlot v13.0 software (Systat Software Inc, London, UK).

3.3.3. Disruption of calcification

Low Ca^{2+}: To control the availability of Ca^{2+}, Harrison's broad spectrum artificial seawater (ASW) (Harrison *et al.*, 1980) was used, with the addition H_2SeO (final concentration 5 nM) and omission of $CaCl_2$. The addition of H_2SeO was made as it has been previously shown that *E. huxleyi* requires selenium for growth (Danbara & Shiraiwa, 1999). Prior to treatment, *C. braarudii* and *E. huxleyi* cells were acclimated at 10 mM Ca^{2+} ASW for several generations (>2 weeks) then treated with a range of Ca^{2+} concentrations from 0 to 10mM (specified).

HEDP: Cells were grown in f/2 FSW with the addition of HEDP (50 µM) (Sigma Aldrich, UK). Prior to inoculation of cells, the pH of the f/2 plus HEDP media was adjusted to pH 8.2 using 1M NaOH and the media was sterile filtered (0.22µm) (PALL, USA).

Ge/Si Manipulation: Low Si seawater was collected in early summer (May 2015) from the Western English Channel (station L4). This batch of seawater was used for all Ge addition experiments and [dSi] determined to be 2.0 µM using a silicate molybdate-ascorbate assay (Kirkwood, 1989). *C. braarudii* cultures were grown in a Ge/Si ratio of 0.2 to disrupt calcification. Ge was added in the form of GeO_2 to a final concentration of 2 or 20 µM (specified). [dSi] was amended by the addition of $Na_2SiO_3.5H_2O$ to give a final [dSi] of 10 or 100 µM (specified). For growth experiments, coccolithophore cultures were

acclimated to the appropriate [dSi] for several generations (at >2 weeks) prior to the investigation.

Very low Si: As it is difficult to routinely obtain natural seawater with [dSi] <1 µM, [dSi] was further depleted using growth of the diatom *Thalassiosira weissflogii* (PLY541) as described previously (Timmermans *et al.*, 2007; Durak *et al.*, 2016), termed diatom deplete seawater (DDSW). Diatoms were removed by sterile filtration and f/4 nutrients were added (without Si). [dSi] was below the level of detection (<0.2 µM) in all DDSW media prepared by this method. Coccolithophore cultures were acclimated to DDSW for several generations (at >2 weeks) prior to the investigation with amended [dSi] (addition of $Na_2SiO_3.5H_2O$) to 20 µM. Prior to inoculation, *C. braarudii* cells were washed with <0.2 µM [dSi] DDSW to avoid carry-over of dSi. Cells were grown in semi-continuous batch cultures, control and very low [dSi] (20 and <0.2 µM respectively) DDSW, subculturing every 9 d into fresh media to maintain cells in exponential growth.

3.3.4. Measurements of photosynthesis

Measurements of chlorophyll fluorescence were taken to assess the performance of the photosynthetic apparatus. The maximum quantum yield of photosystem II (F_v/F_m) was determined using a Z985 AquaPen chlorophyll fluorimeter (Qubit Systems, Kingston, Canada). Cells were dark-adapted for 20 min prior to measurements. Cell densities of > 10, 000 cells ml^{-1} were required to produce consistent F_v/F_m measurements. O_2 evolution measurements were performed using a Firesting O_2 meter with an OXVIAL 4 respiration vial with integrated optical oxygen sensor (Pyro Science, Aachen, Germany). Cells were stirred constantly during measurements and kept at 20 ^{O}C using a water-cooled glass jacket. High cell densities are required for robust O_2 evolution measurements in *C. braarudii* (> 35, 000 cells ml^{-1}). Cells for analysis were grown to late exponential phase in ASW at 10 mM Ca^{2+}, washed and incubated in different Ca^{2+} concentrations (0, 1 and 10 mM) for 24 h prior to being placed in the O_2 vial. A dark period of at least 5 mins was used to record respiration rate and then O_2 evolution was monitored with illumination at 200 µmol photons m^{-2} s^{-1} for 5 minutes.

Analysis of carbon fixation was conducted by determining the particulate organic carbon (POC). Cells were incubated in control and low Ca^{2+} conditions (1 and 10 mM) for 48 h. 250ml of culture was filtered onto pre-combusted (>6 h, 450 °C) GFF filters and stored at -20 °C. POC filters were fumed with 37% concentrated HCl for 4 h in a closed desiccator to remove all inorganic carbon (Zondervan *et al.*, 2002). After drying, (15 h,

55°C), % carbon output was measured using an Elemental Analyser (*EA 1110* CHNS, Carlo-Erba Instruments, Milan, Italy).

3.3.5. Time-lapse microscopy

Light microscopy images were acquired using a DMi8 Inverted Microscope with a DFC700 T colour camera (Leica Microsystems, UK). During time-lapse imaging, cells were placed on a cooled stage at 17^{O}C. For time-lapse imaging of cell division, cells were maintained in the dark and illuminated only for image capture (300 ms exposure, frame rate 5 minutes). Approximately 10-20 cells were viewed simultaneously for each time lapse. Where stated, cells were gently decalcified with 0 mM Ca^{2+} ASW at pH 7.0 for 1 hour before re-suspension in FSW f/2. To monitor the response to Ge treatment, cells were grown in a 40 mL culture and 1 mL aliquots were removed every 24 h for time-lapse imaging over a period of 12 h. Cells were maintained on the microscope in constant light to encourage calcification. Approximately 100-120 cells were viewed simultaneously for these time lapses. Images and sequences were processed using Leica Applications Suite X and ImageJ (Abràmoff *et al.*, 2004) software.

3.3.6. Fluorescence microscopy

Nuclei of Ge-treated cells were stained with Hoechst 33342 (Invitrogen), final concentration 1 µg/ml and incubated in the dark at 15^{O}C for 1 h. The cells were then stained with FM 1-43 (*N*-(3-triethylammoniumpropyl)-4-(4-(dibutylamino) styryl) pyridinium dibromide) (Thermo Fisher, UK) immediately prior to imaging with a DMi8 Inverted Microscope (Leica Microsystems, UK) with an ORCA Flash 4.0 camera (Hamamatsu, Japan). Hoescht 33342 was excited at 395 nm with emission at 435-485 nm. FM 1-43 was excited at 470 nm with emission at 500-550 nm. Extracellular polysaccharides were stained using the fluorescent lectin, FITC-concanavalin A (100 µg/ml). Cells were decalcified *in situ* on the microscope to ensure that the occurrence of paired-cells was not induced by the decalcification process. 1 ml of *C. braarudii* cells were decalcified following the addition of 10 µl of 1 M HCl for 10 mins (final concentration 10 mM HCl). The pH was then restored by the addition of an equal volume of 1 M NaOH. Cells were imaged using a Zeiss LSM 510 laser scanning confocal microscope, with excitation at 488 nm and emission at 500-530 nm (FITC) and 650-715 nm (chlorophyll).

3.3.7. Scanning electron microscopy

Samples for SEM were filtered onto a 13 mm 0.4 µm Isopore filter (Millipore EMD) and rinsed with 5 ml of 1 mM HEPES buffered (pH 8.2) MilliQ water to remove any salt. Filters

were air dried, mounted onto an aluminium stub and sputter coated with 10 nm Pt/Pd (Cressington, USA). Samples were examined using a Phillips XL30S FEG SEM (FEI-Phillips, USA) and imaged in high-resolution secondary electron mode with beam acceleration of 5 kV. SEM was used to score malformed, incomplete and normal coccoliths for each cell examined (> 30 cells per sample).

3.3.8. Immunofluorescence microscopy

Samples were prepared for immunofluorescence microscopy as described in (Durak *et al.*, 2017). Briefly, *C. braarudii* cells were decalcified with Ca^{2+}-free ASW pH 8.0 containing 25 mM EGTA. Cells were then fixed for 10 min in an ASW solution containing 2% glutaraldehyde and 1.7% BSA (bovine serum albumin). Samples were washed three times with a solution of ASW with 1.7% BSA and 0.5% glutaraldehyde and then incubated for 10 min in 0.05% Triton X-100 in ASW. Samples were then washed three times with ASW/1.7% BSA and incubated for a further 20 min. Fixed samples were incubated overnight in a 1/50 dilution of the primary anti-α-tubulin antibody, washed 3x with ASW/1% BSA and then incubated in a 1/150 dilution of the secondary Texas Red-conjugated antibody for 2.5 h. Cells were then washed a final three times with ASW/1.7% BSA. Cells were imaged using a LSM 510 confocal laser scanning microscope (Zeiss, Cambridge, UK). Texas Red was excited at 543 nm, with emission at 575–625 nm. Calcite was imaged using reflectance, with excitation at 633 nm and a short pass emission filter at 685 nm. Nuclei were stained with Hoechst as previously described (Section 3.3.6).

3.4. Results

3.4.1. Disruption of calcification in *C. braarudii*

We examined the physiological effects of disrupting calcification in *E. huxleyi* and *C. braarudii* using multiple independent methodologies: low Ca^{2+} seawater, the addition of HEDP or the addition of Ge. Ge was not applied to *E. huxleyi,* as we have previously demonstrated that this species does not require Si for calcification and is consequently unaffected by Ge, even at very high Ge/Si ratios (Durak *et al.*, 2016). Our previously published work, along with several other reports have shown that calcification was substantially disrupted in *E. huxleyi* cultures grown at 1 mM Ca^{2+} or in the presence of 50 µM HEDP (Sekino & Shiraiwa, 1994; Herfort *et al.*, 2002; Trimborn *et al.*, 2007; Leonardos *et al.*, 2009). All three treatments (low Ca^{2+}, HEDP or Ge) also had profound and specific impacts on the calcification process in *C. braarudii*. Scanning electron microscopy (SEM) revealed the presence of 1-2 incomplete coccoliths in *C. braarudii* cells grown at 1 mM Ca^{2+} for 48 h, suggesting that this treatment interfered with the ability to form new coccoliths but did not cause extensive dissolution of existing coccoliths (Figure 3.1a, Appendix II: Table II.1). Treatment with 50 µM HEDP resulted in grossly malformed coccoliths that could be initially observed after 24 h and were abundant after 72 h. Cells exposed to Ge at a Ge/Si ratio of 0.2 generated highly malformed coccoliths within 24 h that were morphologically distinct from the malformed coccoliths formed following HEDP treatment. Polarised light microscopy of decalcified *C. braarudii* cells after 24 h Ge treatment allowed us to confirm that the coccolith malformations occur internally, within the coccolith vesicle (Appendix II: Figure II.1).

We have previously observed that malformed coccoliths in *C. braarudii* often fail to integrate into the coccosphere and accumulate in the seawater media around the cell (Durak *et al.*, 2016). All three treatments applied to *C. braarudii* cells in this study resulted in a significant increase in discarded coccoliths after 48 h and 72 h (Figure 3.1b), indicating that many of the newly produced coccoliths were not incorporated into the coccosphere. Thus, although the cells continue to calcify and produce coccoliths following treatment with low Ca^{2+}, HEDP or Ge, their ability to maintain a complete coccosphere is compromised.

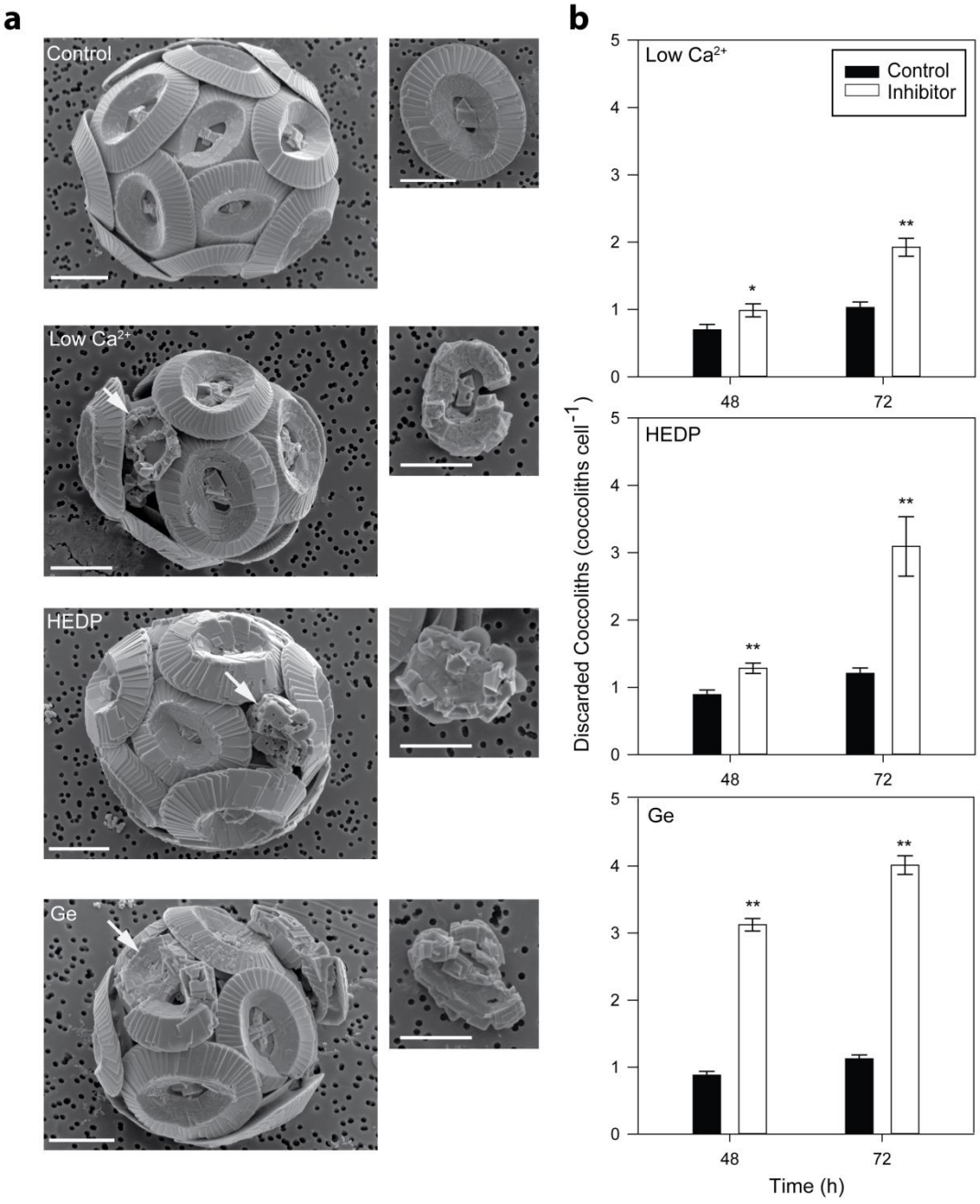

Figure 3.1 Disruption of calcification in *C. braarudii*

a) Representative SEM images of *C. braarudii* cells grown in 1 mM Ca^{2+} (48 h), 5 µM HEDP (24 h) and 0.2 Ge/Si (100 µM Si, 24 h). Incomplete or malformed coccoliths can be observed in response to all three treatments (arrows), whereas these are largely absent from control cells. Incomplete coccoliths are defined as those that exhibit the oval shape of control coccoliths, but calcite precipitation is not complete. Malformed coccoliths are defined as coccoliths with gross defects in crystal morphology and no longer resemble the oval morphology of control coccoliths. Scale bars denote 5 µm. b) Treatments used to disrupt calcification in *C. braarudii* resulted in a significant increase in discarded coccoliths $cell^{-1}$, n=3, p=<0.05 (*) and p=<0.01 (**) when analysed using a one-way ANOVA with Holm-Sidak *post hoc* test. This observation is indicative of incomplete or malformed coccoliths that fail to integrate successfully into the coccosphere. Error bars denote standard error.

3.4.2. Disruption of calcification inhibits growth in *C. braarudii*

Disrupting calcification with 1 mM Ca^{2+} or 50 µM HEDP had dramatically different effects on growth in *E. huxleyi* and *C. braarudii* (Figure 3.2a, b). *E. huxleyi* did not exhibit any significant change in growth at 1 mM Ca^{2+} or 50 µM HEDP confirming previous reports (Sekino & Shiraiwa, 1994; Herfort *et al.*, 2002; Shiraiwa, 2003; Herfort *et al.*, 2004; Trimborn *et al.*, 2007; Leonardos *et al.*, 2009), whereas growth of *C. braarudii* was severely inhibited by both treatments. The growth of *C. braarudii* was also severely inhibited following treatment with Ge (0.2 Ge/Si) for 9 d (Figure 3.2c). Thus, disruption of calcification by multiple methods has little impact on growth in *E. huxleyi*, but results in severe inhibition of growth in *C. braarudii*, suggesting that the requirement for calcification is very different between these species.

The defects in coccolith morphology in response to Ge- and HEDP treatment arise very rapidly, before any defect in growth is observed (Figure 3.2b, c; Appendix II: Table II.1). The coccolith malformations are also distinct from those arising from nutrient limitation or temperature stress (Figure 3.1) (Gerecht *et al.*, 2014; Gerecht *et al.*, 2015).

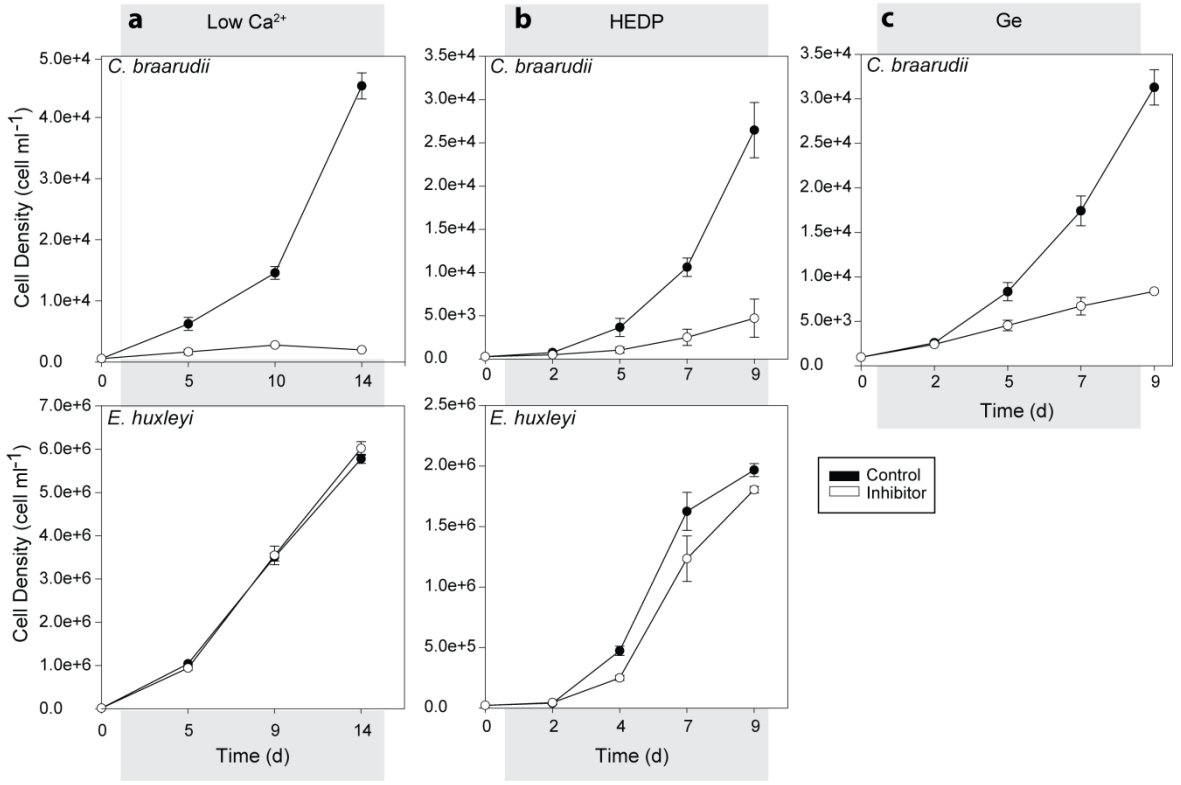

Figure 3.2 Disruption of calcification leads to a reduction in growth in *C. braarudii*

a) Growth of *C. braarudii* and *E. huxleyi* at 1 or 10 mM Ca^{2+} for 14 d. The specific growth rate (SGR) of *E. huxleyi* was not significantly different at 1 mM Ca^{2+} compared to 10 mM Ca^{2+} (0.55 ± 0.006 se d^{-1} and 0.55 ± 0.002 se respectively, p= 0.91, two-tailed t-test), whereas growth of *C. braarudii* was severely inhibited (SGR 0.16 ± 0.01 se d^{-1} compared to the control 0.32 ± 0.01 se, p=<0.05). b) Growth of *C. braarudii* in 50 µM HEDP for 9 d was significantly reduced compared to the control (SGR 0.30 ± 0.05 se d^{-1} and 0.53 ± 0.01 se d^{-1} respectively, p=<0.05), whereas growth of *E. huxleyi* was not significantly different (SGR 50 µM HEDP 0.66 ± 0.03 se d^{-1}, SGR control 0.76 ± 0.08 se, p=0.31). c) Growth of *C. braarudii* in the presence of Ge (0.2 Ge/Si) for 9 d was significantly reduced relative to the control (SGR 0.20 ± 0.04 se d^{-1} compared to 0.38 ± 0.03 se d^{-1} in the control, p<0.05). Error bars denote standard error and in all cases a two-tailed t-test was used (n=3).

3.4.3. Low Si inhibits growth when coccosphere formation is disrupted

We have previously shown that *C. braarudii* exhibits subtle defects in coccolith morphology after 3 d in very low [dSi] (<0.2 µM), although cells monitored for up to 8 d exhibited no decrease in growth rate (Durak *et al.*, 2016). As the requirement for Si is likely to be low in *C. braarudii* (compared to silicified organisms), we grew the cells at very low [dSi] (<0.2 µM) for longer periods (27 d, sub-culturing the cells every 9 d) to ensure that any intracellular pools of Si were depleted. Light microscopy observations at 9 d and 18 d did not reveal clear defects in the coccosphere at <0.2 µM [dSi] (Appendix II: Figure II.2a) compared to the control (20 µM [dSi]) and no effects on growth were observed. However, after transfer to the third sub-culture cells at <0.2 µM [dSi] were observed with incomplete or partial coccospheres after 21 d, whereas cells at 20 µM [dSi] were fully calcified (Appendix II: Figure II.2b). Growth was also greatly reduced at <0.2 µM [dSi] during the third subculture compared with the control (SGR 0.11 ± 0.08 se and 0.29 ± 0.03 se d^{-1} respectively, p=<0.05, n=3, one-tailed t-test) (Figure 3.3a).

To test whether the inhibition of growth due to Si limitation was reversible, we transferred poorly calcified cells grown at <0.2 µM [dSi] for 21 d into media containing <0.2 µM or 20 µM [dSi]. The cells transferred to <0.2 µM [dSi] did not demonstrate any further growth after 21 d and still possessed incomplete or partial coccospheres. However, the cells transferred from <0.2 µM [dSi] to 20 µM [dSi] exhibited fully-formed coccospheres within 7 d of the resupply of Si and growth was partially restored after this time point (Figure 3.3b, Appendix II: Figure II.2c). The delayed growth response to Si addition suggests that the recovery of a Si-dependent process, such as calcification, is responsible for the growth rescue rather than simply the re-supply of Si.

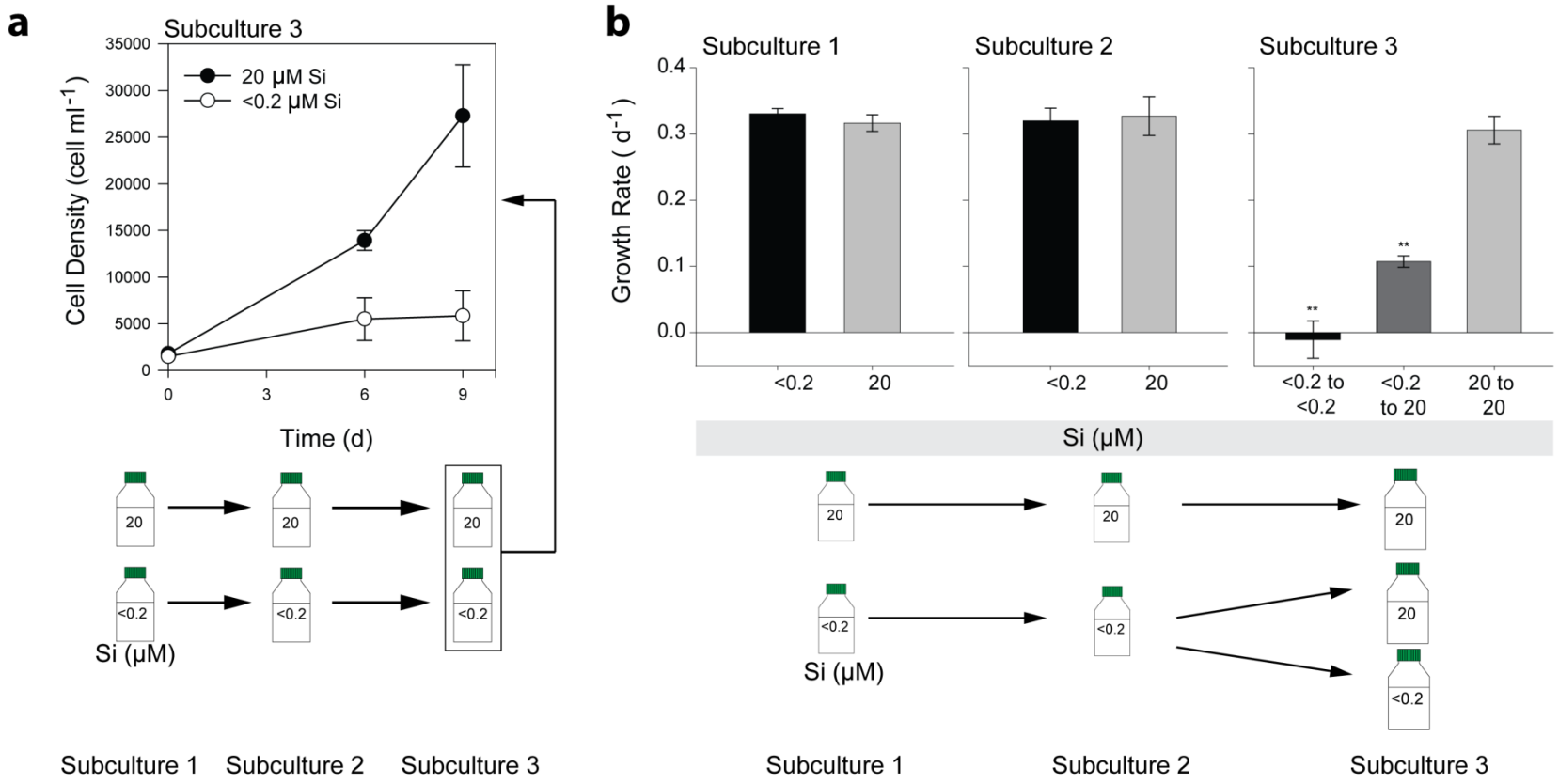

Figure 3.3 Disruption of calcification by limiting Si availability

a) Growth of *C. braarudii* at <0.2 µM [dSi] in semi-continuous batch culture for 27 d. Cells were sub-cultured every 9 d. No effect of Si limitation was observed on growth in the first two sub-cultures (0-9 d, 9-18 d). In the third sub-culture (18-27 d), growth at <0.2 µM [dSi] was greatly reduced compared to cultures maintained at 20 µM [dSi] (n=3). The experiment was repeated two further times with similar results. b) Rescue of Si-limited cultures. Cells grown in <0.2 µM [dSi] for 21 d (sub-cultures 1 and 2) were transferred into media containing <0.2 µM or 20 µM [dSi] (sub-culture 3). Growth in sub-culture 3 was absent at <0.2 µM [dSi]. However, growth was partially restored in cells transferred from <0.2 µM to 20 µM [dSi] (** p=<0.01, SGR calculated 7-14 d after Si resupply, one-way ANOVA with Holm-Sidak *post hoc* test, n=3 biological replicates). Error bars denote standard errors.

3.4.4. Disruption of calcification does not inhibit photosynthesis

We examined whether inhibition of growth following disruption of calcification was due to an effect of calcification on photosynthesis, such as acting as a carbon concentrating mechanism or modulating light entry into the cell. Disruption of calcification with low Ca^{2+} (1 mM), 50 µM HEDP or 20 µM Ge (0.2 Ge/Si ratio) had no impact on the photosynthetic efficiency of photosystem II (quantum yield, F_v/F_m) in *C. braarudii* cells after 72 h treatment (Figure 3.4a, Appendix II: Figure II.3). Similarly, we observed no decrease in the rate of photosynthetic O_2 evolution in cells transferred to 0 or 1 mM Ca^{2+} for 24 h relative to the control (10 mM Ca^{2+}) (p=0.90) (Figure 3.4b). Finally, we investigated carbon fixation by analysing the total particulate organic carbon (POC) content of the cells after 48 h in low Ca^{2+} treatments. There was found to be no significant difference between the POC content of cells in 10 and 1 mM Ca^{2+} treatments (279.5 ± 16.8 and 251.4 ± 14.1 pg $cell^{-1}$ respectively), analysed by a two-tailed t-test (p=>0.05, n=3), which indicates that the cells are fixing carbon in calcification inhibitory conditions. We conclude that direct inhibition of photosynthetic function does not appear to be responsible for the reduction in growth in *C. braarudii* following disruption of calcification. Moreover, the absence of a significant effect on photosynthetic efficiency after 72 h indicated that the treatments used to disrupt calcification do not lead to disruption of general cell function.

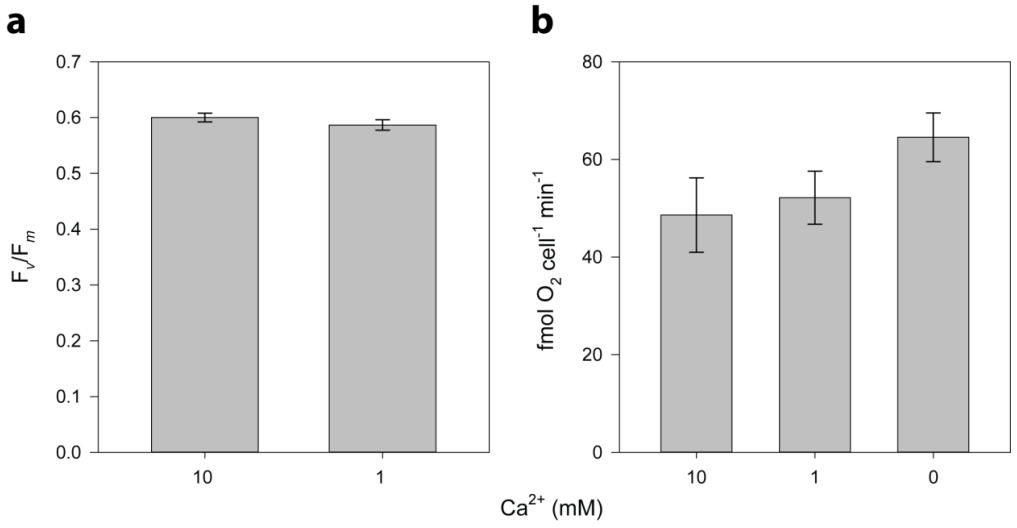

Figure 3.4 Disruption of calcification with low Ca^{2+} does not inhibit photosynthetic activity
a) Photosynthetic efficiency (quantum yield, F_v/F_m) of *C. braarudii* cultures incubated in ASW containing 1 or 10 mM Ca^{2+} for 72 h. No significant difference in F_v/F_m was observed relative to the control (p=>0.05 n=3, two-tailed t-test). b) Photosynthetic O_2 evolution in *C. braarudii* cultures after growth in ASW with 0, 1 or 10 mM Ca^{2+} for 24 h. Disruption of calcification with 0 or 1 mM Ca^{2+} did not result in a statistically significant change in the rate of O_2 evolution (p=>0.05 n=3, one-way ANOVA). Error bars denote standard error. n = 3. The experiment was repeated twice, a representative example is shown.

3.4.5. The role of the coccosphere during cell division

We next investigated whether the inhibition of growth resulted from the inability of *C. braarudii* to form a complete coccosphere. Removal of the coccosphere does not lead to an immediate loss of cell viability in *C. braarudii*: decalcified cells continue to calcify and eventually form a complete new coccosphere (Taylor *et al.*, 2007; Taylor *et al.*, 2017). However, the mechanisms enabling re-organisation of the coccosphere during cell division are not known and it is possible that disrupting calcification interferes with this process. Coccolithophore cells become larger during the day and, once they surpass a size threshold (Müller *et al.*, 2008), divide into two smaller daughter cells during the dark period. Although there are some previous observations of cell division using light microscopy (Parke & Adams, 1960), direct visualisation of the process in live cells has not been reported.

Using time-lapse imaging, we found that dividing *C. braarudii* cells elongate immediately prior to cell division (Figure 3.5). The coccoliths move flexibly to span the fissure between the two daughter cells before closing in a hinge-like motion forming two distinct but attached cells. The coccoliths undergo further rearrangement and once both daughter cells have complete coccospheres the cells separate. The remarkable flexibility in the coccosphere ensures that *C. braarudii* is able to rearrange its closely interlocking coccoliths to cover the dividing cell throughout the entire process. We observed that cells remained attached for a short period after division, but then separated between 4-7 h later (n=4 cells undergoing both division and separation within a 12 h time course; Appendix II: Figure II.4).

Interestingly, secretion of a partially formed or complete coccolith was observed during the process of cell division (Figure 3.5) (38.1% of all division events observed, n=21). This suggests that the intracellular coccolith may interfere with the rearrangement of the cytoskeleton during cell division and is therefore exocytosed, even if it is only partially

formed, which is consistent with previous light microscopy observations noting the absence of an internal coccolith in dividing cells (Parke & Adams, 1960).

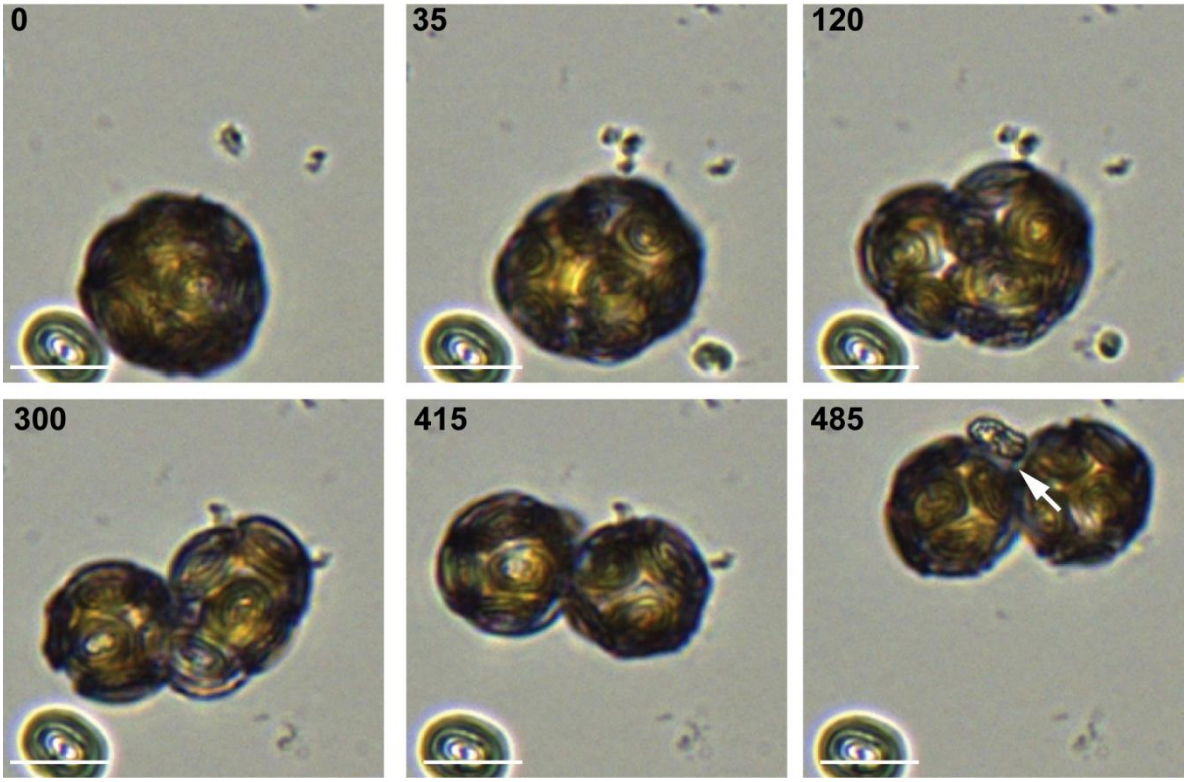

Figure 3.5 Rearrangement of the coccosphere during cell division
Time-lapse light microscopy imaging of *C. braarudii* undergoing cell division recorded over 16 h in the dark (16^{O}C). At the onset of cell division, the cell begins to elongate and the coccoliths move flexibly on the cell surface to maintain a complete coccosphere (35 min). As the cell divides (300 min), the coccosphere rearranges to ensure both daughter cells are fully covered following division (415 min). In the example shown, a partially formed coccolith is secreted during to division (arrowed), implying that cell division occurs regardless of whether coccolith production is completed.

To examine the interaction between calcification and cell division in more detail, we used immunofluorescence microscopy to image the microtubule network during cell division. In dividing cells, a very clear microtubule cable can be observed which spans both cells, persisting even after full separation of the daughter nuclei (Figure 3.6). Intracellular coccoliths are present in nearly all non-dividing cells (85.3 % of cells exhibit distinct coccoliths and a further 11.8 % exhibit smaller accumulations of intracellular calcite, n=68 cells), whereas coccoliths are absent from dividing cells (n=14). These data illustrate the requirement for significant rearrangement of the cytoskeleton during cell division in coccolithophores. The absence of internal coccoliths from dividing cells supports our observation that coccoliths are secreted prior to cell division.

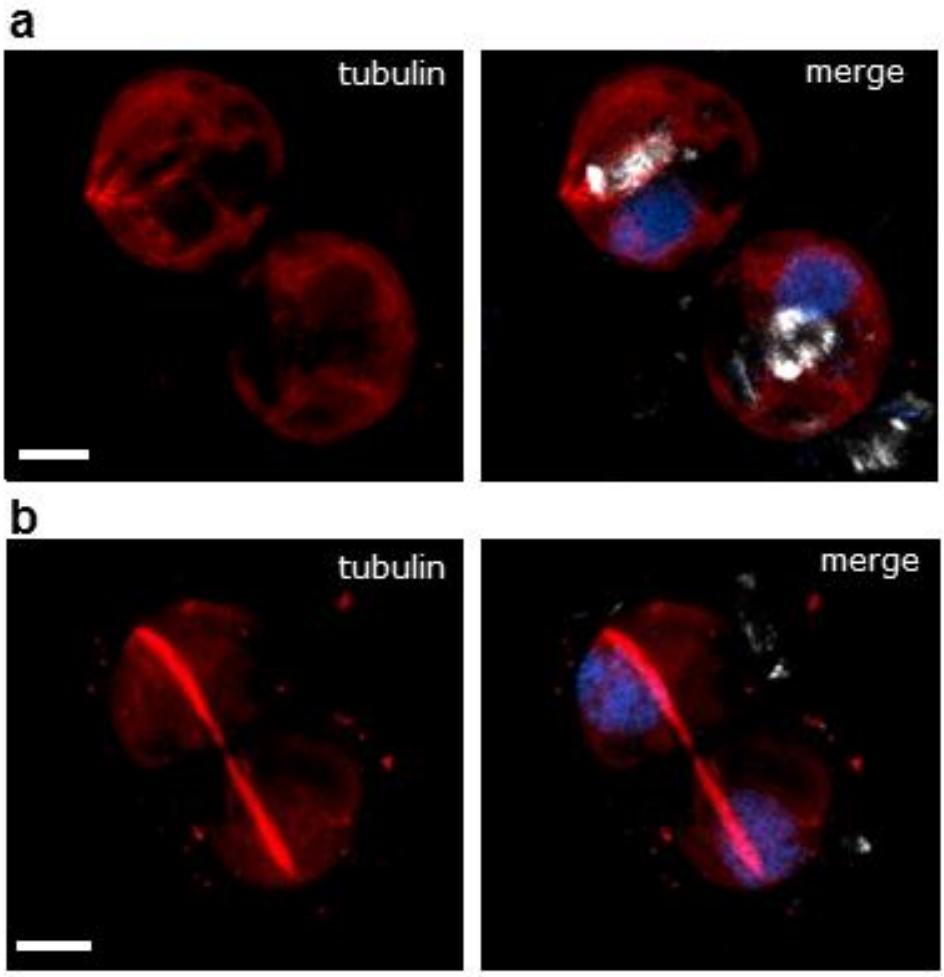

Figure 3.6 Immunofluorescence microscopy of tubulin in dividing cells
The microtubule network was viewed in *C. braarudii* cells using immunofluorescence microscopy. A) 3D projection of a confocal microscopy Z-stack showing the presence of internal coccoliths in non-dividing cells (white). The nuclei are stained with Hoescht (blue) and tubulin is shown in red. Note that there is some background fluorescence caused by fixation with glutaraldehyde. B) The microtubule network in dividing *C. braarudii* cells is characterised by a distinct microtubule cable that spans both daughter cells. Two distinct nuclei can be observed, but intracellular calcite is absent. Image is representative of 14 cells examined. Bar = 5 µm.

3.4.6. Disruption of the coccosphere prevents separation following cell division

To test whether an intact coccosphere was required for entry into the cell cycle, decalcified *C. braarudii* cells were observed by time-lapse microscopy for 12 h. We observed that fully decalcified cells undergo cytokinesis, indicating that the absence of a coccosphere does not prevent entry into and progression through the cell cycle (Appendix II: Figure II.5). However, closer inspection of HEDP- and Ge-treated cells revealed that many cells are present in pairs, comprising two cells closely attached to each other (Figure 3.7). The number of paired cells increased progressively following treatment, with 68 or 60 % of cells present as pairs after treatment with Ge (0.2 Ge/Si)

or 50 µM HEDP for 6 or 7 d respectively (Figure 3.7a, b). The paired-cell phenotype was not apparent in cells grown at 1 mM Ca^{2+} suggesting that the mechanism of growth inhibition may differ in low Ca^{2+} (Figure 3.7c).

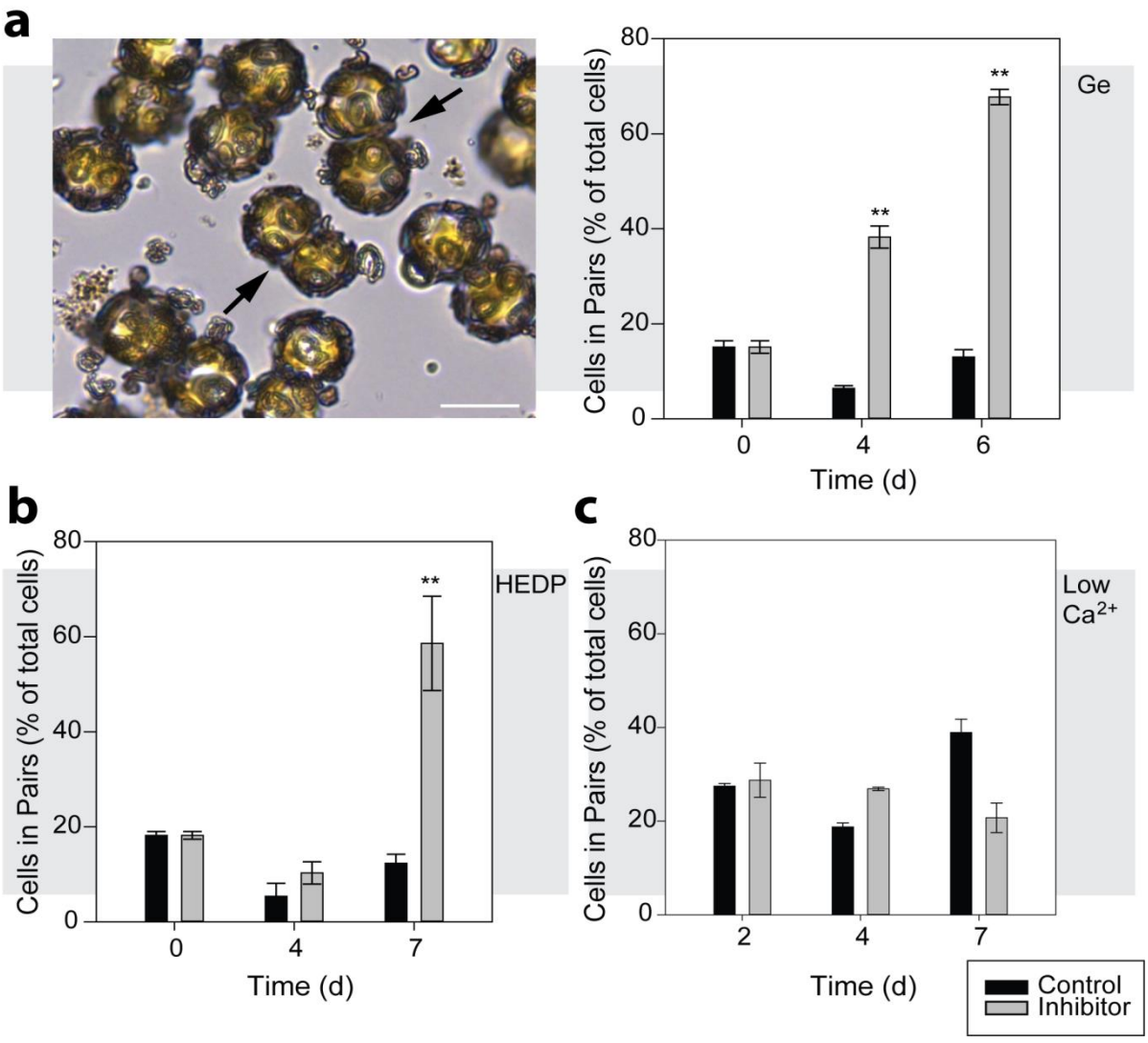

Figure 3.7 Paired cells accumulate in cells with disrupted calcification
a) Paired cells (arrowed) accumulate in Ge-treated *C. braarudii* cells (2 µM Ge, 0.2 Ge/Si). The graph shows the percentage of cells present as pairs (viewed by light microscopy). n>100 cells for each measurement. Scale bar denotes 20 µm. b) Percentage of cells present as pairs in *C. braarudii* cells treated with 50 µM HEDP. c) Percentage of cells present as pairs in *C. braarudii* cells grown in ASW at 1 mM Ca^{2+}, relative to control cells at 10 mM Ca^{2+}. No increase in cells in pairs was observed in the low Ca^{2+} treatment. **denotes $p<0.01$, one-tailed *t*-test. n=3 replicates for all treatments. Error bars denote standard error.

Although flow cytometry is commonly used to measure cell cycle progression in unicellular organisms, we found that the fragile *C. braarudii* cells were not amenable to this approach. Furthermore, flow cytometry cannot adequately distinguish between two cells that remain attached to each other and a cell in G2/M phase. We therefore used time-lapse microscopy to enable the direct observation of cell division, coccolith production and calcification status of individual Ge-treated cells. Importantly, this also allowed us to obtain detailed information on the status of the coccosphere in individual cells prior to division. A culture of *C. braarudii* cells treated with Ge (0.2 Ge/Si) was sampled every 24 h over a period of 5 d to generate a series of individual 12 h time-lapse recordings. These images revealed that the initial secretion of malformed coccoliths occurs within 6 h of Ge treatment, suggesting that Ge has a rapid impact on coccolithogenesis (Figure 3.8a, Appendix II: Figure II.6). The continued production of malformed coccoliths could be observed on successive days, leading to a progressive decrease in the integrity of the coccosphere, with most cells possessing severely defective coccospheres after 5 d (Figure 3.8a, Appendix II: Figure II.7). Time-lapse observation of individual cells indicated that the paired cells form when cells divide but fail to separate (Figure 3.8b). Examination of each paired cell (n>500 paired cells examined) indicated that in every case both daughter cells exhibited significant defects in coccosphere integrity. The number of cells exhibiting the paired-cell phenotype increased dramatically over the course of the experiment, from 4% after 24 h, through to 89.5 % after 96 h (Figure 3.8c). The increasing proportion of cells present as pairs therefore correlates with both the decrease in the integrity of the coccosphere and the decrease in growth rate in Ge-treated cells (Figure 3.2).

DNA staining showed that the paired cells represented two individual daughter cells, each with a single nucleus and a distinct plasma membrane (Figure 3.8d). No clear difference in DNA content was observed between control and Ge treated cells. We did not observe any further rounds of cell division in paired cells in time-lapse images (i.e. leading to the formation of tetrad cell arrangements). This indicates that there is a cell cycle arrest following the initial division, which is most likely the underlying cause of growth inhibition.

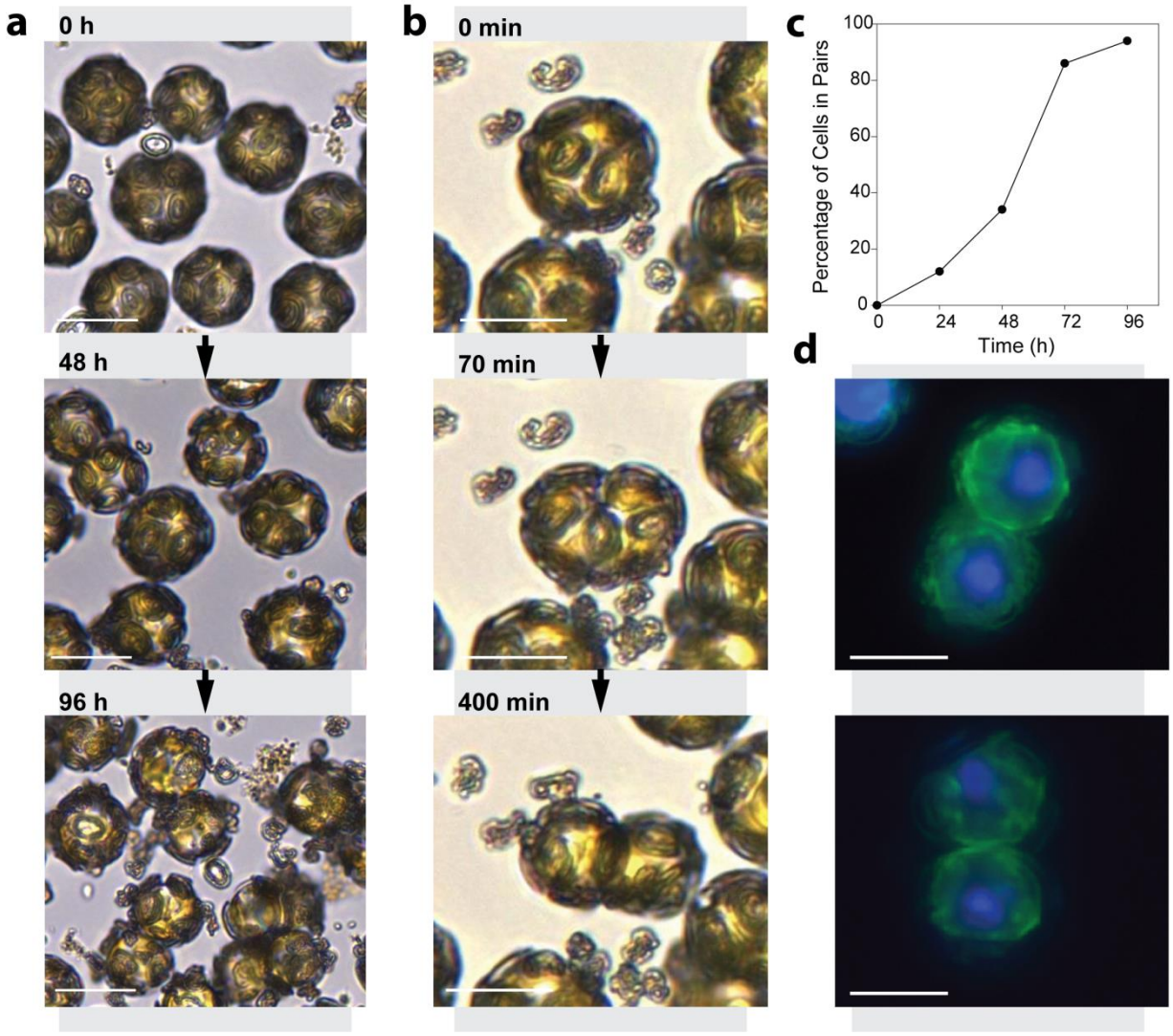

Figure 3.8 Progressive disruption of the coccosphere in *C. braarudii* cells treated with Ge
a) Time-lapse light-microscopy showing the progressive degradation of the coccosphere and the accumulation of paired cells in *C. braarudii* cells treated with 2 µM Ge (0.2 Ge/Si) over a 96 h period. Cells exhibit intact coccospheres at T-0, but start to produce malformed coccoliths soon after the addition of Ge. After 96 h, most cells exhibit incomplete coccospheres and many are present as paired cells. b) Time-lapse light-microscopy showing the formation of a cell pair after 3 d of Ge treatment (0.2 Ge/Si). Parent cells with partial coccospheres divide but daughter cells fail to fully separate. Frame labels represent minutes passed. c) The percentage of paired cells after treatment with 2 µM Ge (0.2 Ge/Si) over 5 d (n= >500 cells counted). d) Epifluorescence microscopy of paired *C. braarudii* cells. The nuclei were stained with Hoechst (blue) and the plasma membrane was stained with FM 1-43 (green). Cells were not decalcified prior to imaging. Each paired cell examined had completed cytokinesis with two defined nuclei and a distinct plasma membrane. Scale bars represent 20 µm.

3.4.7. A polysaccharide-rich organic layer contributes to cell adhesion in the absence of the coccosphere

Transmission electron microscopy indicates that *C. braarudii* possesses an organic layer around the cell, which likely aids in the organisation of the coccosphere and its adhesion to the cell body (Taylor *et al.*, 2007). Polysaccharides in this organic layer around decalcified *C. braarudii* cells, were visualised by microscopy of the fluorescent lectin, FITC-concanavalin A (Figure 3.9a). 3D reconstruction of the polysaccharide layer from untreated cells (i.e. those with an intact coccosphere prior to decalcification) revealed that its structure was not uniform, with distinct oval-shaped regions present at regular intervals that were not stained by FITC-conA. The mean maximal diameter of the non-stained regions was 4.22 ± 0.16 se µm (n=15), which is similar to the inner diameter of the shield elements of the coccolith, suggesting that these regions may correspond to apertures in the polysaccharide layer that form around each coccolith. The distinct structural properties of the polysaccharide layer, which are retained even after decalcification, are likely to contribute to the dynamic re-organisation of the coccosphere throughout the processes of cell expansion and division.

In situ decalcification of paired cells from a Ge-treated culture (after 96 h) revealed that each cell was surrounded by a distinct polysaccharide layer, further confirming that the paired cells are two individual cells (Figure 3.9a). Direct contact between the polysaccharide layers surrounding each cell suggests that the polysaccharide contributes to cell-cell adhesion. The polysaccharide layer was more irregular and the number of non-stained regions associated with the coccoliths were significantly decreased (p=<0.001) in Ge-treated cells when compared to the control over 48 and 96 h (Figure 3.9b). As Ge-treated cells have partially-formed or incomplete coccospheres at 96 h due to the inability of malformed coccoliths to integrate into the coccosphere, the data support the hypothesis that the non-stained regions of the polysaccharide layer are apertures that correspond to the position of the coccoliths. We conclude that the absence

of an intact coccosphere in Ge-treated cells interferes with normal separation of dividing cells and results in cell-cell adhesion via the polysaccharide layer.

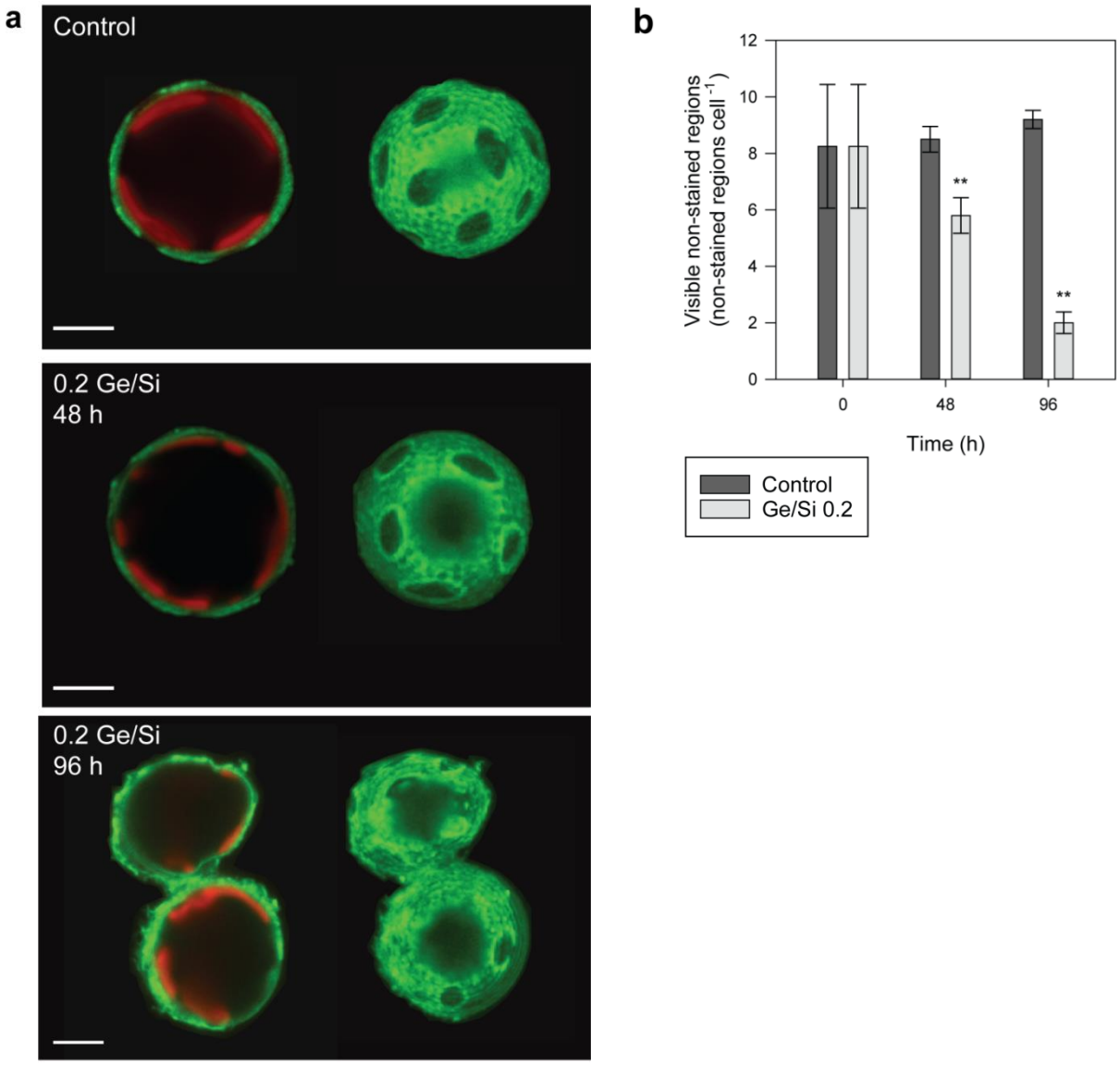

Figure 3.9 A structured polysaccharide layer is involved in organisation of the coccosphere
a) Confocal microscopy imaging of a decalcified *C. braarudii* cells stained with the lectin FITC-conA (green). An external polysaccharide layer can be observed that is distinct from the faint staining present at the plasma membrane. Chlorophyll autofluorescence is also shown (red). 3D reconstructions of the polysaccharide layer in 0.2 Ge/Si (10 µM Si) treated cells for 96 h revealed cells exhibiting the paired-cell phenotype. Paired cells were first identified by light microscopy and then decalcified in situ to ensure that adhesion between cells were not a result of the decalcification process. Each cell in a pair is surrounded by a continuous polysaccharide layer (FITC-conA, green) with polysaccharide clearly visible at the connection point between the two cells. 3D reconstructions of the control polysaccharide layer reveals distinct non-stained oval-shaped regions in the polysaccharide layer. 3D reconstructions of the cells in 0.2 Ge/Si (10 µM Si) at 48 and 96 h also show a reduction in the distinct non-stained oval-shaped regions in the polysaccharide layer. Scale bars denote 5 µm. b) The number of visible non-stained regions cell^{-1} was scored at T0, 48 and 96 h. There was a significant reduction in visible non-stained regions in Ge-treated cells when compared to the control at 48 and 96 h (Mann-Whitney U test p=<0.01, n=20). Scale bars denote standard error.

3.5. Discussion

Our results show that disruption of calcification has dramatically different impacts on the physiology of *C. braarudii* and *E. huxleyi*. Growth of *C. braarudii* was severely inhibited following disruption of calcification by Ge, low Si, HEDP and low Ca^{2+}, whereas *E. huxleyi* grew normally when calcification was disrupted by these latter two treatments. Whilst it is possible that Ge or HEDP may have additional impacts on the metabolism of *C. braarudii*, these treatments are not generally toxic to haptophytes, as concentrations much higher than those required to disrupt calcification have little impact on the growth of *E. huxleyi* and *C. carterae* (Sekino & Shiraiwa, 1994; Asahina, 2004; Durak *et al.*, 2016). Similarly, whilst Ca^{2+} is essential for many cellular processes, lowering seawater Ca^{2+} to 1 mM does not severely inhibit the growth of other marine phytoplankton (Herfort *et al.*, 2004; Trimborn *et al.*, 2007; Leonardos *et al.*, 2009; Müller *et al.*, 2015). Furthermore, the impact of low Si on growth of *C. braarudii* at <0.1 µM Si was only observed following disruption of the coccosphere, suggesting that the effect on growth was specific to the defect in calcification. The combined evidence from these four independent methodologies suggests that there is an essential requirement for calcification in *C. braarudii* but not *E. huxleyi.*

Our data highlight the dynamic nature of the coccosphere in *C. braarudii* and demonstrate the need for coordination between calcification and the cell cycle. Calcification and cell division in coccolithophores are to some extent temporally separated, with cell division occurring primarily in the dark, whereas calcification is largely limited to G1 phase in the light (Paasche, 2001). Our time-lapse observations of dividing *C. braarudii* cells illustrate the rearrangement of the coccosphere during this process and the need for flexible organisation of the coccosphere as the cells grow and expand between divisions. *C. braarudii* cells possess ≤8 coccoliths immediately after cell division, but this increases to ≥16 coccoliths in cells that are ready for division (Gibbs *et al.*, 2013). The coccosphere of *C. braarudii* therefore represents a highly dynamic single layer of interlocking coccoliths that is maintained throughout changes in cell volume and the process of cell division. It appears that the polysaccharide layer surrounding the cell (Taylor *et al.*, 2007) contributes to the organisation of the coccosphere. This layer is not a simple gelatinous mass but has a distinct structure which appears to be formed by the presence of coccoliths on the cell surface. The layer also demonstrates sufficient structural integrity (evidenced by the retention of coccolith-related features in this layer following decalcification) and may play a role in the rapid rearrangement of the coccosphere during cell division, which indicates that coccoliths are able to move within the polysaccharide layer relative to each other and that their position is not rigidly fixed.

Our experiments provide strong evidence that disruption of calcification inhibits growth in *C. braarudii* as well as insight into the cellular mechanisms through which these treatments act to inhibit growth. In Ge- and HEDP-treated cells, we find that the adhesive properties of the organic layer likely prevent cells with disrupted coccospheres from separating after cell division. Paired-cells were also observed in Si-limited cells with disrupted coccospheres. As paired cells fail to divide further, they may be prevented from reaching a critical size that is required for entry into S phase, leading to cell cycle arrest. Entry into S phase of the cell cycle in *E. huxleyi* is triggered by the increase in cell size above a certain threshold (Müller *et al.*, 2008). Under conditions where cells can calcify normally and maintain a complete coccosphere, the area of direct contact between dividing cells would be minimal, preventing adhesion between dividing cells. Thus, the defect in growth in cells treated with Ge, HEDP or low Si appears to result primarily from the inability to maintain a coccosphere following disruption of calcification. We did not find any evidence for a direct cell cycle arrest in Si-limited cells analogous to that seen in diatoms (Vaulot *et al.*, 1987; Brzezinski *et al.*, 1990). Si-limitation takes much longer to disrupt calcification than treatment with Ge. We presume that coccolithophores have a low requirement for Si and it takes many generations for the intracellular pool of Si to become fully depleted. The rapid impact of Ge suggests that Ge does not simply act as a competitive inhibitor of Si uptake, but also acts to disrupt the intracellular role of Si, as observed in diatoms and choanoflagellates (Azam & Volcani, 1981; Marron, A. O. *et al.*, 2016).

C. braarudii cells grown at 1 mM Ca^{2+} did not exhibit a paired-cell phenotype, indicating that the growth arrest from this treatment did not arise from cell adhesion following disruption of the coccosphere. Whilst other marine phytoplankton are able to grow at 1 mM Ca^{2+} (Müller *et al.*, 2015), it is possible that in *C. braarudii* the huge demand for Ca^{2+} in calcification leads to a broad disruption of cellular Ca^{2+} homeostasis that interferes with Ca^{2+}-dependent processes required for growth and cell division. Evidence in support of this hypothesis comes from studies in *Chrysotila* (formerly *Pleurochrysis*) *haptonemofera*, which demonstrates that the growth of calcifying cells is inhibited at 0.5 mM Ca^{2+}, whereas non-calcifying cells grow normally at this concentration (Katagiri *et al.*, 2010). Low Ca^{2+} does not disrupt growth in calcifying *E. huxleyi* cells, which may be a reflection of its ability to greatly vary rates of coccolith production (Paasche, 1998). The mechanisms of Ca^{2+} uptake and partitioning in *E. huxleyi* may also differ from those in other coccolithophores (Sviben *et al.*, 2016; Gal *et al.*, 2017). The absence of a paired-cell phenotype in *C. braarudii* in low Ca^{2+} may also relate to the influence of low external Ca^{2+} on the physical properties of the extracellular polysaccharides, as many algal

polysaccharides such as pectins and alginates are cross-linked by Ca^{2+} and exhibit vastly different properties at lower Ca^{2+} concentrations (Corpe, 1964; Haug, 1976; Matoh & Kobayashi, 1998; Domozych *et al.*, 2014).

The differing requirement to maintain a coccosphere between *C. braarudii* and *E. huxleyi* suggests further mechanistic differences in the calcification process. This may relate to the different organisation of the coccosphere in the two species, as the assembly of the coccosphere in *E. huxleyi* is less structured and can consist of multiple layers of coccoliths (Paasche, 2001). The coccosphere represents a uniform barrier that may help to protect the cell against external influences such as excessive light levels, grazing by bacteria and zooplankton, or infection from pathogens. Monteiro *et al.* (2016) proposed that the requirement to protect the cell from grazing pressure may even have driven the evolution of calcification in coccolithophores around 250 MYA. In *C. braarudii,* selective pressure to maintain the coccosphere appears to have resulted in an inability to grow when calcification is disrupted. We found no evidence to suggest that the inhibition of growth in *C. braarudii* was related to impaired photosynthetic function, although our analyses largely focussed on the light dependent reactions of photosynthesis (F_v/F_m and O_2 evolution) it was also demonstrated that carbon fixation continued after 48 h of calcification disruption. Therefore we can reasonably conclude our data for *C. braarudii* supports conclusions from *E. huxleyi* that calcification does not act primarily to support photosynthesis in coccolithophores under standard laboratory conditions (Bach *et al.*, 2013).

To examine whether the requirement to maintain the coccosphere may be widespread amongst other species, we performed a survey of the coccolithophore species held in major algal culture collections (Table S2). Only two lineages demonstrate the ability to routinely grow in a non-calcified form in the diploid stage of the life cycle. The first of these groups contains solely *E. huxleyi*, whose ability to grow without coccoliths is well documented (Klaveness, 1972; Paasche, 2001). Interestingly, there are no reports that the closely-related species *Gephyrocapsa* and *Reticulofenestra* are able to grow in a non-calcified state, although all these coccolithophores within the Noelaerhabdaceae are closely related to *Isochrysis,* which has completely lost the ability to calcify. The second group is composed of species from the Pleurochrysidaceae (*Chrysotila*) and the Hymenomonadaceae *(Ochrosphaera, Hymenomonas*) in which the coccosphere is composed of many small coccoliths (Marsh & Dickinson, 1997; Marsh, 2006). All other coccolithophore species are fully calcified in healthy, actively growing diploid cultures. This finding suggests that maintenance of the coccosphere in the diploid life cycle stage is a requirement for growth in many coccolithophore species and that commonly used

model organisms in laboratory studies such as *E. huxleyi* and *C. carterae* are not typical of coccolithophores as a whole. Many species of coccolithophore produce small holococcoliths in their haploid life cycle stage, which are distinct from the much larger heterococcoliths produced by the diploid. Intriguingly, the coccolithophore species that do not produce holoccoliths are also the species that can exist as non-calcified diploids (e.g. *Emiliania*, *Chrysotila*, *Hymenomonas*) (De Vargas *et al.*, 2007). While it is not clear whether shared cellular mechanisms contribute to the formation of hetero- and holococcoliths, it is interesting that these species exhibit a lower requirement for calcification in both life cycle stages.

The essential requirement for an intact coccosphere in species such as *C. braarudii* could potentially influence their ecology and their response to future changes in ocean carbonate chemistry. The data presented here indicates that subtle impacts on calcification (such as those induced by low Si) may result in a progressive decline of the integrity of the coccosphere that eventually results in inhibition of growth. Significant increases in seawater CO_2 (pCO_2 >1000 µatm) result in a substantial decrease in both growth rate and calcification rate in *C. braarudii* and also lead to the production of malformed coccoliths (Langer *et al.*, 2006b; Müller *et al.*, 2010; Krug, 2011; Bach, 2015). It is interesting that prolonged growth of *C. braarudii* at elevated CO_2 (>45 d), resulted in a progressive decline in growth rate (Muller 2010). Clearly, the responses of coccolithophores to changes in seawater carbonate chemistry are complex and will involve many aspects of cellular physiology, but it is possible that accumulated defects in coccolith morphology and resultant decline in coccosphere integrity could directly contribute to high CO_2-related growth defects in *C. braarudii*. This is an important consideration, as it reflects a potential direct impact of decreased calcification on physiology, which is not observed for *E. huxleyi*.

In summary, our results show that the ability of diploid *E. huxleyi* cells to persist in a non-calcifying form is not typical of all coccolithophores. The requirement for calcification in *C. braarudii* is primarily due to its need to maintain a full coccosphere, indicating that it is the coccosphere, rather than simply the ability to precipitate calcite, that is central to its ecology.

4. Molecular characterisation of Si transporters in *Coccolithus braarudii*

4.1. Abstract

Biomineralisation by marine phytoplankton, specifically calcification by coccolithophores and silicification by diatoms play an important role in ocean biogeochemical cycles. It was previously thought that coccolithophores do not require silicon (Si) which allowed them to often succeed diatoms following Si depletion by diatom silicification. However, recent research has identified that some coccolithophores possess two types of putative Si transporter: SITs, which are directly related to Si transporters found in diatoms, and a novel group of related proteins known as SITLs. We have examined the regulation of SITL expression in *Coccolithus braarudii* under a variety of growth conditions to explore the cellular role of these novel Si transporters. The data presented here demonstrates that SITL expression is regulated in response to available Si in *C. braarudii*, specifically Si replenishment following a period of starvation. This expression regulation implies that that there is a need to actively transport Si in *C. braarudii.* SITL expression is also only detected in the diploid, heterococcolith-bearing life stage and absent in the haploid, holococcolith-bearing life stage. These findings indicate that Si is likely involved specifically in heterococcolith calcification. Finally we identified the presence of SITL expression in a natural *C. braarudii* population off the coast of Plymouth, framing our findings in an environmental context. These findings are relevant for discussions on the evolution of Si transporters and the role of Si in coccolithophore calcification.

4.2. Introduction

The use of silicon (Si) is highly taxonomically diverse, utilised by a broad range of organisms from bacteria to humans (Birchall, 1995). Si is most commonly involved in the production of siliceous structures (Simpson & Volcani, 2012) which occur in a variety of organisms, many of which are found in the protists (Knoll & Kotrc, 2015). Si utilisation is common throughout the tree of life but many of its cellular mechanisms and roles remain unknown.

In the marine environment the diatoms dominate the use of dissolved Si (dSi). Diatoms are globally abundant, microscopic algae that are found in the photic zone of the oceans and are of huge ecological importance due to their high levels of productivity (Falkowski *et al.*, 1998). Diatoms are encased Si frustules, shell-like structures that are incredibly intricate and have even inspired modern structural engineering and have biotechnological applications (Henstock *et al.*, 2015). As a result of their high dSi usage, diatoms have been attributed to the reduction in the availability of dSi since their evolution (Sullivan & Volcani, 1981; Marron, Alan O. *et al.*, 2016). The current oceanic average is approximately 70 µM but is often less than 10 µM in surface oceans (Treguer *et al.*, 1995).

Although Si is the second most abundant element in the Earth's crust (Lutgens *et al.*, 2014), it has become a limiting nutrient for diatoms in surface waters and is an important factor in their ecology. Crucially, available Si from silica dissolution is very slow and as a result, diatom blooms can deplete dSi in the surface ocean sufficiently to prevent their own further growth. If other nutrients such as nitrate or phosphate are still available, then Si limitation is thought to contribute to seasonal succession in phytoplankton groups, whereby an initial diatom spring bloom can be followed by subsequent blooms of non-siliceous phytoplankton. There is evidence that the low availability of Si is an important contributory factor in the formation of blooms by the coccolithophore *Emiliania huxleyi.* Blooms in areas such as the North Atlantic, the Black Sea and off the Patagonian shelf have been associated with low dSi availability (Leblanc *et al.*, 2009; Balch *et al.*, 2014; Hopkins *et al.*, 2015). Therefore the availability of dSi is thought to influence not only the ecology of diatoms directly but other major phytoplankton groups as well.

Diatoms transport Si from the environment in the form $Si(OH)_4$ through Si transporters (SITs) (Hildebrand *et al.*, 1997; Amo & Brzezinski, 1999). SITs are Na-coupled active transporters formed of membrane associated proteins. The structure of SITs has been well studied, they have 10 trans-membrane domains (TMDs), formed of two identical five

TMD sets (Figure 4.1a). The transport site is thought to be within EGxQ and GRQ motifs, found at TMD2-3 and TMD7-8 (Thamatrakoln *et al.*, 2006; Thamatrakoln & Hildebrand, 2007). Diatoms have multiple SITs which may be involved in different stages of silicification, the cell cycle and have different functions (Thamatrakoln *et al.*, 2006; Thamatrakoln & Hildebrand, 2007; Mock *et al.*, 2008; Sapriel *et al.*, 2009; Shrestha & Hildebrand, 2015). SITs are regulated in response to Si availability, i.e. their expression is up-regulated in response to Si limiting conditions, in both laboratory culture (Shrestha *et al.*, 2012; Smith *et al.*, 2016; Brembu *et al.*, 2017) and natural populations (Durkin *et al.*, 2012).

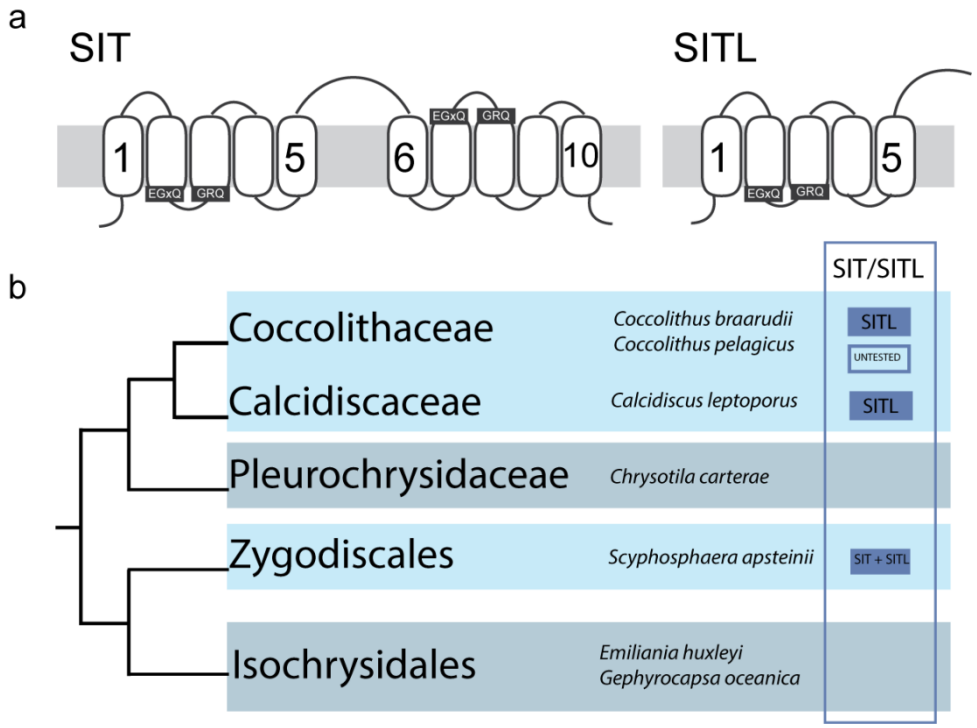

Figure 4.1 The structure and distribution of SITs and SITLs in coccolithophores
(a) A schematic image of the domain architecture of the SITs and the SITLs indicating the approximate position of the transmembrane domains and of the conserved motifs. (b) A schematic tree adapted from Durak *et al.* (2016), based on multiple gene phylogenies (Liu *et al.*, 2010), transcriptome (Keeling *et al.*, 2014) and genome (Nordberg *et al.*, 2013) analysis to show the distribution of SITs and SITLs in coccolithophores. Interestingly there is a lack of identified Si transporters in two distinct groups, the Pleurochrysidaceae and Isochrysidales. Repeated section 2.2.

Recently SITs have also been identified in other important marine organisms including silicified choanoflagellates (Marron *et al.*, 2013) and a silicified haptophyte (Durak *et al.*, 2016). Perhaps more surprising was the identification that some coccolithophores, calcifying haptophytes, have been identified as having SITs (*Scyphosphaera apsteinii*) and SITLs (*Coccolithus braarudii and Calcidiscus leptoporus*) (Durak *et al.*, 2016) (Figure 4.1). It is important to note that not all species of coccolithophore have Si transporters,

with the globally abundant, bloom forming *E. huxleyi* (Tyrrell & Merico, 2004) notably absent from the group. The coccolithophore SITLs are very similar to SITs but only have five TMDs, rather than the full 10. The coccolithophores with SIT/Ls utilise Si within the calcification process (Durak *et al.*, 2016), but the precise role Si plays and the function of the Si transporters are not yet understood. In order to begin investigating this, we can examine the coccolithophore SIT/L expression to see how it compares to diatoms. If coccolithophores have a characteristic expression pattern relating to the availability of Si then there is an indication there is a need to actively transport Si.

Until now investigations have focussed on the diploid heterococcolith bearing life stage. Coccolithophores also have a haploid life stage. In some species, haploid cells are also calcified by coccoliths known as holococcoliths. Holococcoliths are a simple rhomb crystal structure and are thought to be formed externally (Rowson *et al.*, 1986) unlike the complicated, internally formed heterococcoliths. It is not currently known whether Si is involved in the holococcolith calcification process. To fully elucidate what role Si plays in calcification, investigation into the involvement of Si and SIT/Ls in the haploid life stage is required.

The wide distribution of these transporters in ecologically important marine organisms makes their characterisation of particular interest. However, all previous studies have focussed on laboratory culture studies. Although these are incredibly useful for manipulating the conditions in which the algae are subjected, we do not know for sure if their responses mimic those in the natural world. The revelation that coccolithophores require Si has great influence on the current understanding of phytoplankton ecology and should be grounded in environmental studies where ever possible.

This investigation aims to further characterise SITLs in coccolithophores. We have chosen to utilise *C. braarudii* due to its ease of culture, ecological relevance (Daniels *et al.*, 2016) and holococcolith formation in the haploid life stage. In this investigation we explored the regulation of SITLs in *C. braarudii* to address a number of aims:

1. **To quantify the active draw-down of Si from seawater media in cultures of *C. braarudii*.** This would be a strong indication of Si being utilised by coccolithophores with SITLs. Comparison to diatoms and coccolithophores without SITLs will indicate the extent of the Si requirement in this species.

2. **To design and validate a quantitative PCR (qPCR) methodology to quantify the expression of SITLs in *C. braarudii*.** No previous investigations have

quantified gene expression changes in *C. braarudii* therefore full validation of the methodology and reference genes are required.

3. **Establish if SITLs are regulated in response to environmentally available [dSi] in *C. braarudii*.** Diatoms regulate their SIT expression in response to available [dSi], i.e. in Si limiting conditions SITs are up-regulated. If we can establish whether or not SITLs in *C. braarudii* have a characteristic expression pattern in response to available [dSi] then we can reason that there is a need to actively transport Si in *C. braarudii*.

4. **Investigate if SITLs regulated at different life cycle stages in *C. braarudii*.** Calcification differs between diploid and haploid coccolithophores, any changes in expression between these two life cycle stages may give us a greater understanding of the role Si plays in calcification.

5. Identify *C. braarudii* SITL expression in natural populations. All previous work has been conducted in laboratory culture. If we can positively identify the expression of SITLs in natural populations we can compare our observations *in vivo* and *in vitro*.

4.3. Materials and Methods

4.3.1. Algal strains and culture Conditions

Coccolithophores, diploid *C. braarudii* (PLY182g), haploid *C. braarudii* (RCC3777), diploid *E. huxleyi* (CCMP1516) and diatom *Thalassiosira weissflogii* (PLY541) cultures were grown in filtered seawater (FSW) with added f/2 nutrients (Guillard & Ryther, 1962). Cells were illuminated with 55-65 µmol photons m^{-2} s^{-1} on an 16:8 h light:dark cycle and incubated at 15^{O}C. The FSW was collected in May from the Western English Channel, after the diatom spring bloom, to ensure naturally low [dSi] concentrations (≤2 µM). Where FSW with very low [dSi] was required (<2 µM), the diatom *T. weissflogii* (PLY541) was used to further deplete the [dSi] as described previously (Durak *et al.*, 2015). The diatom-depleted seawater was used with the addition of f/4 nutrients (without Si). The [dSi] was determined using a silicate molybdate-ascorbate assay (Kirkwood, 1989). Measurements from the Si draw-down experiment were conducted at UNCW Centre for Marine Science using an AutoAnalyzer3 (Bran Luebbe, Germany) with a standard range of 1.66 to 4.99 µM [dSi]. The [dSi] in environmental samples collected off Plymouth were measured at Plymouth Marine Laboratory in collaboration with Malcolm Woodward. The [dSi] was amended by the addition of $Na_2SiO_3.5H_2O$ where required. For growth experiments, coccolithophore cultures were acclimated to the appropriate [dSi] for several generations (1 month) prior to the investigation. All culture experiments were conducted in triplicate.

4.3.2. SITL Expression Analysis

All qPCR experiments were designed to follow MIQE guidelines (Bustin & Nolan, 2004).

4.3.2.1. RNA Extraction and cDNA Synthesis

20 ml of exponential growth phase culture (approximately 20, 000 cells ml^{-1}) was centrifuged at 3800 *g* for 5 min at 4^{O}C. The supernatant was removed and discarded. Cell pellets were stored at -80^{O}C prior to extraction. Total RNA was extracted using Isolate II RNA Mini Kit (Bioline), as per manufacturers' cell culture extraction instructions with additional elution stage to improve RNA yield.

Extractions were treated with RQ1 RNase-free DNase (Qiagen) to remove any DNA contamination. Extractions were subsequently checked for purity using a Nanodrop 1000 (Thermo Fisher Scientific) (A_{260}/A_{280} ratios > 1.80) and quantified using Quantifluor Single-tube RNA System (Promega) and a 100 ng $µl^{-1}$ standard.

50 ng of cDNA was synthesised per sample/standard using a SensiFAST cDNA Synthesis Kit (Bioline) as per instructions with additional No Reverse-Transcriptase Controls (NRTCs) for each treatment to ensure no DNA contamination occurred. cDNA and NRTCs were stored at -20^{O}C prior to analysis.

4.3.2.2. Primer Design

The published *C. braarudii* transcriptome (MMETSP0164) from the Marine Microbial Eukaryote Transcriptome Sequencing Project (MMETSP) (Keeling *et al.*, 2014) was utilised to design species specific primers for qPCR experiments. Primers were designed using Geneious R8 (Kearse *et al.*, 2012) with Primer3 v2.3.4 (Rozen & Skaletsky, 1999) for *C. braarudii* genes SITL, EFL, RPS1 and TATA Box1. The primers were designed to be approximately 150 bp long for optimal qPCR amplicon length. To ensure specificity, all primer sequences were BLASTED against NCBI GenBank and MMETSP (Keeling *et al.*, 2014) coccolithophore transcriptome sequences.

Multiple primers were designed from each gene and their efficiency tested using gradient PCR. All primers were additionally checked against *E. huxleyi* cDNA to ensure no non-specific amplification was occurring. Full details of primers selected for qPCR is found in

Table 4.1.

Table 4.1 Primer details for qPCR

Gene Name	Full Name	Target	Sequence ID	Primer Name	Primer Sequence	Annealing Site	Amplicon Length
SITL	Diatom-like Si Transporter	Query	CAMNT_0025525031	CbrSITL_F	CGCTGGCATGAATCAAGGTG	104-123	150
				CbrSITL_R	CATATTCCTCCGCACGTCGT	234-253	
EFL	Elongation Factor	Reference	CAMNT_0025499507	CbrEFL_F	GTGCACCACCAAGGAGTTCT	288-307	172
				CbrEFL_R	GTGGTTGCCCTTTTGGATGG	440-459	
RPS1	Ribosomal Protein S1	Reference	CAMNT_0025558139	CbrRPS1_F	GCGTCGGAGAAGACAGACTC	801-820	150
				CbrRPS1_R	GGGAGACATGCTCAAGAACCA	930-950	
TATB	TATA Box Binding Protein	Reference	CAMNT_0025539907	CbrTAT_F	TGCCCGATACGAAGATGAGC	134-153	150
				CbrTAT_R	TCGCCTCTTGTGACGTCAAG	264-283	

4.3.2.3. PCR Efficiency

C. braarudii cDNA was serially diluted (1:5) to generate a five concentration efficiency curve. All efficiency curves of optimised reference genes had an R^2 value ≥99.5% and efficiencies were between 100-105% (Table 4.2). At this stage TATB was rejected as a reference gene due to the high calculated amplification efficiency and low R^2 value, indicated (grey) in Table 4.2. Two reference genes, EFL and RPS1 will be referred to from now on.

Table 4.2 Standard Curve Reaction Efficiencies

Gene	Target	R	R^2	M	B	Efficiency
SITL	Query	0.997	0.995	3.23	19.5	1.04
EFL	Reference	0.999	0.998	3.20	13.1	1.05
RPS1	Reference	0.998	0.997	3.33	17.6	1.00
TATB	Reference	0.997	0.993	2.96	21.4	1.18

4.3.2.4. qPCR Reactions

Reactions were conducted using a Rotorgene 6000 cycle (Qiagen, USA) in 10 or 20 µl reaction volumes of SensiFAST No-ROX Kit (Bioline, UK). Following primer optimisation, PCR reactions were conducted with 400 nM final primer concentration for EFL reactions and 200 nM final concentrations for SITL and RPS1 reactions. PCR cycles were conducted with 95^{O}C 2 min hold, followed by 40 cycles of 95^{O}C denaturing for 5 s, 62^{O}C annealing for 10 s and 72^{O}C extension step (acquisition at end of extension step) for 20 s. A high resolution melt (HRM) curve, 72 - 95^{O}C with 1^{O}C ramp was conducted after amplification to ensure the amplicon had a comparable melting temperature when compared to positive control. NRTCs and no template controls were included in all reactions. All standards, samples and controls were run in duplicate. All qPCR reaction efficiencies were >90% and all PCR products were run on gel electrophoresis to ensure correct amplicon size.

Data was analysed using Relative Expression Software Tool (REST©) (Pfaffl *et al.*, 2002) and SigmaPlot v 13.0.

4.3.3. *C. braarudii* SITL Expression in Natural Populations

4.3.3.1. Sample Site and Collection Method

Samples were collected at L4 Station, 10 nautical miles SW of Plymouth. 15 and 50 µM plankton nets were towed behind *RV Sepia* for 10 min and the contents resuspended in 2 L of surface seawater. The samples were kept at 5^{O}C for 2 h following collection and

prior to centrifugation. Samples were taken for RNA extraction, and microscopy (details below).

200 ml of sample from each net were centrifuged at 3800 g at 4^{O}C for 10 min to pellet the plankton. The supernatant was removed and the pellets were stored at -80^{O}C prior to RNA extraction.

The map of L4 Station was produced using ArcGIS 10.2.2.

4.3.3.2. Microscopy

To positively identify *C. braarudii* in the L4 plankton tow, initial observation was conducted by light microscopy using a Leica DMi8 Inverted Microscope with a DFC7000 T colour camera (Leica Microsystems, UK). To confirm this observation, 10 ml of the 15 µM net plankton sample was prepared for scanning electron microscopy (SEM). Samples for SEM were filtered onto a 13 mm 0.4 µm Isopore filter (Millipore EMD) and rinses with 5 ml MilliQ water to remove any salt. Filters were air dried, mounted onto an aluminium stub and sputter coated with 10 nM Au/Pd (Emitech K550, Quorum Technologies, UK). The sample was analysed using a Jeol JSM-6610LV SEM.

4.3.3.3. Genetic Analysis

The RNA was extracted, cDNA prepared and qPCR conducted as previously described. qPCR reactions for *C. braarudii* were conducted for SITL and EFL genes. Positive qPCR amplicons of both genes were sent to SourceBioscience (Rochdale, UK) for chain termination sequencing with PCR clean-up. The sequences were inspected using BioEdit v7.2.5 (Hall, 1999) and analysed using Geneious 8.0 (Kearse *et al.*, 2012).

4.4. Results

4.4.1. Uptake of [dSi] by coccolithophores

In order to establish the extent of the requirement for Si in *C. braarudii* we compared the uptake of [dSi] in the diatom *T. weissflogii*, a coccolithophore without SITLs, *E. huxleyi,* and a coccolithophore with SITLs, *C. braarudii* (Figure 4.2a). All cultures were in mid-exponential growth phase when analysed (Figure 4.2b). As expected diatom *T. weissflogii* removed almost all [dSi] from the seawater media over the 5 d period. No detectable difference in [dSi] between the two coccolithophores was observed.

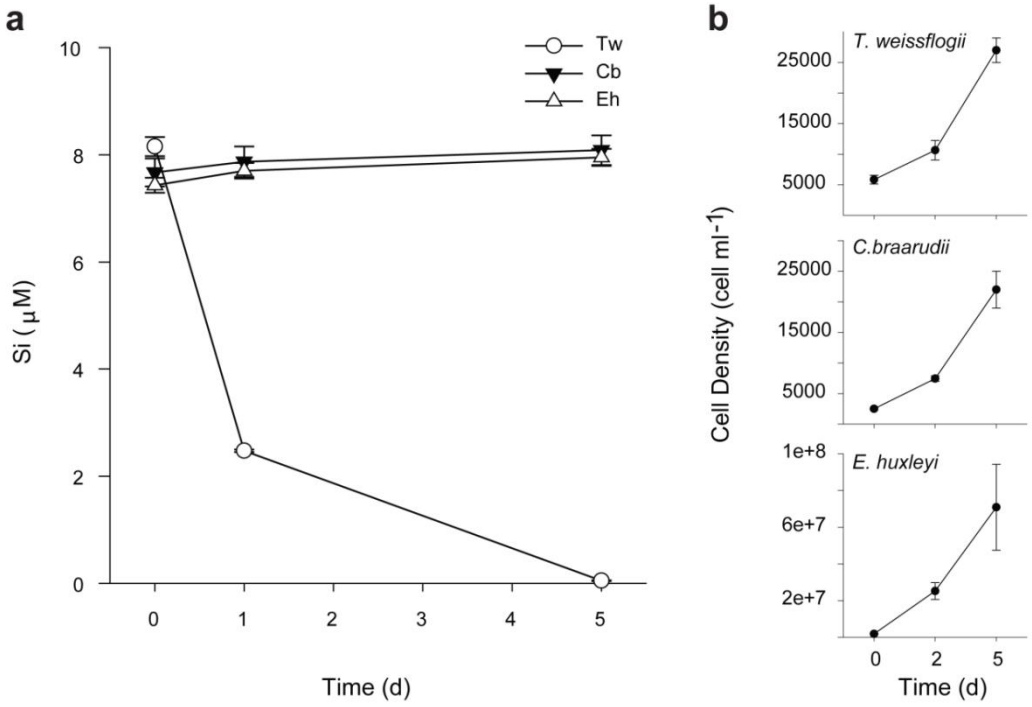

Figure 4.2. Uptake of [dSi] by *T. weissflogii, C. braarudii* and *E. huxleyi*
Concentration of [dSi] in the seawater media was measured over 5 d (a) for cultures containing diatom *T. weissflogii* and coccolithophores *C. braarudii* (SITL) and *E. huxley* (no SITL). *T. weissflogii* removed all available [dSi] over the incubation period, while the coccolithophores *C. braarudii* and *E. huxleyi* exhibited no change in [dSi]. All cultures were in mid-exponential growth phase (b). Error bars denote standard error.

As coccolithophores are not silicified organisms and we see no detectable evidence of [dSi] uptake in the cultures of *C. braarudii*, it is reasonable to hypothesise the requirement for Si is small. In our previous experiments (section 3.4.3) high density cultures (>30, 000 cell ml^{-1}) were achieved prior to Si starvation effects, here the cell densities are lower (22, 000 cell ml^{-1} after 5 d, Figure 4.2b) which may not be dense enough to remove a detectable amount of dSi over the 5 d period. We must also consider that *C. braarudii* may have an intracellular reserve of Si or that they may not be actively up taking Si this time. Although the active uptake was not detectable under these experimental conditions,

examining the expression of the SITL may shed light on whether the transporters are expressed under these conditions. Thereby implying that *C. braarudii* has the potential to uptake Si if necessary.

4.4.2. SITL expression during changing Si availability

To our knowledge this is the first expression study to have been conducted on *C. braarudii* to date. Therefore in order to utilise qPCR to investigate the expression of SITLs a set of reference genes and SITL (query) primers were designed against *C. braarudii* transcriptome (MMETSP0164) and their efficiency validated (section 4.3.2). qPCR was conducted in accordance with MIQE standards (Bustin & Nolan, 2004). The use of two reference genes (EFL and RPS1) was successful in normalising the expression changes in SITLs under various experimental conditions. It was possible to account for any contamination or non-specific amplification using the HRM and gel electrophoresis quality control method. Good replication was observed between biological replicates (n=3) and technical replicates (n=2) (qPCR duplicates). As a result we are confident the assay developed here is robust and produces an accurate depiction of SITL gene expression in *C. braarudii.*

In order to investigate the response of *C. braarudii* SITLs to changing [dSi] we grew cultures in DDSW with [dSi] amended to 10 µM for one month. Cells were then transferred to control (10 µM) and very low (0.22 µM) Si conditions (**Figure 4.3** schematic). Changes in SITL and reference gene expression were analysed following 1 and 8 d of incubation. The fold change expression of the SITLs transferred to very low Si relative to the control was not significantly different following 1 d (*P(H1)* = 0.697) or 8 d of incubation (*P(H1)* = 0.298) when analysed using Pfaffl method (**Figure 4.3**, full Pfaffl output, 6.6.Appendix III: Table III.1). These data show there is no upregulation of SITLs in response to a rapid decrease in the availability of [dSi] in *C. braarudii* over an 8 d period.

The previous data (Figure 4.2) indicated that the requirement for Si is very low in *C. braarudii*. This may explain why there is no immediate expression response to the reduction in [dSi]. It is possible that an intracellular Si pool may not be fully depleted under the experimental conditions. The 0.22 µM Si may not be low enough to initiate Si starvation over a period of 8 d and therefore we do not see the upregulation of SITLs under these circumstances. It is very difficult to achieve lower [dSi] DDSW as the diatoms cannot grow and uptake the Si past these low concentrations.

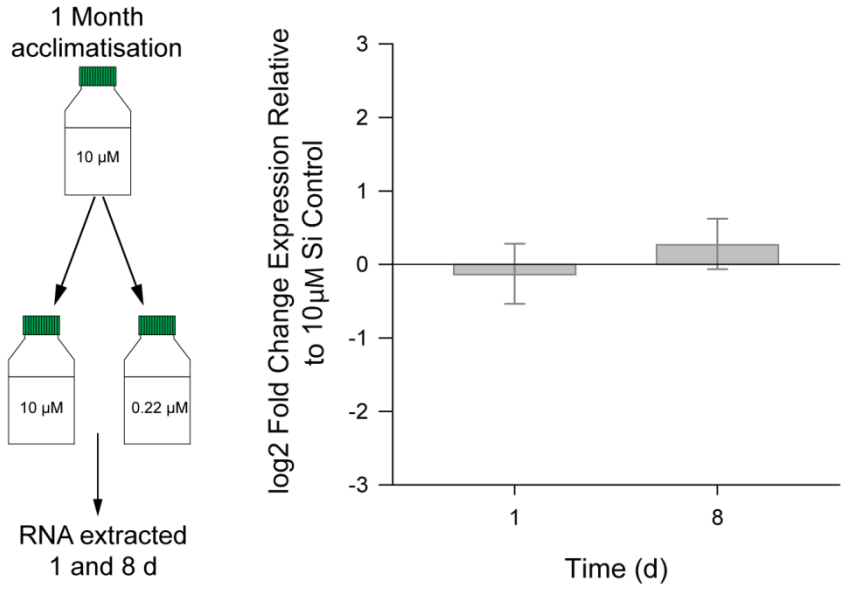

Figure 4.3 The expression of SITLs in response to Si reduction
C. braarudii cultures were grown in 10 µM Si for one month then transferred to control (10 µM) and very low (0.22 µM) Si conditions (schematic). Labels denote [dSi]. Gene expression of the low Si conditions SITLs relative to the control was analysed after 1 and 8 d of incubation. No significant difference was observed over 8 d of incubation when calculated using Pfaffl method (n=3, *P(H1)*= 0.697 and 0.298 respectively). Error bars denote standard error.

Additionally, we investigated whether *C. braarudii* SITL expression responded to Si resupply conditions following a period of Si starvation. We acclimated *C. braarudii* in DDSW (0.22 µM Si) for one month prior to experimentation to enable Si starvation conditions to be established (**Figure 4.4** schematic). After 48 h there was no down regulation of SITLs in all three treatments. After 96 h (5 d) there was down regulation in the higher Si addition treatments (20 and 100 µM) with the 100 µM treatment exhibiting a statistically significant down-regulation of SITLs when compared to the Si starvation control (*P(H1)*=0.045) analysed using the Pfaffl method (**Figure 4.4**, full Pfaffl output Appendix III: Table III.2).

The down-regulation of SITLs in the 100 µM Si treatment is likely to be because of the switch to Si diffusion from active transport, it has been shown in diatom models the concentrations greater than 30 µM allow Si diffusion across the plasma membrane to take place (Thamatrakoln & Hildebrand, 2008).

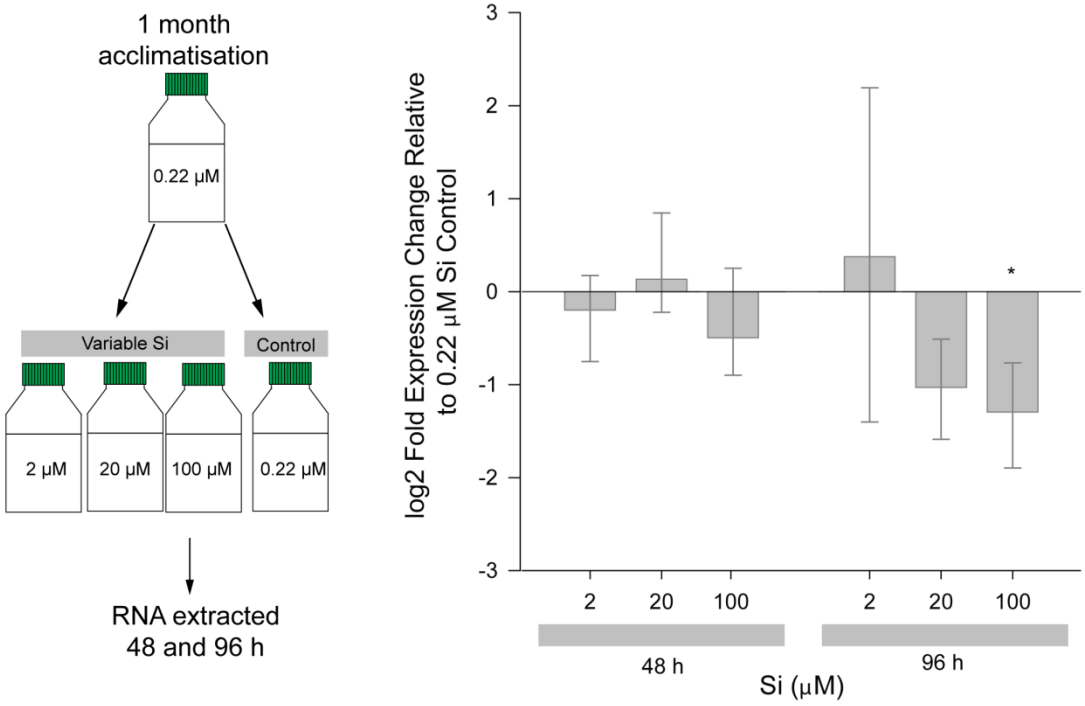

Figure 4.4 Expression of SITLs in response to Si replenishment
C. braarudii cultures were grown in 0.22 µM Si for one month then transferred to 0.22 (control), 2, 20 and 100 µM Si (schematic). Labels denote [dSi]. SITL expression was analysed relative to the control after 48 and 96 h. No significant difference in the 2, 20 and 100 µM Si was observed after 48 h of incubation when calculated using Pfaffl method (n=3, *P(H1)*= 0.842, 0.721 and 0.481 respectively). After 96 h SITLs were down regulated in 20 and 100 µM Si treatments, with a statistically significant down regulation in the 100 µM Si treatment (n=3, *P(H1)*=0.045). Error bars denote standard error.

4.4.3. SITL expression changes in response to life cycle stage

Following the identification of a Si requirement for calcification in diploid *C. braarudii* (Chapter 2) (Durak *et al.*, 2016) we explored whether SITLs were involved solely in heterococcolith formation during the diploid life stage or whether they were also utilised during holococcolith formation in the haploid life cycle stage. Holococcolith formation is distinct from heterococcolith formation and is thought to occur externally (Rowson *et al.*, 1986). The distinction between SITL function would aid the identification of the role Si and SITLs play in coccolithophores.

No expression of a SITL transcript was detected by qPCR implying SITLs are completely down-regulated in the haploid stage. The reference genes (EFL and RPS1) were expressed reasonably consistently between diploid and haploid, shown in both the expression data (**Figure 4.5**a) and accompanying gel electrophoresis images (**Figure**

4.5b). From this data we can conclude that SITL expression and the utilisation of Si are only involved in the diploid, heterococcolith bearing life stage.

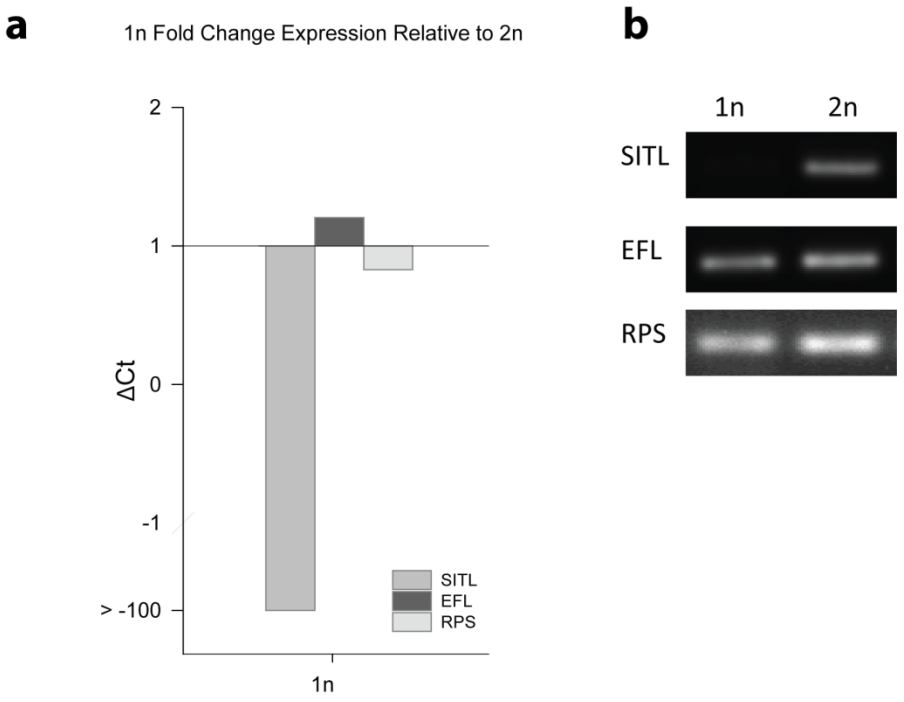

Figure 4.5 The expression of SITL, EFL and RPS1 genes in haploid *C. braarudii*
The haploid life cycle stage of *C. braarudii* exhibits complete down regulation of SITLs when compared to the diploid (2n) expression. Reference genes EFL and RPS1 are similar between haploid (1n) and diploid (2n) expression data. Gel electrophoresis bands show consistent amplification between haploid (1n) and diploid (2n) in EFL, RPS1 but no amplification was observed in haploid (1n) SITL.

We attempted to corroborate the gene expression data with protein expression data. However, we were unable to obtain robust immunoblots from three independent antibodies raised against SITL peptides. Further work is needed to optimise this technique in *C. braarudii* and other coccolithophores.

4.4.4. SITL expression in natural populations

All experiments on coccolithophore SITLs to date have been conducted on laboratory cultures. We investigated whether the *C. braarudii* SITLs were expressed in a natural population off Plymouth, specifically at L4 sample station (**Figure 4.6**a). *C. braarudii* is an infrequent visitor to this station (2017) so we monitored the weekly plankton samples between August and September 2017 using light microscopy (LM) looking for this species. *C. braarudii* was positively identified August (14.8.17) using LM (**Figure 4.6**b) and confirmed this observation using SEM (**Figure 4.6**c).

The [dSi] of L4 surface water was measured at the same time as *C. braarudii* was identified. The surface [dSi] was 0.66 µM (Observatory, 2017), a low concentration and within the range we have found functional expression of SITLs in laboratory culture studies (0.22 – 100 µM). The [dSi] at L4 station was constantly <5 µM during 2017, with lows of <1 µM throughout the summer months (Observatory, 2017). L4 station is consistently within the [dSi] range whereby we have detected SITL expression in our laboratory experiments.

Following the visual identification, we extracted total RNA and positively identified EFL and SITL sequences for *C. braarudii* using qPCR (**Figure 4.6**d). Initially we utilised gel electrophoresis and HRM to select amplicons for sequencing. All sequenced amplicons ran comparatively to standards on gel electrophoresis with no primer dimers (**Figure 4.6**d) and all fell between SITL standard melting temperature range (86.8 – 87.8^{O}C) and EFL standard melting temperature range (87.5 – 88.6^{O}C).

Sanger sequencing was used to validate the qPCR data, we found that the environmental SITL consensus sequence and our laboratory culture reference sequence aligned with a 100% match over the 150bp amplicon. EFL environmental consensus sequence matched the reference sequence 95% over 174 bp amplicon length. The eight base differences in identities in EFL sequence may be due to sequence variation between the natural population and the laboratory culture or due to sequencing error. More environmental sequences would be needed to resolve this difference. Full alignments see Appendix III: Figure III.1.

The environmental consensus sequences were additionally searched against the NCBI BLAST search engine using the blastn function (Altschul *et al.*, 1990). The SITL top hit was *Calcidiscus leptoporus* SITL (Sequence ID: KR677451.1) at 90% identities. The EFL top BLAST hit was *Micromonas commode* EFL (Sequence ID: XM_002502902.1) at 93% identities. These matches are not as strong as those reported above. There are currently no *C. braarudii* EFL and SITL sequences deposited in the NCBI database. The data show *C. braarudii* SITLs are expressed in the natural population at L4 station off Plymouth and not just in laboratory culture.

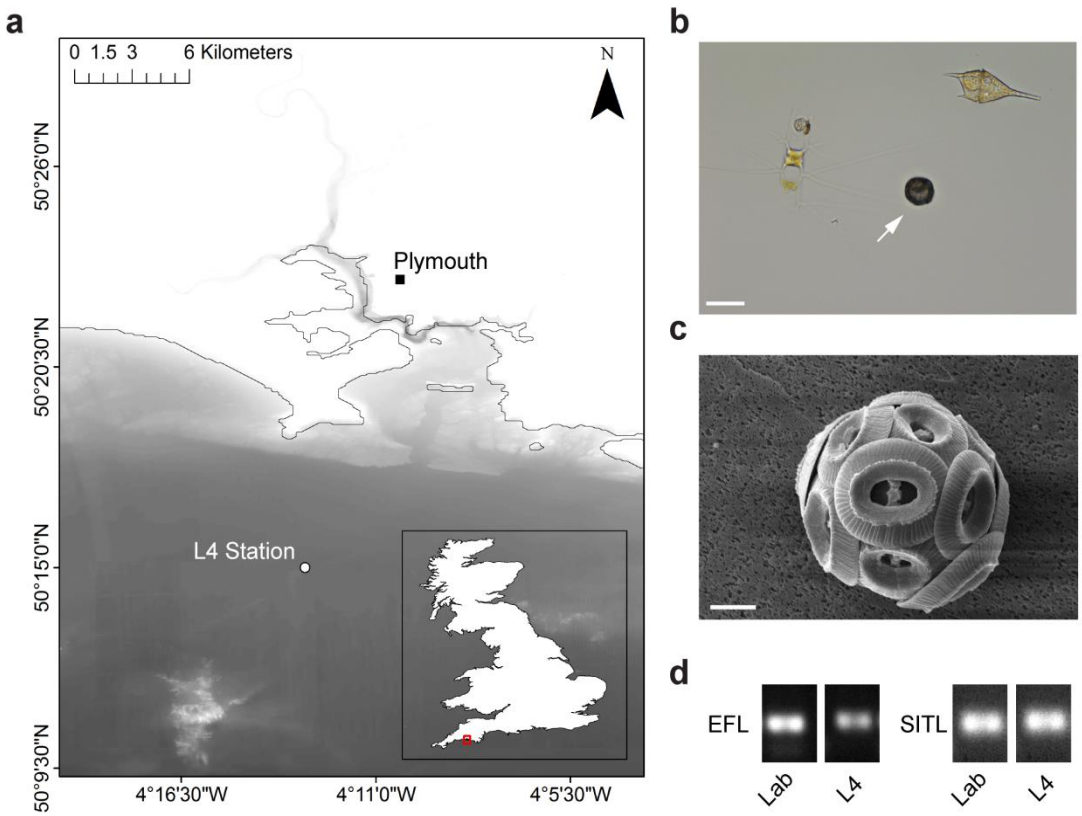

Figure 4.6 Expression of SITLs in natural coccolithophore populations
We analysed L4 station (a) plankton tow net samples for the presence of *C. braarudii* using light microscopy (b). When *C. braarudii* was positively identified the observation was confirmed using scanning electron microscopy (c). EFL and SITL sequences were successfully amplified from RNA extracted from L4 sample, confirming the presence and expression of *C. braarudii* SITLs in natural population.

4.5. Discussion

In this investigation we show that SITL expression in the ecologically important *C. braarudii* (Daniels *et al.*, 2014) can be characterised by qPCR. The data indicate *C. braarudii* consistently expresses SITLs in low [dSi] conditions and responds to a surge in Si by down-regulating SITL expression. Additionally we clarified that SITL expression is closely associated with heterococcolith calcification in the diploid life cycle stage and is not linked to the haploid life stage. Finally, we positively identified the active expression of SITLs in a natural population of *C. braarudii* at L4 station off Plymouth, UK. This interesting observation takes work previously based in laboratory culture and frames it in an environmental context.

C. braarudii is not a silicified organism but it has an obligate requirement for Si in calcification. Our data show that the requirement for Si is low, when considering the Si draw-down and the Si starvation SITL expression data. These data contrast to that in diatom literature whereby SITs have been shown to be highly regulated in response to Si depletion (Shrestha *et al.*, 2012; Smith *et al.*, 2016; Brembu *et al.*, 2017). It is important to note that diatoms rapidly deplete their internal and extracellular [dSi] due to the extensive silicification and Si uptake (Sullivan & Volcani, 1981) and therefore need to increase their Si transporters to meet demand. This is not the case in coccolithophores. Our data shows SITLs are functional in laboratory culture across an environmentally relevant range of [dSi] (0.22-10 µM) and in the environmental samples, which were isolated from waters with a [dSi] of 0.66 µM. We can reasonably conclude that *C. braarudii* is likely to consistently require SITL expression in average surface water conditions of ≤10 µM [dSi] and that these are down-regulated when [dSi] is abundant. We are yet to identify the exact role Si plays in coccolithophore calcification; once this is elucidated it may be possible to calculate a Si budget for each species of coccolithophore. This revelation would provide an interesting insight into the evolution and ecology of coccolithophores.

The down-regulation of SITLs in response to replenishment of [dSi] is likely due to the lack of necessity to actively transport Si under these conditions. In this case we may compare *C. braarudii* to the existing model in diatoms; following Si starvation diatoms respond with a period of Si replenishment known as surge uptake, whereby SITs are still expressed. A similar response may have been observed in *C. braarudii*, whereby there was no down-regulation of SITLs after 48 h despite the fact that the dSi is now concentrated enough to diffuse across the cell membrane (Johnson & Volcani, 1978; Thamatrakoln & Hildebrand, 2008). When the Si is recovered in diatoms, the SITs are

subsequently down-regulated (Shrestha *et al.*, 2012). We also see a down-regulation of SITLs in high [dSi] after 96 h (5 d) in *C. braarudii*. The diatom SIT response occurs over a period of hours (<9 h) whereas the SITL expression responds over 5 d. The different mechanisms behind Si sensing and transport, and the reliance on the element for essential life processes between these two algal groups are likely to be the reason underlying this time-frame distinction.

It has been suggested that SITLs may be an evolutionary precursor to the SITs. Eukaryotic Si transporter sequences fall into three groups; Group 1 SITLs, Group 1 SITs and Group 2 (containing both SIT/Ls). The coccolithophore SITLs are classed as Group 1 SITLs and are considered predecessors to the Group 1 SITs found in organisms including coccolithophore *S. apsteinii*, the silicified haptophyte *Prymnesium neolepis* and the diatoms. The SIT system is thought to be evolved from a fusion of two five TMDs SITLs, whereby the fusion may confer beneficial properties that are absent in the SITLs (Marron, Alan O. *et al.*, 2016). An interesting candidate to expand this research is the coccolithophore *S. apsteinii*, which has both SITLs and SITs (Durak *et al.*, 2016). Here we may find an evolutionary link between the two systems and a check point in the evolution of the transporters and insight into their functional differences.

One functional difference may be the Si transporting capabilities of each system, i.e. the SITL system may be less efficient than that of the SIT system. The consistent expression of SITLs in low [dSi] conditions demonstrates that the low Si requirement in *C. braarudii* can be satisfied by the function of SITLs. This is also likely to be the case for the closely related *C. leptoporus* which also has SITLs (Durak *et al.*, 2016). In contrast, *S. apsteinii* may have a higher requirement of Si. We know *S. apsteinii* has a very different coccosphere to *C. braarudii* and *C. leptoporus,* with considerably larger barrel-shaped lopadoliths and flat disk-shaped muroliths in a dimorphic arrangement. Si has also been identified within the coccolith composition (Drescher *et al.*, 2012). Differences in the coccoliths or their production may infer a greater requirement for Si for calcification in this species. The presence of both transporters may therefore have evolved to meet the higher Si demands. It is likely that SITs are more efficient at transporting Si as the silicified haptophyte *P. neolepis*, which clearly has a higher Si requirement, has SITs and not SITLs present in its transcriptome. The SITs are known to provide enough Si for extensively silicified organisms including diatoms, whereas SITLs may not. It is important to note that as SITLs have not been extensively characterised, they may have properties that differ to SITs that are not yet known. More work to characterise the efficiency of the SITL transporters is necessary to explore this hypothesis.

The lower Si requirement may also have an impact on the required accompanying mechanisms to Si transport in coccolithophores. Diatoms have a complex Si sensory mechanism (Shrestha & Hildebrand, 2015) and a suite of Si transport associated genes (Hildebrand *et al.*, 1998; Armbrust *et al.*, 2004), whether or not coccolithophores have an extended Si sensory mechanism is yet to be divulged but their consistent expression below the Si diffusion threshold may imply it is not crucial in these calcified organisms. It is likely that coccolithophores utilise a more primitive Si system than diatoms to meet their lower Si demands.

It is important to consider the environmental conditions at the time of evolution and the influences this may have on the coccolithophore SITLs. The coccolithophores which have SIT/Ls are considered to be from the more ancestral lineages in modern extant species (Liu *et al.*, 2010; Durak *et al.*, 2016) and therefore likely to retain certain ancestral features. The evolution of calcification in coccolithophores can be traced phylogenetically and in the fossil record to approximately 220 million years ago (MYA) (Brown *et al.*, 2004; De Vargas *et al.*, 2007). The available [dSi] at the 220 MYA was approximately 1 mM, considerably higher than in modern oceans (Siever, 1991; Treguer *et al.*, 1995). It has been suggested that coccolithophores evolved SITLs to cope with the high [dSi] in their environment, the presence of Si in the intracellular space is likely to be controlled due to the tendency of Si to polymerise, which can be destructive to cellular function (Marron, Alan O. *et al.*, 2016). It is also possible that the SITLs evolved to replenish the Si needed for calcification when environmental [dSi] began to decrease rapidly with the evolution of the diatoms 140 MYA (Gersonde & Harwood, 1990). The requirement for Si in calcification may have preceded the SIT/L evolution in the high [dSi] world coccolithophores originated in. It is unlikely SITLs evolved to transport Si in an environment whereby Si can easily diffuse across membranes (>30 µM) but may have evolved to cope with the diatom induced decreasing [dSi] experienced by modern lineages of coccolithophore.

The environmental conditions experienced by modern coccolithophores are influenced by their life cycle stage, we can expand this to include the lack of a Si requirement in the haploid stage of *C. braarudii*. Interestingly the haploid cells have been shown to have a greater affinity to oligotrophic, nutrient poor conditions when compared to the diploid stage in both laboratory (Houdan *et al.*, 2006) and environmental investigations (Kleijne, 1993). Although studies have not considered Si a limiting factor, the lack of requirement for Si in the haploid stage may aid towards this difference in niche occupation between the two ploidy stages.

Additionally, this distinction between ploidy stages sheds light on the role of Si in coccolithophores. Previous studies identified the role of Si in calcification (Durak *et al.*, 2016), but we cannot be sure that Si does not play a role in other cellular functions. As we have shown that the haploid does not have a requirement for Si active transport, this suggests that the Si is not actively involved in any other cellular processes, specifying its role in heterococcolith calcification. As the haploid holococcoliths are relatively simple (Rowson *et al.*, 1986), we may hypothesise that the Si is related to a process which enables the formation of the complex heterococcolith structure found in diploid cells. The lack of SITL expression in haploid *C. braarudii* has aided our understanding of the Si requirement and this distinction may enable the identification of the precise role Si plays in future studies.

The lack of SITLs in some species of coccolithophore is also an interesting consideration. The large-bloom formers, *E. huxleyi* and *Gephyrocapsa oceanica* are amongst those species without SITLs (Durak *et al.*, 2016). It has been hypothesised that SITLs may have been lost in the isochrysodale lineage (Marron, Alan O. *et al.*, 2016), enabling these species to maximise on low [dSi] conditions following diatom blooms (Leblanc *et al.*, 2009; Balch *et al.*, 2014; Hopkins *et al.*, 2015). The considerable cell densities required to form a bloom of this magnitude may be extensive enough to limit Si in surface waters. This may be a contributing factor to the lack of large blooms in species such as *C. braarudii* and *Coccolithus pelagicus.* Whether or no these species have an alternative mechanism to Si compared to species with SIT/Ls is yet to be revealed. This may highlight an interesting difference in the calcification mechanisms between these species.

Although the mechanism for Si utilisation is not yet fully understood, it is clear the exposition of this mechanism will greatly aid our understanding of modern coccolithophore ecology and ocean biogeochemical cycling. The progress made here to characterise the SITL transporters system in *C. braarudii* provides a good model that can be utilised in other species of coccolithophore and wider organisms. With more widespread characterisation of the SITL family we can shed light on both their evolution and their roles in non-siliceous organisms.

5. Investigating Coccolith Associated Polysaccharides

5.1. Abstract

Coccolithophores are globally abundant marine microalgae characterised by their ability to form calcite platelets (coccoliths). The coccoliths are produced internally in a special Golgi-derived vesicle. Current evidence indicates that calcite precipitation in the coccolith vesicle is modulated by coccolith associated polysaccharides (CAPs). The mature coccolith is extruded from the cell whereby it forms a protective covering on the cell surface, known as the coccosphere. Previous research into CAPs has focussed on their ability to modulate the precipitation of calcite. Here we demonstrate the presence of a large amount of insoluble polysaccharide associated with the external coccoliths that differs between species in structure and composition. Our data suggest that this polysaccharide is extruded with the coccoliths. Once extruded, the polysaccharides play a role in the adhesion of the coccoliths to the cell surface and contribute to the overall organisation of the coccosphere. Finally, we combine previous research and data presented here to define CAPs as a broad group of polysaccharides encompassing intracoccolith polysaccharides; internal, calcite precipitation-modulating polysaccharides; and external polysaccharides involved in cell surface-adhesion of the completed coccolith and organisation of the coccosphere.

5.2. Introduction

Coccolithophores are photosynthetic unicellular marine algae that are characterised by their ability to form intricate calcite platelets known as coccoliths (Taylor *et al.*, 2017). Coccoliths are produce internally in a specially Golgi-derived coccolith vesicle (CV) and extruded to the cell surface (Young & Henriksen, 2003; Brownlee & Taylor, 2004). Coccolithophores are globally abundant, with some species forming vast blooms that can be visible from space (Westbroek *et al.*, 1993), making them important global producers and significant contributors to the ocean carbon cycle (Rost & Riebesell, 2004). The important role coccolithophores play in biogeochemical cycling has driven much research investigating the underlying cellular mechanisms of calcification and the roles of the extracellular coccoliths.

Coccolithophores transport Ca^{2+} and HCO^{-} from the environment into the CV whereby the precipitation of calcite occurs (Brownlee & Taylor, 2004). Once extruded, coccoliths are organised into an extracellular layer covering the cell surface, known as the coccosphere. There is considerable variability in the morphology of coccoliths and the nature of the coccosphere between species. For example, heavily-calcified placolith-bearing species such as *Coccolithus braarudii* or *Calcidiscus leptoporus* exhibit a single layer of interlocking coccoliths (Young *et al.*, 2003). The cosmopolitan bloom forming species *Emiliania huxleyi* also produces placoliths, but these can be arranged into multiple layers within its coccosphere (Paasche, 2001). *Scyphosphaera apsteinii* produces dimorphic coccoliths, the flat muroliths and barrel-shaped lopadoliths. These form a single layer on the cell surface, but are not interlocking (Young *et al.*, 2003). The proportion of muroliths and lopadoliths in the coccosphere can vary due to environmental conditions (Drescher *et al.*, 2012). The coccosphere of all species likely forms a protective covering around the cell (Monteiro *et al.*, 2016), which must be both flexible (to enable cell growth and division) but also tightly organised to ensure full covering of the cell surface and prevent excess shedding of coccoliths. The mechanisms supporting the arrangement of coccoliths on the cell surface and their tethering to the plasma membrane have not been closely investigated. There are several reports describing an organic layer surrounding the cell, which is integrated with the coccoliths (Van der Wal, P *et al.*, 1983; Van der Wal, P. *et al.*, 1983b; Marsh, 1994; Taylor *et al.*, 2007) (Chapter 3: Figure 3.9). Polysaccharides are known to contribute significantly to this layer, but the nature of these polysaccharides and their contribution to the very different coccospheres found in coccolithophores are not known.

Although little is known about the extracellular polysaccharides in coccolithophores, there has been considerable interest in the role of polysaccharides in modulating calcite precipitation. These polysaccharides are collectively referred to as coccolith associated polysaccharides (CAPs) (Westbroek *et al.*, 1973; De Jong *et al.*, 1976), and are considered to be a crucial component in the calcification process. CAPs are predominantly classified as water-soluble acidic polysaccharides primarily composed of neutral monosaccharides, acidic sulphate esters and uronic acid residues (De Jong *et al.*, 1976). The uronic acid residues are pivotal in modulating calcification because their carboxyl groups ($COOH^-$) bind to Ca^{2+} cations and impede calcite precipitation at key points in coccolith production. Studies both *in vivo* and *in vitro* have demonstrated that CAPs regulate the precipitation of calcite in various species of coccolithophore (Borman *et al.*, 1982; Borman *et al.*, 1987; Ozaki *et al.*, 2007; Henriksen & Stipp, 2009; Kayano *et al.*, 2011; Gal *et al.*, 2016).

As well as studies into the role, the localisation of CAPs has been investigated, with observations of polysaccharide situated internally in the CV in *Emiliania huxleyi* (Van der Wal, P *et al.*, 1983) and *Chrysotila carterae* (formerly *Pleurochrysis carterae*) (Van der Wal, P. *et al.*, 1983b; Marsh, 1994). These studies also described CAPs associated with extracellular coccoliths after they are fully formed and extruded to the cell surface. With research focussed on the role of CAPs in modulation of calcification, their structural organisation and potential roles in relation to the extruded coccolith have not been extensively investigated.

Interestingly, CAPs show diversity across different coccolithophore species. Firstly the number of major soluble CAPs reported ranges from one in *Emiliania huxleyi* (Borman *et al.*, 1987) to three in *C. carterae* (Marsh, 2003). It has been proposed that the additional polysaccharides in *C. carterae* may function as a component of a Ca^{2+} delivery system, possibly replacing the function of the reticular body, a membrane-rich organelle that is not found in *Chrysotila* species (Marsh & Dickinson, 1997), but which is a predominant feature in other species such as *E. huxleyi* and *C. braarudii* (Taylor et al, 2007, 2017). Secondly, the chemical composition, specifically the uronic acid content, of CAPs differs between both species and strains (Borman *et al.*, 1987; Lee *et al.*, 2016). It is thought that these differences may influence the shaping of the calcite crystals (Marsh & Dickinson, 1997) and may reflect adaptations to the calcite saturation in the environment the species inhabits (Lee *et al.*, 2016).

A degree of ambiguity surrounds the nature and roles of CAPs due to the aforementioned diversity between species and because many investigations use different polysaccharide extraction procedures (

Table 5.1). These include targeting the whole cell, isolated coccoliths or intracoccolith extractions. Note that these intracoccolith extractions have previously been referred to as intracrystalline (Westbroek *et al.*, 1973; Lee *et al.*, 2016) but as the localisation of polysaccharides internally in calcite crystals is subject to debate we shall refer to these fractions as intracoccolith in this discussion. Additionally, the majority of investigations have focussed on the water-soluble component of the CAPs albeit stable insoluble polysaccharides are also associated with the coccoliths (Van der Wal, P *et al.*, 1983). Although many studies refer to CAPs collectively, it is likely the varied extraction techniques have included a combination of different polysaccharides, both those derived from the coccolith vesicle and those found extracellularly. Whether these polysaccharides are similar in structure and function is yet to be established. In particular, closer examination of the extracellular polysaccharides associated with the coccoliths is required to understand their involvement in coccolithophore calcification.

In this study, we examine the extracellular roles of polysaccharides associated with coccoliths. We identify the presence of insoluble polysaccharides associated with both the cell body and the coccoliths in all species investigated. These polysaccharides differ in physical structure and composition between species. Further investigation into *C. braarudii* revealed that the extracellular polysaccharides are likely produced internally with the coccolith and play a subsequent role in the adhesion and organisation of the coccosphere.

Table 5.1 Coccolith Associated Polysaccharide Extraction Fractions

Reference	Fraction*	Species	Polysaccharide Isolation
Gal *et al.* (2016)	Coccoliths	*Chrysotila carterae*	EDTA
Lee *et al.* (2016)	Intracoccolith	*Emiliania huxleyi*, *Gephyrocapsa oceanica*, *Calcidiscus leptoporus & Coccolithus pelagicus*	EDTA
Kayano *et al.* (2011)	Whole cell	*E. huxleyi*	TCA
Kayano and Shiraiwa (2009)	Whole cell	*E. huxleyi*	TCA
Henriksen and Stipp (2009)	Coccoliths	*E. huxleyi*	EDTA
Ozaki *et al.* (2007)	Whole Cell, Coccoliths	*Chyrysotila haptonemofera*	EDTA
Ozaki *et al.* (2004)	Whole cell	*E. huxleyi*, *G. oceanica & C. carterae*	EDTA
Henriksen, K. *et al.* (2004)	Coccoliths	*E. huxleyi*	EDTA
Marsh *et al.* (1992)	Whole Cell	*C. carterae*	TCA
Marsh *et al.* (1992**)**	Coccoliths	*C. carterae*	EDTA
Borman *et al.* (1987)	Coccoliths	*E. huxleyi*	EDTA
Borman *et al.* (1982)	Coccoliths	*E. huxleyi*	EDTA
Fichtinger-Schepman *et al.* (1981)	Coccoliths	*E. huxleyi*	EDTA
Fichtinger-Schepman *et al.* (1981)	Coccoliths	*E. huxleyi*	EDTA
De Jong *et al.* (1976)	Coccoliths	*E. huxleyi*	EDTA
Westbroek *et al.* (1973)	Intracoccolith	*E. huxleyi*	EDTA

* Fractions are defined as [1]Whole cell: the whole cell was subjected to polysaccharide extraction without any prior treatment. [2]Coccoliths: the coccoliths were separated from the cell body and all polysaccharides associated extracted. [3]Intracocclith: the coccoliths were separated and all organic material on the outside of the coccoliths removed before calcite dissolved and intracoccolith polysaccharides extracted.

5.3. Materials and Methods

5.3.1. Algal strains and culture conditions

C. braarudii (PLY182g) (formerly *Coccolithus pelagicus* ssp *braarudii*), *C. leptoporus* (RCC1130), *C. carterae* (PLY406) and *E. huxleyi* (CCMP1516) were grown in filtered seawater (FSW) with added f/2 nutrients (Guillard & Ryther, 1962). *S. apsteinii* (RCC 1456) was grown in FSW with added f/2 and 10% K medium. Cells were grown in batch cultures, incubated at 15^{O}C and illuminated with 65-75 µmol photons m^{-2} s^{-1} in a 16:8 light:dark cycle.

5.3.2. Decalcification of coccolithophores

Coccolithophores were allowed to settle and excess f/2 media removed. To decalcify, the cells were washed in Harrison's broad spectrum artificial seawater (ASW) (Harrison *et al.*, 1980), without $CaCl_2$ and pH adjusted to 7.0 with HCl. Cells were washed twice to remove any residual Ca^{2+} and adjust the pH, with time allowed for cells to settle between washes. Cells were incubated in the ASW for approximately 30 min to decalcify, allowed to settle and were finally re-suspended in FSW f/2 media prior to staining.

5.3.3. Staining and confocal microscopy

Extracellular polysaccharides were stained using the fluorescent lectins Concanavalin A (conA) (100 µg/ml) and Wheat Germ Agglutinin (WGA) (100 µg/ml) conjugated to either FITC or Texas Red (specified) (all lectins: Invitrogen, UK). Cells were imaged using a Zeiss LSM 510 laser scanning confocal microscope or a Bio-Rad Radiance confocal system on a Nikon upright microscope, with excitation at 488 nm and emission at 500-530 nm (FITC) and 650-715 nm (chlorophyll). Where stated, certain samples were also visualised using a Nikon Ti epifluorescence microscope with a Photometrics Evolve EM-CCD camera (excitation 475-495 nm, emission 505-535 nm).

5.3.4. Electron microscopy

Samples for SEM were filtered onto a 13 mm 0.4 µm Isopore filter (Millipore EMD) and rinsed with 5 ml of 1 mM HEPES buffered (pH 8.2) MilliQ water to remove any salt. Filters were air dried, mounted onto aluminium stubs and sputter coated with 10 nm Pt/Pd (Cressington, USA). Samples were examined using a Phillips XL30S FEG SEM (FEI-

Phillips, USA) and imaged in high-resolution secondary electron mode with beam acceleration of 5 kV.

5.3.5. Coccolith preparation

Late exponential phase cultures were harvested by centrifugation at 4800 g, 4^{O}C for 5 min. Cells were resuspended in 10 ml of f/2 FSW and subjected to probe sonication (Sonics Vibra Cell VCX750) at 30% amplification for two 10 second pulses, cells were mixed by inverting the tube between pulses. The cell debris and coccoliths were pelleted and the supernatant removed. The pellet was resuspended in 50% Percoll® (Sigma-Aldrich, UK) to separate the cell debris and coccoliths by density centrifugation. The mixture was centrifuged at 4800 g, 4^{O}C for 20 min. The density centrifugation step was repeated twice to ensure a clean coccolith preparation. The Percoll® was then removed from the coccoliths by washing three times in NH_4HCO_3 0.5 M. The coccolith preparation was then subjected to polysaccharide extraction.

A sample of the coccolith preparation was cleaned by incubating in 10% NaClO at room temperature overnight to remove all organic material. The coccoliths were pelleted and the supernatant removed. The cleaned calcite was then stained using FITC conA to test if the lectin bound non-specifically to the coccoliths.

5.3.6. Polysaccharide extractions

Coccolith preparations were used for polysaccharide extractions. Polysaccharides were extracted using cold 80% ethanol (three washes). Soluble polysaccharides and calcite were subsequently removed using 0.1 M EDTA (three washes). Polysaccharides were further cleaned using three additional ethanol washes to ensure all other cellular material was removed, pellets were then air dried and stored at -20^{O}C prior to GC-MS.

5.3.7. GC-MS preparation and analysis

The composition of polysaccharides extracted from the coccolith preparations for *C. braarudii, S. apsteinii, C. carterae* and *E. huxleyi* using gas chromatography – mass spectrometry (GC-MS). Due to the necessity to grow large volumes of culture to have enough material to extract (approximately 1 L per extraction), we were unable to use *C. leptoporus* as it was not possible to grow enough biomass.

Alcohol-insoluble polysaccharide pellets were hydrolysed by heating to 105^{O}C for 2 h in the presence of 2 M trifluoroacetic acid (TFA) (200 µl). TFA only blanks were also included. 50 µl of hydrolysed sample was centrifuged at 13, 000 g for 10 min to remove any solid material. 40 µl of supernatant was transferred to glass MS vials and 10 µl of internal standard added (myo-inositol, final concentration 2 µM). Samples were completely dried down using an evaporator (GeneVac EZ-2). 20 µl of 20 mg ml^{-1} methoxyamine hydrochloride dissolved in pyridine was added to each sample and they were incubated at 37^{O}C for 2 h. 35 µl of N-methyl-N-trimethylsilyltrifluoroacetamide (MSTFA) was then added and the samples returned to 37^{O}C for a further 30 min, before analysis on the GC-MS. Methoxyamine hydrochloride in pyridine derivatises the carbonyl groups, then MSTFA containing 1% trimethylchlorosilane (catalyst) derivatises carboxyl, hydroxyl, amino, imino or sulphonyl groups. Derivatising agents were all from purchased from Sigma-Aldrich, UK.

Blanks (TFA) and sugar standards were treated in the same way, along with a derivatisation agent only blank. A 10 and 1 µM standard mix were prepared containing glucose, galactose, mannose, xylose, arabinose, fucose, galacturonic acid, glucuronic acid and myo-inositol.

Derivatised samples were analysed using an Agilent 7200 series accurate mass Q-TOF GC-MS together with a 7890A GC system (Agilent Technologies, Santa Clara, USA), equipped with an electron ionisation ion source. 5 µl of each sample was injected into a non-deactivated, baffled glass liner with a 12:1 split ratio (14.448 ml min^{-1} split flow) and the inlet temperature was maintained at 250^{O}C. A 3ml/minute septum purge flow was applied. A Zebron semi-volatiles (Phenomenex, Torrance, USA) column (30 m x 250 µm x 0.25 µm) coupled with a 10 m guard column, was maintained at a constant helium flow of 1.2ml min^{-1}. The temperature gradient of the GC was ramped up at a rate of 15^{O}C min^{-1}, from 70^{O}C to 310^{O}C over 16 min, and then held at 310^{O}C for a further 6 min. The total run time of 22 min, was followed by a 7 min backflush at 310^{O}C to clean the column at the end of every run. The MS emission current and emission voltage were held at 35 µA and 70 eV respectively, and the MS was automatically calibrated after every run. The mass range was set from 50 to 600 amu, with an acquisition rate of 5 spectra s^{-1}, and a solvent delay of 3.5 min.

Data were analysed using Agilent technologies MassHunter qualitative and quantitative software.

5.4. Results

5.4.1. Localisation of extracellular polysaccharides using lectin FITC-conA

C. braarudii, S. apsteinii , C. leptoporus , C. carterae and *E. huxleyi* represent a range of sizes, coccolith morphologies (Figure 5.1), biogeographical distributions and cover a range of clades from the coccolithophore phylogeny (Liu *et al.*, 2010). In order to examine the distribution of extracellular polysaccharides, we first used fluorescent conjugates of the lectin Concanavalin A (conA), which binds primarily to D-mannose and D-glucose residues.

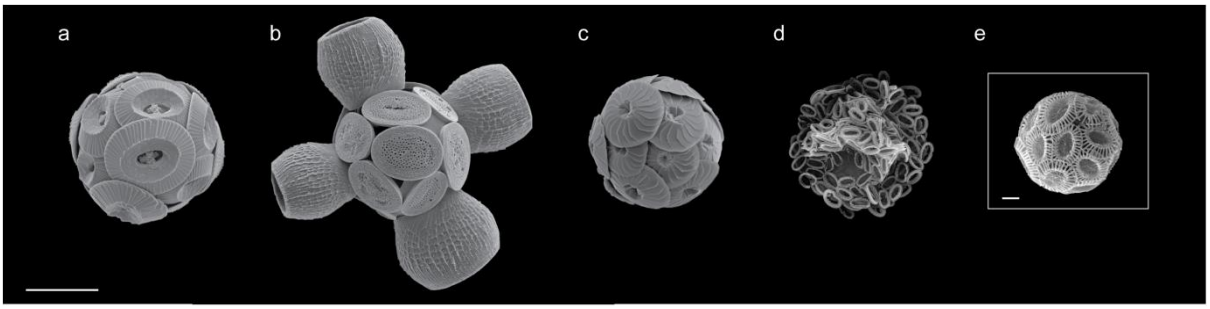

Figure 5.1 Scanning electron microscopy images of coccolithophore species in this study
a) *Coccolithus braarudii*, b) *Scyphosphaera apsteinii*, c) *Calcidiscus leptoporus*, d) *Chrysotila carterae* and e) *Emiliania huxleyi*. Scale bars represent 10 µm (a-d) and 1 µm (e).

FITC-conA bound positively to decalcified cells of all five species (Figure 5.2), indicating that cells from each species are coated in a layer of insoluble polysaccharide containing D-glucose and/or D-mannose residues. Some structural diversity was observed in the polysaccharide layers between species. *C. braarudii* (Figure 5.2a) has a distinctly structured polysaccharide layer, with ellipsoidal intervals in the staining which has previously been reported (Chapter 3: Figure 3.9). Interestingly, this distinctive structural layer was not observed in the closely related species *C. leptoporus*. We observed some irregularities in the staining of the polysaccharide layer of *C. leptoporus* (Figure 5.2b), but these clearly differ from the regularly spaced oval-shaped areas seen in *C. braarudii* and may be a result of natural inconsistencies in the polysaccharide layer. In the other species the polysaccharide formed a smooth consistently stained layer on the cell surface (Figure 5.2c-e).

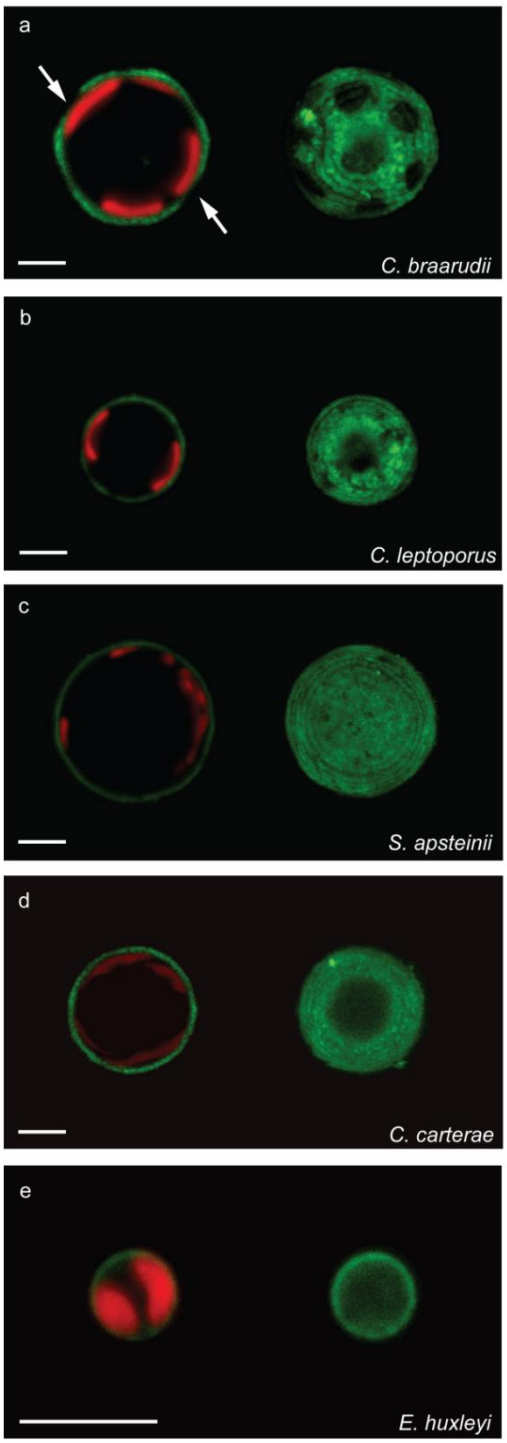

Figure 5.2 Polysaccharide layer found on the cell surface of decalcified coccolithophores
Confocal microscopy imaging of decalcified coccolithophores that were stained with the lectin FITC-conA (green). Chlorophyll autofluorescence is also shown (red). The staining revealed a layer of polysaccharide on the cell surface of all five species. The 2D slice images and 3D reconstructions are shown to reveal the structure of the polysaccharide. *C. braarudii* (a) exhibits ellipsoidal intervals in the FITC-conA staining. *C. leptoporus* (b) shows some irregularities in the polysaccharide layer whereas all other species (c-e) have a smooth consistent layer. Scale bars represent 5 µm.

To investigate the localisation of the insoluble polysaccharide within the coccosphere, FITC-conA was also applied to calcified cells and discarded coccoliths. All five species exhibited positive staining (lectin staining summarised Table 5.2). Images of fully calcified *C. braarudii* and *S. apsteinii* are presented show polysaccharide integrated within the coccosphere (Figure 5.3).

C. braarudii cells revealed staining patterns with similar dimensions to coccoliths. It was not possible to determine whether this is due to polysaccharide coating the coccoliths or the impression of coccolith on the underlying polysaccharide layer. However, imaging of discarded coccoliths indicated that they were positively stained by FITC-conA, indicating an extracellular coating of polysaccharide (Figure 5.3c, Figure 5.1a SEM for comparison). Imaging of calcified *S. apsteinii* revealed the cell body, lopadoliths and discarded muroliths (Figure 5.3b, d) were all positively stained. Interestingly there is no clear murolith staining on the calcified cell but the discarded murolith is positively stained, there may have been some inconsistencies exhibited in the staining in FITC-WGA which highlights the necessity to observe multiple cells and discarded coccoliths.

These observations show the polysaccharide layer with glucose and/or mannose residues surrounds both the cell and the coccoliths, clearly integrated within the whole coccosphere. These observations are consistent with existing literature on *E. huxleyi* and *C. carterae* (Van der Wal, P *et al.*, 1983; van der Wal, P. *et al.*, 1983a).

Table 5.2 Results of polysaccharide lectin staining in coccolithophores

Species	**conA**		**WGA**	
	Calcified	Decalcified	Calcified	Decalcified
Coccolithus braarudii	✓	✓	×	×
Scyphosphaera apsteinii	✓	✓	✓	✓
Calcidiscus leptoporus	✓	✓	×	×
Chrysotila carterae	✓	✓	×	×
Emiliania huxleyi	✓	✓	×	×

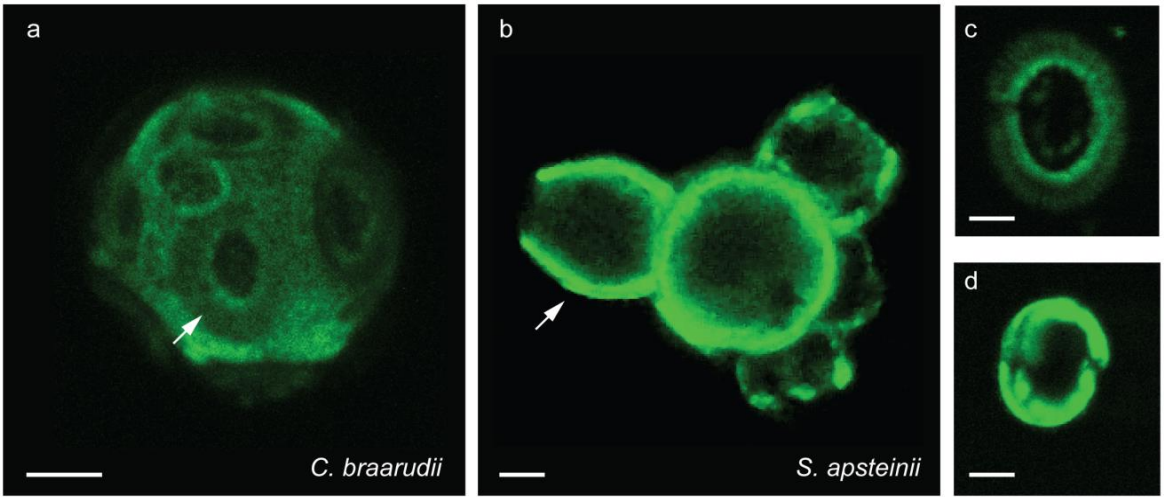

Figure 5.3 Polysaccharide layer associated with coccosphere
Confocal microscopy imaging of calcified coccolithophores *C. braarudii* (a) and *S. apsteinii* (b) that were stained with the lectin FITC-conA. The polysaccharide is clearly shown associated with the coccospheres (a-b) and discarded coccoliths (c-d) in both species. Scale bars represent 5 µm (a-b) and 2 µm (c-d).

In contrast to untreated coccoliths, we observed no fluorescent staining of *C. braarudii* coccoliths treated with sodium hypochlorite to remove organic material. (Appendix IV: Figure IV.1), indicating that the lectin binds specifically to the polysaccharides associated with the cell body and the coccosphere. As an additional control, we utilised Texas Red-conA to ensure there was no non-specific binding due to the fluorophore conjugated to the lectin. We observed identical staining patterns in cells treated with FITC and Texas Red conjugates of conA (Appendix IV: Figure IV.2).

5.4.2. Localisation of extracellular polysaccharides using lectin FITC-WGA

Wheat germ agglutinin (WGA) binds to N-acetyl-D-glucosamine and sialic acid residues in polysaccharides. Interestingly, FITC-WGA staining was negative in all species except *S. apsteinii* (Figure 5.1b), which exhibited positive staining when both calcified (Figure 5.4a, b) and decalcified (Figure 5.4c, d). WGA clearly stained lopadoliths and muroliths, as well as a layer surrounding the cell body. In decalcified cells, the gentle decalcification process occasionally left polysaccharide remnants that closely resemble the shape of the lopadoliths (Figure 5.4c, d). It is likely that these are polysaccharides associated with the coccoliths prior to decalcification, either externally and/or intracoccolith. This staining pattern suggests that *S. apsteinii* produces a polysaccharide that contains N-acetyl-D-

glucosamine and/or sialic acid residues and therefore differs in composition from those of the other four species.

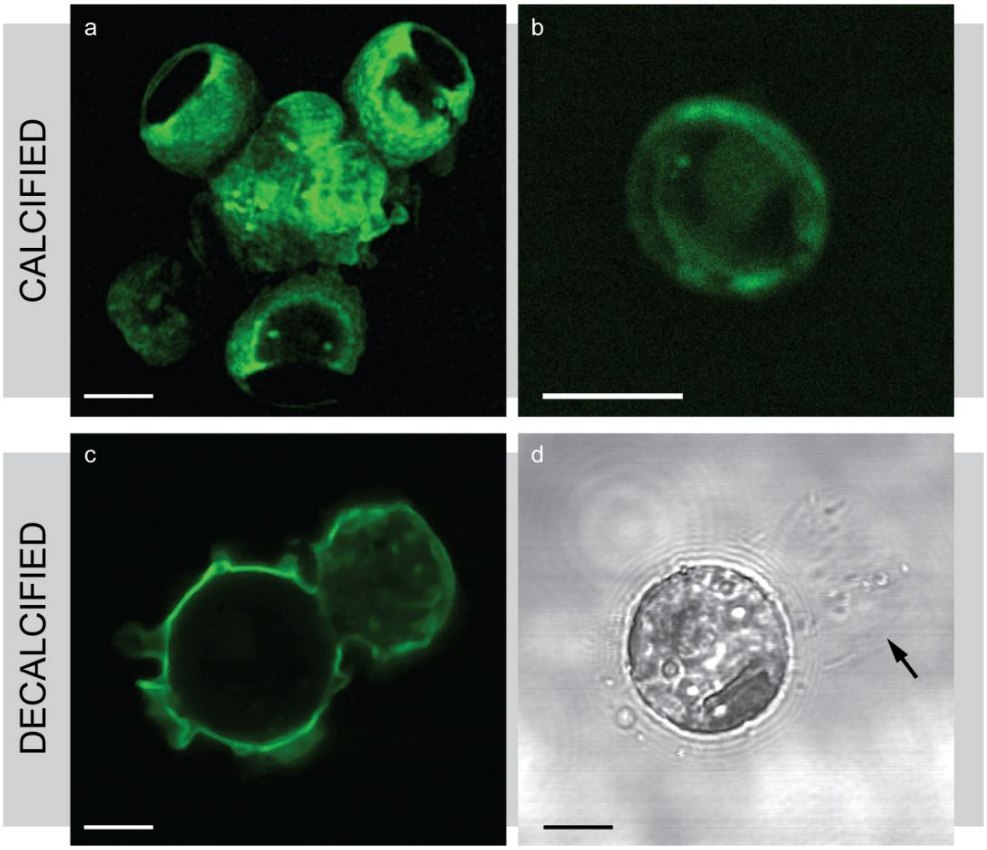

Figure 5.4 Wheat germ agglutinin staining in *S. apsteinii*
Confocal microscopy imaging of FITC-WGA staining in *S. apsteinii* revealed positive staining on a fully-calcified cell (a) and a discarded murolith (b). The decalcified images (c-d) show positive FITC-WGA staining of a polysaccharide residue that closely resembles the shape of a lopadolith (c), the polysaccharide can also be seen (arrow) in the accompanying transmission image (d). Scale bars represent 5 µm.

To identify if the two lectins applied to *S. apsteinii* localised to different regions of the extracellular polysaccharide, we utilised FITC-conA and Texas Red-WGA simultaneously on the same sample of decalcified cells. We found that both lectins positively stain the cell body (Figure 5.5). The data also shows that the residual-lopadolith polysaccharide stained positive for Texas Red-WGA but not FITC-conA. Although the FITC-conA stained the calcified lopadoliths we did not visualise any residual-lopadolith polysaccharide staining in any FITC-conA decalcified *S. apsteinii* cells. It is possible that the residual-lopadolith polysaccharides were not present but it is also possible that only FITC-WGA

stains these structures. The WGA positive residual-lopadolith polysaccharides may be intracoccolith polysaccharides that are revealed after decalcification.

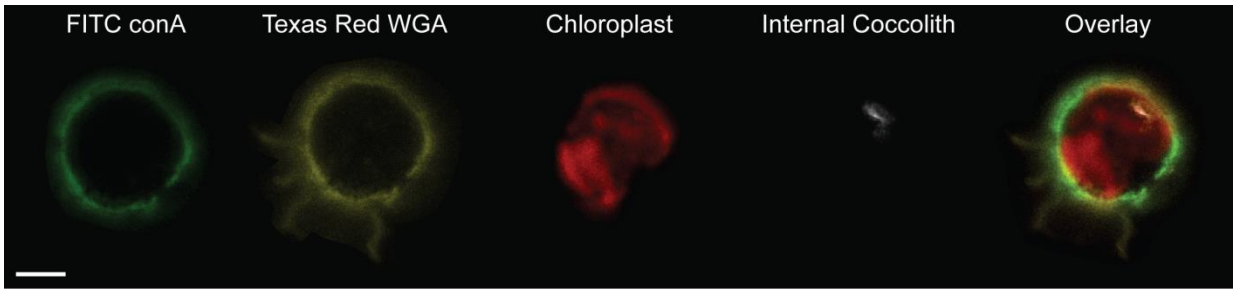

Figure 5.5 Differential localisation of lectin stains in *S. apsteinii*
Confocal microscopy imaging of FITC-conA and Texas Red-WGA staining in *S. apsteinii*. Both lectins localise around the cell body but on Texas Red-WGA is found on the residual-lopadolith polysaccharides (yellow). Chlorophyll autofluorescence and internal coccolith are also shown. Scale bar represents 5 µm.

5.4.3. Polysaccharide extraction and composition analysis

To examine the composition of the extracellular coccolith polysaccharides, coccoliths were isolated from the cell debris and the ethanol insoluble polysaccharides were extracted. To ensure isolation of targeted polysaccharide during the coccolith preparation, FITC-conA was utilised to stain coccoliths and extracted polysaccharide at various stages throughout the process: following lysis of the cells to release the coccoliths; following density centrifugation and removal of Percoll®; and following the ethanol extraction procedure. The staining data (Figure 5.2, Figure **5.3**) suggests that the polysaccharide coating the cell body and the coccoliths may be the same. All samples were positively stained by FITC ConA confirming the presence of the target polysaccharide throughout the extraction process (Appendix IV: Figure IV.3).

Nine sugars were identified in reference to known standards in the GC-MS data (Figure 5.6). Previous analysis of *E. huxleyi* also identified a similar polysaccharide composition when analysing water-soluble CAPs (Fichtinger-Schepman *et al.*, 1979; Fichtinger-Schepman *et al.*, 1981). There were some monosaccharides that were relatively consistent between species, xylose, arabinose (both pentose monosaccharides) and rhamnose (a hexose sugar). In others there were clear differences, notably glucose which made up a higher proportion of known sugars *C. braarudii* (28.9 % ±0.7 SE) and *S. apsteinii* (33.3% ±3.5 SE) than *E. huxleyi* (19.7% ±1.3 SE) and *C. carterae* (19.9%

±6.1 SE). Two monosaccharides are of particular interest, glucuronic acid and galacturonic acid monohydrate, as they are uronic acids, a charged component found in other CAP studies (De Jong *et al.*, 1976; Lee *et al.*, 2016) and known to modulate the precipitation of calcite (Borman *et al.*, 1982; Ozaki *et al.*, 2007; Kayano & Shiraiwa, 2009). Glucuronic acid and galacturonic acid monohydrate have been combined to calculate the total uronic acid (TUA) proportion of known sugars. TUA made up a higher proportion of known sugars in *E. huxleyi* (9.31% ±1.6 SE) and *C. carterae* (6.2% ±1.8 SE) compared to *C. braarudii* (1.51% ±0.8 SE) and *S. apsteinii* (0.8% ±0.5 SE).

The GC-MS analysis identified both glucose and mannose residues in all species (Figure 5.6) which corresponds with the FITC-conA lectin staining seen in calcified cells (Figure 5.3, Figure 5.4). It was not possible to identify the N-acetyl-D-glucosamine or sialic acid that the FITC-WGA binds to as no standards were available at the time of analysis.

Further analysis is needed to resolve this likely monosaccharide component of the S. apsteinii coccolith polysaccharide.

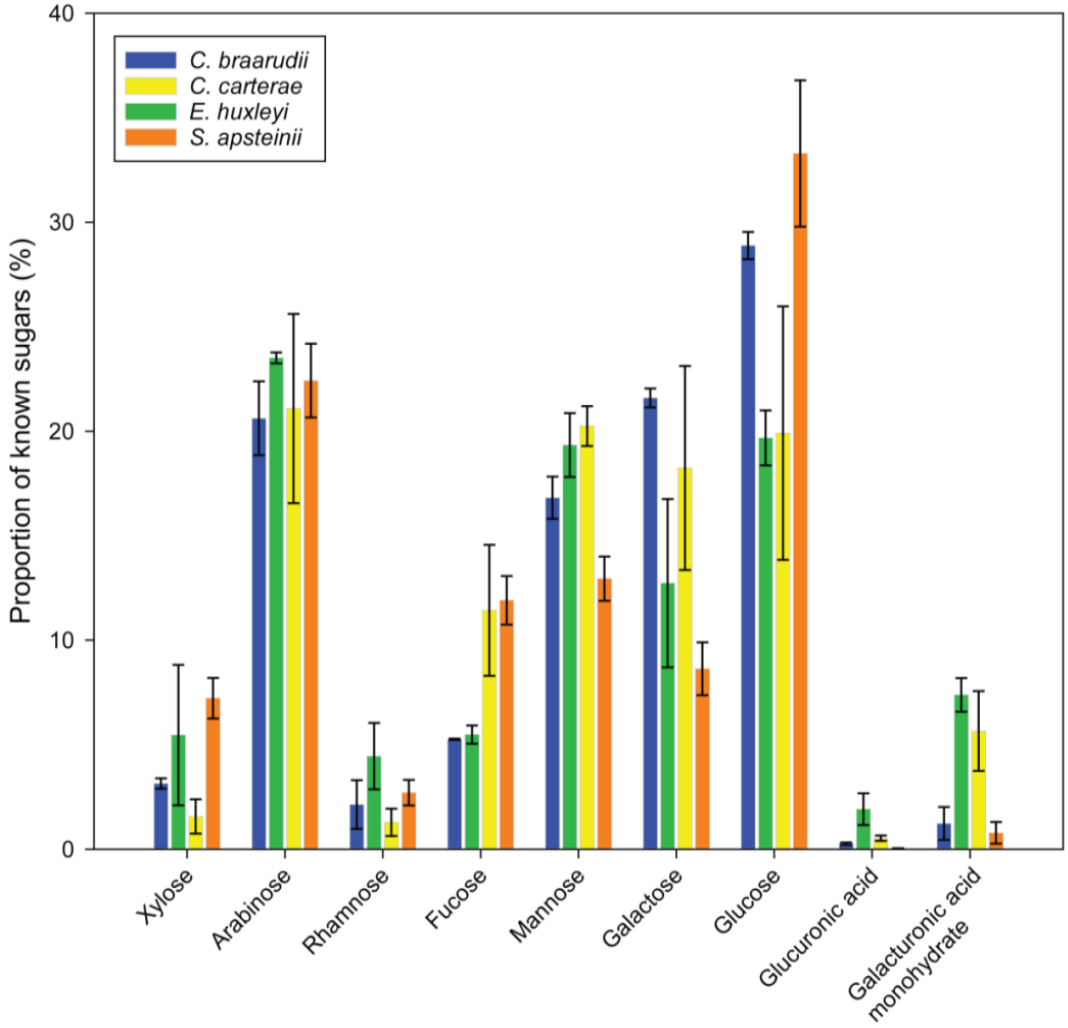

Figure 5.6 Coccolith polysaccaride composition
GC-MS analysis identified known monosaccharides in the insoluble coccolith polysaccharide fraction, when compared to a known standard. The monosaccharide content is present as proportion of known sugars. The data demonstrates variation in monosaccharide content between species. Error bars denote standard error.

5.4.4. Production and role of extracellular polysaccharides in *C. braarudii*

We chose to examine the nature of the extracellular polysaccharide surrounding *C. braarudii* cells in greater detail, due to the distinctive polysaccharide morphology observed in decalcified cells (Figure 5.2a). As these features are preserved even after decalcification, it suggests that the polysaccharide layer in *C. braarudii* possesses structural properties that may contribute to the organisation of the coccosphere. Figure

5.7a shows that in partially decalcified cells the coccoliths correspond exactly to regions unstained by FITC-conA. However, the outer diameter of the coccoliths is considerably larger than the unstained region, which exhibited a similar diameter to the baseplate of the coccolith. It is possible that the movement of the coccoliths through the polysaccharide layer or the positioning within the coccosphere in *C. braarudii* causes the formation of the ellipsoidal structures visualised in the FITC-conA staining.

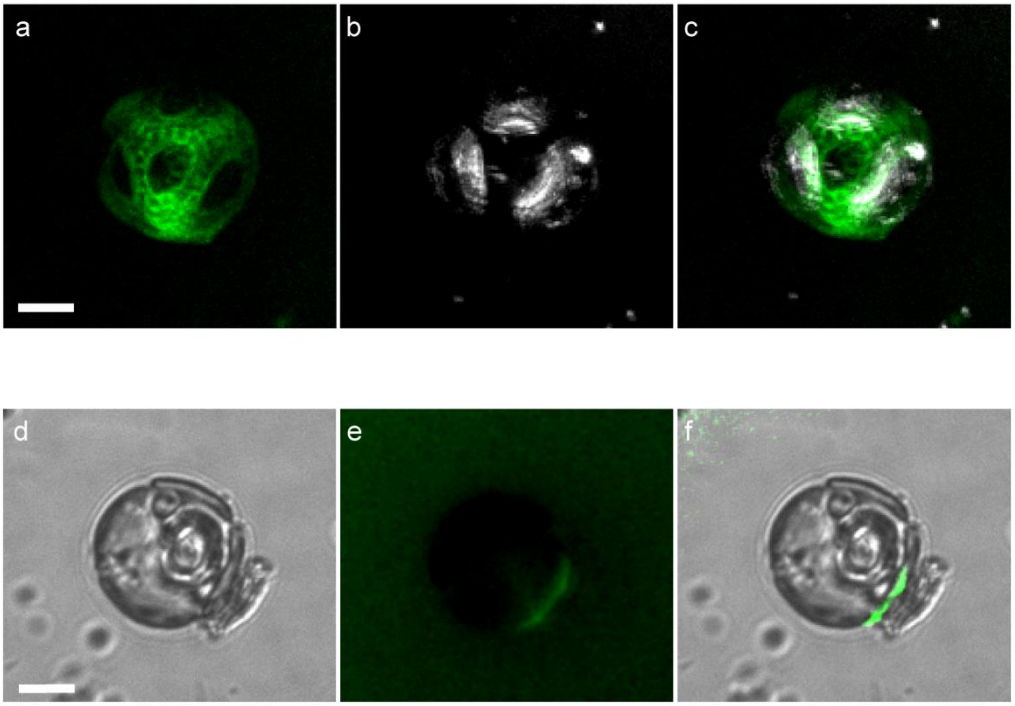

Figure 5.7 The extracellular polysaccharide is associated with the coccoliths in *C. braarudii*
FITC-conA stained partially decalcified *C. braarudii* images show the ellipsoidal intervals in staining (a) and the coccoliths (b). When the two are overlayed (c), the coccoliths correspond extactly to the regions unstained by FITC-conA. Previously decalcified *C. braarudii* with the extracellular polysaccaride layer removed were allowed to recalcify (d). Newly produced FITC-conA stained polysaccaride (e) is localised on the underside of the newly produced coccolith (f).

Further imaging of decalcified cells demonstrated that a small proportion of cells have lost the polysaccharide layer, presumably due to the experimental manipulations associated with decalcification (Appendix IV: Figure IV.4a-d). Several cells were observed where the polysaccharide layer was partially detached (n=3), allowing us to confirm that the polysaccharide layer possesses considerable structural integrity even when dissociated from the cell (Appendix IV: Figure IV.4e-f).

The occurrence of decalcified cells lacking a polysaccharide layer allowed us to examine how this layer was formed during coccolith secretion. When these cells were allowed to re-calcify, we found that the newly produced coccoliths exhibited a localised layer of FITC-conA stained polysaccharide on the underside of the coccolith (Figure 5.7e-f). The data suggests that the insoluble polysaccharide is produced internally and extruded with the coccolith, an observation that correlates with previous polysaccharide studies (Van der Wal, P *et al.*, 1983; Van der Wal, P. *et al.*, 1983b; Marsh, 1994). The polysaccharide layer therefore appears to be formed by the aggregation of polysaccharides secreted with each coccolith, rather than pre-formed as a complete layer. The close association of polysaccharide with the underside of the coccolith may indicate that these polysaccharides are involved in adhering the coccoliths to the cell surface, aiding the formation and structure of the complete coccosphere.

Like most phytoplankton cells, the surface area of a coccolithophore cell increases substantially as its volume increases throughout the cell cycle. The cell must therefore continuously produce new coccoliths to ensure that its surface area remains fully covered. This suggests that each new coccolith must be secreted through the existing polysaccharide layer, which must therefore retain a substantial flexibility. To determine whether coccoliths were secreted through the polysaccharide layer, we imaged coccolith secretion in decalcified cells in which the polysaccharide layer remained intact. The newly-secreted coccoliths were observed external to the polysaccharide layer, indicating that they can pass through the layer. In addition, coccoliths produced in these cells were coated with polysaccharide on both the underside and the topside of the coccolith (Appendix IV: Figure IV.5). We hypothesise that the coccolith is coated with polysaccharide as it moves through the existing polysaccharide layer on the cell surface.

5.5. Discussion

Our results demonstrate that coccolithophores are coated in a layer of insoluble polysaccharide that differs between species in structure and composition. We suggest that this polysaccharide is extruded with the coccoliths, plays a role in the adhesion of the coccoliths to the cell surface and contributes to the organisation of the coccosphere. While these polysaccharides are clearly associated with the coccosphere, they may be distinct from the polysaccharides identified in previous studies and commonly referred to as coccolith associated polysaccharides (CAPs).

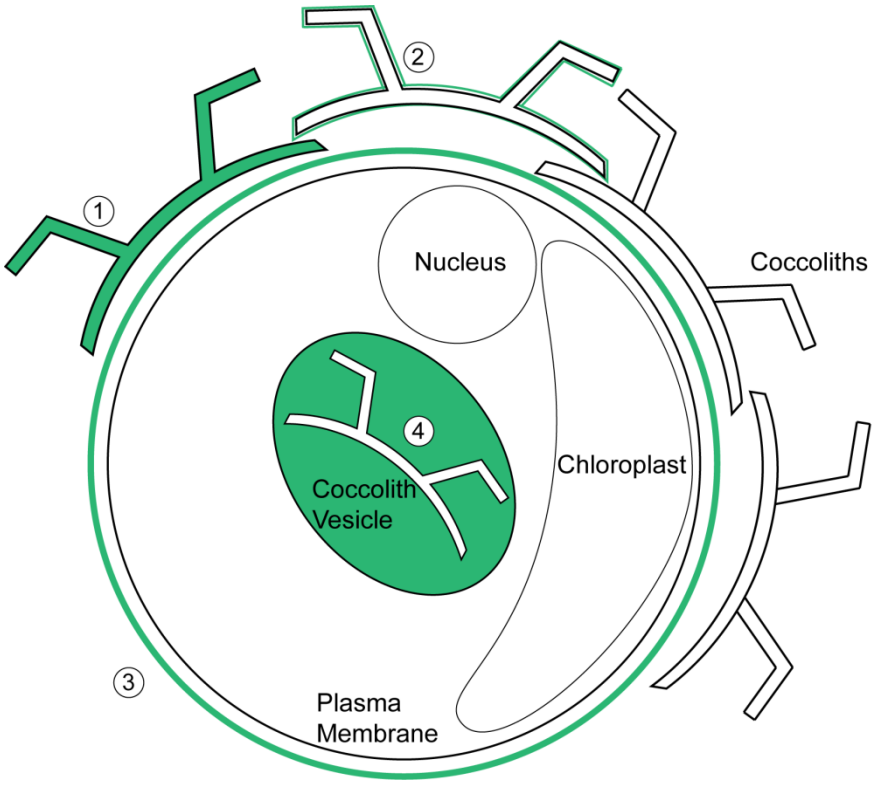

Figure 5.8 The localisation of coccolith associated polysaccharides
The localisation of coccolith associated polysaccharides identified in previous research and this study: intracoccolith (1), coating the coccolith surface (2), on the cell surface (3) and associated with the coccolith vesicle (4).

Previous research has focussed on the ability of CAPs to modulate the precipitation of calcite within the coccolith vesicle, with little research conducted on extracellular role of polysaccharides. Here we show that there is a large proportion of polysaccharide extruded with the coccolith that coats the coccosphere. Combining our research with previous studies we find that the term CAPs potentially includes polysaccharides in four

distinct locations (summarised Figure 5.8). These are intracoccolith polysaccharides found within the coccolith structure; polysaccharides coating the surface of coccoliths; polysaccharides covering the cell body; and polysaccharides within the coccolith vesicle actively involved in the modulation of calcite precipitation. Interestingly, our observations of *C. braarudii* suggest that these extracellular CAPs may originate from the coccolith vesicle as they are extruded with the newly formed coccolith. The biochemical characterisation conducted here indicates the ethanol-insoluble extracellular polysaccharides studied here may have similar components to the water-soluble polysaccharides that play a role in calcite precipitation (Fichtinger-Schepman *et al.*, 1979; Fichtinger-Schepman *et al.*, 1981; Borman *et al.*, 1982; Ozaki *et al.*, 2007; Kayano *et al.*, 2011).

The uronic acid residues identified by GC-MS analysis are of interest as they have been shown to modulate the precipitation of calcite (Borman *et al.*, 1982; Ozaki *et al.*, 2007). In this study the uronic acid proportion of total sugars (in the form of glucuronic acid and galacturonic acid monohydrate) was higher in *E. huxleyi* and *C. carterae* in comparison to *C. braarudii* and *S. apsteinii*. A similar result has been observed previously whereby *E. huxleyi* exhibited a higher uronic acid content in the soluble intracoccolith CAP to *Coccolithus pelagicus* and *C. leptoporus* (Lee *et al.*, 2016). The uronic acid content in *E. huxleyi* was found to correlate with carbon availability and the extent of calcification exhibited by the morphotypes studied, highest in R and A (RCC1216 and RCC1256 respectively) and lowest in type B (RCC1212), here we examined RCC1516 which is morphotype A. This was not the case in other species, whereby the more heavily calcified genus *Coccolithus* (Daniels et al., 2014) had a lower uronic acid content than the more lightly calcified *E. huxleyi* both in Lee *et al.* (2016) and in this study. It appears counter intuitive that more heavily calcified species would have less calcite precipitation modulation residues but it is possible that uronic acid may play a more significant role in *E. huxleyi* calcification than the other species studied. How this differs is not yet understood. Another study found sulphate esters in soluble polysaccharides extracted from *E. huxleyi* coccoliths (Fichtinger-Schepman *et al.*, 1979; Fichtinger-Schepman *et al.*, 1981). Sulphate esters also carry a negative charge and therefore may also bind to Ca^{2+} ions. It is also important to note that Lee *et al.* (2016) and Fichtinger-Schepman *et al.* (1981) have isolated different polysaccharide fractions to this study (soluble intracoccolith, soluble coccolith respectively). It is possible that the polysaccharides recovered within the insoluble external coccolith polysaccharide fraction isolated here

are also involved in calcite modulation or that we have extracted a combination of these polysaccharide fractions. We do not yet know the consistency of composition between all polysaccharide fractions; it would be very interesting to compare the composition from all localisations in the future (Figure 5.8).

It is probable that the insoluble layer of polysaccharide found on the exterior of the coccolith imparts some kind of protection from the environment. A previous study suggests the organic covering prevents dissolution of the calcite in unfavourable conditions (Henriksen, Karen *et al.*, 2004). Our data also suggests the stability of the polysaccharide over time in *C. braarudii* as the layer maintains its structure when the coccoliths are dissolved and when the polysaccharide itself is removed from the cell body. This is supported by studies that found polysaccharides extracted from coccolith-containing ancient sediments were still functional in protecting coccoliths from dissolution (Sand *et al.*, 2014). In future ocean conditions the potential for dissolution of calcite structures will increase (Tyrrell *et al.*, 2008), whether these polysaccharides are able to reduce this pressure in coccolithophores should be considered and explored.

In addition to protection from dissolution, extracellular polysaccharide appears to play an adhesive role in securing newly produced coccoliths to the cell surface. The presence of polysaccharide coating the cell body in all species examined suggests that polysaccharides are likely to perform this role in all coccolithophores. These adhesive properties are likely to cover a range of coccosphere morphologies from a single layer of interlocking placoliths in *C. braarudii*; a dimorphic arrangement of non-interlocking coccoliths in *S. apsteinii*; and may even facilitate unusual coccosphere arrangements such as the many layers of coccoliths that can encase *E. huxleyi* under certain conditions (Paasche, 2001). The evidence presented here suggests the extracellular polysaccharide plays an important organisational role in the different coccospheres.

C. braarudii exhibited a distinct structural polysaccharide whereby the ellipsoidal intervals in lectin stained polysaccharide are thought to be formed by the presence of coccoliths within the coccosphere, evidenced here and suggested in previous work (Chapter 3: Figure 3.9). It is surprising that the closely related *C. leptoporus* exhibits no definitive structure similar to *C. braarudii* (Liu *et al.*, 2010) as it has similar structured coccosphere with a similar number of coccoliths per cell (~ 15 coccolith cell^{-1}) (Langer *et al.*, 2006b). The data presented here shows that the structured polysaccharide is associated with the organisation of the coccoliths in *C. braarudii,* a species which always

maintains a complete coccosphere in healthy cultures (Chapter 3) (Taylor *et al.*, 2007). The extracellular polysaccharide described here is clearly important in maintaining the coccosphere which in turn is essential for successful growth and cell division (Chapter 3), the polysaccharide clearly plays an important role within this species.

The smooth nature of the polysaccharides seen on other species' cell body may be due to the greater turn-over of coccoliths or dynamic nature of their coccospheres. For example, *E. huxleyi* produces between 23-36 coccoliths per cell in optimal growing conditions and as many as 20 of these are discarded (Paasche, 1998; Paasche, 1999; Paasche, 2001). In contrast *C. braarudii* cells are covered with 8-20 coccoliths (Gibbs *et al.*, 2013) and typically discard less than one coccolith per cell in optimal growing conditions (Durak *et al.*, 2016). *C. carterae* produces a high number of small coccoliths (Figure 5.1) and has a comparable cell size to species bearing larger coccoliths. Both *E. huxleyi* and *C. carterae* are likely to have many more coccoliths move through the polysaccharide on the cell body than *C. braarudii*. *S. apsteinii* has a dynamic coccosphere because of its dimorphic coccolith arrangement. The ratio of lopadoliths to muroliths has been shown to shift in varying light intensities (Drescher *et al.*, 2012). In this species, the adaptive coccosphere may result in a higher coccolith turnover and be a contributing factor why no structured polysaccharide is observed.

Diversity in the composition and functional roles of CAPs between species is important when the energetic cost of polysaccharide production is considered. Previous research assessing the cost/benefit of calcification in coccolithophores has endeavoured to calculate the cost of producing these polysaccharides. Recent estimates suggest that the single intracoccolith CAPs produced by *E. huxleyi* and *C. braarudii* require 7% and 0.2% of total cellular fixed organic carbon respectively (Monteiro *et al.*, 2016). In contrast, production of multiple CV-associated CAPs in *C. carterae* was calculated to cost 50% of the total fixed organic carbon, a significantly higher cost of production (Brownlee & Taylor, 2004). The large range in these calculations is due to different assumptions over the role of CAPs. The former estimates are based primarily on the amounts of intracoccolith CAPs recovered from purified coccoliths, whereas the latter calculation assumes CAPs are involved in the stoichiometric delivery of Ca^{2+} to the coccolith vesicle. Our results indicate that the cost of extracellular polysaccharide must also be considered in future calculations. This is clearly crucial as there is an abundance of extracellular

polysaccharide produced by each species examined here and no true estimate of cost can be achieved without considering the whole CAP produced.

In this study we have expanded on the current understanding of CAPs and added to their biological importance within coccolithophore calcification. CAPs are a group of polysaccharides involved in coccolith precipitation, coccolith adhesion, organisation and protection of the coccosphere. It is also likely that greater diversity and function remains to be fully understood. However, it is imperative that their abundance and role should be taken in to account in considerations of energy budgeting and response of coccolithophores to future ocean conditions.

6. General Discussion

6.1. Introduction

This thesis set out to identify differences in mechanisms related to calcification between coccolithophore species. Previous work had largely focussed on the globally abundant *Emiliania huxleyi* but less focus had been given to other ecologically important species. The use of *Coccolithus braarudii* and other species in this thesis revealed some contrasting and interesting revelations in coccolithophore biology.

Firstly the findings highlighted the importance and organisation of the coccosphere for growth and cellular fitness in *C. braarudii*. Additionally these data provided additional insight into the relationship between photosynthesis and calcification, informing the discussion on the role of calcification. A novel requirement for Si in heterococcolith calcification in species with Si transporters (SITLs) adds to the components of the calcification mechanism known to the field. Moreover, novel observations of cell division and coccolith associated polysaccharides (CAPs) add to the understanding of coccolithophore biology. All these findings (summarised Figure 6.1) have implications for the evolution and current ecology of coccolithophores.

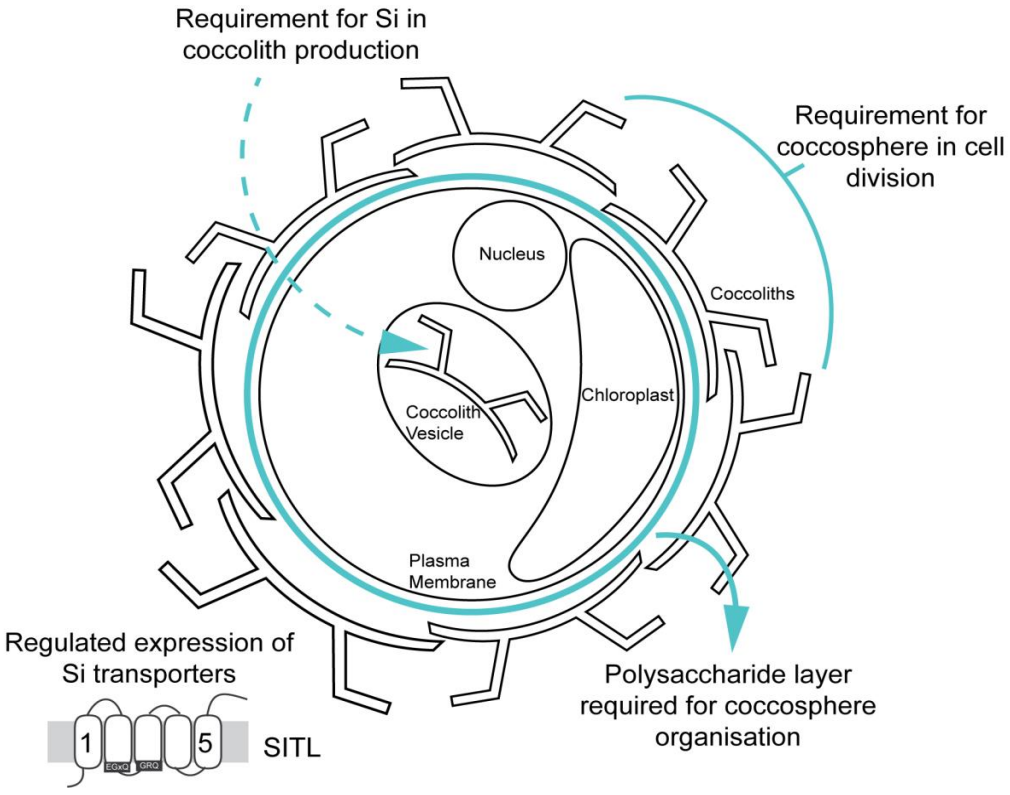

Figure 6.1 Key Findings
Cell schematic highlighting the key findings in *C. braarudii* presented in this thesis.

6.2. Discussing the role of calcification

6.2.1. Importance of the coccosphere in *C. braarudii*

The data presented here adds new significance to the necessity and organisation of the coccosphere in *C. braarudii* through potential protective and mechanical roles. Although it is known that some coccolithophores do not need to calcify, a coccosphere is considered a crucial feature of diploid coccolithophores in the environment. Diploid cultures that no longer calcify were invariably calcified on initial isolation (Paasche, 2001; Marsh, 2003). The suggested original evolutionary role of calcification in coccolithophores is to infer protection upon the cells but in modern coccolithophores it may also infer additional benefits depending on species (Dixon, 1900; Monteiro *et al.*, 2016). Other studies have also suggested protection as a crucial role for coccosphere maintenance, even showing the mechanical-protection capabilities of the *E. huxleyi* coccosphere (Jaya et al., 2016*)*. Additional protective characteristics were observed during cell division, whereby the coccoliths extend protectively over the dividing cells until the cytokinesis event has occurred. However, the current study did not demonstrate any direct protective role of the coccoliths but the obligate requirement for a complete coccosphere for growth in *C. braarudii* would infer any resulting protection upon the cell.

The concept of the importance of the coccosphere in *C. braarudii* is supported by the equal division of the parental coccoliths between daughter cells, observed here and in previous studies whereby *C. braarudii* was recorded as having 16 coccoliths prior to division, and 8 following (Gibbs *et al.*, 2013; Sheward *et al.*, 2014). The coccosphere also plays an important mechanical role during the process of cell separation following division. Without an intact coccosphere cells remain attached following an initial round of cell division and a subsequent cell division arrest follows, leaving cells in a paired formation. Across the coccolithophores the coccosphere is a diverse feature encompassing variable coccolith types, dimorphic arrangements and degrees of coverage (Young *et al.*, 2003) and more research is required to explore the widespread reliance on an intact coccosphere. However, as very few lineages of coccolithophore grow in laboratory culture in a non-calcified form (Appendix II: Table II.2) then we can hypothesise that the requirement may be relatively widespread.

This study has also identified an important role for extracellular polysaccharides in the organisation of the coccosphere. It has expanded upon the definition of coccolith-associated polysaccharides (CAPs) to include those polysaccharides that are extruded with the fully formed coccoliths and adhere the coccoliths to the cell surface. When using low Ca^{2+} as a calcification disruption technique we suggested a disruption of the production of polysaccharide may be partly responsible for the breakdown in the calcification mechanism. A previous study in *Chrysotila haptonemofera* (formerly *Pleurochrysis*) also suggested low Ca^{2+} conditions reduce polysaccharide production (Katagiri *et al.*, 2010). Since the extracellular CAP is integral in coccosphere organisation and the coccosphere is integral for cellular fitness in *C. braarudii*, any disruption in the former will negatively impact the cell.

6.2.2. Calcification as a potential carbon concentrating mechanism

Photosynthesis, and more specifically carbon concentrating mechanisms (CCMs), have also been suggested as the driving role behind calcification. Algal CCMs function by providing CO_2 to the active site of Rubisco in aquatic environments where CO_2 is limiting (Reinfelder, 2011; Falkowski & Raven, 2013). There is some evidence for CO_2 limitation in coccolithophores as studies have observed a direct response to moderately higher CO_2 concentrations causing increased growth and calcification in laboratory cultures of *E. huxleyi* and *G. oceanica* (Sett *et al.*, 2014). This implies that CO_2 availability is limiting growth in coccolithophores. Additionally, a recent study found that increasing CO_2 has prompted the increase in probability of coccolithophores occurrence in the North Atlantic from approximately 2% in 1965 to 20% in 2010 (Rivero-Calle *et al.*, 2015). However, this study predicts that the CO_2 induced increase in growth rate will level out at 500 ppm. *E. huxleyi* is known to have a low affinity CCM (Reinfelder, 2011) and is able to switch between CO_2 and HCO_3^- as a primary carbon source (Kottmeier *et al.*, 2016). Since calcification produces protons (H^+) as a by-product of calcite precipitation if HCO_3^- is used as the external substrate, these H^+ could be used to drive the dehydration of HCO_3^- to CO_2 (Paasche, 2001).

The data presented here does not support the hypothesis that calcification functions as a CCM in *C. braarudii* as we observed no reduction in photosynthetic activity when calcification was severely impacted. These findings correlate with existing research and support the conclusions from recent literature. As the majority of other studies have been conducted in *E. huxleyi*, supporting information in another species is an important addition.

Studies have shown that it is possible to inhibit calcification through reducing external Ca^{2+}, as was done here, whilst photosynthesis and growth remains unaffected (Herfort *et al.*, 2002; Trimborn *et al.*, 2007; Leonardos *et al.*, 2009). Bach *et al.* showed that by manipulating the external carbonate chemistry rather than providing a source of dissolved inorganic carbon (DIC) for photosynthesis, that calcification appeared to be in direct competition with photosynthesis for available DIC. These results indicate calcification does not function as a CCM but that the two may utilise the same intracellular pool of DIC in *E. huxleyi* (Buitenhuis *et al.*, 1999; Riebesell *et al.*, 2000; Zondervan *et al.*, 2001; Bach *et al.*, 2013). Other investigations have also shown that this is likely in *C. braarudii* (Rickaby et al., 2010) and that *C. carterae* was also observed to have a decreased level of calcification at low available DIC (Zhou *et al.*, 2012). However, *Gephyrocapsa oceanica,* a closely related species to *E. huxleyi* (Liu *et al.*, 2010), was found to have independent pools of DIC for calcification and photosynthesis when examined using carbon isotopic fractionation (Rickaby *et al.*, 2010). The further exploration of these mechanisms and expansion into other species will greatly progress the field and clarify the differences described here. Understanding these mechanisms will also be important as *p*CO2 increases in the future.

6.3. Introducing Si as a potential component to the calcification mechanism

The calcification mechanism in coccolithophores requires the transport of calcification substrates from the environment to specially derived organelles for the formation of the coccoliths. HCO_3^- and Ca^{2+} are transported from the surrounding seawater into the coccolith vesicle (CV). Certain candidate putative transporter proteins have been identified, in the form of HCO_3^- -Na^+ co-transporters and -Cl^- antiporters (Buitenhuis *et al.*, 1999; Herfort *et al.*, 2002; Mackinder *et al.*, 2010). Ca^{2+} is thought to be transported into the cell through ion channels down a strong Ca^{2+} gradient, it is then proposed to be actively transported into the CV (or precursor compartment) with Ca^{2+}/H^+ antiporters which are likely to operate at intracellular membranes to bring about loading of Ca^{2+} (Mackinder *et al.*, 2010; Mackinder *et al.*, 2011; Holtz *et al.*, 2013). Subsequently, nucleation of calcite crystals occurs in a proto-coccolith ring around an organic base-plate scale. The formation of calcite is thought to be strongly regulated by CAPs and specific proteins (Van der Wal, P. *et al.*, 1983b; Marsh, 2003; Kayano & Shiraiwa, 2009; Hirokawa, 2013; Gal *et al.*, 2016). The CAPs, CV and surrounding cytoplasmic structures are thought to shape the coccoliths into their species-specific form (Young *et al.*, 1999).

Once the coccolith is fully formed, the CV fuses with the plasma membrane to extrude the coccolith onto the cell surface.

Si and Si transporters have been identified as new components that appear to be directly involved in the calcification mechanism in some species of coccolithophore. Through extensive germanium (Ge) cell physiology experiments and SITL expression studies it was possible to identify that Si is likely involved with the heterococcolith calcification in diploid coccolithophores and as a result, we can confidently conclude that SITLs are strong candidates as a calcification-related genes in *C. braarudii*. Further work is required to fully elucidate the role, one such step that would take us closer to understanding would be the mass-spectrometry analysis of the Si content of coccoliths and whether this differs between species with and without SIT/Ls, as we know it has already been identified in *S. apsteinii* lopadoliths (Drescher *et al.*, 2012).

Previous studies into calcification-related genes have been problematic as there is a significant lack of genetic manipulation tools for any coccolithophore species. As a result currently much data supporting molecular mechanisms of calcification is speculative or correlative. However, progress has been made in the identification of potential calcification relevant genes in *E. huxleyi* including GPA, a Ca^{2+}-binding protein associated with CAPs (Corstjens *et al.*, 1998; Wahlund *et al.*, 2004; Quinn *et al.*, 2006); carbonic anhydrases (Quinn *et al.*, 2006); and genes which have been found to be involved in biomineralisation in other organisms (Nguyen *et al.*, 2005). Mackinder *et al.* (2011) combined physiological experiments with gene expression studies to show the upregulation of putative HCO_3^- transporter and a Ca^{2+}/H^+ ion exchanger belonging to the CAX family.

In order to suggest that Si transport is involved specifically in the calcification process we also utilised a multi-disciplinary approach. The availability of the *E. huxleyi* genome (v1) (Nordberg *et al.*, 2013) and the Marine Microbial Eukaryotic Transcriptome Sequencing Project (MMETSP) (Keeling *et al.*, 2014) were pivotal in the analysis of multiple species of coccolithophores, identifying those with and without SITs and SITLs (Durak *et al.*, 2016). Additionally, the sequences extracted from these databases were utilised to design primers for gene expression analysis of query and reference sequences presented here. Finally, combining physiological culture based studies with the gene expression analysis enabled the confident identification of the requirement for Si in heterococcolith calcification. Although it is possible that Si does have additional roles in

coccolithophores, the primary impact of Si disruption is an effect on calcification. Therefore it is possible to conclude that Si and SITLs are very likely to be directly involved in the calcification mechanisms. This makes SITs and SITLs the best candidates for a calcification related gene in coccolithophores to date, with the perhaps exception of GPA. This is a surprising revelation to the field of calcification, whereby the transporters of Ca^{2+} and HCO_3^- may have been considered likelier candidates.

6.4. The evolution of calcification

The data presented here identified the requirement for calcification in *C. braarudii* and the need for Si within the calcification process. We know that the Si requirement is more widespread, excluding the Noelaerhabdaceae and Pleurochrysidaceae (Durak *et al.*, 2016). It is also possible to suggest the requirement for calcification may also be more widespread due to the inability of many species of coccolithophore to grow in a non-calcified form in laboratory culture (Figure 6.2). A caveat here is the inability to culture many coccolithophore species and a sufficient number of strains for each. However, these requirements may shed light on the evolution of the calcification process. It is possible that certain clades of coccolithophores retain ancestral requirements and others, such as the Noelaerhabdaceae, may have lost certain limiting calcification features.

6.4.1. Holococcolith formation

A possible example of evolutionary loss of a calcification mechanism is holococcolith production. Holococcoliths are formed by some species of coccolithophore during the haploid life cycle stage but are absent in other species, such as *E. huxleyi* (distribution Figure 6.2). Phylogenetic analyses predicts holococcoliths to have evolved prior to the divergence of the Isochrysidales (the lineage containing Noelaerhabdaceae), which occurred 220 million years ago (MYA) by the earliest estimate (Medlin *et al.*, 2008; Liu *et al.*, 2010). Holococcoliths did not appear in the fossil record until much later (185 MYA) but their fragile structure has been predicted to reduce their preservation in the geological record. Early coccolithophores were also thought to predominantly occur in coastal waters where conditions for preservation in the sediments are unfavourable (Young *et al.*, 2005).Therefore, early emergence cannot be ruled out. The mechanism of holococcolith calcification is thought to be complex but has not yet been fully elucidated (Rowson *et al.*, 1986; Young *et al.*, 1999) and to date, their primary role is not yet known.

It is widely suggested that holococcolith calcification is unlikely to have evolved more than once due to its complexity and it is more likely that the ability has been lost (see Figure 6.2). This loss would have had to occur twice in both a clade of coastal Coccolithales (which includes Pleurochrysidaceae and Hymenomonadaceae) (Young *et al.*, 2005) and in the Isochrysidales (Medlin *et al.*, 2008; Liu *et al.*, 2010).

A driver behind holococcolith gene loss may be a trade-off between the cost of production and the benefits inferred. Haploid life cycle stages are thought to be more tolerant of oligotrophic environments (Houdan *et al.*, 2006) and therefore coccolithophores may switch to the haploid stage to cope in these environments. Species that do not produce holococcoliths may be greater suited to oligotrophic environments as they do not have the energetic cost of holococcolith calcification. However, not enough is known about the ecology and physiology of haploid coccolithophore to have confidence in this hypothesis. More research is needed in this field. To contextualise, holococcolith calcification is a candidate for loss in multiple lineages whereas heterococcolith calcification is only suggested to be lost in one lineage, the Isochrysidales (further discussion section 6.4.3). This observation suggests that the benefits conferred by heterococcolith calcification outweigh the cost inferred whereas in contrast, the benefits may not outweigh the cost of production in holococcolith calcification in the environments that haploid cells inhabit.

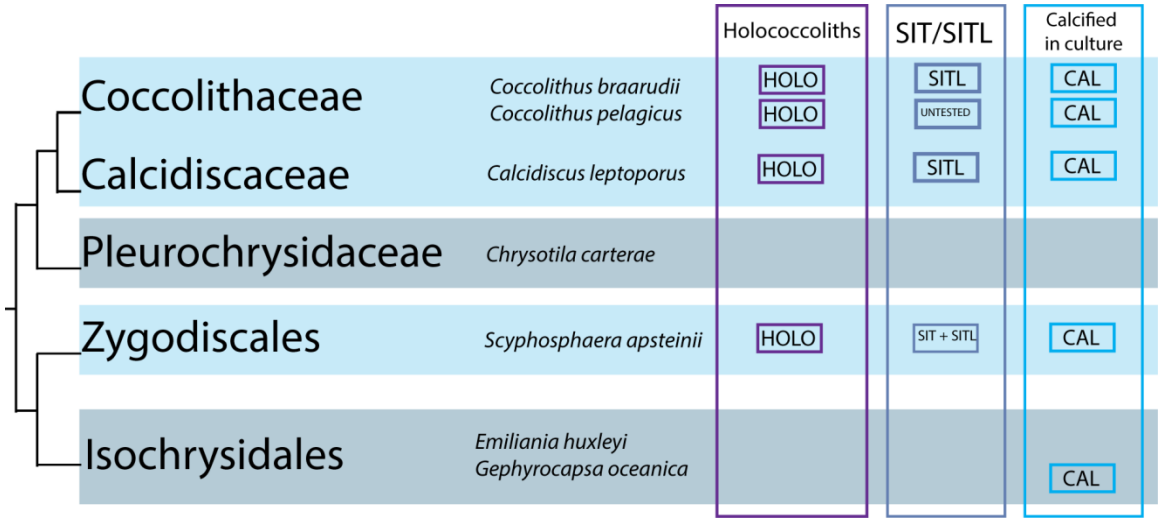

Figure 6.2 Distribution of holococcoliths, Si-transporters and calcification state in culture
A schematic tree based on multiple gene phylogenies (Liu *et al.*, 2010) to show the distribution of holococcolith production in the haploid life stage (Young *et al.*, 2003), Si-transporters (Durak *et al.*, 2016) and calcification state in laboratory culture. Some species, *E. huxleyi* and *C. carterae* are able

to grow in a non-calcified state in laboratory culture with no perceived negative impacts on cellular fitness.

6.4.2. Si transporters

The requirement for Si has potentially been lost in some lineages of coccolithophores (distribution Figure 6.2). The wider scale distribution of SITs and SITLs provides evidence for loss of Si transporters in certain haptophytes. The distribution of Si transporter genes through many major eukaryotic lineages is thought to have originated by either vertical inheritance from the eukaryotic last common ancestor or by multiple horizontal/endosymbiotic gene transfer events (Marron, Alan O. *et al.*, 2016). Either way, multiple occurrences of gene loss of SIT/Ls would have therefore have had to occur to produce the distribution we observe today (Marron, Alan O. *et al.*, 2016). It is possible that the two coccolithophore lineages known not to have Si transporters, Noelaerhabdaceae and Pleurochrysidaceae, have been examples of these multiple gene loss events. This hypothesis is supported by the monophyly in the haptophyte SITs and SITLs. Marron, Alan O. *et al.* (2016) describe the origin of SITs from a gene encoding a five trans-membrane domain protein that diversified into SITLs observed today. The SITLs subsequently duplicated to form SITs, which makes the SITL the ancestral state of the descendant SIT. Coccolithophores are an excellent study organism for the further understanding of SITs and SITLs. They have species with potential gene loss, demonstrated successful expression studies in a species with SITLs, and include a species which has both SITs and SITLs, *Scyphosphaera apsteinii* (Durak *et al.*, 2016).

However, the lack of ability to genetically manipulate coccolithophores is a large hindrance to the field. The ability to target the Si transporters for gene knockout or to express fluorescent fusion proteins in species with SITLs or in *S. apsteinii* where both SITs and SITLs are found would enable the full characterisation of their function and localisation. These approaches have been highly successful in studies on other algae including diatoms (Kroth, 2007) and the green alga *Chlamydomonas* (Hippler, 2017). The recent focus of this yet unachieved goal within the community is both exciting and holds great prospect for advances in the future.

6.4.3. Obligate requirement for calcification

Previously, it has been suggested that within Isochrysidales there is evidence of the independent emergence of calcification as *Isochrysis sp.* are non-calcifying species and

E. huxleyi exhibits differences in calcification mechanisms to other coccolithophores. (De Vargas *et al.*, 2007). This may explain the differing calcification requirement identified between *C. braarudii* and *E. huxleyi* in this thesis. *Emiliania* is a relatively modern genus that diverged approximately 250,000 years ago (Thierstein *et al.*, 1977). More recently, over the last 70,000 years, they have been a dominant component of global phytoplankton communities (Bijma *et al.*, 2001) and have the ability to form vast blooms (Westbroek *et al.*, 1993). The differences in *E. huxleyi* calcification include the absence of an organic base-plate during calcite production (Klaveness, 1972), the absence of holococcoliths in the haploid phase in *E. huxleyi* and closely related *Gephyrocapsa sp.* (Cros *et al.*, 2000) and the ability of *E. huxleyi* to grow in culture in a non-calcified state (Paasche, 1998). De Vargas *et al.* (2007) suggest these features as potential evidence of a genus that is evolving a sophisticated calcification mechanism and as evidence for the multiple independent emergences of calcification. However, it is also important to note that calcification may have been lost by *Isochrysis.* The loss of calcification is perhaps more plausible since it would require a singular event whereas the alternative would require calcification evolving at least twice within the coccolithophores.

More work on the requirement for calcification would help explore these two theories as we do not yet know how widely the obligate requirement for calcification is distributed outside *C. braarudii*. However, the current data suggest that very few examples grow well in a non-calcified state (distribution shown Figure 6.2, and in more detail Appendix II: Table II.2).

6.5. Ecological impacts

6.5.1. Environmental conditions at the time of coccolithophore evolution

It is clear that environmental conditions have played a role in the evolution of calcification in coccolithophores. It has been suggested that the mechanisms for calcification were already in place in the cells and that environmental conditions at the time drove them into novel roles resulting in calcification (Westbroek & Marin, 1998).

Coccolithophores originated in a period of high Ω necessary for calcification due to an oversaturation of carbonate around 220 MYA, this is thought to be a result of erosion and absence of calcification activities at that time (Walker *et al.*, 2002). As a result the availability of HCO_3^- is considered sufficient for coccolithophore calcification. Ca^{2+} was also abundant 220 MYA and at higher concentration than in modern oceans, approximately 15 mM

whereas modern oceans have an average Ca^{2+} of 10 mM (Hönisch *et al.*, 2012). Therefore both components of calcification were readily available.

The available dissolved Si (dSi) at 220 MYA was approximately 1 mM, considerably higher compared to an average of 70 µM in modern oceans and less than 10 µM in surface waters due primarily to proliferation of diatoms (Siever, 1991; Treguer *et al.*, 1995). Coccolithophores are therefore likely to have evolved a requirement for Si in calcification when Si was in abundance. The requirement for Si in calcification may have preceded the emergence of SIT and SITL transporters in coccolithophores. Si, in the form of silicic acid, diffuses across membranes at concentrations >30 µM. Coccolithophore SITL transporters may have evolved in parallel with the decreasing availability of [dSi] and the evolution of the diatoms 140 MYA (Gersonde & Harwood, 1990). The SITLs may have evolved to cope with this reduction and transport the required Si for calcification. It has also been proposed that Si transporters evolved to regulate intracellular Si (Marron, Alan O. *et al.*, 2016), however it is not currently clear how this would work mechanistically since modern Si transporters operate as influx carriers driven by Na^+ co-transport. The original evolutionary role of Si transporters in coccolithophores remains elusive but the data reported in this thesis implies that today, most coccolithophores inhabit environments where Si must be actively transported to meet their needs.

6.5.2. Current coccolithophore ecology

The findings presented in this thesis also relate to current coccolithophore ecology, highlighting the physiological difference between species, markedly between *C. braarudii* and *E. huxleyi*. A lot is known about *E. huxleyi* as it is the most ubiquitous of all the coccolithophores, found in many surface ocean environments. It has the ability to form vast blooms with cell densities as high as 10^8 cells L^{-1}, recorded in the Norwegian Fjords (Birkenes & Braarud, 1952; Berge, 1962). *E. huxleyi* is considered a euryhaline species, able to grow at salinities ranging from 41 ppt in the Red Sea (Winter *et al.*, 1979) to 11 ppt in the Sea of Azov (Bukry, 1974) and a eurythermal species with a temperature range of 1 - 30^{O}C (Okada & McIntyre, 1979). It is also considered to be nutrient tolerant as they inhabit both eutrophic and oligotrophic environments and light tolerant as they occupy the to top 200 m of the ocean (Winter *et al.*, 2006). There is a high amount of variation between strains in a variety of categories, including morphotype, abundance of coccoliths (Paasche, 2001), genotype variation (Young & Westbroek, 1991) and response changing

carbon chemistry (Langer *et al.*, 2009). All considered, *E. huxleyi* is clearly a highly adaptive species that has had considerable ecological success for the last 73, 000 years (Thierstein *et al.*, 1977).

It is occasionally difficult to identify *C. braarudii* in the literature preceding 2003 as at this time this species was grouped within the species *Coccolithus pelagicus.* Following molecular analysis of genes tufa (translation elongation factor), ITS (internal transcribed spacer region) rDNA and 18S (small subunit) rDNA, *C. pelagicus* was separated into two species: *C. braarudii* and *C. pelagicus* (Sáez *et al.*, 2003). *C. braarudii* has a more restricted distribution than *E. huxleyi*, being largely found in temperate waters, in particular coastal and upwelling areas (Giraudeau *et al.*, 1993; Cachao & Moita, 2000; Geisen *et al.*, 2002; Parente *et al.*, 2004; Ziveri *et al.*, 2004; Cubillos *et al.*, 2012). *C. pelagicus* has a more Northerly distribution of the two, found in the Arctic Ocean and sub-polar Northern Hemisphere (McIntyre & Bé, 1967; Daniels *et al.*, 2014). The *Coccolithus* species are known to bloom, with records of *C. pelagicus* blooming to cell densities of 10^6 cells L^{-1} off Scotland (Milliman, 1980). *C. braarudii* is thought to favour nutrient-rich environments in the diploid phase and is more tolerant to oligotrophic environments when in the haploid phase (Houdan *et al.*, 2006). *C. braarudii* is an important producer of calcium carbonate in the environments it inhabits. A study by Daniels *et al.* (2014) revealed that the cellular calcite content of *C. pelagicus* (16.6 pmol calcite $cell^{-1}$) and *C. braarudii* (38.7 pmol calcite $cell^{-1}$) is typically 30-80 times greater than *E. huxleyi* (0.43 - 0.52 pmol calcite $cell^{-1}$). Therefore even with the higher growth rate exhibited by *E. huxleyi*, *C. braarudii* was shown to be a significant producer of calcite in mixed communities and crucial contributor to biogenic calcite production. *C. braarudii* may be less abundant than *E. huxleyi* but its calcite production is highly influential on the environments it inhabits.

C. braarudii is less ubiquitous and has a more specific ecological niche than *E. huxleyi*, which correlates with the findings presented here. Requiring calcification for growth and a reliance on Si are likely to add to the limitations upon *C. braarudii*. For example, this may contribute to an inability to successfully colonise areas of the oceans that exhibit unfavourable carbonate chemistry, such as the Baltic Sea, which exhibits a low calcite saturation state in winter (Tyrrell *et al.*, 2008). The role of calcification in relation to proposed costs and benefits was recently modelled using the Darwin model and current ecological data. (Monteiro *et al.*, 2016). This model highlighted that different species may

have differing advantages inferred from calcification within the broad category of protection. *C. braarudii* would be a really interesting candidate species to investigate further due to the pressures of an obligate calcification requirement and a reliance on Si. Although the study also focussed on the cost of calcification, we have presented a case for including the transport costs of Si and the increased metabolic costs in regard to extracellular CAPs which are not considered in current calculations. As we learn more about calcification we may be able to revise our cost calculations to build an accurate picture of the trade-offs coccolithophore will to undergo to calcify.

6.5.3. Response to future ocean scenarios

As well as current ecology it is important to consider future ocean conditions and the pressures predicted to impact coccolithophores by ocean acidification and ocean warming. Increasing CO_2 levels have widely been considered a threat to calcifying organisms (Doney *et al.*, 2009). Atmospheric CO_2 is at equilibrium with the ocean surface waters such that CO_2 released by anthropogenic activity leads to an increase in ocean pCO_2. Consequently the ocean pH will be reduced and the carbonate (CO_3^{2-}) ion concentration lowered. As a result the saturation state (Ω) of the ocean is reduced and conditions for the formation calcareous structures is less favourable (Doney *et al.*, 2012).

Research based largely on laboratory studies of *E. huxleyi* suggests that, while significant variability exists between different studies and strains, calcification rates are likely to be lower under future ocean conditions (Findlay *et al.*, 2011; Hoppe *et al.*, 2011; Meyer & Riebesell, 2015), albeit, the reduction in growth by *E. huxleyi* under more extreme ocean acidification scenarios appears to be principally due to sensitivity to reduced pH and not an effect of the decreased calcification rate (Bach *et al.*, 2011; Taylor *et al.*, 2011; Bach *et al.*, 2013; Bach *et al.*, 2015). Other coccolithophore species are also likely to exhibit decreased calcification rates under future ocean scenarios (Langer *et al.*, 2006a). Here we provide evidence that subtle defects in calcification can have a detrimental effect on the ecological success of *C. braarudii* over time. The essential requirement for an intact coccosphere in species such as *C. braarudii* could potentially influence their response to future changes in ocean carbonate chemistry. Previous studies have shown that significant increases in seawater CO_2 (pCO_2 >1000 µatm) result in a substantial decrease in both growth rate and calcification rate in *C. braarudii*, with clear evidence of substantially malformed coccoliths (Müller *et al.*, 2010; Bach *et al.*, 2011; Krug, 2011).

The effects of ocean acidification on coccolithophores have been shown to be intertwined with temperature (Sett *et al.*, 2014). Coccolithophore data has been varied, with some laboratory studies demonstrating that *E. huxleyi* may be able to adapt well to warming (Schlüter *et al.*, 2014) and others demonstrating a poleward expansion in this species (Winter *et al.*, 2014). Gibbs *et al.* (2016) demonstrated that warming temperatures were the principal driver in range retentions of coccolithophores, resulting in a shift to higher latitudes despite the more adverse ocean chemistry conditions for calcification. Adverse ocean acidification effects were only evidenced when combined with increased temperatures. We may consider how this effect would influence an obligate calcifier such as *C. braarudii.* A temperature induced range shift may have an indirect detrimental impact on the species ability to calcify which may result in an inability to grow. However, the study by Gibbs *et al.* (2016) targeted holococcoliths and *Braarudosphaera sp.,* whose genetic status as a coccolithophore still remains unresolved (Chapter 1: section 1.3), therefore we must use caution in interpreting the findings with respect diploid coccolithophore requirements.

Whilst it is clear that the response of coccolithophores to future changes in seawater carbonate chemistry will involve many aspects of cellular physiology, the results presented here demonstrate that accumulated defects in coccolith morphology can disrupt the formation of the coccosphere and prevent the cells from undergoing successive divisions. Therefore, the predicted disruption of calcification in *C. braarudii* by elevated CO_2 may directly influence the growth and survival of this species in future oceans.

6.6. Concluding Remarks

The data presented in this thesis provides novel insights into coccolithophore biology and enforces the importance of studying a range of species. Although *E. huxleyi* has been the research focus for many years, this thesis clearly demonstrates there are species within the calcifying haptophytes that exhibit a large degree of variation to the considered model coccolithophore. *C. braarudii* is another excellent study species due to its ease of culture and dichotomous characteristics when compared to *E. huxleyi*. Additionally, aspects of the calcification mechanisms in *C. braarudii* may represent the ancestral state within the coccolithophores.

The work described in this thesis is based on the combination of multidisciplinary studies. Combining physiology, cell biology, molecular and environmental approaches has led to the advances made here. This multidisciplinary approach is considered essential to

inform modelling and ecological studies, as has occurred in previous works (Monteiro *et al.*, 2016).

Finally, coccolithophores are complex and their calcification activities are globally pivotal in biogeochemical cycling. We still do not fully understand the mechanisms behind calcification and how they will respond the future ocean conditions but a fully integrated approach encompassing many disciplines is essential to fully elucidate the complex biology behind these enigmatic microalgae.

Appendix I: Chapter 2 Supplementary Information

nature COMMUNICATIONS

ARTICLE

Received 4 Aug 2015 | Accepted 23 Dec 2015 | Published 4 Feb 2016

DOI: 10.1038/ncomms10543 OPEN

A role for diatom-like silicon transporters in calcifying coccolithophores

Grażyna M. Durak[1,*,†], Alison R. Taylor[2,*], Charlotte E. Walker[1], Ian Probert[3], Colomban de Vargas[3], Stephane Audic[3], Declan Schroeder[1], Colin Brownlee[1,4] & Glen L. Wheeler[1]

Biomineralization by marine phytoplankton, such as the silicifying diatoms and calcifying coccolithophores, plays an important role in carbon and nutrient cycling in the oceans. Silicification and calcification are distinct cellular processes with no known common mechanisms. It is thought that coccolithophores are able to outcompete diatoms in Si-depleted waters, which can contribute to the formation of coccolithophore blooms. Here we show that an expanded family of diatom-like silicon transporters (SITs) are present in both silicifying and calcifying haptophyte phytoplankton, including some globally important coccolithophores. Si is required for calcification in these coccolithophores, indicating that Si uptake contributes to the very different forms of biomineralization in diatoms and coccolithophores. Significantly, SITs and the requirement for Si are absent from highly abundant bloom-forming coccolithophores, such as *Emiliania huxleyi*. These very different requirements for Si in coccolithophores are likely to have major influence on their competitive interactions with diatoms and other siliceous phytoplankton.

[1] Marine Biological Association, The Laboratory, Citadel Hill, Plymouth, Devon PL1 2PB, UK. [2] Department of Biology and Marine Biology, University of North Carolina Wilmington, 601 South College Road, Wilmington, North Carolina, 28403-5915, USA. [3] Station Biologique de Roscoff, Place Georges Teissier, 29680 Roscoff, France. [4] School of Ocean and Earth Sciences, University of Southampton, National Oceanography Centre, Southampton SO14 3ZH, UK. * These authors contributed equally to this work. † Present address: University of Konstanz, Department of Chemistry, Physical Chemistry, Universitätsstr. 10, Box 714, D-78457 Konstanz, Germany. Correspondence and requests for materials should be addressed to C.B. (email: cbr@mba.ac.uk) or to G.W. (email: glw@mba.ac.uk).

The biomineralized phytoplankton are major contributors to marine primary productivity and play a major role in carbon export to the deep oceans by promoting the sinking of organic material from the photic zone[1,2]. The two primary forms of biomineralization found in marine plankton are the precipitation of silica (by diatoms, chrysophytes, synurophytes, dictyochophytes, choanoflagellates and radiolarians) and calcium carbonate (by coccolithophores, foraminifera, ciliates and dinoflagellates)[3]. These processes require very different chemistries and exhibit no known shared mechanisms. Both silicification and calcification appear to have evolved independently on multiple occasions. However, since in many cases the underlying cellular mechanisms have not been elucidated, the evolutionary processes remain unclear. Improved knowledge of the cellular mechanisms of biomineralization will allow us to understand the impact of past climatic events on the major phytoplankton lineages and better predict their response to future environmental change.

The haptophyte algae are of particular interest in the evolution of biomineralization as they include closely related silicified and calcified representatives. The coccolithophores (Calcihaptophycidae)[4] produce an extracellular covering of ornate calcium carbonate plates (coccoliths) and are major contributors to biogenic calcification in the ocean[3]. The most abundant coccolithophore species in modern oceans are *Emiliania huxleyi* and *Gephyrocapsa oceanica*, which belong to the Noelarhabdaceae. These species have a small cell size and are able to form extensive blooms. Larger coccolithophores species such as *Coccolithus braarudii* and *Calcidiscus leptoporus* are less numerous, but as they are heavily calcified they are important contributors to global calcification[5]. Much of our understanding of coccolithophore biology comes from the study of *E. huxleyi*, but emerging evidence suggests that there is considerable physiological diversity among coccolithophores[6].

Though the biomineralized haptophytes are predominately calcified, a representative was recently described, *Prymnesium neolepis* (formerly *Hyalolithus neolepis*), which is covered with silica scales and resembles a 'silicified coccolithophore'[7–9]. The silica scales are produced intracellularly and then deposited outside the plasma membrane, in a manner analogous to coccolith secretion[8,10]. The Prymnesiales are estimated to have diverged from the coccolithophores around 280 Myr ago[11] and *P. neolepis* is the only known extensively silicified haptophyte. Understanding whether common cellular mechanisms contribute to silica scale production in *P. neolepis* and coccolith formation in the coccolithophores may help us to understand how these different forms of biomineralization have evolved in the haptophytes and also in other phytoplankton lineages.

Silicification by marine phytoplankton has both contributed to and been influenced by the marked changes in the biogeochemistry of Si in the surface ocean. The diatoms, representing the dominant silicifying phytoplankton in current oceans, appeared only relatively recently in the fossil record (120 Myr ago) and their expansion in the Cenozoic resulted in the extensive depletion of silicate from the surface ocean, leading to the decline of heavily silicified sponges and decreased silicification in radiolarians[12–15]. Si has therefore become a limiting nutrient for modern silicifying phytoplankton and is an important factor in competitive interactions with non-silicifying taxa. As the regeneration of available Si from silica dissolution is slow, diatom blooms can deplete Si in the surface ocean sufficiently to prevent further growth. If other nutrients such as nitrate or phosphate are still available, then Si limitation can contribute to seasonal succession, where an initial diatom spring bloom is followed by subsequent blooms of non-siliceous phytoplankton. There is evidence that the low availability of Si is an important contributory factor in the formation of some coccolithophore blooms. Major *E. huxleyi* blooms in areas such as the North Atlantic, the Black Sea and off the Patagonian shelf have been associated with low silicate availability[16–18]. These observations support the view that the ecological niche of coccolithophores is partly defined by conditions that reduce competition with the fast-growing resource-efficient diatoms, such as in areas of low silicate where other nutrients (for example, nitrate and phosphate) remain available[19].

To further understand the evolution of biomineralization in haptophytes, we characterized the cellular mechanisms underlying silica scale formation in *P. neolepis*. We examine commonalities with other silicified organisms and determine whether any common cellular mechanisms contribute to biomineralization in silicified and calcified haptophytes. Surprisingly, given that it is generally assumed that coccolithophores lack a requirement for Si, we identify that diatom-like Si transporters are present in haptophytes, not only in the silicified *P. neolepis* but also in some important calcifying coccolithophore species. We demonstrate that Si plays an important role in formation of calcite coccoliths in these coccolithophores, but that the requirement for Si is significantly absent from the most abundant species in present day oceans, *E. huxleyi*. The findings have important implications for the evolution of the biomineralized phytoplankton and their distribution in both past and modern oceans.

Results

Mechanisms of biomineralization in a silicifying haptophyte. The known mechanisms of biosilicification in eukaryotes involve a number of common elements; a mechanism for Si uptake, an acidic silica deposition vesicle and an organic matrix for catalysing and organizing silica precipitation[20]. However, there is little evidence for shared mechanisms at the molecular level, suggesting that silicification has evolved independently in many lineages. We therefore examined the mechanisms of silicification in *P. neolepis*, using both molecular and physiological approaches. At low Si concentrations, Si uptake in diatoms is performed by a family of Na^+-coupled high-affinity Si transporters (SITs), although diatoms may also acquire Si by diffusive entry at higher Si concentrations[21,22]. Silicified sponges and land plants do not contain SITs, but use alternative mechanisms for Si transport[23,24]. A search for putative Si transporters in the transcriptome of *P. neolepis* strain PZ241 (Supplementary Fig. 1) identified a single gene bearing similarity to the SITs (*PnSIT1*). PnSIT1 exhibits 24.9–29.3% identity and 39.8–47.0% similarity to diatom SITs at the amino-acid level (sequences used for comparison were *Cylindrotheca. fusiformis* AAC49653.1, *Thalassiosira. pseudonana* ABB81826.1 and *Phaeodactylum tricornutum* ACJ65494.1). SITs have only previously been identified in siliceous stramenopiles (diatoms and chrysophytes) and choanoflagellates[25–27]. Many features of PnSIT1 are conserved with these SITs, including the 10 predicted transmembrane regions and the pair of motifs (EGxQ and GRQ) between TM2-3 and TM7-8 (ref. 27; Supplementary Fig. 2). We also identified a homologue of the Si efflux protein, Lsi2 in *P. neolepis* (Supplementary Table 1). Lsi2 is related to the bacterial arsenate transporter ArsB and mediates Si efflux in plant cells[28]. Lsi2 is also present in diatoms and its transcriptional regulation is highly similar to SIT2 in *Thalassiosira pseudonana*, although its cellular role has not yet been characterized[29]. The identification of Lsi2 in *P. neolepis* suggests that it may play a conserved role in siliceous phytoplankton.

We next determined the presence of an acidic silica deposition vesicle in *P. neolepis* using the fluorescent dye HCK-123, which partitions into acidic compartments and labels nascent silica

(Fig. 1a,b). We found that newly formed silica scales are secreted at the posterior pole of the cell, indicating that the principal cellular components involved in scale formation (silica precipitation in acidic non-Golgi-derived vesicles) are distinct from those involved in coccolith formation (calcite precipitation in alkaline Golgi-derived vesicles and secretion at the anterior pole of the cell)[10,30].

A search of the *P. neolepis* transcriptome for mechanisms involved in silica precipitation did not reveal homologues of any of the known silica-associated proteins from diatoms (silaffins, pleuralins and frustulins) or sponges (silicateins)[20,31] (Supplementary Table 1). As some of these proteins have a low complexity amino-acid composition and may not be identified by sequence similarity searches, we directly analysed the organic components released by NH_4F dissolution of the silica scales. We identified two major organic components using Tricine/SDS–PAGE; a lipocalin-like protein and long-chain polyamines (LCPAs; Fig. 1c). The lipocalin-like protein contains two proline-/lysine-rich regions surrounding a lipocalin domain and represents a novel silica-associated protein (LPCL1, Fig. 1d, Supplementary Fig. 3). The LCPAs from *P. neolepis* are composed of *N*-methylated oligopropyleneimine repeats, similar to the silica-associated LCPAs previously characterized from diatoms and sponges[32,33], but differ from these LCPAs as the repeat units are linked to a lysine residue rather than putrescine, ornithine or spermidine (diatoms), or butaneamine (sponges) residues (Fig. 1e, Supplementary Fig. 4). Diatoms possess a series of unusual orthologues of the genes involved in polyamine synthesis that are proposed to play a specific role in the formation of LCPAs[34]. Homologues of these modified genes for polyamine synthesis were not found in the *P. neolepis* transcriptome, indicating that these modifications may be specific to diatoms.

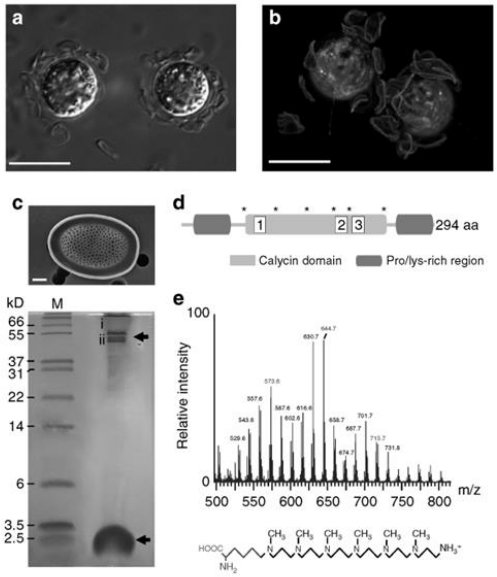

Figure 1 | Molecular mechanisms of silica scale production in *P. neolepis*. (**a**) Differential interference contrast (DIC) microscopy image of *P. neolepis* cells displaying the loose covering of silica scales. Scale bar, 10 µm. (**b**) Confocal microscopy of a *P. neolepis* cell showing incorporation of the fluorescent dye HCK-123 into newly formed silica scales (green). Chlorophyll autofluorescence is shown in red. The 3D-projection was generated from compiling a Z-stack of 15 images. Scale bar, 10 µm. (**c**) Tricine/SDS–PAGE of organic components released after dissolution of silica scales with NH_4F. A SEM image of an isolated silica scale is also shown (Scale bar, 1 µm). The higher molecular weight component around 50 kDa is a single protein that runs as two bands (i, ii), whereas the low-molecular-weight components around 2.5 kDa are long-chain polyamines (LCPA). M, molecular-weight markers. (**d**) Domain organization of the lipocalin-like protein (LPCL1) identified from both protein bands in NH_4F extracted silica scales. The approximate positions of the proline/lysine-rich regions and the calycin domain (IPR012674) are shown. Also shown are the positions of six highly conserved cysteines (asterisk) that may be involved in the formation of disulphide bridges. (**e**) Long-chain polyamines (LCPAs) from *P. neolepis* silica scales. Electrospray ionization mass spectrometry (ESI-MS) of the low-molecular-weight NH_4F-soluble fraction of silica scales revealed a series of mass peaks separated by 71 Da (highlighted in red), characteristic of *N*-methyl propyleneimine units. The additional mass peaks ±14 Da may indicate different methylation states, as is commonly observed in LCPAs. The proposed structure of the LCPAs in *P. neolepis* is shown with the putative lysine residue is highlighted in red.

An expanded family of SITs in haptophytes. Our analyses indicate that there are some similarities in the biosilicification mechanisms between *P. neolepis* and diatoms, including the silica deposition vesicle and the LCPAs. However, the silica-associated proteins bear no similarity and the only known silicification-related gene products common to both organisms are the Si transporters (SITs and Lsi2). To examine the origins of SITs and Lsi2 in *P. neolepis*, we performed sequence similarity searches of the *Emiliania huxleyi* genome and 24 other haptophyte transcriptomes (including six species of coccolithophore) from the Marine Microbial Eukaryote Transcriptome data set (http://marinemicroeukaryotes.org/)[35]. Homologues of the Si-associated protein LPCL1 from *P. neolepis* were not found in other haptophytes (Supplementary Tables 1 and 2). However, we identified a SIT homologue in the calcifying coccolithophore *Scyphosphaera apsteinii* that was highly similar to PnSIT1 (66% identity, 76.2% similarity at the amino-acid level). In addition, we found that three coccolithophores (*S. apsteinii*, *Coccolithus braarudii* and *Calcidiscus leptoporus*) possess a SIT-like protein that only contains five transmembrane regions (Fig. 2a,b). The Si efflux protein Lsi2 was not found in these coccolithophores, or in any other haptophyte, with the exception of the non-mineralized prymnesiophyte, *Haptolina ericina*.

Comparison of the two haptophyte SITs with 33 other SIT sequences originating from diatoms, chrysophytes and choanoflagellates indicated that all of the highly conserved amino-acid residues identified by Marron *et al.*[26] were also conserved in haptophytes (Supplementary Fig. 2). The single 5TM domain of the SIT-like (SITL) proteins displays a high sequence similarity to the N- and C-terminal 5TM domains of SITs. SITLs also possess the highly conserved EGxQ and GRQ motifs that are proposed to play a role in binding Si[26,27], as well as many of the other amino-acid residues that were identified as being highly conserved in SITs (Supplementary Fig. 2). The 5TM + 5TM inverted repeat topology of the SITs is characteristic of Na^+-coupled transporters with a LeuT fold and is also found in many other membrane transporters[36,37]. The inverted repeat topology in these transporters is thought to have evolved following gene duplication and fusion of a related transporter that initially existed as a homodimer with inverted symmetry[38]. Homodimerization of the SITLs may therefore result in a membrane transporter with similar properties to the SITs and it is likely that SITs evolved from a protein resembling the SITLs.

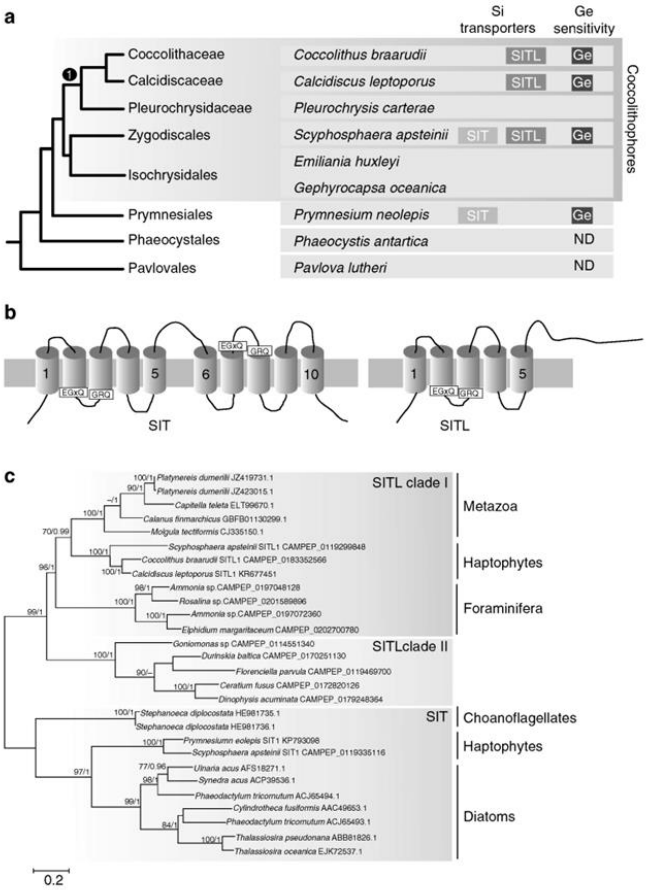

Figure 2 | An expanded family of diatom-like Si-transporters (SITs) in haptophytes. (**a**) Phylogenetic relationships between haptophytes. The schematic tree shows the currently accepted phylogenetic relationships of the major haptophyte lineages based on multigene phylogenies[11]. Representative species of each group are indicated, along with the presence of SITs or SITLs in these species. Sensitivity to Ge is shown in red, ND, not determined. ❶ Coccolithales. (**b**) A schematic image of the domain architecture of the SITs and the SITLs indicating the approximate position of the transmembrane domains and of the conserved motifs. (**c**) A maximum likelihood phylogenetic tree based on an alignment of selected SITL proteins with SITs (aligned to the N-terminal SIT domain). Final alignment size was 157 amino acids. The SITLs form a well-supported monophyletic clade. Within the SITLs two distinct clades can be observed. SITL clade I contains haptophytes, metazoa and foraminifera, whereas SITL clade II contains dinoflagellates, a cryptophyte and a dictyochophyte. Bootstrap values >70% (100 bootstraps) and Bayesian posterior probabilities >0.95 (10,000,000 generations) are shown above nodes. Scale bar, substitutions per site.

SITLs were not found in any other haptophytes or in diatoms, but were present in a range of other eukaryotes, including foraminifera, dinoflagellates and metazoa (such as the polychaetes, *Capitella teleta* and *Platynereis dumerilii* and the copepod *Calanus finmarchicus*) (Fig. 2c). Many calanoid copepods have silicified teeth[39] and SITLs may provide a mechanism for Si transport in these ecologically important zooplankton. However, not all of the species that possess SITLs are silicified. The foraminifera and the coccolithophores are the predominant contributors to calcification in our oceans and so the identification of SITLs in these lineages is particularly intriguing.

The SITs from *P. neolepis* and *S. apsteinii* form a strongly supported monophyletic clade, suggesting a common evolutionary origin for the haptophyte SITs (Fig. 2c, Supplementary Fig. 5). To explain the limited distribution of SITs, Marron *et al.*[26] proposed that horizontal gene transfer (HGT) of SITs may have occurred between stramenopiles and choanoflagellates. However, there is no phylogenetic evidence to support recent HGT of SITs between stramenopiles, choanoflagellates or the haptophytes. The SITL proteins form a monophyletic clade distinct from true SITs, suggesting that they represent a novel but closely related group of transporter proteins (Fig. 2c). When aligned to the SITLs, the

individual N- and C-terminal regions of SITs form strongly supported clades, suggesting that the SITs found in stramenopiles, choanoflagellates and haptophytes arose from a single gene duplication event, rather than from a series of more recent duplication events in each lineage (Supplementary Fig. 5). Phylogenetic analyses of Lsi2 provided no indication that haptophytes acquired this gene by recent HGT (Supplementary Fig. 6).

A novel role for Si in coccolithophore calcification. Calcified coccolithophores emerged in the early Mesozoic (c. 220 Myr ago)[11], when Si concentrations in the surface oceans were considerably higher than in present day. The distribution of the SITs and SITLs in haptophytes suggests that these transporters were present in ancestral haptophytes, including the last common ancestor of the coccolithophores. Although Si has not been generally identified as a component of calcite coccoliths, a recent study showed that Si is a minor component of the two forms of heterococcolith (muroliths and lopadoliths) found in *S. apsteinii*[40]. In many calcifying systems, calcite precipitation occurs by the crystallization of amorphous calcium carbonate (ACC). Recent evidence indicates that silica can modulate the crystallization of calcium carbonate *in vitro* by acting to modulate the metastability of ACC and facilitate ordered calcite crystal formation[41–44]. We therefore hypothesized that Si uptake via SITs or SITLs may contribute to calcification in coccolithophores.

To test this hypothesis, we used the Si analogue germanium (Ge), which competitively inhibits Si uptake in diatoms[22] and also prevents Si scale production in *P. neolepis* (Supplementary Fig. 7). In diatoms, Ge/Si ratios <0.01 do not have an inhibitory effect, but ratios >0.05 inhibit Si uptake and also disrupt Si metabolism within the cell[45–47]. Other silicifying algae, such as the chrysophytes *Synura petersenii* and *Paraphysomonas vestita*, are also sensitive to Ge, although growth in *Paraphysomonas* is only inhibited at much higher Ge/Si ratios than diatoms[48,49]. In contrast, non-silicified algae are reported to be largely unaffected by Ge[50]. Our initial experiments to screen for Ge sensitivity in coccolithophores were conducted in low-Si seawater ($<0.1\,\mu M$), to ensure high Ge:Si ratios (>1). Observations with light microscopy and scanning electron microscopy (SEM) identified that coccolith formation in *S. apsteinii* was severely disrupted by the addition of $1\,\mu M$ Ge, with 73% of cells displaying highly malformed coccoliths after 72 h (compared with 3.3% in Si-replete seawater; Fig. 3). The cup-shaped lopadoliths were severely misshapen, frequently exhibiting additional disorganized calcite precipitation at the apical rim, and the smaller disk-shaped muroliths also exhibited malformation. The addition of $5\,\mu M$ Ge to *C. braarudii* and *C. leptoporus* resulted in the production of severely malformed coccoliths that failed to integrate into the coccosphere and were shed into the surrounding seawater (Fig. 3). In all three species, addition of $100\,\mu M$ Si suppressed the disruptive effects of Ge on coccolith morphology, suggesting that Ge acts competitively with Si.

To examine the relationship between Ge and Si in greater detail, we grew *C. braarudii* cells at three different Si concentrations (2, 20 and $100\,\mu M$) and examined the effect of a range of Ge concentrations (0.5–$20\,\mu M$ Ge; Fig. 4). Because high Ge/Si ratios completely inhibit biosynthesis and growth in diatoms[46], we also assessed the physiological status of the Ge-treated coccolithophores. We found that the inhibitory effects of Ge on calcification (assessed by the accumulation of discarded coccoliths in the media) are dependent on the ratio of Ge/Si, rather than the absolute concentration of Ge. For example, $2\,\mu M$ Ge results in the production of many aberrant coccoliths at $2\,\mu M$ Si, but its impacts at 20 and $100\,\mu M$ Si are progressively reduced. The inhibitory effects of Ge on calcification in *C. leptoporus* and *S. apsteinii* were also dependent on the Ge/Si ratio (Supplementary Fig. 8). These data support the hypothesis that Ge is acting to competitively inhibit an aspect of Si uptake and/or metabolism that is required for production of coccoliths.

At high Ge/Si ratios (>1) both growth and calcification (accumulation of discarded coccoliths) were inhibited in *C. braarudii*. (Fig. 4). The maximum quantum yield of photosystem II (F_v/F_m) was only reduced at the very highest Ge/Si ratios. It is possible that the inhibition of growth results from the severe disruption of the calcification process. No effects on growth or photosynthetic efficiency were observed at low Ge/Si ratios, while coccolith defects were still observed, demonstrating that Ge had specifically disrupted calcification (Figs 4 and 5). The unique coccolith morphology of Ge-treated cells is distinct from defects in calcification caused by other stressors, such as nutrient limitation or high temperature[51].

Detailed examination of Si-limited coccolithophores provided direct evidence for a requirement for Si in the calcification process. In Si-replete cultures, defects in coccolith morphology were almost completely absent (Figs 3 and 5). However, highly aberrant coccoliths were consistently observed at a low frequency in both *C. braarudii* and *C. leptoporus* cultures after transfer to very low Si seawater (without Ge) for 72 h (Fig. 3a,b). In addition to the appearance of highly aberrant coccoliths, many cells exhibited more subtle but significant defects in coccolith morphology due to Si limitation, such as disorganization of the overlapping elements of the distal shield (termed 'blocky' morphology; Fig. 3a). Growth of *C. braarudii* was not inhibited after 8 days in very low Si ($<0.1\,\mu M$; Supplementary Fig. 9), indicating that the defects in calcification are not caused by a general disruption of cellular physiology. Defective coccolith morphology was also apparent in *C. braarudii* and *C. leptoporus* cultures grown at $2\,\mu M$ Si, compared to Si-replete cells grown at $100\,\mu M$ Si (Fig. 5, Supplementary Fig. 8). This is an important observation as it shows calcification defects may occur at ecologically relevant Si concentrations. The slower growing *S. apsteinii* did not exhibit obvious defects in calcification after transfer to low Si for 72 h, but after 8 days clear defects in coccolith formation were observed, such as missing muroliths or incomplete lopadoliths (Supplementary Fig. 10).

In combination, our results using Ge treatment and Si limitation strongly suggest that Si is required for calcification in certain coccolithophores. The dramatic effects of Ge on these species are surprising as most non-siliceous algae are considered to be insensitive to Ge[50,52]. However, many previous studies on coccolithophore physiology have focussed on *E. huxleyi*, a coccolithophore that lacks SITs or SITLs in its genome. When we examined the impact of Ge on *E. huxleyi* at very low Si ($<0.1\,\mu M$ Si), we found no effects on calcification, with normal coccospheres produced even in the presence of $20\,\mu M$ Ge (Fig. 6a). Concentrations of Ge up to $20\,\mu M$ also had no impact on the growth or photosynthetic efficiency of *E. huxleyi* at $2\,\mu M$ Si (Fig. 6b), in clear contrast to the marked effects of Ge on *C. braarudii*. Furthermore, no Ge sensitivity was observed in two further coccolithophore species in which SITs or SITLs appear absent (from their available transcriptome sequence data); *G. oceanica*, a coccolithophore that is closely related to *E. huxleyi*, and *Pleurochrysis carterae* (Fig. 6a, Supplementary Fig. 11). Our results suggest that Si plays an important role in calcification in coccolithophores that possess SITs and/or SITLs, but this requirement for Si is not universal and is notably absent from the abundant bloom-forming coccolithophore species in modern oceans (the Noelaerhabdaceae)[4].

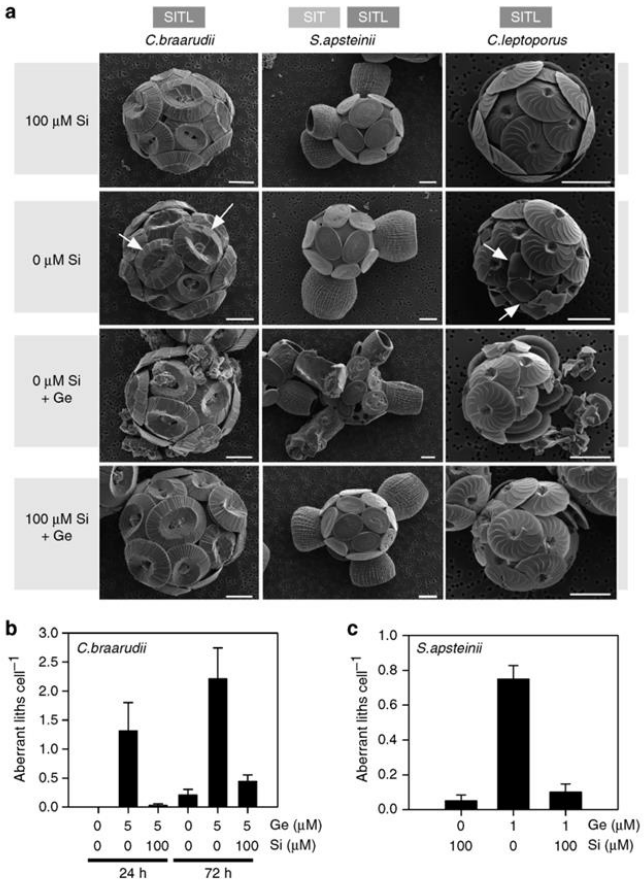

Figure 3 | A role for Si in coccolith formation. (**a**) Representative SEM micrographs demonstrating the effects of Si limitation and Ge addition on coccolith production. *C. braarudii, S. apsteinii* and *C. leptoporus* were incubated for 72 h in very low Si seawater (<0.1 µM), which was amended with Ge (1 µM for *S. apsteinii* or 5 µM for the other two species). *C. braarudii* and *C. leptoporus* cells grown in very low Si appeared superficially similar to cells grown in Si-replete seawater (100 µM Si), but closer inspection revealed that many 'blocky' coccoliths are apparent (arrowed), indicating a calcification defect related to the lack of Si. The addition of Ge resulted in the production of highly aberrant coccoliths in all three species. In *C. braarudii* these aberrant liths fail to integrate fully into the coccosphere and were often shed into the media. Both types of heterococcolith in *S. apsteinii* (the large cup-shaped lopadoliths and the small plate-like muroliths) exhibit extensive malformations. In *C. leptoporus* the aberrant coccoliths are all co-localized, suggesting that the newly formed liths in this species are secreted in a similar position in the coccosphere. The addition of 100 µM Si to Ge-treated cells markedly reduced the inhibitory effects on calcification. Scale bar, 5 µm. (**b**) Quantification of the production of aberrant coccoliths in *C. braarudii* grown in very low Si media for 24 and 72 h, amended with 5 µM Ge or 5 µM Ge + 100 µM Si. For this experiment, only highly aberrant coccoliths were scored and more subtle coccolith malformations such as the 'blocky' coccoliths observed under low Si were not scored. $n = 40$ cells. For discarded liths 4–7 fields of view were scored containing at least 40 cells. The experiment was repeated four times and representative results are shown. (**c**) Quantification of the production of aberrant lopadoliths in *S. apsteinii* grown in low Si media for 72 h, amended with 1 µM Ge, or 1 µM Ge + 100 µM Si. $n = 40$ cells. The experiment was repeated four times and representative results are shown. Error bars denote s.e.

Discussion

While *P. neolepis* is the only known haptophyte exhibiting extensive silicification, our results point towards a much broader role for Si in haptophyte physiology. *P. neolepis* exhibits key similarities with other silicifying eukaryotes, but there is no evidence that silicification in this lineage arose from recent HGT. The mechanisms for silicification in *P. neolepis* have most likely been assembled independently from existing cellular components. Although *P. neolepis* contains a Si transporter belonging to the SIT family, the identification of a SIT in the coccolithophore *S. apsteinii* suggests that the presence of this family of Si transporters greatly predates the emergence of silicification in the haptophytes and may therefore have played an alternative role before being recruited for biomineralization. In diatoms, Thamatrakoln and Hildebrand[22] have proposed that SITs may have played an ancestral role in preventing

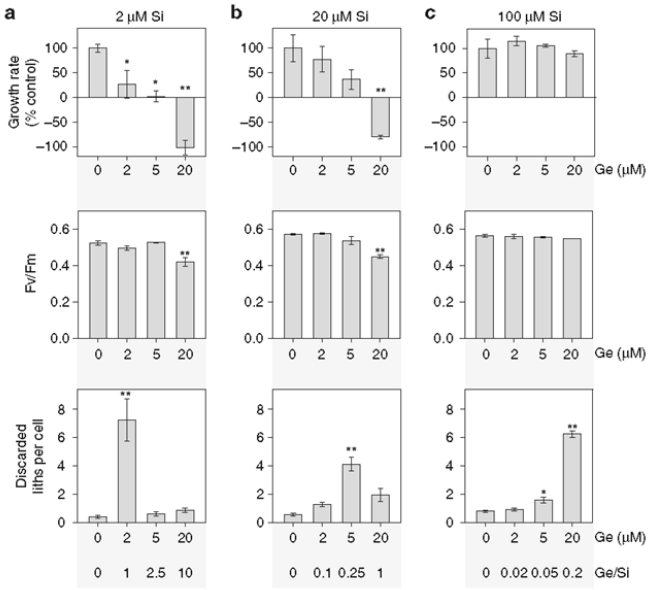

Figure 4 | The inhibitory effects of Ge are dependent on the Ge/Si ratio. (**a**) *C. braarudii* cells were treated with 0, 2, 5 or 20 µM Ge for 48 h in seawater containing 2 µM Si. Effects on coccolith morphology were determined by counting the mean number of discarded liths relative to the cell density. Specific growth rate (per day) and photosynthetic efficiency (the quantum yield of photosystem II, F_v/F_m) were also determined. *$P<0.05$ and **$P<0.01$ denote treatments that differ significantly from the 0 µM Ge control (one-way ANOVA with Holm–Sidak *post hoc* test, $n=3$). Error bars denote standard errors. (**b**) *C. braarudii* cells treated as in **a** but in seawater containing 20 µM Si. (**c**) *C. braarudii* cells treated as in **a** but in seawater containing 100 µM Si. Ge had a much lower impact on coccolithophore physiology at higher Si concentrations, suggesting that Ge acts competitively with Si.

excessive accumulation of intracellular Si in the Si-rich waters of Mesozoic oceans, before they were recruited for frustule formation.

SITs exhibit a very limited distribution in eukaryotes (stramenopiles, haptophytes and choanoflagellates). In the absence of evidence for HGT, an alternative explanation is that this distribution results from multiple losses of a gene that was present in the last common ancestor of these lineages. However, as this ancestor was most likely close to the last common ancestor of all eukaryotes, this scenario requires gene loss of SITs on a massive scale. Two factors that may have contributed to the loss of SITs in eukaryotes are the potential functional redundancy between SITs and SITLs and the extensive depletion of Si from surface oceans in the Cenozoic. However, an alternative scenario that does not require such extensive gene loss is possible as the phylogenetic position of the haptophytes is not fully resolved. Recent phylogenomic evidence suggests a specific association between haptophytes and stramenopiles[53,54], with Stiller *et al.*[54] proposing that haptophytes acquired their plastids following endosymbiosis of a photosynthetic stramenopile belonging to the ochrophyta (which includes diatoms and chrysophytes). The associated endosymbiotic gene transfer therefore provides a mechanism through which the haptophytes may have acquired SITs from stramenopiles. The phylogeny of the SITs is not at odds with this scenario, as the proposed endosymbiosis would have occurred before the extensive radiation of the stramenopiles and the haptophytes, but it does infer that the SITs have been lost extensively in both of these taxonomic groups. This scenario does not explain the presence of SITs in choanoflagellates. Although HGT of SITs to or from choanoflagellates is not supported by the phylogeny, it cannot be ruled out and there is evidence for extensive HGT from algae into choanoflagellates[55].

Clearly, there are broader evolutionary questions relating to the phylogeny of the haptophytes that must be addressed before we can fully determine the origins of the SITs. Further understanding of the function and roles of the SITLs may also provide important insight into these processes. Nevertheless, our results clearly suggest that an expanded family of SITs were present in ancestral haptophytes and that both SITs and SITLs were present in the ancestor of the calcifying coccolithophores. Therefore, it seems likely that this ancestor possessed the capacity for Si uptake. As Si exhibits the ability to modulate calcite precipitation *in vitro*[42,43], its presence in ancestral coccolithophores may even have facilitated the emergence of extensively calcified coccoliths. We have provided evidence of a role for Si in coccolith formation in *S. apsteinii*, *C. braarudii* and *C. leptoporus*. These results identify that Si uptake via SITs is an important common mechanism contributing to very different modes of biomineralization in two of the major phytoplankton lineages, the diatoms and the coccolithophores.

Lsi2 was not found in coccolithophores with SITs and SITLs, suggesting that its cellular role in *P. neolepis* and diatoms may relate to the process of silicification. In plants, Lsi2 is proposed to act as a H^+/silicic acid exchanger, using an inward H^+ gradient to drive the efflux of silicic acid across the plasma membrane[28]. In silicifying organisms, H^+/silicic acid exchangers could act to load the acidic silica deposition vesicle, using the H^+ gradient across the vesicle membrane to drive the accumulation of silicic acid. It will therefore be important to identify the cellular localization of Lsi2 in *P. neolepis* and diatoms.

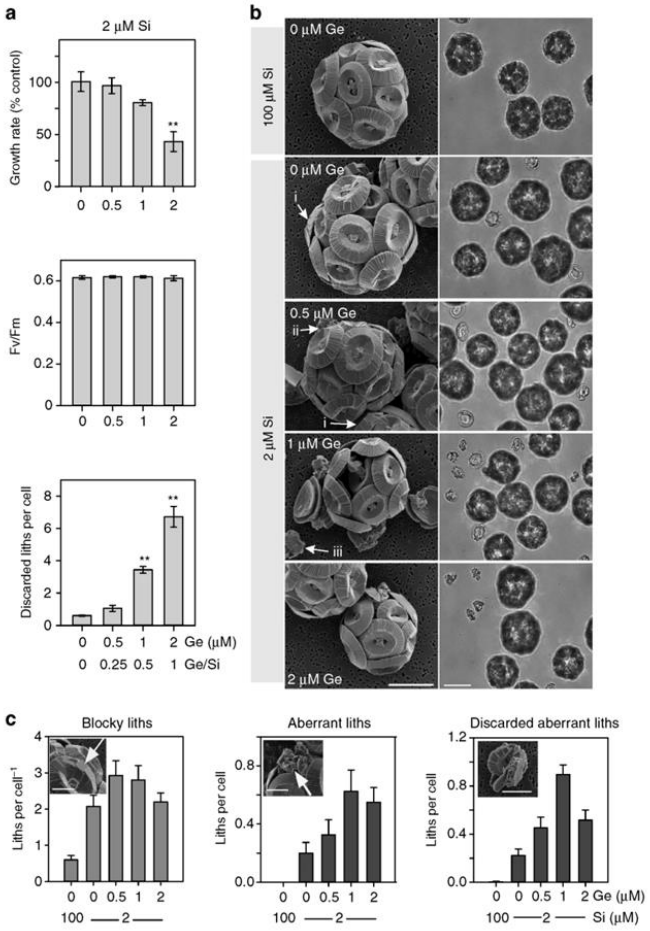

Figure 5 | Ge causes defects in calcification at low Ge/Si ratios. (**a**) *C. braarudii* cells were treated with 0, 0.5, 1 or 2 µM Ge for 48 h in seawater containing 2 µM Si. Growth, photosynthetic efficiency and the number of discarded liths were determined. $^{*}P<0.05$ and $^{**}P<0.01$ denote treatments that differ significantly from the 0 µM Ge control (one-way ANOVA with Holm–Sidak *post hoc* test, $n=3$). (**b**) SEM (left panel) and bright-field microscopy (right panel) images of *C. braarudii* cells grown in Ge for 48 h (conditions described in **a**). Three classes of defective coccolith morphology were observed. (i) 'Blocky' coccoliths where the overlapping arrangement of the distal shield is disrupted, but the shape of the coccolith is preserved. (ii) Aberrant coccoliths with highly disrupted morphology (iii) Discarded aberrant coccoliths that are not successfully integrated into the coccosphere. Note that even without Ge treatment 'blocky' coccoliths can be observed at 2 µM Si, but these are not present at 100 µM Si. Scale bar, 10 µm. (**c**) Quantification of the defective coccolith morphology shown in **b**. At least 40 cells were scored for each treatment. For discarded liths four to seven fields of view were scored containing at least 40 cells. Error bars denote standard errors. Scale bar, 5 µm.

We do not yet know the cellular mechanisms through which Si contributes to the calcification process. Previous workers have identified a role for Si in bone formation in vertebrates[56,57]. However, the primary role of Si in bone formation appears to relate to the synthesis of collagen to form the underlying organic matrix, rather than a direct role in the mineralization process[58,59]. More recently, it has been demonstrated that silica plays an important role in formation of cystoliths, small calcium carbonate deposits that are found in the leaves of some land plants[41,60]. Although silica is only a minor component of cystoliths, it is essential for the formation of the amorphous calcium carbonate phase that comprises the bulk of the structure[60]. These studies suggest that Si could act to modulate coccolith formation through a number of mechanisms. Further elucidation of its precise role will enable important insight into the cellular mechanisms of calcification in coccolithophores, which remain poorly understood.

Significantly, our results suggest that requirement for Si in coccolithophore calcification may have been lost by the Noelaerhabdaceae and Pleurochrysidaceae. There are other potential evolutionary scenarios that we cannot rule out at this stage, such as independent evolution of the Si requirement within the

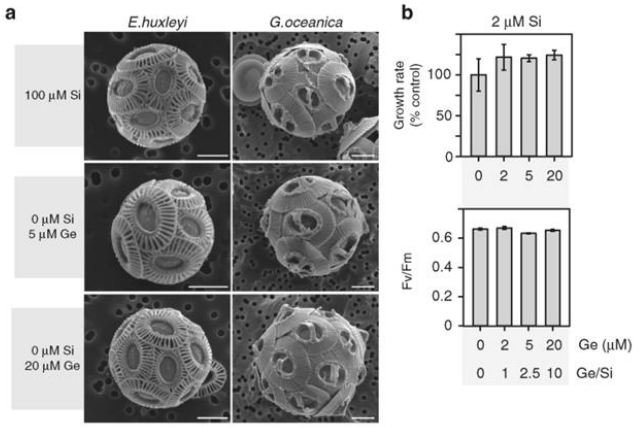

Figure 6 | *Emiliania huxleyi* and *Gephyrocapsa oceanica* are insensitive to Ge. (**a**) Representative SEM micrographs for *E. huxleyi* and *G. oceanica* following treatment for 72 h in low Si (< 0.1 µM) media with different additions of Ge (5 or 20 µM). No effect of Ge on coccolith morphology was observed in either species relative to the control grown in normal seawater media (100 µM Si). Si transporters (SIT/SITL) were not identified the genome of *E. huxleyi* or the transcriptome of *G. oceanica*. Scale bar, 2 µm. The results are representative of three independent experiments. (**b**) *E. huxleyi* cells were treated with 0, 0.5, 1 or 2 µM Ge for 48 h in seawater containing 2 µM Si. Mean specific growth rate and mean F_v/F_m as a measure of photosynthetic efficiency were determined. No significant differences were noted between treatments and the 0 µM Ge control (one-way ANOVA, $n = 3$). The results are representative of two independent experiments. Error bars denote s.e.

Zygodiscales and the Coccolithales, although these scenarios are less parsimonious. The marked decline of surface ocean silicate in the Cenozoic also suggests that loss of the requirement for Si would be more likely than gain. These evolutionary events have important implications for coccolithophore ecology and prompt a re-evaluation of the widely held view that the coccolithophores do not require Si. The Si-requiring coccolithophores identified in this study are important marine calcifiers, with *C. braarudii* and *C. leptoporus* contributing significantly to calcite flux to the deep ocean in large parts of the Atlantic Ocean[5,61]. Although the requirement of these coccolithophores for Si is likely to be considerably lower than that of extensively silicified organisms, Si limitation clearly impairs their ability to calcify. Whether these species encounter significant Si limitation in natural seawaters and can compete effectively for this resource with diatoms and other silicified plankton must be resolved. However, concentrations of silicate in the surface ocean can often reach very low levels, particularly after diatom blooms[62]. It is possible that small fast-growing coccolithophores, which are best suited to exploit the nutrient-depleted waters following a diatom bloom, may have encountered selective pressure to uncouple calcification from Si uptake to avoid Si limitation. The bloom-forming coccolithophores belonging to the Noelaerhabdaceae, such as *E. huxleyi* and *G. oceanica*, may therefore have developed alternative cellular mechanisms to replace the role of Si in coccolith formation. The Noelaerhabdaceae are the most abundant and broadly distributed coccolithophores in modern oceans and their ability to form extensive blooms (often in Si-depleted waters) has likely contributed to their considerable ecological success[16–18]. The differing requirements for Si may therefore have had a profound impact on the physiology of modern coccolithophores and contributed significantly to the evolution and global distribution of this important calcifying lineage.

Methods

Algal strains and culture growth. *Prymnesium neolepis* (NCBI Tax ID 284051) strains TMR5 (RCC3432—Sea of Japan) and PZ241 (RCC1453—Mediterranean Sea) were obtained from the Roscoff Culture Collection. Strain TMR5 was used for all physiological analyses and for RT–PCR. Strain PZ241 was used to generate the transcriptome. Cultures of *P. neolepis* were maintained in filtered seawater (FSW) supplemented with f/2 nutrients (including 100 µM $Na_2SiO_3.5H_2O$) under irradiance of 80–100 µmol s^{-1} m^{-2} (18:6 h light:dark) at 18 °C. Stock cultures of the coccolithophores *Coccolithus braarudii* (formerly *Coccolithus pelagicus* ssp *braarudii)* (PLY182G), *Emiliania huxleyi* (PLY-B92/11) and *Pleurochrysis carterae* (PLY406) were maintained in FSW supplemented with f/2 nutrients (without added Si) and Guillard's vitamins as previously described[40]. *Calcidiscus leptoporus* (RCC1130), *Gephyrocapsa oceanica* (RCC1303) and *Scyphosphaera apsteinii* (RCC1456) were maintained in f/2 supplemented with 10% K medium. All coccolithophore cultures were grown at 15 °C under 80–100 µmol s^{-1} m^{-2} irradiance (14:10 h light:dark).

Manipulation of seawater Si and addition of Ge. To examine the effect of Si and Ge on coccolithophores, we used a batch of seawater from the Western English Channel in which Si was naturally low (measured at 2 µM using the molybdate-ascorbate assay[63]). This batch of seawater was used for all subsequent analyses involving the effect of Ge on coccolithophores, except where very low Si concentrations were required (see below). Si concentration was amended by the addition of $Na_2SiO_3.5H_2O$. Ge was added in the form of GeO_2, to give concentrations ranging from 0.5–20 µM. f/2 nutrients (without Si) were added and all coccolithophore cultures were grown under identical conditions (15 °C under 80–100 µmol s^{-1} m^{-2} irradiance, 14:10 h light:dark). For growth experiments, coccolithophore cultures were acclimated to 2 µM Si for several generations (1–2 weeks) before the onset of the experimental period. For SEM analysis, all cultures were maintained in 100 µM Si for 1–2 weeks before the onset of the experimental period to prevent accumulation of aberrant coccoliths in the control.

Very low Si seawater was prepared using diatoms to deplete Si as described previously[64]. One-litre batches of f/2 FSW (without added Si) were inoculated with the diatom *Thalassiosira weissflogii* and allowed to grow into stationary phase (6–10 days). Diatoms were removed by two passages through 0.2-µm filters and the Si concentration was verified on an autoanalyser (Bran + Luebb, Germany) using a molybdate-ascorbate assay[63]. The initial Si in Gulf Stream Seawater was 5.4 µM and after diatom depletion the Si was below the level of detection (< 0.1 µM, hereto referred to as 0Si f/2 FSW). Before inoculation of treatment media, aliquots of cells were washed at least twice by allowing them to settle, drawing off the overlying media, and resuspending in 0Si f/2 FSW. An inoculum of 0Si f/2 FSW washed cells was then added to a tube of the treatment media and monitored over 72 h. Care was taken to ensure final cell numbers did not exceed 2×10^4 cells per ml for *E. huxleyi*, the most rapidly growing of the three species, thus avoiding any significant changes to the carbonate chemistry of the culture medium over the course of the experimental incubations.

Physiological measurements. Growth rates of coccolithophore cultures were determined by cell counts using a Sedgewick-Rafter counting chamber (*C. braarudii, P. carterae*) or a Neubauer improved haemocytometer (*E. huxleyi*). Specific growth rates (per day) were determined from the initial and final cell densities (N_{t0}, N_{t1}) using the formula $\mu = (\ln(N_{t1}) - \ln(N_{t0}))/t$. For Ge-treated *C. braarudii* cultures, an initial cell density of 1.2×10^4 cells per ml was used to ensure sufficient biomass was available after 48 h for measurements of chlorophyll fluorimetry. For these short-term incubations, the control cultures exhibited a specific growth rate between 0.24–0.35 per day and growth of the Ge-treated cultures is shown as a percentage of the control. For Si-limited cultures, an initial cell density of 4.5×10^3 cells per ml was used and growth was monitored over 8 days. Discarded coccoliths of *C. braarudii* were also counted for selected experiments. As coccolith morphology can be difficult to determine accurately by light microscopy, we did not discriminate between intact and aberrant liths in these analyses. To assess the performance of the photosynthetic apparatus, the maximum quantum yield of photosystem II was determined using a Z985 AquaPen chlorophyll fluorimeter (Qubit Systems, Kingston, Canada). Statistical analyses of these data were performed in SigmaPlot v12.0 software (Systat Software Inc, London, UK).

Fluorescence microscopy of *P. neolepis* silica scales. One millilitre of *P. neolepis* cells was incubated with the fluorescent dye LysoTracker yellow HCK-123 or LysoSensor Yellow/Blue DND-160 (Invitrogen; 1 μM, 10 h). Fluorescently labelled scales were imaged by confocal laser scanning microscopy (Zeiss LSM 510 microscope). HCK-123 was viewed using excitation at 488 nm and emission at 500–550 nm. DND-160 was viewed using multiphoton excitation at 740 nm with emission at 435–485 nm and 500–550 nm. Chlorophyll autofluorescence was also detected (emission 650–710 nm).

Extraction of silica-associated organic components. Organic components were extracted from the silica scales of *P. neolepis* using a modified protocol for diatom frustules[65]. Cells in mid-exponential growth phase were harvested by low pressure filtration and pelleted by centrifugation (500 × *g*, 5 min, Thermo Scientific, Waltham, MA). The cells were disrupted by the addition of 10 ml of lysis buffer (2% SDS, 100 mM EDTA, 0.1 M Tris pH 8.0), vortexed and centrifuged at 6,000*g* for 10 min. The pellet containing the silica scales was washed with lysis buffer a further five times to remove cellular organic material. The silica scales were further purified by centrifugation through a 50% glycerol cushion (3,200*g*, 2 min) to remove any traces of contaminating low-density organic material, such as the smaller organic scales. The purity of the silica scale preparation was assessed by light microscopy (Nikon Ti Eclipse, Tokyo, Japan) and electron microscopy (both SEM and transmission electron microscopy). No contamination with cell debris or organic scales was observed in the purified preparations of silica scales, although organic scales could clearly be viewed in crude cell extracts. To dissolve the silica component of scales, 2 ml of 10 M NH_4F was added to 30–100 mg biosilica sample and vortexed until the pellet was dissolved. 0.5 ml of 6 M HCl was then added to the mixture, vortexed, and the pH was adjusted to 4.5 with 6 M HCl. The sample was incubated at room temperature for 30 min before centrifugation (3,200*g*, 15 min) and the supernatant was transferred to a 3 kDa cut-off filtration column (Amicon) to concentrate and desalt protein. The concentrate was washed sequentially with 5 ml of 500 mM ammonium acetate, 5 ml of 200 mM ammonium acetate and three times with 5 ml of 50 mM ammonium acetate. The sample was then further concentrated to 150–400 μl and analysed using Tricine/SDS–PAGE with Coomassie Blue staining to stain both proteins and LCPAs[66]. Staining with silver stain or Stains-All (Sigma), which do not bind to LCPAs, was used to verify that the lower molecular weight component did not contain protein. A trypsin digest was also conducted, where 10 μl of the NH_4F soluble extract was incubated with 2 μg of TPCK (tosyl phenylalanyl chloromethyl ketone)-treated trypsin in 100 mM Tris-HCl at pH 8.8 at 37 °C (18 h). Analysis by Tricine/SDS–PAGE revealed that the higher molecular weight component had been removed by trypsin, but the low-molecular-weight component (LCPA) remained. To further confirm that silica scales were not contaminated with cellular debris or organic scales, the purified silica scales were extracted with 5 ml buffer (100 mM EDTA, 0.1 M Tris pH 8.0) in the absence of NH_4F dissolution. No organic components were observed following Tricine/SDS–PAGE analysis, indicating that the organic components observed following treatment with NH_4F are released by silica dissolution.

Protein identification from silica scale extract. Following Tricine/SDS–PAGE, protein bands were excised from the gel and analysed by peptide mass fingerprinting using a tryptic digest (Alta Bioscience, Abingdon, UK). The *P. neolepis* transcriptome was used to create a reference proteome. A single protein (LPCL1) was identified, with 8–16 unique peptides identified in each sample. The protein identification was repeated at an alternative facility (Mass Spectrometry Facility, Biosciences, University of Exeter, UK) using an independent protein extract. This gave an identical result identifying 8 unique peptides for LPCL1.

LCPA purification from silica scale extract. LCPAs were separated from the protein fraction by ultrafiltration of 500 μl of the NH_4F soluble extract through a 10 kD MW filtre. The LCPAs were then further purified by cation exchange through 2 ml of high S strong cation exchange resin (Bio-Rad, Hemel Hempstead, UK). The column was prepared by washing sequentially with 10 ml of deionised water, 10 ml of 2 M ammonium acetate and then three further times with deionised water. The NH_4F extraction was diluted (4.5:100) with deionised water and passed through the column. The resin was then washed three times with 1 ml of 200 mM ammonium acetate and polyamines were eluted by 4 sequential additions of 1 ml of 2 M ammonium acetate. The eluant was neutralized with acetic acid and lyophilized. Long-chain polyamines were analysed by electrospray ionization mass spectrometry (ESI-MS) using an amaZon speed mass spectrometer (Bruker, Bremen). Samples were diluted in H_2O/CH_3CN (50/50), and injected by direct infusion at a flow rate of 500 nl min^{-1} using a Captive Spray ion source. MS and MSn spectra were acquired in positive ion mode.

Generation of the *P. neolepis* transcriptome. A 100-ml culture of *P. neolepis* strain PZ241 growing in standard conditions (mid-exponential phase, f/2 + Si, other growth conditions as described above) was used to generate the transcriptome. Cells were collected 4 h into the light cycle by centrifugation (500*g*, 5 min). RNA was extracted using the Trizol method (Invitrogen, Paisley, UK), with additional purification using an RNeasy kit (Qiagen, Venlo, Netherlands). Following reverse transcription using oligo-dT primers, *P. neolepis* complementary DNA was sequenced by Illumina technology, generating 64,548,084 paired end reads of 75 bp (Genoscope, Evry, France). The paired end reads were assembled by Trinity[67], producing 118,473 transcripts, including alternative forms of a total of 83,175 transcripts.

Reverse transcription PCR. Reverse transcription PCR (RT–PCR) was used to verify the expression of selected genes (*LPCL1*, *SIT* and *SITL*) identified in the haptophyte transcriptomes. Fifty-millilitre cultures of *P. neolepis* (TMR5), *C. braarudii*, *C. leptoporus* and *S. apsteinii* were grown in standard conditions (as described above). Cells were collected ~4 h into the light cycle by centrifugation (500*g*, 5 min). RNA was extracted using the Trizol method (Invitrogen), with additional purification using an RNeasy kit (Qiagen). Complementary DNA was synthesized using either oligo-dT primers (*PnSIT1*) or gene specific primers (all other products) using Superscript III reverse transcriptase (Invitrogen). Gene products were then amplified by PCR (95 °C for 30 s, 54 °C for 30 s, 72 °C for 60 s, 35 cycles) (Supplementary Table 3). PCR products were sequenced to confirm the amino-acid sequence of the predicted protein product (Source BioScience, Cambridge, UK). The nucleotide sequences of *P. neolepis* SIT1 and LPCL1 obtained from the TMR5 strain were 100% identical at the nucleotide level to those identified in the PZ241 transcriptome.

Bioinformatic analyses. Known proteins associated with silicification from diatoms, sponges and land plants were used to search the haptophyte transcriptomes (Supplementary Table S1). The additional haptophyte transcriptomes were obtained from the Marine Microbial Eukaryote Sequencing Project (MMETSP; http://camera.calit2.net/mmetsp/)[35]. The genomes of *Emiliania huxleyi* v1.0 and *Thalassiosira pseudonana* v3.0 were obtained from the Joint Genome Institute (JGI; http://genome.jgi.doe.gov/). Further searches were performed at NCBI (http://blast.ncbi.nlm.nih.gov/Blast.cgi), including Transcriptome Shotgun Assembly (TSA) and Expressed Sequence Tag (EST) databases. Databases were searched using BLASTP and TBLASTN. Position-specific iterative BLAST (PSI-BLAST) was used to identify highly conserved motifs in proteins that exhibit low levels of sequence identity (for example, lipocalins). Each potential hit was manually inspected using a multiple sequence alignment to identify conserved residues and then phylogenetic analyses were performed using both neighbour-joining and maximum likelihood methods within the MEGA5 software package to assess the relationship with known proteins[68]. For detailed phylogenetic analysis of SITs and SITLs, multiple sequence alignments were generated using MUSCLE and manually inspected for alignment quality. After manual refinement, GBLOCKS 0.91b was used to remove poorly aligned residues[69] and then ProtTest was used to determine the best substitution model (WAG with gamma and invariant). Maximum likelihood phylogenetic trees were generated using PhyML3.0 software with 100 bootstraps. Bayesian posterior probabilities were calculated using BEAST v1.8, running for 10,000,000 generations[70]. The identification of potential transmembrane domains in SITLs was performed using Phobius and TMHMM.

Electron microscopy. SEM images of *P. neolepis* scales were acquired with a JEOL 5000 and JEOL 7001 F microscopes (Jeol, Japan) at 15 keV accelerating voltage. Scales were collected using lysis buffer (2% SDS, 100 mM EDTA, 0.1 M Tris pH 8.00) as described above, but were additionally cleaned by heating at 95 °C for 10 min in the lysis buffer. Purified *P. neolepis* silica scale material was dried and sputter coated with gold or chromium before imaging. Samples of coccolithophores for SEM were collected by filtration onto a 13-mm 0.4-μm Isopore filter (Millpore EMD), followed by a rinse with 10 ml of 1 mM HEPES buffer (pH 8.2) to remove salts. Filters were air-dried, mounted onto an aluminium stub and sputter coated with 10 nm Pt/Pd (Cressington, USA). Samples were examined with a Phillips XL30S FEG SEM (FEI-Phillips, USA) and imaged in high-resolution secondary

electron mode with beam acceleration of 5 kV. Three categories of coccolith morphology were scored. (i) 'Blocky' coccoliths where the overlapping arrangement of the distal shield is disrupted, but the overall shape of the coccolith is not disrupted (*C. braarudii* and *C. leptoporus* only). (ii) 'Aberrant' coccoliths were classified as coccoliths that clearly departed from the typical morphology for any given species. (iii) 'Discarded aberrant' coccoliths were classed as those aberrant coccoliths that failed to integrate into the coccosphere. To analyse coccolith morphology, at least 40 cells per treatment were scored for the number of malformed coccoliths present in the coccosphere. Coccoliths on the underside of cells could not be scored and the resultant underestimate of coccoliths per cell was assumed to be the same for any given species. Discarded aberrant coccoliths were counted in four to seven random fields of view in which both cells and loose aberrant coccoliths on the filter were scored (at least 40 cells in total were scored for each treatment). Ge-treated cultures for SEM analysis were grown in single replicates. Each experiment was repeated on multiple independent occasions and in each case the effects of Ge were highly reproducible. A representative example of each experiment is shown. Error bars denote standard error.

References

1. De La Rocha, C. L. & Passow, U. Factors influencing the sinking of POC and the efficiency of the biological carbon pump. *Deep Sea Res. Part II* **54,** 639–658 (2007).
2. Schmidt, K., De La Rocha, C. L., Gallinari, M. & Cortese, G. Not all calcite ballast is created equal: differing effects of foraminiferan and coccolith calcite on the formation and sinking of aggregates. *Biogeosciences* **11,** 135–145 (2014).
3. Raven, J. A. & Giordano, M. Biomineralization by photosynthetic organisms: evidence of coevolution of the organisms and their environment? *Geobiology* **7,** 140–154 (2009).
4. De Vargas, C., Aubry, M.-P., Probert, I. & Young, J. in *Evolution of Primary Producers in the Sea* (eds Falkowski, P. & Knoll, A.) (Elsevier, 2007).
5. Daniels, C. J., Sheward, R. M. & Poulton, A. J. Biogeochemical implications of comparative growth rates of *Emiliania huxleyi* and *Coccolithus* species. *Biogeosciences* **11,** 6915–6925 (2014).
6. Rickaby, R. E. M., Henderiks, J. & Young, J. N. Perturbing phytoplankton: response and isotopic fractionation with changing carbonate chemistry in two coccolithophore species. *Clim. Past* **6,** 771–785 (2010).
7. Edvardsen, B. *et al.* Ribosomal DNA phylogenies and a morphological revision provide the basis for a revised taxonomy of the Prymnesiales (Haptophyta). *Eur. J. Phycol.* **46,** 202–228 (2011).
8. Yoshida, M., Noel, M. H., Nakayama, T., Naganuma, T. & Inouye, I. A haptophyte bearing siliceous scales: Ultrastructure and phylogenetic position of *Hyalolithus neolepis* gen. et sp nov (Prymnesiophyceae, Haptophyta). *Protist* **157,** 213–234 (2006).
9. Patil, S., Mohan, R., Shetye, S., Gazi, S. & Jafar, S. A. *Prymnesium neolepis* (Prymnesiaceae), a siliceous Haptophyte from the Southern Indian Ocean. *Micropaleontology* **60,** 475–481 (2014).
10. Taylor, A. R., Russell, M. A., Harper, G. M., Collins, T. F. T. & Brownlee, C. Dynamics of the formation and secretion of hetercoccoliths by *Coccolithus pelagicus* (ssp *braarudii*). *Eur. J. Phycol.* **42,** 125–1336 (2007).
11. Liu, H., Aris-Brosou, S., Probert, I. & de Vargas, C. A time line of the environmental genetics of the haptophytes. *Mol. Biol. Evol.* **27,** 161–176 (2010).
12. Harper, H. E. & Knoll, A. H. Silica, diatoms, and cenozoic radiolarian evolution. *Geology* **3,** 175–177 (1975).
13. Lazarus, D. B., Kotrc, B., Wulf, G. & Schmidt, D. N. Radiolarians decreased silicification as an evolutionary response to reduced Cenozoic ocean silica availability. *Proc. Natl Acad. Sci. USA* **106,** 9333–9338 (2009).
14. Maldonado, M., Carmona, M. G., Uriz, M. J. & Cruzado, A. Decline in Mesozoic reef-building sponges explained by silicon limitation. *Nature* **401,** 785–788 (1999).
15. Sims, P. A., Mann, D. G. & Medlin, L. K. Evolution of the diatoms: insights from fossil, biological and molecular data. *Phycologia* **45,** 361–402 (2006).
16. Balch, W. M. *et al.* Surface biological, chemical, and optical properties of the Patagonian Shelf coccolithophore bloom, the brightest waters of the Great Calcite Belt. *Limnol. Oceanogr.* **59,** 1715–1732 (2014).
17. Hopkins, J., Henson, S. A., Painter, S. C., Tyrrell, T. & Poulton, A. J. Phenological characteristics of global coccolithophore blooms. *Global Biogeochem. Cycles* **29,** 239–253 (2015).
18. Leblanc, K. *et al.* Distribution of calcifying and silicifying phytoplankton in relation to environmental and biogeochemical parameters during the late stages of the 2005 North East Atlantic Spring Bloom. *Biogeosciences* **6,** 2155–2179 (2009).
19. Tyrrell, T. & Merico, A. in *Coccolithophores: From Molecular Processes to Global Impact*. (eds Thierstein, H. R. & Young, J. R.) 75–97 (2004).
20. Kroger, N. & Poulsen, N. Diatoms-from cell wall biogenesis to nanotechnology. *Annu. Rev. Genet.* **42,** 83–107 (2008).
21. Hildebrand, M., Volcani, B. E., Gassmann, W. & Schroeder, J. I. A gene family of silicon transporters. *Nature* **385,** 688–689 (1997).
22. Thamatrakoln, K. & Hildebrand, M. Silicon uptake in diatoms revisited: a model for saturable and nonsaturable uptake kinetics and the role of silicon transporters. *Plant Physiol.* **146,** 1397–1407 (2008).
23. Ma, J. F. *et al.* A silicon transporter in rice. *Nature* **440,** 688–691 (2006).
24. Schroder, H. C. *et al.* Silica transport in the demosponge *Suberites domuncula*: fluorescence emission analysis using the PDMPO probe and cloning of a potential transporter. *Biochem. J.* **381,** 665–673 (2004).
25. Likhoshway, Y. V., Masyukova, Y. A., Sherbakova, T. A., Petrova, D. P. & Grachev, A. M. A. Detection of the gene responsible for silicic acid transport in chrysophycean algae. *Dokl. Biol. Sci.* **408,** 256–260 (2006).
26. Marron, A. O. *et al.* A family of diatom-like silicon transporters in the siliceous loricate choanoflagellates. *Proc. Biol. Sci.* **280,** 20122543 (2013).
27. Thamatrakoln, K., Alverson, A. J. & Hildebrand, M. Comparative sequence analysis of diatom silicon transporters: Toward a mechanistic model of silicon transport. *J. Phycol.* **42,** 822–834 (2006).
28. Ma, J. F. *et al.* An efflux transporter of silicon in rice. *Nature* **448,** 209–212 (2007).
29. Shrestha, R. P. *et al.* Whole transcriptome analysis of the silicon response of the diatom *Thalassiosira pseudonana*. *BMC Genomics* **13,** 499 (2012).
30. Manton, I. Further observations on the fine structure of *Chrysochromulina chiton* with special reference to the haptonema, 'peculiar' golgi structure and scale production. *J. Cell. Sci.* **2,** 265–272 (1967).
31. Shimizu, K., Cha, J., Stucky, G. D. & Morse, D. E. Silicatein alpha: cathepsin L-like protein in sponge biosilica. *Proc. Natl Acad. Sci. USA* **95,** 6234–6238 (1998).
32. Kroger, N., Deutzmann, R., Bergsdorf, C. & Sumper, M. Species-specific polyamines from diatoms control silica morphology. *Proc. Natl Acad. Sci. USA* **97,** 14133–14138 (2000).
33. Matsunaga, S., Sakai, R., Jimbo, M. & Kamiya, H. Long-chain polyamines (LCPAs) from marine sponge: possible implication in spicule formation. *Chembiochem* **8,** 1729–1735 (2007).
34. Michael, A. J. Molecular machines encoded by bacterially-derived multi-domain gene fusions that potentially synthesize, N-methylate and transfer long chain polyamines in diatoms. *FEBS Lett.* **585,** 2627–2634 (2011).
35. Keeling, P. J. *et al.* The Marine Microbial Eukaryote Transcriptome Sequencing Project (MMETSP): illuminating the functional diversity of eukaryotic life in the oceans through transcriptome sequencing. *PLoS Biol.* **12,** e1001889 (2014).
36. Abramson, J. & Wright, E. M. Structure and function of Na^+-symporters with inverted repeats. *Curr. Opin. Struct. Biol.* **19,** 425–432 (2009).
37. Khafizov, K., Staritzbichler, R., Stamm, M. & Forrest, L. R. A study of the evolution of inverted-topology repeats from LeuT-fold transporters using AlignMe. *Biochemistry* **49,** 10702–10713 (2010).
38. Duran, A. M. & Meiler, J. Inverted topologies in membrane proteins: a mini-review. *Comput. Struct. Biotechnol. J.* **8,** e201308004 (2013).
39. Michels, J., Vogt, J., Simon, P. & Gorb, S. N. New insights into the complex architecture of siliceous copepod teeth. *Zoology* **118,** 141–146 (2015).
40. Drescher, B., Dillaman, R. M. & Taylor, A. R. Coccolithogenesis in *Scyphosphaera apsteinii* (Prymnesiophyceae). *J. Phycol.* **48,** 1343–1361 (2012).
41. Gal, A., Weiner, S. & Addadi, L. The stabilizing effect of silicate on biogenic and synthetic amorphous calcium carbonate. *J. Am. Chem. Soc.* **132,** 13208–13211 (2010).
42. Ihli, J. *et al.* Dehydration and crystallization of amorphous calcium carbonate in solution and in air. *Nat. Commun.* **5,** 3169 (2014).
43. Kellermeier, M. *et al.* Stabilization of amorphous calcium carbonate in inorganic silica-rich environments. *J. Am. Chem. Soc.* **132,** 17859–17866 (2010).
44. Zhang, G., Delgado-Lopez, J. M., Choquesillo-Lazarte, D. & Garcia-Ruiz, J. M. Growth behavior of monohydrocalcite ($CaCO_3.H_2O$) in silica-rich alkaline solution. *Cryst. Growth Des.* **15,** 564–572 (2015).
45. Azam, F., Hemmings, B. b. & Volcani, B. E. Germanium incorporation into silica of diatom cell-walls. *Arch. Microbiol.* **92,** 11–20 (1973).
46. Darley, W. M. & Volcani, B. E. Role of silicon in diatom metabolism. A silicon requirement for deoxyribonucleic acid synthesis in the diatom *Cylindrotheca fusiformis* Reimann and Lewin. *Exp. Cell Res.* **58,** 334–342 (1969).
47. Azam, F. & Volcani, B. E. in *Silicon and siliceous structures in biological systems* (eds Simpson, T. L. & Volcani, B. E.) 43–68 (Springer-Velag, 1981).
48. Klaveness, D. & Guillard, R. R. L. Requirement for silicon in *Synura petersenii* (Chrysophyceae). *J. Phycol.* **11,** 349–355 (1975).
49. Lee, R. E. Formation of scales in *Paraphysomonas vestita* and inhibition of growth by germanium dioxide. *J. Protozool.* **25,** 163–166 (1978).
50. Lewin, J. C. Silicon metabolism in diatoms. V. germanium dioxide, a specific inhibitor of diatom growth. *Phycologia* **6,** 1–12 (1966).
51. Gerecht, A. C., Supraha, L., Edvardsen, B., Probert, I. & Henderiks, J. High temperature decreases the PIC/POC ratio and increases phosphorus requirements in *Coccolithus pelagicus* (Haptophyta). *Biogeosciences* **11,** 3531–3545 (2014).
52. Probert, I. & Houdan, A. in *Coccolithophores: From Molecular Processes to Global Impact*. (eds Thierstein, H. R. & Young, J. R.) 217–249 (2004).

53. Miller, J. J. & Delwiche, C. F. Phylogenomic analysis of *Emiliania huxleyi* provides evidence for haptophyte-stramenopile association and a chimeric haptophyte nuclear genome. *Marine Genomics* **21,** 31–42 (2015).
54. Stiller, J. W. *et al.* The evolution of photosynthesis in chromist algae through serial endosymbioses. *Nat. Commun.* **5,** 5764 (2014).
55. Yue, J., Sun, G., Hu, X. & Huang, J. The scale and evolutionary significance of horizontal gene transfer in the choanoflagellate *Monosiga brevicollis*. *BMC Genomics* **14,** 729 (2013).
56. Schwarz, K. & Milne, D. B. Growth-promoting effects of silicon in rats. *Nature* **239,** 333 (1972).
57. Carlisle, E. M. Silicon. A possible factor in bone calcification. *Science* **167,** 279 (1970).
58. Reffitt, D. M. *et al.* Orthosilicic acid stimulates collagen type 1 synthesis and osteoblastic differentiation in human osteoblast-like cells *in vitro*. *Bone* **32,** 127–135 (2003).
59. Carlisle, E. M., Berger, J. W. & Alpenfels, W. F. A silicon requirement for prolyl hydroxylase-activity. *Fed. Proc.* **40,** 886–886 (1981).
60. Gal, A. *et al.* Plant cystoliths: a complex functional biocomposite of four distinct silica and amorphous calcium carbonate phases. *Chemistry* **18,** 10262–10270 (2012).
61. Ziveri, P., Broerse, A. T. C., van Hinte, J. E., Westbroek, P. & Honjo, S. The fate of coccoliths at 48 degrees N 21 degrees W, northeastern Atlantic. *Deep Sea Res. Part II* **47,** 1853–1875 (2000).
62. Yool, A. & Tyrrell, T. Role of diatoms in regulating the ocean's silicon cycle. *Global Biogeochem. Cycles* **17,** 1103 (2003).
63. Zhang, J. Z. & Berberian, G. A. in *Methods for the Determination Of Chemical Substances In Marine And Estuarine Environmental Matrices* (ed Arar, E. J.) 366.360-361–366.360-313 (U.S. Environmental Protection Agency, 1997).
64. Timmermans, K. R., Veldhuis, M. J. W. & Brussaard, C. P. D. Cell death in three marine diatom species in response to different irradiance levels, silicate, or iron concentrations. *Aquat. Microb. Ecol.* **46,** 253–261 (2007).
65. Kroger, N., Deutzmann, R. & Sumper, M. Polycationic peptides from diatom biosilica that direct silica nanosphere formation. *Science* **286,** 1129–1132 (1999).
66. Schagger, H. Tricine-SDS-PAGE. *Nat. Protoc.* **1,** 16–22 d (2006).
67. Haas, B. J. *et al.* De novo transcript sequence reconstruction from RNA-seq using the Trinity platform for reference generation and analysis. *Nat. Protoc.* **8,** 1494–1512 (2013).
68. Tamura, K. *et al.* MEGA5: molecular evolutionary genetics analysis using maximum likelihood, evolutionary distance, and maximum parsimony methods. *Mol. Biol. Evol.* **28,** 2731–2739 (2011).
69. Talavera, G. & Castresana, J. Improvement of phylogenies after removing divergent and ambiguously aligned blocks from protein sequence alignments. *Syst. Biol.* **56,** 564–577 (2007).
70. Drummond, A. J., Suchard, M. A., Xie, D. & Rambaut, A. Bayesian phylogenetics with BEAUti and the BEAST 1.7. *Mol. Biol. Evol.* **29,** 1969–1973 (2012).

Acknowledgements

We thank Roy Moate, Glenn Harper and Peter Bond (University of Plymouth, UK) for help with electron microscopy imaging, Malcolm Woodward (Plymouth Marine Laboratory, UK) for help with silicate analyses, Nicholas Smirnoff and Hannah Florance (University of Exeter, UK) for help with protein sequencing and Nils Kroger and Nicole Poulsen (TU Dresden, Germany) for their guidance on analysing the organic component of the silica scales. This study was funded by EU Interreg IV *Marinexus* grant. GW and CB acknowledge support from NERC grant (NE/J021954/1). ART acknowledges NSF grant IOS 0949744 and the University of North Carolina Wilmington Microscopy Facility.

Author contributions

G.M.D. characterized the mechanisms of silicification in *P. neolepis* and identified the requirement for Si in coccolithophores. A.R.T. performed detailed analysis of coccolithophore calcification. C.E.W. performed additional experiments. S.A., I.P., C.d.V. sequenced the transcriptome of *P. neolepis*. G.M.D., A.R.T., C.B. and G.L.W. designed the study and analysed the data. G.M.D., A.R.T., D.C.S., C.B. and G.L.W. wrote the paper.

Additional information

Sequences from *P. neolepis* and *C. leptoporus* were submitted to GenBank (KP793098-KP793099, KR677451).

Supplementary Information accompanies this paper at http://www.nature.com/naturecommunications

Competing financial interests: The authors declare no competing financial interests.

Reprints and permission information is available online at http://npg.nature.com/reprintsandpermissions/

How to cite this article: Durak, G. M. *et al.* A role for diatom-like silicon transporters in calcifying coccolithophores. *Nat. Commun.* 7:10543 doi: 10.1038/ncomms10543 (2016).

Figure I.1

Appendix II: Chapter 3 Supplementary Information

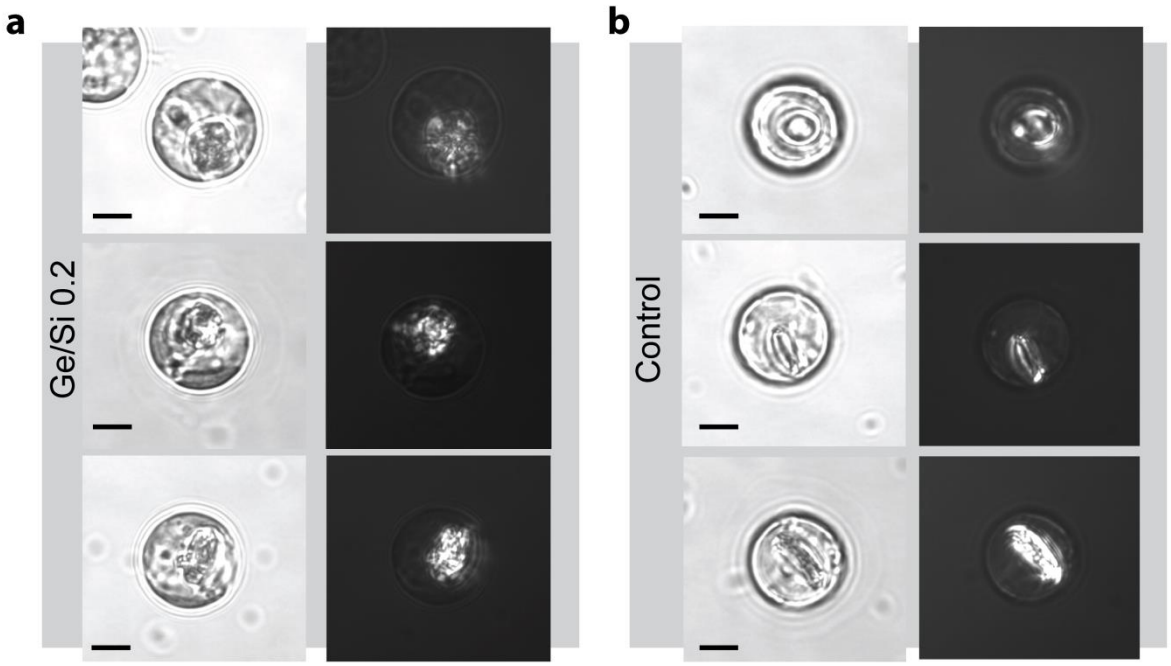

Figure II.1 Images of internal malformed coccoliths
Bright field and polarised light microscopy of decalcified *C. braarudii* cells after 24 h in 0.2 Ge/Si (a) and 0 Ge/Si control (b). Cells were decalcified prior to imaging to clearly visualise the developing internal coccolith. In the Ge treated cells coccoliths are unmistakably malformed. Ge resultant malformations are visible in both the light and polarised light images, especially when compared to the ellipsoidal structure of the control cell internal coccoliths. Scale bars denote 5 µm.

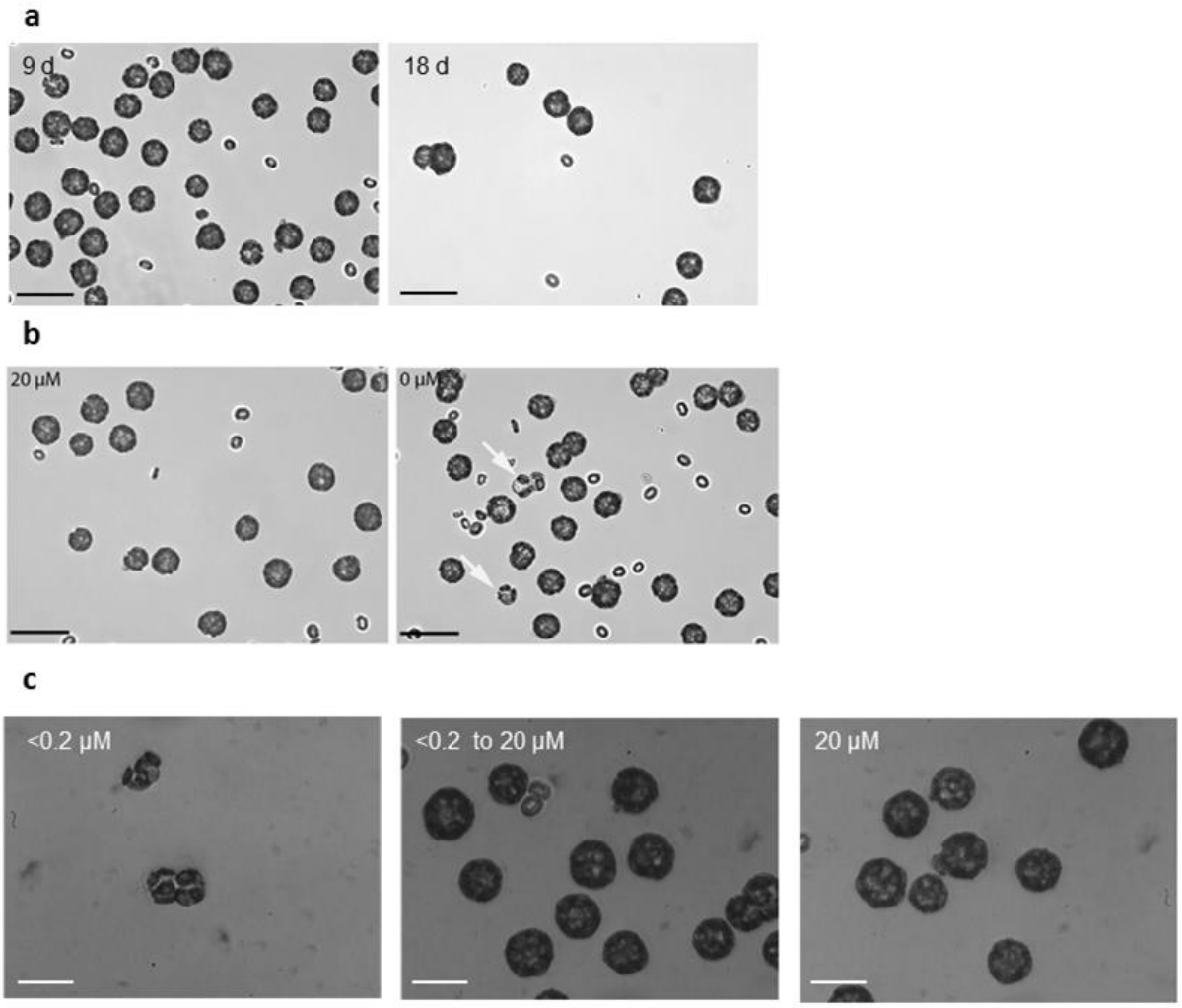

Figure II.2 Images of Si-depleted cultures

C. braarudii cells after 9 and 18 d and 21 d (third sub-culture) in <0.2 µM [dSi]. Cells are fully calcified at 9 and 18 d (a) though partially calcified cells can be observed at <0.2 µM [dSi] after 21 d (b: arrowed). Many cells are present in pairs. c) Bright field images of cells grown in <0.2 µM [dSi] for 21 d and then transferred into <0.2 and 20 µM [dSi]. 7 d after transfer (i.e. 28 d after the initiation of the experiment) cells in <0.2 µM [dSi] are poorly calcified whereas those transferred to 20 µM [dSi] exhibit full coccospheres. Scale bars denote 50 µm.

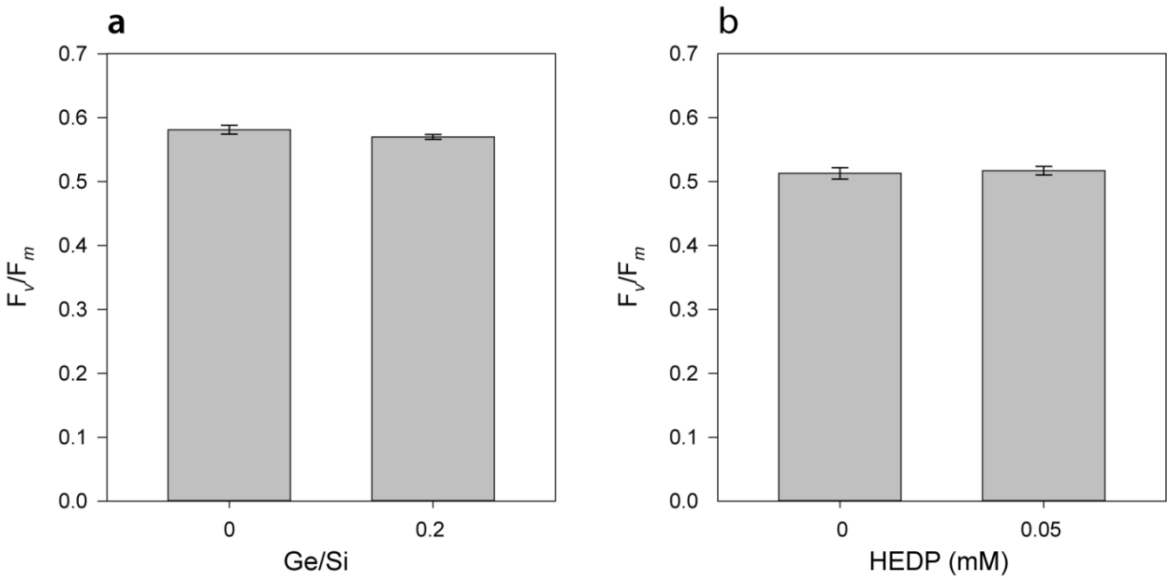

Figure II.3 Photosynthetic efficiency following disruption of calcification
a) The photosynthetic efficiency of photosystem II (F_v/F_m) following treatment of *C. braarudii* cells with 0.2 Ge/Si (100 µM Si) and (b) 0.05 mM HEDP for 72 h. No significant difference was observed in either treatment (p=>0.05, n=3, when analysed using a two-tailed *t*-test). Error bars denote standard error.

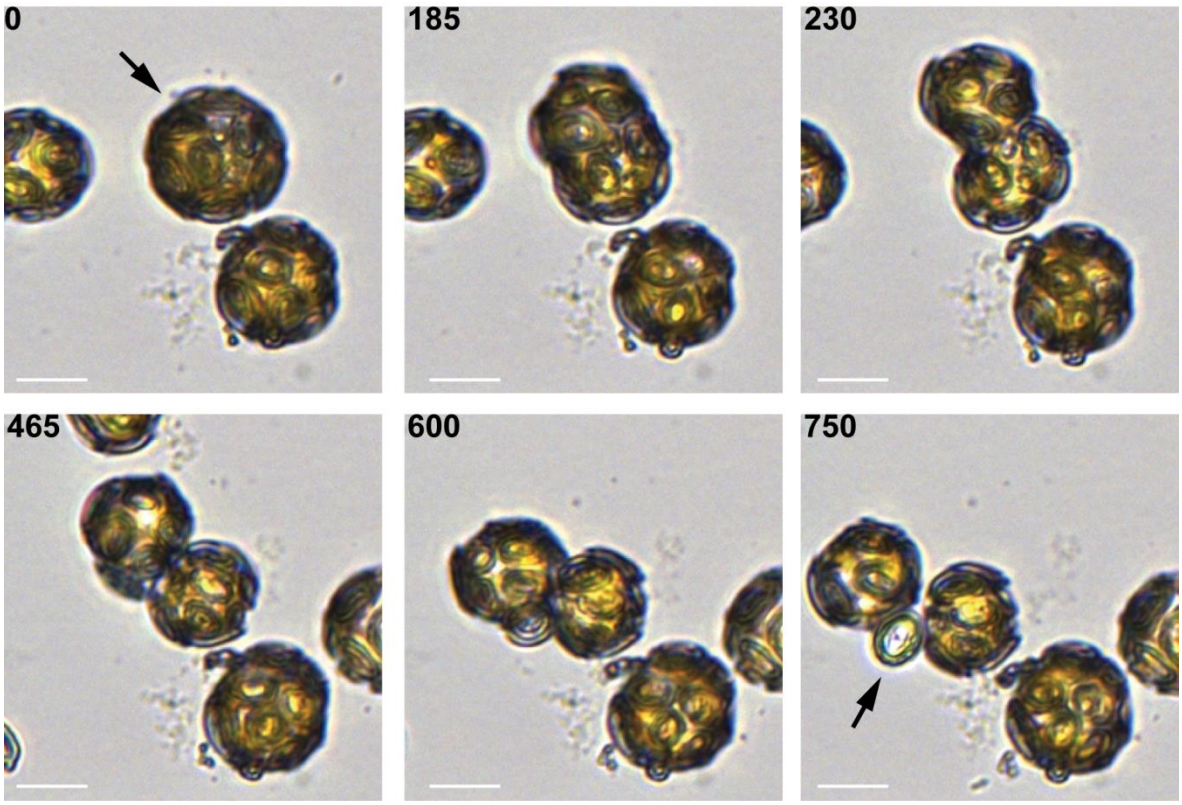

Figure II.4 Time-lapse microscopy of cell division in *C. braarudii*
Time-lapse imaging of *C. braarudii* undergoing cell division recorded over 16 h in the dark (cells were illuminated for 100 ms every 5 minutes in order to record an image). At the onset of cell division, the cell begins to elongate (185 min) and the coccoliths move flexibly on the cell surface to maintain a complete coccosphere. As the cell divides, the coccosphere rearranges to ensure both daughter cells are fully covered following division (230-465 min). The cells separate following rearrangement of the coccospheres (600-750 min) and a complete coccolith is dislodged prior to separation of the two daughter cells (arrowed). Frame labels denote minutes passed and scale bars denote 15 µm.

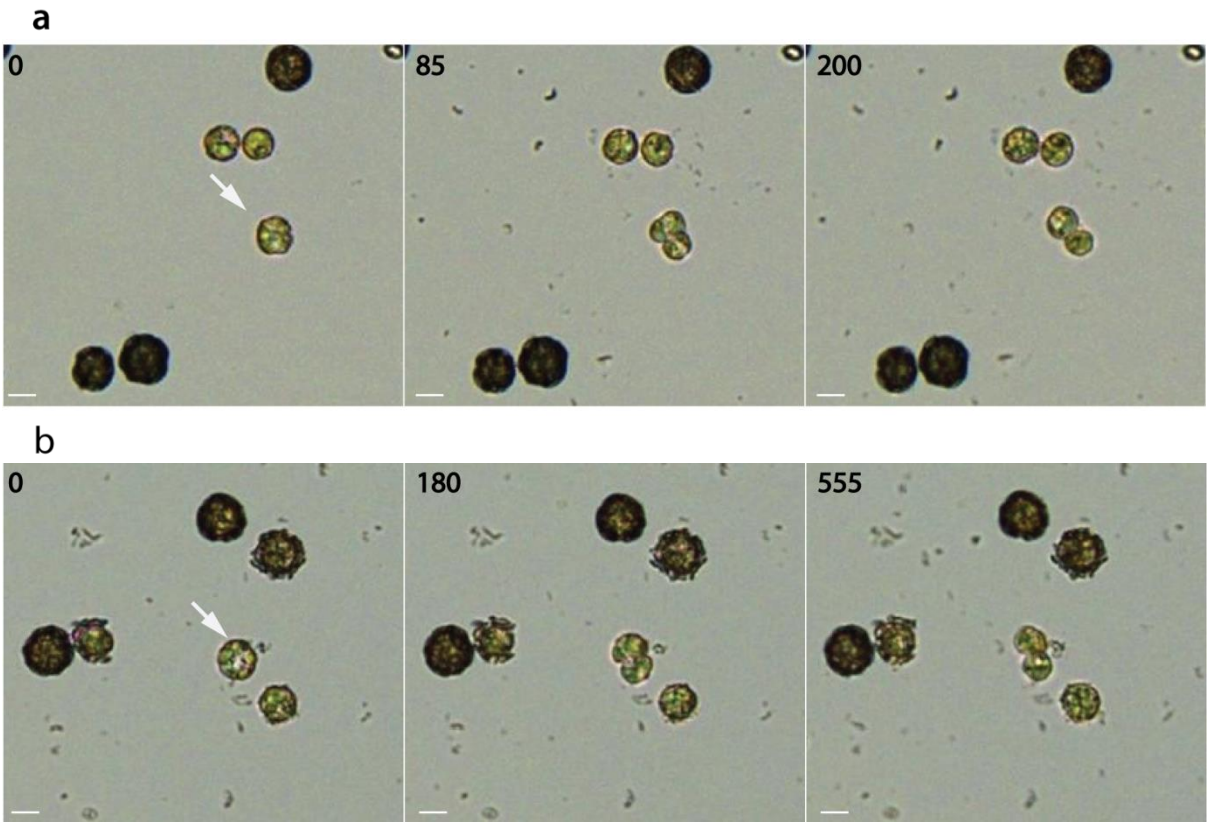

Figure II.5 Cell division can occur in the absence of a coccosphere
C. braarudii cells were decalcified using ASW minus Ca^{2+} pH 7.0 for 1 h. This timescale results in significant numbers of fully decalcified cells. Time-lapse images were recorded for 16 h in the dark (17^{o}C) to observe cell division of the decalcified cells. a, b) examples of fully decalcified cells undergoing cell division (arrows). The cells are able to divide when fully decalcified but remain in pairs after cytokinesis takes place. Frame labels denote minutes passed and scale bars denote 15 µm.

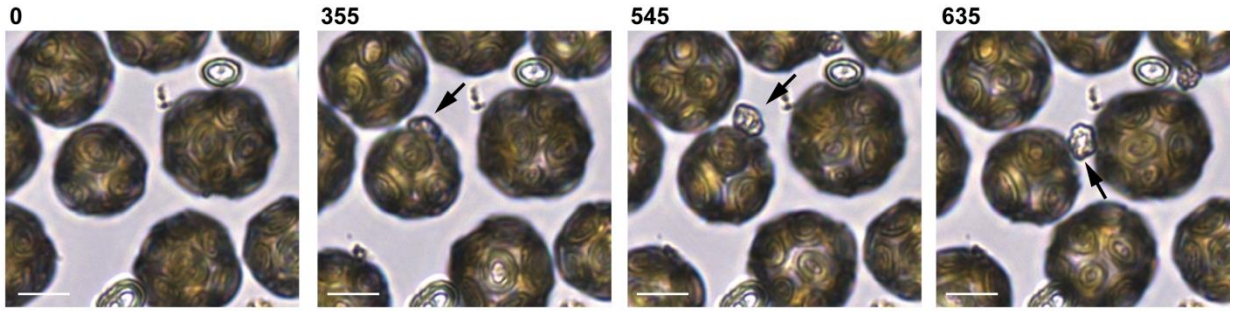

Figure II.6 Malformed coccolith production in Ge-treated cells
C. braarudii cells were incubated in Ge/Si 0.2 (10 µM Si). Time-lapse images were recorded over 16 h in the light (17^{o}C) to observe the effects of Ge. Cells treated with Ge are initially fully calcified. In the example shown, a cell produces a highly malformed coccolith 6 h after addition of Ge (arrow). The malformed coccolith is unable to integrate into the coccosphere and is discarded into the surrounding media. Frame labels denote minutes passed and scale bars denote 10 µm.

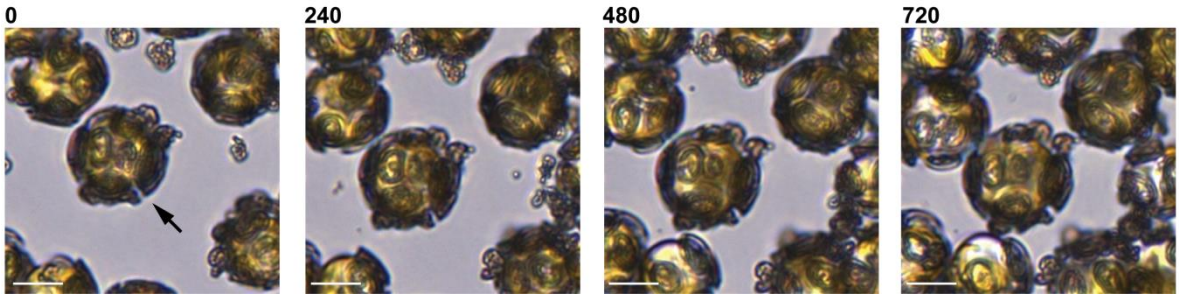

Figure II.7 Ge-treated cells exhibit a progressive disruption of the coccosphere as cell volume increases

Time-lapse LM footage was recorded over 12 h in the light (17^{O}C) to observe the effects of Ge on coccolith production. *C. braarudii* cells were grown in Ge/Si 0.2 (10 µM Si) for 4 d. In control cells, coccoliths are continuously produced and incorporated into the coccosphere as volume of the growing cell increases, ensuring the cell remains covered by a single layer of coccoliths. Ge-treated cells also continue to calcify and exhibit an increase in cell volume during the 12 h time-lapse period. However, as the malformed coccoliths are not integrated into the coccosphere, the coccosphere covers proportionately less of the cell body as the cell expands. As a result, the disruption to the coccosphere is visibly greater at the end of time lapse (720 min) the compared to the start (T0). Frame labels denote minutes passed and scale bars denote 10 µm.

Table II.1 Disruption of calcification in *C. braarudii* by low Ca^{2+}, HEDP or Ge, determined as the percentage of incomplete or malformed coccoliths in the coccosphere.

Inhibitor		**24 h**		**48 h**		**72 h**	
		Control	Inhibitor	Control	Inhibitor	Control	Inhibitor
Low Ca^{2+}	Incomplete (%)	9.42*	8.49	12.53	20.69	6.56	29.75
	Total Coccoliths Scored	456	412	431	435	457	437
Ge	Malformed (%)	0.00	4.03	0.76	13.74	0.38	11.08**
	Total Coccoliths Scored	552	521	526	502	526	469
HEDP	Malformed (%)	0.41	3.24	0.21	15.40	0.00	25.00
	Total Coccoliths Scored	487	432	475	435	471	471

Incomplete: where calcification of the coccolith has begun but stopped before completion

Malformed: coccoliths exhibiting gross defects in morphology, e.g. irregular shaping of the calcite crystals

* *C. braarudii* cells grown in ASW typically exhibit an elevated level of incomplete coccoliths relative to cells grown in natural seawater.

** Coccoliths generated during Ge treatment are highly malformed and often fail to integrate into the coccosphere.

Table II.2 The calcification status of diploid coccolithophore strains in algal culture collections

Family	Species	Isolates often become partially- or non-calcified in laboratory culture?*	Examples of non-calcified diploid strains in culture collections	Reports of non-calcified strains in literature
Calcidiscaceae	*Calcidiscus leptoporus*	NO	None	
	Calcidiscus quadriperforatus	NO	None	
	Oolithotus fragilis	NO	None	
	Umbilicosphaera sibogae	NO	None	
	Umbilicosphaera foliosa	NO	None	
	Umbilicosphaera hulburtiana	NO**	None	
Coccolithaceae	*Coccolithus pelagicus*	NO	None	
	Coccolithus braarudii	NO	None	
Hymenomonadaceae	*Ochrosphaera neapolitana*	YES	CCAP932/1; RCC1358; RCC1365	
	Hymenomonas coronata	YES	RCC1337	
Pleurochrysidaceae	*Chrysotila carterae*	YES	CCMP645; RCC1402	Marsh & Dickinson, 1997; Marsh, 2006
	Chrysotila dentata	YES	CCAP904/1; RCC1394	
	Chrysotila pseudoroscoffensis	YES	CCAP912/1; CCAP913/2; CCAP913/3; CCAP961/3	
Helicosphaeraceae	*Syracosphaera pulchra*	NO	None	
	Helicosphaera carteri	NO	None	
Pontosphaeraceae	*Scyphosphaera apsteinii*	NO	None	
Noelaerhabdaceae	*Gephyrocapsa oceanica*	NO	None	
	Emiliania huxleyi	YES	CCMP370; CCMP373; CCMP374; CCMP379; CCMP1280; CCMP1516; CCMP2090	Klaveness, 1972; Paasche, 2001

*Non-calcified strains are defined as diploid strains which can persist in a non-calcified state without any adverse effects on cell fitness; calcified strains are those in which healthy diploid cultures do not exhibit non-calcified cells. **A single isolate (strain RCC1474) was observed to grow in a non-calcified state for a prolonged period, although it has subsequently regained a calcified state (I. Probert -personal communication).

Appendix III: Chapter 4 Supplementary Information

Table III.1 REST Output: Si Reduction Response

Time (d)	Control (Si µM)	Test (Si µM)	Gene	Type	Reaction Efficiency	Expression	Standard Error	95% Confidence Interval	*P(H1)*	Result*
1	10	0.22	EFL	REF	0.95	1.054				
			RPS1	REF	0.90	0.648				
			SITL	QUERY	0.92	0.908	0.690 – 1.216	0.554 – 1.349	0.697	NS
8	10	0.22	EFL	REF	0.95	0.959				
			RPS1	REF	0.90	1.042				
			SITL	QUERY	0.92	1.205	0.956 – 1.541	0.854 – 1.673	0.298	NS

* Statistical significance of the normalised expression change. NS: not statistically significant

Table III.2 REST Output: Si Replenishment Response

Time (h)	Control (Si µM)	Test (Si µM)	Gene	Type	Reaction Efficiency	Expression	Standard Error	95% Confidence Interval	*P(H1)*	Result*
48	0	2	EFL	REF	0.99	1.136				
			RPS1	REF	1.0	0.881				
			SITL	QUERY	0.97	0.872	0.594- 1.129	0.545 – 1.187	0.842	NS
		20	EFL	REF	0.99	0.738				
			RPS1	REF	1.0	1.355				
			SITL	QUERY	0.97	1.097	0.857 – 1.799	0.612 – 1.799	0.721	NS
		100	EFL	REF	0.99	1.018				
			RPS1	REF	1.0	0.982				
			SITL	QUERY	0.97	0.710	0.537 – 1.191	0.366 – 1.276	0.481	NS
96	0	2	EFL	REF	0.99	0.618				
			RPS1	REF	1.0	1.617				
			SITL	QUERY	0.97	1.298	0.379 – 4.575	0.333 – 5.488	0.608	NS
		20	EFL	REF	0.99	1.473				
			RPS1	REF	1.0	0.679				
			SITL	QUERY	0.97	0.490	0.333 – 0.702	0.293 – 0.842	0.080	NS
		100	EFL	REF	0.99	1.507				
			RPS1	REF	1.0	0.664				
			SITL	QUERY	0.97	0.408	0.269 – 0.588	0.236 – 0.706	0.045	DOWN

* Statistical significance of the normalised expression change. NS: not statistically significant

a) EFL L4 consensus and *C. braarudii* MMETSP EFL Sequence Alignment

```
> (modified) Alignment of 2 sequences: EFL 1A 2A Consensus - Edited, CAMNT_0025
499507


Identities = 167/174 (95%),
Positives = 169/174 (97%), Gaps = 0/174 (0%)

EFL 1A 2A Consensus - Edited     1 GTGCACCACCAAGGAGTTCTTCACGGAGAAGTGGCACTACACCATCATTGACGCCCCGGG  60
                                   GTGCACCACCAAGGAGTTCTTCACGGAGAAGTGGCACTACACCATCATTGACGC CC GG
CAMNT_0025499507               288 GTGCACCACCAAGGAGTTCTTCACGGAGAAGTGGCACTACACCATCATTGACGCGCCTGG 347

EFL 1A 2A Consensus - Edited    61 TCACCGTGATTTCATCAAGAACATGATTTCCGGTGCCGCCCAGGCTGACGTCGCCCTGCT 120
                                   TCACCGTGATTTCATCAAGAACATGAT TCCGGTGCCGC CAGGCTGACGTCGC CTGCT
CAMNT_0025499507               348 TCACCGTGATTTCATCAAGAACATGATCTCCGGTGCCGCGCAGGCTGACGTCGCTCTGCT 407

EFL 1A 2A Consensus - Edited   121 CATGGTTCCCGCNGACGGTAACTTCACCACCGCCATCCAANAGGGCAACCACAA 174
                                   CATGGTTCCCGC+GACGGTAACTTCACCACCGCCATCCAA+AGGGCAACCACAA
CAMNT_0025499507               408 CATGGTTCCCGCCGACGGTAACTTCACCACCGCCATCCAAAAGGGCAACCACAA 461
```

b) SITL L4 consensus and *C. braarudii* MMETSP SITL Sequence Alignment

```
> (modified) Alignment of 2 sequences: L4 SITL Consensus, CAMNT_0025525031

Identities = 150/150 (100%),
Positives = 150/150 (100%), Gaps = 0/150 (0%)

L4 SITL Consensus      2 CGCTGGCATGAATCAAGGTGGTTTTGGCACGAGTATGCGCCGCACTACGCCGCGTTATCC  61
                         CGCTGGCATGAATCAAGGTGGTTTTGGCACGAGTATGCGCCGCACTACGCCGCGTTATCC
CAMNT_0025525031     104 CGCTGGCATGAATCAAGGTGGTTTTGGCACGAGTATGCGCCGCACTACGCCGCGTTATCC 163

L4 SITL Consensus     62 ATGCGTTGTTGTGACGGTGTTTTGTTGAGCCGCTCGCTCGCGCTTGAACTGGAGGAGCAG 121
                         ATGCGTTGTTGTGACGGTGTTTTGTTGAGCCGCTCGCTCGCGCTTGAACTGGAGGAGCAG
CAMNT_0025525031     164 ATGCGTTGTTGTGACGGTGTTTTGTTGAGCCGCTCGCTCGCGCTTGAACTGGAGGAGCAG 223

L4 SITL Consensus    122 TGCCATACACACGACGTGCGGAGGAATATG 151
                         TGCCATACACACGACGTGCGGAGGAATATG
CAMNT_0025525031     224 TGCCATACACACGACGTGCGGAGGAATATG 253
```

Figure III.1 Alignments of EFL and SITL environmental and reference sequences
EFL (a) and SITL (b) L4 environmental consensus sequences aligned with *C. braarudii* MMETSP EFL and SITL reference sequences.

Appendix IV: Chapter 5 Supplementary Information

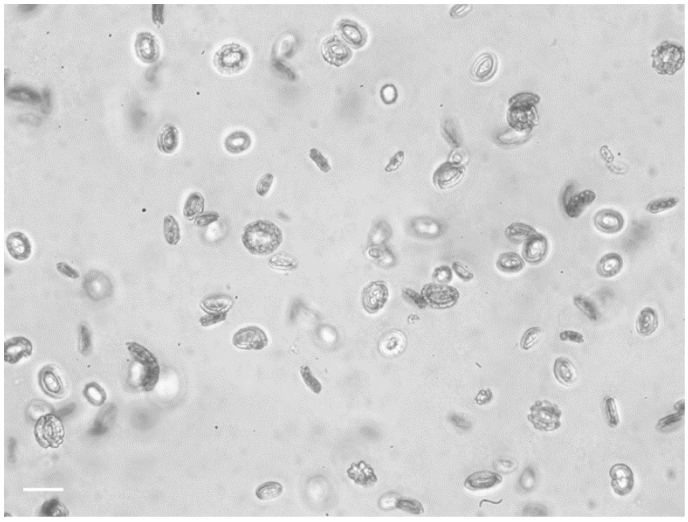

Figure IV.1 FITC-conA does not bind to calcite
Bright field image of *C. braarudii* coccoliths treated with sodium hypochlorite to remove all organic material. No non-specific binding of FITC-conA to calcite was observed in this sample. Scale bar denotes 5 µm.

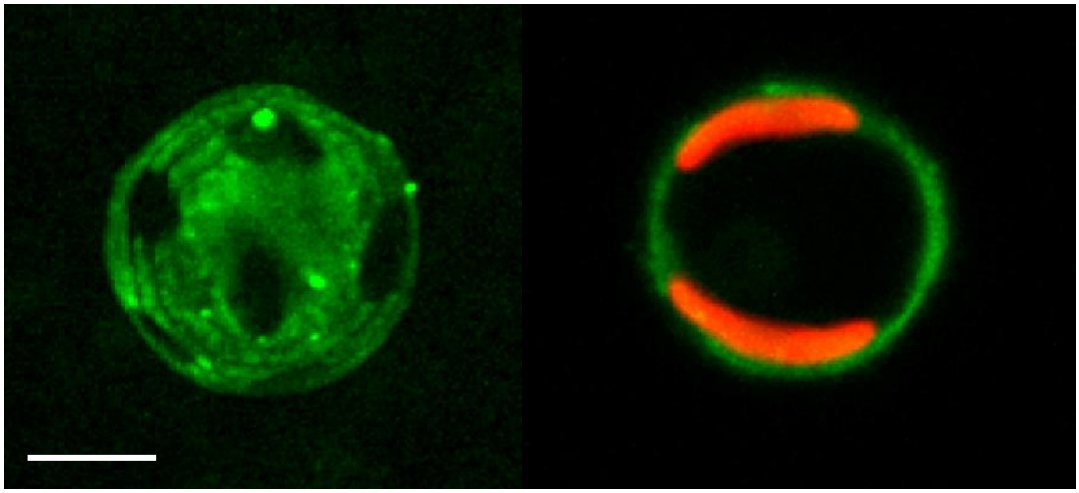

Figure IV.2 Confocal microscopy of Texas Red-conA stained decalcified *C. braarudii*
The 3D reconstruction shows ellipsoidal intervals in the Texas Red-conA staining. Chlorophyll autofluorescence is also shown (red). Texas Red-conA staining is comparable to FITC-conA indicating that there was no non-specific binding due to the fluorophore conjugated to the lectin. Scale bar denotes 10 µm.

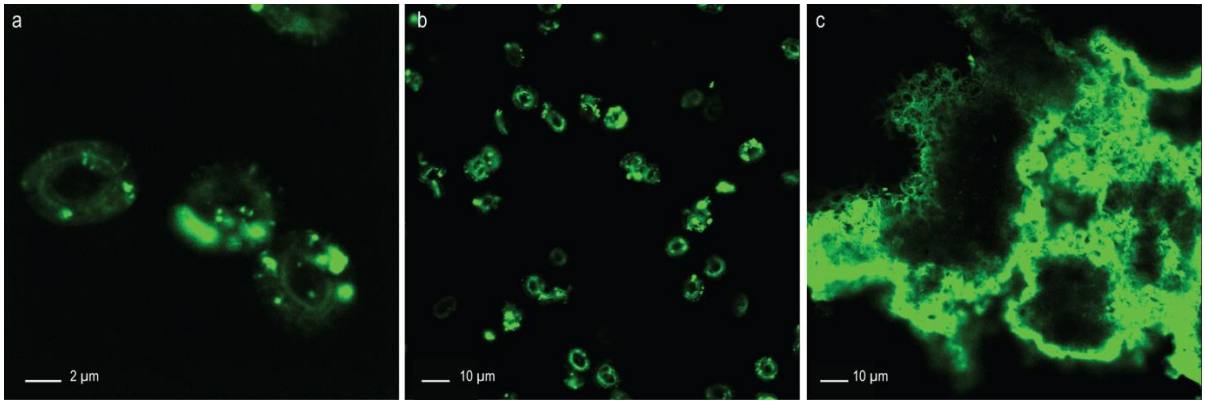

Figure IV.3 FITC-conA staining of polysaccharide extractions
FITC-conA stained coccoliths following (a) cell lysis, (b) density centrifugation and (c) a portion of the polysaccharide pellet post-extraction procedure. FITC-conA staining visualised in calcified cells is maintained throughout the polysaccharide extraction process.

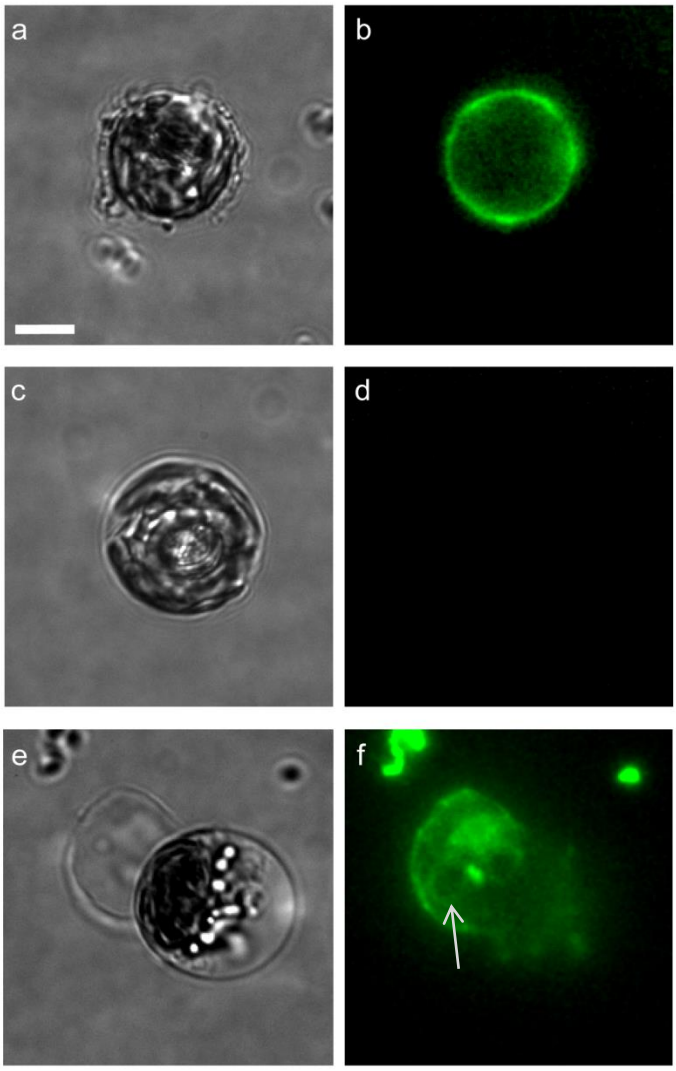

Figure IV.4 Detachment of the extracellular polysaccharide layer
FITC-conA staining of *C. braarudii* cells with an attached polysaccharide layer (a-b) and without an attached polysaccharide layer (c-d). The detached polysaccharide layer can remain intact even when removed from the cell body (e-f) whereby the oval-shaped structure is still visible (arrow). These images were captured on a Nikon Ti epifluorescent microscope. Scale bar denotes 5 µm and is applied to all images.

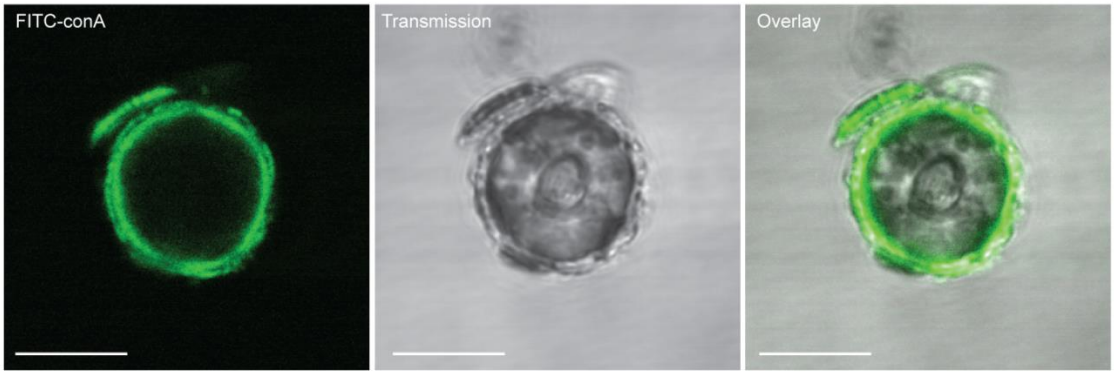

Figure IV.5 Extracellular polysaccharide coats the cell and the coccoliths
FITC-conA stained partially decalcified *C. braarudii* shows that the extracellular polysaccharide is localised on the cell body and coats the singular coccolith visualised on the cell surface. It is likely that the polysaccharide coats the coccolith as it moves through the extracellular layer. Scale bars denote 10 µm.

References

2017. Western Channel Observatory L4 Phytoplankton Time-series.In Observatory WC. http://www.westernchannelobservatory.org.uk/l4_phytoplankton.

Abràmoff MD, Magalhães PJ, Ram SJ. 2004. Image processing with ImageJ. *Biophotonics international* **11**(7): 36-42.

Aitken ZH, Luo S, Reynolds SN, Thaulow C, Greer JR. 2016. Microstructure provides insights into evolutionary design and resilience of *Coscinodiscus sp*. frustule. *Proceedings of the National Academy of Sciences* **113**(8): 2017-2022.

Altschul SF, Gish W, Miller W, Myers EW, Lipman DJ. 1990. Basic local alignment search tool. *Journal of Molecular Biology* **215**(3): 403-410.

Amo YD, Brzezinski MA. 1999. The chemical form of dissolved Si taken up by marine diatoms. *Journal of Phycology* **35**(6): 1162-1170.

Archer D. 1996. A data-driven model of the global calcite lysocline. *Global Biogeochemical Cycles* **10**(3): 511-526.

Armbrust EV, Berges JA, Bowler C, Green BR, Martinez D, Putnam NH, Zhou S, Allen AE, Apt KE, Bechner M. 2004. The genome of the diatom *Thalassiosira pseudonana*: ecology, evolution, and metabolism. *Science* **306**(5693): 79-86.

Asahina M. 2004. *Inhibition of Crystal Growth in Coccolith Formation of Pleurochrysis Carterae by a potent Scale Inhibitor, (1-Hydroxyethylidene) Bisphosphonic Acid (HEBP)*: Universidade de Vigo: Servicio de Publicaciones.

Azam F, Hemmingsen BB, Volcani BE. 1973. Germanium incorporation into the silica of diatom cell walls. *Archives of Microbiology* **92**(1): 11-20.

Azam F, Volcani B 1981. Germanium-silicon interactions in biological systems. *Silicon and siliceous structures in biological systems*: Springer, 43-67.

Bach L. 2015. Reconsidering the role of carbonate ion concentration in calcification by marine organisms. *Biogeosciences Discussions* **12**: 6689-6722.

Bach LT, Bauke C, Meier K, Riebesell U, Schulz KG. 2012. Influence of changing carbonate chemistry on morphology and weight of coccoliths formed by *Emiliania huxleyi*. *Biogeosciences (BG)* **9**(8): 3449-3463.

Bach LT, Mackinder LC, Schulz KG, Wheeler G, Schroeder DC, Brownlee C, Riebesell U. 2013. Dissecting the impact of CO_2 and pH on the mechanisms of photosynthesis and calcification in the coccolithophore *Emiliania huxleyi*. *New Phytol* **199**(1): 121-134.

Bach LT, Riebesell U, Georg Schulz K. 2011. Distinguishing between the effects of ocean acidification and ocean carbonation in the coccolithophore *Emiliania huxleyi*. *Limnology and Oceanography* **56**(6): 2040-2050.

Bach LT, Riebesell U, Gutowska M, Federwisch L, Schulz KG. 2015. A unifying concept of coccolithophore sensitivity to changing carbonate chemistry embedded in an ecological framework. *Progress in Oceanography*.

Balch W, Drapeau D, Bowler B, Lyczkowski E, Lubelczyk L, Painter S, Poulton A. 2014. Surface biological, chemical, and optical properties of the Patagonian Shelf coccolithophore bloom, the brightest waters of the Great Calcite Belt. *Limnology and Oceanography* **59**(5): 1715-1732.

Balch WM, Holligan PM, Kilpatrick KA. 1992. Calcification, photosynthesis and growth of the bloom-forming coccolithophore, *Emiliania huxleyi*. *Continental Shelf Research* **12**(12): 1353-1374.

Basharina TN, Danilovtseva EN, Zelinskiy SN, Klimenkov IV, Likhoshway YV, Annenkov VV. 2012. The effect of titanium, zirconium and tin on the growth of diatom *Synedra acus* and morphology of its silica valves. *Silicon*: 1-11.

Baumann K-H, Böckel B, Frenz M 2004. Coccolith contribution to South Atlantic carbonate sedimentation. In: Thierstein HR, Young JR eds. *Coccolithophores: From Molecular Processes to Global Impact*. Berlin, Heidelberg: Springer Berlin Heidelberg, 367-402.

Berge G. 1962. Discoloration of the sea due to *Coccolithus huxleyi* "bloom". *Sarsia* **6**(1): 27-40.

Bienert GP, Schüssler MD, Jahn TP. 2008. Metalloids: essential, beneficial or toxic? Major intrinsic proteins sort it out. *Trends in Biochemical Sciences* **33**(1): 20-26.

Bijma J, Altabet M, Conte M, Kinkel H, Versteegh G, Volkman J, Wakeham S, Weaver P. 2001. Primary signal: Ecological and environmental factors—Report from Working Group 2. *Geochemistry, Geophysics, Geosystems* **2**(1).

Birchall J. 1995. The essentiality of silicon in biology. *Chemical Society Reviews* **24**(5): 351-357.

Birkenes E, Braarud T. 1952. Phytoplankton in the Oslo Fjord during a" *Coccolithus Huxleyi*-summer".-Avh. norske Vidensk. *Akad. Mat.-Nat. Kl* **2**.

Borman AH, de Jong EW, Huizinga M, Kok DJ, Westbroek P, Bosch L. 1982. The Role in $CaCO_3$ Crystallization of an Acid Ca^{2+}-Binding Polysaccharide Associated with Coccoliths of *Emiliania huxleyi*. *European Journal of Biochemistry* **129**(1): 179-183.

Borman AH, De Jong EW, Thierry R, Westbroek P, Bosch L. 1987. Coccolith-Associated Polysaccharides from cells of *Emiliania huxleyi* (Haptophyceae). *Journal of Phycology* **23**: 118-125.

Bown P. 1998. *Calcareous nannofossil biostratigraphy*: Chapman and Hall; Kluwer Academic.

Bown PR, Lees JA, Young JR 2004. Calcareous nannoplankton evolution and diversity through time. *Coccolithophores*: Springer, 481-508.

Brand LE. 2006. Physiological ecology of marine. *Coccolithophores*: 39.

Brembu T, Chauton MS, Winge P, Bones AM, Vadstein O. 2017. Dynamic responses to silicon in Thalasiossira pseudonana - Identification, characterisation and classification of signature genes and their corresponding protein motifs. *Scientific Reports* **7**(1): 4865.

Brown PR, Lees JA, Young JR 2004. Calcareous nannoplankton evolution and diversity through time. *Coccolithophores*: Springer, 481-508.

Brownlee C, Taylor A 2004. Calcification in coccolithophores: A cellular perspective. In: Thierstein H, Young J eds. *Coccolithophores*: Springer Berlin Heidelberg, 31-49.

Brzezinski M, Olson R, Chisholm S. 1990. Silicon availability and cell-cycle progression in marine diatoms. *Marine ecology progress series. Oldendorf* **67**(1): 83-96.

Buitenhuis ET, De Baar HJ, Veldhuis MJ. 1999. Photosynthesis and calcification by Emiliania huxleyi (Prymnesiophyceae) as a function of inorganic carbon species. *Journal of Phycology* **35**(5): 949-959.

Buitenhuis ET, van der Wal P, de Baar HJW. 2001. Blooms of *Emiliania huxleyi* are sinks of atmospheric carbon dioxide: A field and mesocosm study derived simulation. *Global Biogeochemical Cycles* **15**(3): 577-587.

Bukry D. 1974. Coccoliths as Paleosalinity Indicators--Evidence from Black Sea: Biology.

Burki F, Okamoto N, Pombert J-F, Keeling PJ. 2012. The evolutionary history of haptophytes and cryptophytes: phylogenomic evidence for separate origins. *Proceedings of the Royal Society B: Biological Sciences* **279**(1736): 2246-2254.

Bustin SA, Nolan T. 2004. Pitfalls of quantitative real-time reverse-transcription polymerase chain reaction. *Journal of biomolecular techniques: JBT* **15**(3): 155.

Cachao M, Moita M. 2000. *Coccolithus pelagicus*, a productivity proxy related to moderate fronts off Western Iberia. *Marine Micropaleontology* **39**(1-4): 131-155.

Cavalier-Smith T. 1982. The origins of plastids. *Biological Journal of the Linnean Society* **17**(3): 289-306.

Cavalier-Smith T. 2003. Protist phylogeny and the high-level classification of Protozoa. *European Journal of Protistology* **39**(4): 338-348.

Chemistry RSo 2018. Periodic Table. http://www.rsc.org/periodic-table: Royal Society of Chemistry.

Chiu S-J, Lee M-Y, Chen H-W, Chou W-G, Lin L-Y. 2002. Germanium oxide inhibits the transition from G2 to M phase of CHO cells. *Chemico-biological interactions* **141**(3): 211-228.

Clapham DE. 1995. Calcium signaling. *Cell* **80**: 259-268.

Corpe WA. 1964. Factors influencing growth and polysaccharide formation by strains of Chromobacterium violaceum. *Journal of bacteriology* **88**(5): 1433-1441.

Corstjens PLAM, Van Der Kooij A, Linschooten C, Brouwers G-J, Westbroek P, Jong EWdV-d. 1998. GPA, A CALCIUM-BINDING PROTEIN IN THE COCCOLITHOPHORID EMILIANIA HUXLEYI (PRYMNESIOPHYCEAE). *Journal of Phycology* **34**(4): 622-630.

Cros L, Kleijne A, Zeltner A, Billard C, Young JR. 2000. New examples of holococcolith–heterococcolith combination coccospheres and their implications for coccolithophorid biology. *Marine Micropaleontology* **39**(1–4): 1-34.

Cubillos JC, Henderiks J, Beaufort L, Howard WR, Hallegraeff GM. 2012. Reconstructing calcification in ancient coccolithophores: Individual coccolith weight and morphology of *Coccolithus pelagicus* (sensu lato). *Marine Micropaleontology* **92**: 29-39.

Danbara A, Shiraiwa Y. 1999. The requirement of selenium for the growth of marine coccolithophorids, *Emiliania huxleyi, Gephyrocapsa oceanica* and *Helladosphaera sp*.(Prymnesiophyceae). *Plant and Cell Physiology* **40**(7): 762-766.

Daniels CJ, Poulton AJ, Young JR, Esposito M, Humphreys MP, Ribas-Ribas M, Tynan E, Tyrrell T. 2016. Species-specific calcite production reveals Coccolithus pelagicus as the key calcifier in the Arctic Ocean. *Marine Ecology Progress Series* **555**: 29-47.

Daniels CJ, Sheward RM, Poulton AJ. 2014. Biogeochemical implications of comparative growth rates of *Emiliania huxleyi* and *Coccolithus* species. *Biogeosciences* **11**(23): 6915-6925.

Darley WM, Volcani B. 1969. Role of silicon in diatom metabolism: a silicon requirement for deoxyribonucleic acid synthesis in the diatom *Cylindrotheca fusiformis* Reimann and Lewin. *Experimental Cell Research* **58**(2): 334-342.

Davis AK, Hildebrand M. 2008. A self-propagating system for Ge incorporation into nanostructured silica. *Chemical Communications*(37): 4495-4497.

De Jong EW, Bosch L, Westbroek P. 1976. Isolation and Characterization of a Ca^{2+} Binding Polysaccharide Associated with Coccoliths of *Emiliania huxleyi* (Lohmann) Kamptner. *European Journal of Biochemistry* **70**(2): 611-621.

De Vargas C, Aubry MP, Probert I, Young JN 2007. Origin and Evolution of Coccolithophores: From Coastal Hunters to Oceanic Farmers. In: Falkowski P, Knoll AH eds. *Evolution of Primary Producers in the Sea*: Academic Press.

Dixon HH. 1900. On the structure of coccospheres and the origin of coccoliths. *Proceedings of the Royal Society of London* **66**(424-433): 305-315.

Domozych DS, Sørensen I, Popper ZA, Ochs J, Andreas A, Fangel JU, Pielach A, Sacks C, Brechka H, Ruisi-Besares P. 2014. Pectin metabolism and assembly in the cell wall of the charophyte green alga Penium margaritaceum. *Plant Physiology* **165**(1): 105-118.

Doney SC, Fabry VJ, Feely RA, Kleypas JA. 2009. Ocean Acidification: The Other CO_2 Problem. *Ann Rev Mar Sci* **1**(1): 169-192.

Doney SC, Ruckelshaus M, Duffy JE, Barry JP, Chan F, English CA, Galindo HM, Grebmeier JM, Hollowed AB, Knowlton N. 2012. Climate change impacts on marine ecosystems. *Marine Science* **4**.

Dorrell RG, Gile G, Mccallum G, Méheust R, Bapteste EP, Klinger CM, Brillet-Guéguen L, Freeman KD, Richter DJ, Bowler C. 2017. Chimeric origins of ochrophytes and haptophytes revealed through an ancient plastid proteome. *Elife* **6**.

Drescher B, Dillaman RM, Taylor AR. 2012. Coccolithogenesis in *Scyphosphaera apsteinii* (Prymnesiophyceae). *Journal of Phycology* **48**(6): 1343-1361.

Durak GM, Brownlee C, Wheeler GL. 2017. The role of the cytoskeleton in biomineralisation in haptophyte algae. *Scientific Reports* **7**(1): 15409.

Durak GM, Taylor AR, Walker CE, Probert I, de Vargas C, Audic S, Schroeder D, Brownlee C, Wheeler G. 2015. A role for diatom-like silicon transporters in calcifying coccolithophores. *Nature Communications* **In press**.

Durak GM, Taylor AR, Walker CE, Probert I, De Vargas C, Audic S, Schroeder D, Brownlee C, Wheeler GL. 2016. A role for diatom-like silicon transporters in calcifying coccolithophores. *Nat Commun* **7**.

Durkin CA, Marchetti A, Bender SJ, Truong T, Morales R, Mock T, Armbrust E. 2012. Frustule-related gene transcription and the influence of diatom community composition on silica precipitation in an iron-limited environment. *Limnology and Oceanography* **57**(6): 1619-1633.

Edvardsen B, Eikrem W, Throndsen J, Sáez AG, Probert I, Medlin LK. 2011. Ribosomal DNA phylogenies and a morphological revision provide the basis for a revised taxonomy of the Prymnesiales (Haptophyta). *European Journal of Phycology* **46**(3): 202-228.

Falkowski PG, Barber RT, Smetacek V. 1998. Biogeochemical Controls and Feedbacks on Ocean Primary Production. *Science* **281**(5374): 200-206.

Falkowski PG, Katz ME, Milligan AJ, Fennel K, Cramer BS, Aubry MP, Berner RA, Novacek MJ, Zapol WM. 2005. The Rise of Oxygen over the Past 205 Million Years and the Evolution of Large Placental Mammals. *Science* **309**(5744): 2202-2204.

Falkowski PG, Raven JA. 2013. *Aquatic photosynthesis*: Princeton University Press.

Fichtinger-Schepman AMJ, Kamerling JP, Versluis C, Vliegenthart JFG. 1981. Structural studies of the methylated, acidic polysaccharide associated with coccoliths of Emiliania huxleyi (lohmann) kamptner. *Carbohydrate Research* **93**(1): 105-123.

Fichtinger-Schepman AMJ, Kamerling JP, Vliegenthart JFG, De Jong EW, Bosch L, Westbroek P. 1979. Composition of a methylated, acidic polysaccharide associated with coccoliths of *Emiliania huxleyi* (Lohmann) Kamptner. *Carbohydrate Research* **69**(1): 181-189.

Findlay HS, Calosi P, Crawfurd K. 2011. Determinants of the PIC : POC response in the coccolithophore Emiliania huxleyi under future ocean acidification scenarios. *Limnology and Oceanography* **56**(3): 1168-1178.

Gal A, Hirsch A, Siegel S, Li C, Aichmayer B, Politi Y, Fratzl P, Weiner S, Addadi L. 2012. Plant cystoliths: a complex functional biocomposite of four distinct silica and amorphous calcium carbonate phases. *Chemistry-A European Journal* **18**(33): 10262-10270.

Gal A, Sviben S, Wirth R, Schreiber A, Lassalle-Kaiser B, Faivre D, Scheffel A. 2017. Trace Element Incorporation into Intracellular Pools Uncovers Calcium Pathways in a Coccolithophore. *Advanced Science* **4**(10).

Gal A, Weiner S, Addadi L. 2010. The stabilizing effect of silicate on biogenic and synthetic amorphous calcium carbonate. *J Am Chem Soc* **132**(38): 13208-13211.

Gal A, Wirth R, Kopka J, Fratzl P, Faivre D, Scheffel A. 2016. Macromolecular recognition directs calcium ions to coccolith mineralization sites. *Science* **353**(6299): 590-593.

Geisen M, Billard C, Broerse AT, Cros L, Probert I, Young JR. 2002. Life-cycle associations involving pairs of holococcolithophorid species: intraspecific variation or cryptic speciation? *European Journal of Phycology* **37**(4): 531-550.

Gerecht AC, Šupraha L, Edvardsen B, Langer G, Henderiks J. 2015. Phosphorus availability modifies carbon production in Coccolithus pelagicus (Haptophyta). *Journal of Experimental Marine Biology and Ecology* **472**: 24-31.

Gerecht AC, Šupraha L, Edvardsen B, Probert I, Henderiks J. 2014. High temperature decreases the PIC/POC ratio and increases phosphorus requirements in *Coccolithus pelagicus* (Haptophyta). *Biogeosciences* **11**(13): 3531-3545.

Gersonde R, Harwood DM 1990. 25. Lower Cretaceous diatoms from ODP LEG 113 Site 693 (Weddel sea). Part 1: Vegetative cells. *Proc ODP Sci Res*. 365-402.

Gibbs SJ, Bown PR, Ridgwell A, Young JR, Poulton AJ, O'Dea SA. 2016. Ocean warming, not acidification, controlled coccolithophore response during past greenhouse climate change. *Geology* **44**(1): 59-62.

Gibbs SJ, Poulton AJ, Brown PR, Daniels CJ, Hopkins J, Young JR, Jones HL, Thiemann GJ, O'Dea SA, Newsam C. 2013. Species-specific growth response of coccolithophores to Palaeocene–Eocene environmental change. *Nature Geoscience* **6**: 5.

Giraudeau J, Monteiro PM, Nikodemus K. 1993. Distribution and malformation of living coccolithophores in the northern Benguela upwelling system off Namibia. *Marine Micropaleontology* **22**(1-2): 93-110.

Gordon R, Losic D, Tiffany MA, Nagy SS, Sterrenburg FA. 2009. The glass menagerie: diatoms for novel applications in nanotechnology. *Trends in biotechnology* **27**(2): 116-127.

Green J, Course P. 1983. Extracellular calcification in Chrysotila lamellosa (Prymnesiophyceae). *British Phycological Journal* **18**(4): 367-382.

Guan W, Gao K. 2010. Impacts of UV radiation on photosynthesis and growth of the coccolithophore *Emiliania huxleyi* (Haptophyceae). *Environmental and Experimental Botany* **67**(3): 502-508.

Guillard RRL, Ryther JH. 1962. Studies of marine planktonic diatoms. *Canadian Journal of Microbiology* **8**(2): 229-239.

Hagino K, Onuma R, Kawachi M, Horiguchi T. 2013. Discovery of an endosymbiotic nitrogen-fixing cyanobacterium UCYN-A in *Braarudosphaera bigelowii* (Prymnesiophyceae). *PLoS One* **8**(12): e81749.

Hall TA 1999. BioEdit: a user-friendly biological sequence alignment editor and analysis program for Windows 95/98/NT. *Nucleic acids symposium series*: [London]: Information Retrieval Ltd., c1979-c2000. 95-98.

Hansen FC, Witte HJ, Passarge J. 1996. Grazing in the heterotrophic dinoflagellate *Oxyrrhis marina*: size selectivity and preference for calcified *Emiliania huxleyi* cells. *Aquatic microbial ecology* **10**(3): 307-313.

Harris RP. 1994. Zooplankton grazing on the coccolithophore *Emiliania huxleyi* and its role in inorganic carbon flux. *Marine Biology* **119**(3): 431-439.

Harrison PJ, Waters RE, Taylor F. 1980. A Broad Spectrum Artificial Sea Water Medium for Coastal and Open Ocean Phytoplankton. *Journal of Phycology* **16**(1): 28-35.

Harvey EL, Bidle KD, Johnson MD. 2015. Consequences of strain variability and calcification in *Emiliania huxleyi* on microzooplankton grazing. *Journal of Plankton Research* **37**(6): 1137-1148.

Haug A. 1976. The influence of borate and calcium on the gel formation of a sulfated polysaccharide from Ulva lactuca. *Acta chemica Scandinavica. Series B: Organic chemistry and biochemistry* **30**(6): 562-566.

Heath CR, Leadbeater BCS, Callow ME. 1995. Effect of inhibitors on calcium carbonate deposition mediated by freshwater algae. *Journal of Applied Phycology* **7**(4): 367-380.

Henriksen K, Stipp SLS. 2009. Controlling biomineralization: the effect of solution composition on coccolith polysaccharide functionality. *Crystal Growth and Design* **9**(5): 2088-2097.

Henriksen K, Stipp SLS, Young JR, Marsh ME 2004. Biological control on calcite crystallization: AFM investigation of coccolith polysaccharide function. *American Mineralogist*. 1709.

Henriksen K, Young J, Bown P, Stipp S. 2004. Coccolith biomineralisation studied with atomic force microscopy. *Palaeontology* **47**(3): 725-743.

Henstock JR, Canham LT, Anderson SI. 2015. Silicon: The evolution of its use in biomaterials. *Acta Biomaterialia* **11**: 17-26.

Herfort L, Loste E, Meldrum F, Thake B. 2004. Structural and physiological effects of calcium and magnesium in *Emiliania huxleyi* (Lohmann) Hay and Mohler. *Journal of Structural Biology* **148**(3): 307-314.

Herfort L, Thake B, Roberts J. 2002. Acquisition and use of bicarbonate by *Emiliania huxleyi*. *New Phytologist* **156**(3): 10.

Hildebrand M, Dahlin K, Volcani B. 1998. Characterization of a silicon transporter gene family in *Cylindrotheca fusiformis*: sequences, expression analysis, and identification of homologs in other diatoms. *Molecular and General Genetics MGG* **260**(5): 480-486.

Hildebrand M, Volcani BE, Gassmann W, Schroeder JI. 1997. A gene family of silicon transporters. *Nature* **385**(6618): 688.

Hippler M. 2017. *Chlamydomonas: Molecular Genetics and Physiology*: Springer.

Hirokawa Y. 2013. Localization and Associative Strength of Acid Polysaccharides in Coccoliths of <i>Pleurochrysis haptonemofera</i> (Haptophyta) Predicted from Their Extractability from Partially Decalcified Coccoliths. *Open Journal of Marine Science* **03**(01): 48-54.

Hoffmann R, Kirchlechner C, Langer G, Wochnik AS, Griesshaber E, Schmahl WW, Scheu C. 2015. Insight into *Emiliania huxleyi* coccospheres by focused ion beam sectioning. *Biogeosciences* **12**(3): 825-834.

Holtz L-M, Thoms S, Langer G, Wolf-Gladrow DA. 2013. Substrate supply for calcite precipitation in Emiliania huxleyi: assessment of different model approaches. *Journal of Phycology* **49**(2): 417-426.

Hönisch B, Ridgwell A, Schmidt DN, Thomas E, Gibbs SJ, Sluijs A, Zeebe R, Kump L, Martindale RC, Greene SE, et al. 2012. The Geological Record of Ocean Acidification. *Science* **335**(6072): 1058-1063.

Hopkins J, Henson SA, Painter SC, Tyrrell T, Poulton AJ. 2015. Phenological characteristics of global coccolithophore blooms. *Global Biogeochemical Cycles* **29**(2): 239-253.

Hoppe CJM, Langer G, Rost B. 2011. Emiliania huxleyi shows identical responses to elevated pCO2 in TA and DIC manipulations. *Journal of Experimental Marine Biology and Ecology* **406**(1–2): 54-62.

Houdan A, Probert I, Van Lenning K, Lefebvre S. 2005. Comparison of photosynthetic responses in diploid and haploid life-cycle phases of *Emiliania huxleyi* (Prymnesiophyceae). *Marine Ecology Progress Series* **292**: 139-146.

Houdan A, Probert I, Zatylny C, Véron B, Billard C. 2006. Ecology of oceanic coccolithophores. I. Nutritional preferences of the two stages in the life cycle of Coccolithus braarudii and Calcidiscus leptoporus. *Aquatic microbial ecology* **44**(3): 291.

Jaya BN, Hoffmann R, Kirchlechner C, Dehm G, Scheu C, Langer G. 2016. Coccospheres confer mechanical protection: New evidence for an old hypothesis. *Acta Biomaterialia* **42**: 258-264.

Johnson RN, Volcani BE. 1978. The uptake of silicic acid by rat liver mitochondria. *Biochemical Journal* **172**(3): 557-568.

Jolly WL. 1966. *The chemistry of non-metals*. Englewood Cliffs, New Jersey: Prentice-Hall Inc. .

Jordan RW, Green JC. 1994. A check-list of the extant Haptophyta of the world. *Journal of the Marine Biological Association of the United Kingdom* **74**(01): 149-174.

Katagiri F, Takatsuka Y, Fujiwara S, Tsuzuki M. 2010. Effects of Ca and Mg on growth and calcification of the coccolithophorid *Pleurochrysis haptonemofera*: Ca requirement for cell division in coccolith-bearing cells and for normal coccolith formation with acidic polysaccharides. *Marine Biotechnology* **12**(1): 42-51.

Katz ME, Fennel K, Falkowski PG. 2007. Geochemical and biological consequences of phytoplankton evolution. *Evolution of Primary Production in the Sea*: 405-430.

Kayano K, Saruwatari K, Kogure T, Shiraiwa Y. 2011. Effect of coccolith polysaccharides isolated from the coccolithophorid, *Emiliania huxleyi*, on calcite crystal formation in in vitro $CaCO_3$ crystallization. *Marine Biotechnology* **13**(1): 83-92.

Kayano K, Shiraiwa Y. 2009. Physiological regulation of coccolith polysaccharide production by phosphate availability in the coccolithophorid *Emiliania huxleyi*. *Plant Cell Physiol* **50**(8): 1522-1531.

Kearse M, Moir R, Wilson A, Stones-Havas S, Cheung M, Sturrock S, Buxton S, Cooper A, Markowitz S, Duran C. 2012. Geneious Basic: an integrated and extendable desktop software platform for the organization and analysis of sequence data. *Bioinformatics* **28**(12): 1647-1649.

Keeling PJ, Burki F, Wilcox HM, Allam B, Allen EE, Amaral-Zettler LA, Armbrust EV, Archibald JM, Bharti AK, Bell CJ, et al. 2014. The Marine Microbial Eukaryote Transcriptome Sequencing Project (MMETSP): illuminating the functional diversity of eukaryotic life in the oceans through transcriptome sequencing. *PLoS Biol* **12**(6): e1001889.

Kegel JU, John U, Valentin K, Frickenhaus S. 2013. Genome variations associated with viral susceptibility and calcification in *Emiliania huxleyi*. *PLoS One* **8**(11): e80684.

Keller MD, Selvin RC, Claus W, Guillard RR. 1987. Media for the culture of oceanic ultraphytoplankton1, 2. *Journal of Phycology* **23**(4): 633-638.

Kirkwood DS. 1989. Simultaneous determination of selected nutrients in sea water. . ICES.

Klaas C, Archer DE. 2002. Association of sinking organic matter with various types of mineral ballast in the deep sea: Implications for the rain ratio. *Global Biogeochemical Cycles* **16**(4).

Klaveness D. 1972. *Coccolithus Huxleyi (Lohmann) Kamptner: Morphological Investigations on the Vegetative Cell and the Process of Coccolith Formation*.

Klaveness D, Guillard RR. 1975. The requirement for silicon in *Synura petersenii* (Chrysophyceae). *Journal of Phycology* **11**(3): 349-355.

Kleijne D. 1993. *Morphology, taxonomy and distribution of extant coccolithophorids (calcereous nanoplankton).* Ph.D, Free University of Amsterdam.

Knoll AH. 2003. Biomineralization and evolutionary history. *Reviews in mineralogy and geochemistry* **54**(1): 329-356.

Knoll AH, Kotrc B 2015. Protistan skeletons: a geologic history of evolution and constraint. *Evolution of lightweight structures*: Springer, 1-16.

Kolb A, Strom S. 2013. An inducible antipredatory defense in haploid cells of the marine microalga *Emiliania huxleyi* (Prymnesiophyceae). *Limnology and Oceanography* **58**(3): 932-944.

Kottmeier DM, Rokitta SD, Rost B. 2016. H^+ driven increase in CO_2 uptake and decrease in uptake explain coccolithophores' acclimation responses to ocean acidification. *Limnology and Oceanography* **61**(6): 2045-2057.

Kröger N, Deutzmann R, Sumper M. 1999. Polycationic Peptides from Diatom Biosilica That Direct Silica Nanosphere Formation. *Science* **286**(5442): 1129-1132.

Kroth PG 2007. Genetic Transformation. *Protein Targeting Protocols*: Springer, 257-267.

Krug SA. 2011. *Coccolithophores in an acidifying ocean: from single strain to multiple species approaches.* Christian-Albrechts Universität Kiel.

Langer G, Bode M. 2011. CO_2 mediation of adverse effects of seawater acidification in Calcidiscus leptoporus. *Geochemistry, Geophysics, Geosystems* **12**(5).

Langer G, Geisen M, Baumann K-H, Kläs J, Riebesell U, Thoms S, Young JR. 2006a. Species-specific responses of calcifying algae to changing seawater carbonate chemistry. *Geochemistry, Geophysics, Geosystems* **7**(9): Q09006.

Langer G, Geisen M, Baumann K-H, Kläs J, Riebesell U, Thoms S, Young JR. 2006b. Species-specific responses of calcifying algae to changing seawater carbonate chemistry. *Geochemistry, Geophysics, Geosystems* **7**(9): n/a-n/a.

Langer G, Nehrke G, Probert I, Ly J, Ziveri P. 2009. Strain-specific responses of *Emiliania huxleyi* to changing seawater carbonate chemistry. *Biogeosciences* **6**(11): 2637-2646.

Leblanc K, Hare C, Feng Y, Berg G, DiTullio G, Neeley A, Benner I, Sprengel C, Beck A, Sanudo-Wilhelmy S. 2009. Distribution of calcifying and silicifying phytoplankton in relation to environmental and biogeochemical parameters during the late stages of the 2005 North East Atlantic Spring Bloom. *Biogeosciences* **6**: 2155-2179.

Lee RBY, Mavridou DAI, Papadakos G, McClelland HLO, Rickaby REM. 2016. The uronic acid content of coccolith-associated polysaccharides provides insight into coccolithogenesis and past climate. **7**: 13144.

Lee RE. 1978. Formation of scales in *Paraphysomonas vestita* and the inhibition of growth by germanium dioxide. *Journal of Eukaryotic Microbiology* **25**(2): 163-166.

Leonardos N, Read B, Thake B, Young JR. 2009. No mechanistic dependence of photosynthesis on calcifcation in the coccolithophorid *Emiliania huxleyi* (Haptophyta). *Journal of Phycology* **45**(5): 1046-1051.

Lewin J. 1966. Silicon Metabolism in Diatoms. V. Germanium Dioxide, a Specific Inhibitor of Diatom Growth. *Phycologia* **6**(1): 1-12.

Lewin RA. 1992. What the haptonema is for. *Nature* **356**: 195.

Liu H, Aris-Brosou S, Probert I, de Vargas C. 2010. A time line of the environmental genetics of the haptophytes. *Mol Biol Evol* **27**(1): 161-176.

Lutgens FK, Tarbuck EJ, Tasa DG. 2014. *Essentials of geology*: Pearson Higher Ed.

Mackinder L, Wheeler G, Schroeder D, Riebesell U, Brownlee C. 2010. Molecular Mechanisms Underlying Calcification in Coccolithophores. *Geomicrobiology Journal* **27**(6-7): 585-595.

Mackinder L, Wheeler G, Schroeder D, von Dassow P, Riebesell U, Brownlee C. 2011. Expression of biomineralization-related ion transport genes in *Emiliania huxleyi*. *Environmental Microbiology* **13**(12): 3250-3265.

Mann S, Ozin GA. 1996. Synthesis of inorganic materials with complex form. *Nature* **382**(6589): 313-318.

Marin F, Smith M, Isa Y, Muyzer G, Westbroek P. 1996. Skeletal matrices, muci, and the origin of invertebrate calcification. *Proceedings of the National Academy of Sciences* **93**(4): 1554-1559.

Marron AO, Alston MJ, Heavens D, Akam M, Caccamo M, Holland PWH, Walker G. 2013. A family of diatom-like silicon transporters in the siliceous loricate choanoflagellates. *Proceedings of the Royal Society B: Biological Sciences* **280**(1756): 20122543.

Marron AO, Chappell H, Ratcliffe S, Goldstein RE. 2016. A model for the effects of germanium on silica biomineralization in choanoflagellates. *Journal of The Royal Society Interface* **13**(122): 20160485.

Marron AO, Ratcliffe S, Wheeler GL, Goldstein RE, King N, Not F, de Vargas C, Richter DJ. 2016. The Evolution of Silicon Transport in Eukaryotes. *Mol Biol Evol* **33**(12): 3226-3248.

Marsh M. 1994. Polyanion-mediated mineralization — assembly and reorganization of acidic polysaccharides in the Golgi system of a coccolithophorid alga during mineral deposition. *Protoplasma* **177**(3-4): 108-122.

Marsh M, Chang D, King G. 1992. Isolation and characterization of a novel acidic polysaccharide containing tartrate and glyoxylate residues from the mineralized scales of a unicellular coccolithophorid alga Pleurochrysis carterae. *Journal of Biological Chemistry* **267**(28): 20507-20512.

Marsh ME. 1996. Polyanion-mediated mineralization — a kinetic analysis of the calcium-carrier hypothesis in the phytoflagellatePleurochrysis carterae. *Protoplasma* **190**(3-4): 181-188.

Marsh ME. 2003. Regulation of $CaCO_3$ formation in coccolithophores. *Comparative Biochemistry and Physiology Part B: Biochemistry and Molecular Biology* **136**(4): 743-754.

Marsh ME. 2006. Biomineralization in Coccolithophores. *Biomineralization: Progress in Biology, Molecular Biology and Application*.

Marsh ME, Dickinson DP. 1997. Polyanion-mediated mineralization — mineralization in coccolithophore (*Pleurochrysis carterae*) variants which do not express PS2, the most abundant and acidic mineral-associated polyanion in wild-type cells. *Protoplasma* **199**(1): 9-17.

Martin-Jézéquel V, Hildebrand M, Brzezinski MA. 2000. Silicon metabolism in diatoms: implications for growth. *Journal of phycology* **36**(5): 821-840.

Matoh T, Kobayashi M. 1998. Boron and calcium, essential inorganic constituents of pectic polysaccharides in higher plant cell walls. *Journal of Plant Research* **111**(1): 179-190.

McIntyre A, Bé AW 1967. Modern coccolithophoridae of the Atlantic Ocean—I. Placoliths and cyrtoliths. *Deep Sea Research and Oceanographic Abstracts*: Elsevier. 561-597.

Medlin L, Sáez A, Young J. 2008. A molecular clock for coccolithophores and implications for selectivity of phytoplankton extinctions across the K/T boundary. *Marine Micropaleontology* **67**(1-2): 69-86.

Meyer J, Riebesell U. 2015. Reviews and Syntheses: Responses of coccolithophores to ocean acidification: a meta-analysis. *Biogeosciences* **12**(6): 1671-1682.

Milliman J, Troy P, Balch W, Adams A, Li Y-H, Mackenzie F. 1999. Biologically mediated dissolution of calcium carbonate above the chemical lysocline? *Deep Sea Research Part I: Oceanographic Research Papers* **46**(10): 1653-1669.

Milliman JD. 1980. Coccolithophorid production and sedimentation, Rockall Bank. *Deep Sea Research Part A. Oceanographic Research Papers* **27**(11): 959-963.

Milliman JD. 1993. Production and accumulation of calcium carbonate in the ocean: Budget of a nonsteady state. *Global Biogeochemical Cycles* **7**(4): 927-957.

Mock T, Samanta MP, Iverson V, Berthiaume C, Robison M, Holtermann K, Durkin C, BonDurant SS, Richmond K, Rodesch M. 2008. Whole-genome expression profiling of the marine diatom *Thalassiosira pseudonana* identifies genes involved in silicon bioprocesses. *Proceedings of the National Academy of Sciences* **105**(5): 1579-1584.

Monteiro FM, Bach LT, Brownlee C, Bown P, Rickaby REM, Poulton AJ, Tyrrell T, Beaufort L, Dutkiewicz S, Gibbs S, et al. 2016. Why marine phytoplankton calcify. *Science Advances* **2**(7).

Müller M, Antia A, LaRoche J. 2008. Influence of cell cycle phase on calcification in the coccolithophore *Emiliania huxleyi*. *Limnology and Oceanography* **53**(2): 506-512.

Müller M, Schulz K, Riebesell U. 2010. Effects of long-term high CO 2 exposure on two species of coccolithophores. *Biogeosciences (BG)* **7**(3): 1109-1116.

Müller MN, Barcelos e Ramos J, Schulz KG, Riebesell U, Kaźmierczak J, Gallo F, Mackinder L, Li Y, Nesterenko PN, Trull TW, et al. 2015. Phytoplankton calcification as an effective mechanism to alleviate cellular calcium poisoning. *Biogeosciences* **12**(21): 6493-6501.

Nanninga HJ, Tyrrell T. 1996. Importance of light for the formation of algal blooms by *Emiliania huxleyi*. *Marine Ecology Progress Series* **136**: 195-203.

Nguyen B, Bowers RM, Wahlund TM, Read BA. 2005. Suppressive subtractive hybridization of and differences in gene expression content of calcifying and noncalcifying cultures of Emiliania huxleyi strain 1516. *Appl Environ Microbiol* **71**(5): 2564-2575.

Nordberg H, Cantor M, Dusheyko S, Hua S, Poliakov A, Shabalov I, Smirnova T, Grigoriev IV, Dubchak I. 2013. The genome portal of the Department of Energy Joint Genome Institute: 2014 updates. *Nucleic acids research* **42**(D1): D26-D31.

Observatory WC 2017. Western Channel Observatory L4 surface nutrients data.In Laboratory PM. www.westernchannelobservatory.org.uk.

Okada H, McIntyre A. 1979. Seasonal distribution of modern coccolithophores in the western North Atlantic Ocean. *Marine Biology* **54**(4): 319-328.

Ozaki N, Ozaki M, Kogure T, Sakuda S, Nagasawa H. 2004. Structural and functional diversity of acidic polysaccharides from various species of coocolithophorid algae. *Thalassas: An international journal of marine sciences* **20**(1): 59-68.

Ozaki N, Sakuda S, Nagasawa H. 2007. A novel highly acidic polysaccharide with inhibitory activity on calcification from the calcified scale "coccolith" of a coccolithophorid alga, Pleurochrysis haptonemofera. *Biochemical and Biophysical Research Communications* **357**(4): 1172-1176.

Paasche E. 1964. *A Tracer Study of the Inorganic Carbon Uptake During Coccolith Formation and Photosynthesis in the Coccolithophorid Coccolithus Huxleyi*: Scandinavian Society for Plant Physiology.

Paasche E. 1998. Roles of nitrogen and phosphorus in coccolith formation in *Emiliania huxleyi* (Prymnesiophyceae). *European Journal of Phycology* **33**(1): 33-42.

Paasche E. 1999. Reduced coccolith calcite production under light-limited growth: a comparative study of three clones of Emiliania huxleyi (Prymnesiophyceae). *Phycologia* **38**(6): 508-516.

Paasche E. 2001. A review of the coccolithophorid *Emiliania huxleyi* (Prymnesiophyceae), with particular reference to growth, coccolith formation, and calcification-photosynthesis interactions. *Phycologia* **40**(6): 503-529.

Parente A, Cachão M, Baumann K-H, de Abreu L, Ferreira J. 2004. Morphometry of *Coccolithus pelagicus* sl (Coccolithophore, Haptophyta) from offshore Portugal, during the last 200 kyr. *Micropaleontology* **50**(Suppl_1): 107-120.

Parke M, Adams I. 1960. The motile (*Crystallolithus hyalinus* Gaarder & Markali) and non-motile phases in the life history of *Coccolithus pelagicus* (Wallich) Schiller. *Journal of the Marine Biological Association of the United Kingdom* **39**(2): 263-274.

Patwardhan SV. 2011. Biomimetic and bioinspired silica: recent developments and applications. *Chemical Communications* **47**(27): 7567-7582.

Pfaffl MW, Horgan GW, Dempfle L. 2002. Relative expression software tool (REST©) for group-wise comparison and statistical analysis of relative expression results in real-time PCR. *Nucleic acids research* **30**(9): e36-e36.

Poulton AJ, Adey TR, Balch WM, Holligan PM. 2007. Relating coccolithophore calcification rates to phytoplankton community dynamics: Regional differences and implications for carbon export. *Deep Sea Research Part II: Topical Studies in Oceanography* **54**(5–7): 538-557.

Poulton AJ, Painter SC, Young JR, Bates NR, Bowler B, Drapeau D, Lyczsckowski E, Balch WM. 2013. The 2008 *Emiliania huxleyi* bloom along the Patagonian Shelf: Ecology, biogeochemistry, and cellular calcification. *Global Biogeochemical Cycles* **27**(4): 1023-1033.

Quinn P, Bowers RM, Zhang X, Wahlund TM, Fanelli MA, Olszova D, Read BA. 2006. cDNA microarrays as a tool for identification of biomineralization proteins in the coccolithophorid Emiliania huxleyi (Haptophyta). *Appl Environ Microbiol* **72**(8): 5512-5526.

Read BA, Kegel J, Klute MJ, Kuo A, Lefebvre SC, Maumus F, Mayer C, Miller J, Monier A, Salamov A, et al. 2013. Pan genome of the phytoplankton Emiliania underpins its global distribution. *Nature* **499**(7457): 209-213.

Reinfelder JR. 2011. Carbon concentrating mechanisms in eukaryotic marine phytoplankton. *Ann Rev Mar Sci* **3**: 291-315.

Rickaby REM, Henderiks J, Young JN. 2010. Perturbing phytoplankton: response and isotopic fractionation with changing carbonate chemistry in two coccolithophore species. *Climate of the Past* **6**(6): 771-785.

Ridgwell A, Schmidt DN, Turley C, Brownlee C, Maldonado MT, Tortell P, Young JR. 2009. From laboratory manipulations to Earth system models: scaling calcification impacts of ocean acidification. *Biogeosciences* **6**(11): 2611-2623.

Ridgwell A, Zeebe R. 2005. The role of the global carbonate cycle in the regulation and evolution of the Earth system. *Earth and Planetary Science Letters* **234**(3-4): 299-315.

Riebesell U, Zondervan I, Rost B, Tortell PD, Zeebe R, Morel F, M. M. 2000. Reduced calcification of marine plankton in response to increased atmospheric CO_2. *Nature chemistry* **407**: 4.

Rivero-Calle S, Gnanadesikan A, Del Castillo CE, Balch WM, Guikema SD. 2015. Multidecadal increase in North Atlantic coccolithophores and the potential role of rising CO_2. *Science* **350**(6267): 1533-1537.

Rost B, Riebesell U 2004. Coccolithophores and the biological pump: responses to environmental changes. *Coccolithophores: From*.

Rowson JD, Leadbeater BS, Green J. 1986. Calcium carbonate deposition in the motile (Crystallolithus) phase of *Coccolithus pelagicus* (Prymnesiophyceae). *British Phycological Journal* **21**(4): 359-370.

Rozen S, Skaletsky H. 1999. Primer3 on the WWW for general users and for biologist programmers. *Bioinformatics methods and protocols*: 365-386.

Sáez AG, Probert I, Geisen M, Quinn P, Young JR, Medlin LK. 2003. Pseudo-cryptic speciation in coccolithophores. *Proceedings of the National Academy of Sciences* **100**(12): 7163-7168.

Safonova T, Annenkov V, Chebykin E, Danilovtseva E, Likhoshway YV, Grachev M. 2007. Aberration of morphogenesis of siliceous frustule elements of the diatom *Synedra acus* in the presence of germanic acid. *Biochemistry (Moscow)* **72**(11): 1261-1269.

Sand K, Pedersen C, Sjoberg S, Nielsen J, Makovicky E, Stipp S. 2014. Biomineralization: long-term effectiveness of polysaccharides on the growth and dissolution of calcite. *Crystal Growth & Design* **14**(11): 5486-5494.

Sanders D, Pelloux J, Brownlee C, Harper JF. 2002. Calcium at the crossroads of signaling. *The Plant Cell* **14**(suppl 1): S401-S417.

Sapriel G, Quinet M, Heijde M, Jourdren L, Tanty V, Luo G, Le Crom S, Lopez PJ. 2009. Genome-wide transcriptome analyses of silicon metabolism in *Phaeodactylum tricornutum* reveal the multilevel regulation of silicic acid transporters. *PLoS One* **4**(10): e7458.

Schlüter L, Lohbeck KT, Gutowska MA, Gröger JP, Riebesell U, Reusch TBH. 2014. Adaptation of a globally important coccolithophore to ocean warming and acidification. *Nature Climate Change* **4**: 1024.

Sekino K, Shiraiwa Y. 1994. Accumulation and Utilization of Dissolved Inorganic Carbon by a Marine Unicellular Coccolithophorid, *Emiliania huxleyi*. *Plant and Cell Physiology* **35**(3): 353-361.

Sett S, Bach LT, Schulz KG, Koch-Klavsen S, Lebrato M, Riebesell U. 2014. Temperature modulates coccolithophorid sensitivity of growth, photosynthesis and calcification to increasing seawater pCO(2). *PLoS One* **9**(2): e88308.

Sheward RM, Daniels CJ, Gibbs SJ 2014. Growth rates and biometric measurements of coccolithophores (*Coccolithus pelagicus, Coccolithus braarudii, Emiliania huxleyi*) during experiments: PANGAEA.

Shiraiwa Y. 2003. Physiological regulation of carbon fixation in the photosynthesis and calcification of coccolithophorids. *Comparative Biochemistry and Physiology Part B: Biochemistry and Molecular Biology* **136**(4): 775-783.

Shrestha RP, Hildebrand M. 2015. Evidence for a regulatory role of diatom silicon transporters in cellular silicon responses. *Eukaryotic Cell* **14**(1): 29-40.

Shrestha RP, Tesson B, Norden-Krichmar T, Federowicz S, Hildebrand M, Allen AE. 2012. Whole transcriptome analysis of the silicon response of the diatom *Thalassiosira pseudonana*. *BMC Genomics* **13**(1): 499.

Siever R. 1991. Silica in the oceans: Biological-geochemical interplay. *Scientists on gaia*: 287-295.

Sikes CS, Wilbur KM. 1982. Functions of coccolith formation. *Limnology and Oceanography* **27**(1): 18-26.

Simpson T 1981. Effects of germanium on silica deposition in sponges. *Silicon and siliceous structures in biological systems*: Springer, 527-550.

Simpson TL, Gil M, Connes R, Diaz JP, Paris J. 1985. Effects of germanium (Ge) on the silica spicules of the marine sponge *Suberites domuncula*: transformation of spicule type. *Journal of Morphology* **183**(1): 117-128.

Simpson TL, Volcani BE. 2012. *Silicon and siliceous structures in biological systems*: Springer Science & Business Media.

Smith SR, Glé C, Abbriano RM, Traller JC, Davis A, Trentacoste E, Vernet M, Allen AE, Hildebrand M. 2016. Transcript level coordination of carbon pathways during silicon starvation-induced lipid accumulation in the diatom Thalassiosira pseudonana. *New Phytologist* **210**(3): 890-904.

Steinmetz JC 1994. Sedimentation of coccolithophores. *Coccolithophores*: Cambridge University Press Cambridge, 179-197.

Stiller JW, Schreiber J, Yue J, Guo H, Ding Q, Huang J. 2014. The evolution of photosynthesis in chromist algae through serial endosymbioses. *Nat Commun* **5**: 5764.

Suffrian K, Schulz KG, Gutowska MA, Riebesell U, Bleich M. 2011. Cellular pH measurements in Emiliania huxleyi reveal pronounced membrane proton permeability. *New Phytol* **190**(3): 595-608.

Sullivan C, Volcani B 1981. Silicon in the cellular metabolism of diatoms. *Silicon and siliceous structures in biological systems*: Springer, 15-42.

Sutton J, J. EM, A. MW, L. CP. 2010. Oceanic distribution of inorganic germanium relative to silicon: Germanium discrimination by diatoms. *Global Biogeochemical Cycles* **24**(2).

Sviben S, Gal A, Hood MA, Bertinetti L, Politi Y, Bennet M, Krishnamoorthy P, Schertel A, Wirth R, Sorrentino A, et al. 2016. A vacuole-like compartment concentrates a disordered calcium phase in a key coccolithophorid alga. *Nat Commun* **7**: 11228.

Takano Y, Hagino K, Tanaka Y, Horiguchi T, Okada H. 2006. Phylogenetic affinities of an enigmatic nannoplankton, *Braarudosphaera bigelowii* based on the SSU rDNA sequences. *Marine Micropaleontology* **60**(2): 145-156.

Taylor AR, Brownlee C, Wheeler G. 2017. Coccolithophore Cell Biology: Chalking Up Progress. *Ann Rev Mar Sci* **9**: 283-310.

Taylor AR, Chrachri A, Wheeler G, Goddard H, Brownlee C. 2011. A Voltage-Gated H+ Channel Underlying pH Homeostasis in Calcifying Coccolithophores. *PLoS Biol* **9**(6): e1001085.

Taylor AR, Russell MA, Harper GM, Collins TfT, Brownlee C. 2007. Dynamics of formation and secretion of heterococcoliths by *Coccolithus pelagicuss sp.braarudii*. *European Journal of Phycology* **42**(2): 125-136.

Thamatrakoln K, Alverson AJ, Hildebrand M. 2006. Comparative sequence analysis of diatom silicon transporters: toward a mechanistic model of silicon transport. *Journal of Phycology* **42**(4): 822-834.

Thamatrakoln K, Hildebrand M. 2007. Analysis of *Thalassiosira pseudonana* silicon transporters indicates distinct regulatory levels and transport activity through the cell cycle. *Eukaryotic Cell* **6**(2): 271-279.

Thamatrakoln K, Hildebrand M. 2008. Silicon uptake in diatoms revisited: a model for saturable and nonsaturable uptake kinetics and the role of silicon transporters. *Plant Physiology* **146**(3): 1397-1407.

Thierstein HR, Geitzenauer KR, Molfino B, Shackleton NJ. 1977. Global synchroneity of late Quaternary coccolith datum levels Validation by oxygen isotopes. *Geology* **5**(7): 400.

Thierstein HR, Young JR. 2004. *Coccolithophores: From Molecular Processes to Global Impact*: Springer.

Thompson AW, Foster RA, Krupke A, Carter BJ, Musat N, Vaulot D, Kuypers MMM, Zehr JP. 2012. Unicellular Cyanobacterium Symbiotic with a Single-Celled Eukaryotic Alga. *Science* **337**(6101): 1546-1550.

Timmermans KR, Veldhuis MJ, Brussaard CP. 2007. Cell death in three marine diatom species in response to different irradiance levels, silicate, or iron concentrations. *Aquatic microbial ecology* **46**(3): 253-261.

Treguer P, Nelson DM, Van Bennekom AJ, DeMaster DJ, Leynaert A, Quéguiner B. 1995. The silica balance in the world ocean: a reestimate. *Science* **268**(5209): 375-379.

Tréguer PJ, Rocha CLDL. 2013. The World Ocean Silica Cycle. *Annual Review of Marine Science* **5**(1): 477-501.

Trimborn S, Langer G, Rost B. 2007. Effect of varying calcium concentrations and light intensities on calcification and photosynthesis in *Emiliania huxleyi*. *Limnology and Oceanography:* **52**(5): 2285-2293.

Tsutsui H, Takahashi K, Asahi H, Jordan RW, Nishida S, Nishiwaki N, Yamamoto S. 2016. Nineteen-year time-series sediment trap study of Coccolithus pelagicus and Emiliania huxleyi (calcareous nannoplankton) fluxes in the Bering Sea and subarctic Pacific Ocean. *Deep Sea Research Part II: Topical Studies in Oceanography* **125-126**: 227-239.

Tyrrell T, Merico A 2004. *Emiliania huxley*i: bloom observations and the conditions that induce them. In: Thierstein H, Young J eds. *Coccolithophores*: Springer Berlin Heidelberg, 75-97.

Tyrrell T, Schneider B, Charalampopoulou A, Riebesell U. 2008. Coccolithophores and calcite saturation state in the Baltic and Black Seas. *Biogeosciences* **5**(2): 485-494.

Van der Wal P, De Jong E, Westbroek P, De Bruijn W, Mulder-Stapel A. 1983. Ultrastructural polysaccharide localization in calcifying and naked cells of the coccolithophorid *Emiliania huxleyi*. *Protoplasma* **118**(2): 157-168.

van der Wal P, de Jong EW, Westbroek P, de Bruijn WC, Mulder-Stapel AA. 1983a. Polysaccharide localization, coccolith formation, and golgi dynamics in the coccolithophorid *Hymenomonas carterae*. *Journal of Ultrastructure Research* **85**(2): 139-158.

Van der Wal P, Dejong EW, Westbroek P, Debruijn WC, Mulderstapel AA. 1983b. Polysaccharide localization, coccolith formation, and golgi dynamics in the coccolithophorid *Hymenomonas carteraeJournal of Ultrastructure Research* **85**(2): 139-158.

van Emburg PR, de Jong EW, Daems WT. 1986. Immunochemical localization of a polysaccharide from biomineral structures (coccoliths) of Emiliania huxleyi. *Journal of Ultrastructure and Molecular Structure Research* **94**(3): 246-259.

Vaulot D, Olson RJ, Merkel S, Chisholm SW. 1987. CELL-CYCLE RESPONSE TO NUTRIENT STARVATION IN 2 PHYTOPLANKTON SPECIES, THALASSIOSIRA-WEISSFLOGII AND HYMENOMONAS-CARTERAE. *Marine Biology* **95**(4): 625-630.

Wahlund TM, Hadaegh AR, Clark R, Nguyen B, Fanelli M, Read BA. 2004. Analysis of expressed sequence tags from calcifying cells of marine coccolithophorid (Emiliania huxleyi). *Marine Biotechnology* **6**(3): 278-290.

Walker LJ, Wilkinson BH, Ivany LC. 2002. Continental drift and Phanerozoic carbonate accumulation in shallow-shelf and deep-marine settings. *The Journal of geology* **110**(1): 75-87.

Westbroek P, Brown CW, Bleijswijk Jv, Brownlee C, Brummer GJ, Conte M, Egge J, Fernández E, Jordan R, Knappertsbusch M, et al. 1993. A model system approach to biological climate forcing. The example of *Emiliania huxleyi*. *Global and Planetary Change* **8**(1–2): 27-46.

Westbroek P, De Jong E, Dam W, Bosch L. 1973. Soluble intracrystalline polysaccharides from coccoliths of *Coccolithus huxleyi* (Lohmann) kamptner (I). *Calcified Tissue International* **12**(1): 227-238.

Westbroek P, Marin F. 1998. A marriage of bone and nacre. *Nature* **392**(6679): 861-862.

Wilson WH, Tarran GA, Schroeder D, Cox M, Oke J, Malin G. 2002. Isolation of viruses responsible for the demise of an *Emiliania huxleyi* bloom in the English Channel. *Journal of the Marine Biological Association of the United Kingdom* **82**(03): 369-377.

Winter A, Henderiks J, Beaufort L, Rickaby REM, Brown CW. 2014. Poleward expansion of the coccolithophore Emiliania huxleyi. *Journal of Plankton Research* **36**(2): 316-325.

Winter A, Jordan RW, Roth PH 2006. Biogeography of living coccolithophores in oceanic waters. In: Winter A, Siesser WG eds. *Coccolithophores*: Cambridge University Press.

Winter A, Reiss Z, Luz B. 1979. Distribution of living coccolithophore assemblages in the Gulf of Elat ('Aqaba). *Marine Micropaleontology* **4**: 197-223.

Winter A, Siesser WG. 2006. *Coccolithophores*: Cambridge University Press.

Xu J, Bach LT, Schulz KG, Zhao W, Gao K, Riebesell U. 2016. The role of coccoliths in protecting Emiliania huxleyi against stressful light and UV radiation. *Biogeosciences* **13**(16): 4637-4643.

Yamashiro H. 1995. The effects of HEBP, an inhibitor of mineral deposition, upon photosynthesis and calcification in the scleractinian coral, *Stylophora pistillata*. *Journal of Experimental Marine Biology and Ecology* **191**(1): 57-63.

Yool A, Tyrrell T. 2003. Role of diatoms in regulating the ocean's silicon cycle. *Global Biogeochemical Cycles* **17**(4).

Yoshida M, Noël M-H, Nakayama T, Naganuma T, Inouye I. 2006. A Haptophyte Bearing Siliceous Scales: Ultrastructure and Phylogenetic Position of *Hyalolithus neolepis* gen. et sp. nov. (Prymnesiophyceae, Haptophyta). *Protist* **157**(2): 213-234.

Young J, Geisen M, Cros L, Kleijne A, Sprengel C, Probert I, Østergaard J. 2003. A guide to extant coccolithophore taxonomy. *Journal of Nannoplankton Research* **1**(1): 1-125.

Young JR. 1987. Possible functional interpretations of coccolith morphology. *Abh. Geol. B.-A* **39**: 305-313.

Young JR, Davis SA, Bown PR, Mann S. 1999. Coccolith Ultrastructure and Biomineralisation. *Journal of Structural Biology* **126**(3): 195-215.

Young JR, Geisen M, Probert I. 2005. A review of selected aspects of coccolithophore biology with implications for paleobiodiversity estimation. *Micropaleontology* **51**(4): 267-288.

Young JR, Henriksen K. 2003. Biomineralization within vesicles: the calcite of coccoliths. *Reviews in mineralogy and geochemistry* **54**(1): 189-215.

Young JR, Westbroek P. 1991. Genotypic variation in the coccolithophorid species *Emiliania huxleyi*. *Marine Micropaleontology* **18**(1): 5-23.

Zhou C, Jiang Y, Liu B, Yan X, Zhang W. 2012. The relationship between calcification and photosynthesis in the coccolithophorid Pleurochrysis carterae. *Acta Ecologica Sinica* **32**(1): 38-43.

Ziveri P, Baumann K-H, Böckel B, Bollmann J, Young JR 2004. Biogeography of selected Holocene coccoliths in the Atlantic Ocean. *Coccolithophores*: Springer, 403-428.

Ziveri P, de Bernardi B, Baumann K-H, Stoll HM, Mortyn PG. 2007. Sinking of coccolith carbonate and potential contribution to organic carbon ballasting in the deep ocean. *Deep Sea Research Part II: Topical Studies in Oceanography* **54**(5–7): 659-675.

Zondervan I, Rost B, Riebesell U. 2002. Effect of CO_2 concentration on the PIC/POC ratio in the coccolithophore *Emiliania huxleyi* grown under light-limiting conditions and different daylengths. *Journal of Experimental Marine Biology and Ecology* **272**(1): 55-70.

Zondervan I, Zeebe RE, Rost B, Riebesell U. 2001. Decreasing marine biogenic calcification: A negative feedback on rising atmospheric pCO2. *Global Biogeochemical Cycles* **15**(2): 507-516.